



HAL
open science

New optimisation and characterisation methods of tannin-based foams for thermal insulation of buildings

Clara Delgado Sánchez

► **To cite this version:**

Clara Delgado Sánchez. New optimisation and characterisation methods of tannin-based foams for thermal insulation of buildings. Material chemistry. Université de Lorraine, 2017. English. NNT : 2017LORR0246 . tel-01820656

HAL Id: tel-01820656

<https://theses.hal.science/tel-01820656>

Submitted on 22 Jun 2018

HAL is a multi-disciplinary open access archive for the deposit and dissemination of scientific research documents, whether they are published or not. The documents may come from teaching and research institutions in France or abroad, or from public or private research centers.

L'archive ouverte pluridisciplinaire **HAL**, est destinée au dépôt et à la diffusion de documents scientifiques de niveau recherche, publiés ou non, émanant des établissements d'enseignement et de recherche français ou étrangers, des laboratoires publics ou privés.



AVERTISSEMENT

Ce document est le fruit d'un long travail approuvé par le jury de soutenance et mis à disposition de l'ensemble de la communauté universitaire élargie.

Il est soumis à la propriété intellectuelle de l'auteur. Ceci implique une obligation de citation et de référencement lors de l'utilisation de ce document.

D'autre part, toute contrefaçon, plagiat, reproduction illicite encourt une poursuite pénale.

Contact : ddoc-theses-contact@univ-lorraine.fr

LIENS

Code de la Propriété Intellectuelle. articles L 122. 4

Code de la Propriété Intellectuelle. articles L 335.2- L 335.10

http://www.cfcopies.com/V2/leg/leg_droi.php

<http://www.culture.gouv.fr/culture/infos-pratiques/droits/protection.htm>



THÈSE

Pour l'obtention du titre de:

DOCTEUR de L'UNIVERSITÉ DE LORRAINE

Spécialité: Chimie

Présentée par:

CLARA DELGADO SÁNCHEZ

Nouvelles méthodes d'optimisation et de caractérisation de mousses à base de tanins pour l'isolation thermique du bâtiment

Thèse soutenue publiquement le 5 Décembre 2017 à Epinal devant le jury composé de:

Mme Alice MIJA	Maître de conférences, HDR, Université de Nice-Sophia Antipolis	Rapporteur
Mme Fatima CHARRIER-EL BOUHTOURY	Maître de conférences, HDR, Université de Pau et des Pays de l'Adour	Rapporteur
M. Damien ERRE	Professeur, Université de Reims Champagne-Ardenne	Examineur
Mme Vanessa FIERRO	Directrice de Recherches au CNRS, Institut Jean Lamour	Directrice de thèse
M. Alain CELZARD	Professeur, Institut Jean Lamour, Université de Lorraine	Co-directeur de thèse

*Institut Jean Lamour –UMR 7198- Département N2EV – Equipe 402
ENSTIB - BP 21042 - 88051 Épinal Cedex 9
Université de Lorraine – Pôle M4 - Collegium Sciences et Technologie*

Remerciements

Je tiens tout d'abord à remercier les membres du jury de ma soutenance de thèse et donc, en substance, les rapporteurs Mme Alice Mija, maître de conférences à l'Université de Nice - Sophia Antipolis, et Mme Fatima Charrier-El Bouhtoury, maître de conférences à l'Université de Pau et des Pays de l'Adour, ainsi que l'examineur M. Damien Erre, professeur à l'Université de Reims Champagne-Ardenne qui ont passé leur temps à lire soigneusement cette mémoire. Je vous remercie pour tous les commentaires positifs et toutes vos contributions sur vos domaines d'expertise qui me permettent d'enrichir mes connaissances.

Je remercie aussi tout particulièrement mon directeur de thèse M. Alain Celzard pour m'avoir laissé l'autonomie nécessaire dans ce type de travail tout en étant présent pour me guider, pour avoir été assez critique et strict avec moi afin d'obtenir ma meilleure version, pour m'avoir aidé dans mes moments de doutes et surtout pour avoir en plus confiance en moi que je n'avais en moi-même. Je tiens également à remercier Mme Vanessa Fierro, ma directrice de thèse, pour sa gentillesse, sa compréhension, ses attentions et ses connaissances pendant ces années. Ce fût un honneur de travailler avec eux.

Je tiens à remercier toutes les personnes qui m'ont aidé à mener à bien mon travail de recherche. D'une part, l'équipe de Serge et lui-même qui m'ont accueilli dans son laboratoire à Lille pendant une semaine et que m'a permis de développer la connaissance d'un autre domaine. Et, d'autre part, à tous les gens de l'atelier de l'ENSTIB qui m'ont aidé avec plusieurs reprises.

Tout au long de ces trois ans j'ai rencontré beaucoup de gens, certains j'en ai connu plus à fond, d'autres un peu moins, certains ont été éphémères et d'autres ont été avec moi tout le temps, mais sans aucun doute tous font partie de cette aventure et je vous remercie pour tout ce que vous m'avez apporté. Particulièrement, je vais donner une immense merci à mon cher Philippe Gadonneix qui a toujours été là pour m'aider à mener à terme toutes les expériences du laboratoire, pour résoudre tous mes problèmes et atténuer mes dégâts, pour prendre soin de moi, me faire sourire et me donner (ou m'enlever) tranquillité. Je remercie aussi Andrzej pour m'apporter ses connaissances et son savoir-faire nombreuses fois au début de ma thèse et aussi pour ses discussions qui m'ont rendu plus forte. Je veux et je dois surtout remercier Maxime de m'accueillir à bras ouverts et sans mesure, merci de me faire confiance, d'être ma bouée de

sauvetage avec tous mes doutes, de m'aider avec tout et surtout d'être mon ami. Je voudrais également remercier Sébastien, mon éternel collègue de bureau, pour son soutien tout au long de la thèse, bien que nous ayons eu des millions de discussions, nous avons toujours compris et aidé entre nous. A Ángela le quiero agradecer que me haya dejado entrar a formar parte de su vida, que haya siempre confiado en mí y me haya cuidado prácticamente como una madre. A mon Italien, Giuseppe, merci d'avoir donné la vie au bureau, car il était difficile d'être mon partenaire des peines et des joies et il a été super bien à la hauteur. A mi Jime bonita que llegó a mi vida cuando más la necesitaba para aportarme tranquilidad, cariño y amor, mil gracias amiga. A Clément, je le remercie beaucoup de m'avoir fait rire chaque matin avec son "tour de magie". Benoit et Perrine pour nous avoir fait sentir comme de la famille. Et un grand merci aussi à Karakashoviii (Blagoj), à l'inégalée Zelig, Taher, mis mexicanitos (Victor y Judih), César, Balazs, Ousamma, Touraya, Asma, Quentin, Romain, Damien, Imane, Saman, Vincent..... et beaucoup plus.

Quiero darle las GRACIAS a una persona muy importante, Fran. Gracias por ser mi cielo y mi todo, por estar conmigo en los mejores momentos y sobre todo en los peores, por ser mi apoyo incondicional, alegrarte con cada uno de mis logros y animarme y darme cariño siempre que lo necesitaba. No habría podido tener un mejor compañero de viaje. Te quiero.

Me quiero también acordar de todos mis amigos que siempre han estado ahí cuando los he necesitado y que me han apoyado incondicionalmente. Mis amigos de la universidad, que ahora son algunos como mis hermanos y los quiero mil: mi Sergio y mi chulito Antonio que están ahí al pie del cañón todos los días, mi nena Almu, Adri, Julio, Manolo, etc. Y mil gracias también a mis amigas de toda la vida porque no importa la distancia ni lo poco o mucho que hablemos o nos veamos, ellas y sus peques siempre estarán ahí cuando las necesite. Muchas personas se vienen a mi mente en estos momentos, no los cito a todos porque si no esto sería interminable.

Termino agradeciéndole a toda mi familia y, especialmente, a mis padres y mi hermana, que pese a estar físicamente separados han estado y sé que estarán siempre junto a mí, apoyándome, acompañándome, aguantándome y queriéndome incondicionalmente en todo momento. Son lo mejor de mi vida. Gracias a ellos he llegado hasta aquí.

“Sólo aquellos que se arriesgan a ir muy lejos, pueden llegar a saber lo lejos que pueden ir”

“Only those who will risk going too far can possibly find out how far one can go”

T.S. Eliot

A mi hermana

Table of contents

RESUME DE LA THESE	7
INTRODUCTION GENERALE	21
CHAPTER I: STATE OF THE ART	25
I/1. Global context	27
I/1.1. Energy, resources and environmental issues	27
I/1.2. Current market of insulating materials	28
I/2. Natural precursor of rigid foams - Tannin	30
I/2.1. Definition and extraction	30
I/2.2. Classification and structure	32
I/2.3. Reactivity	34
I/2.3.1 Reactions with aldehydes	34
I/2.3.2 Reactions with hexamine	36
I/2.3.3 Reactions with furfuryl alcohol	38
I/2.4. Economic aspect and applications	40
I/3. Tannin foams	42
I/3.1. Generalities about foams	42
I/3.1.1 Solid foams	42
I/3.2. Introduction to tannin foams	45
I/3.3. Formulations of tannin foams	46
I/3.4. Structure and main physical properties of tannin foams	52
I/3.4.1 Structure	52
I/3.4.2 Mechanical properties	54
I/3.4.3 Thermal properties	55
I/3.4.4 Acoustic properties	56
I/3.4.5 Fire behaviour	56
I/3.4.6 Liquid sorption properties	57
I/3.4.7 Bio-adsorbent	58

I/4.	Objective of the thesis	59
I/5.	Bibliography	60

CHAPTER II: STABILITY ANALYSIS AND OPTIMISATION OF MERINGUE TANNIN-BASED FOAMS 67

II/1.	Introduction	69
II/2.	Experimental	71
II/2.1.	Foam preparation	71
II/2.2.	Foam capacity	72
II/2.3.	Foam stability	73
II/2.3.1	Basics of the optical analyser	73
II/2.3.2	Assessment of foams' destabilisation phenomena	75
II/3.	Results and discussion	78
II/3.1.	Foaming capacity	78
II/3.2.	Foam stability	79
II/3.2.1	Effect of crosslinker	80
II/3.2.2	Effect of stirring time	83
II/3.2.3	Effect of surfactant amount	86
II/3.2.4	Effect of temperature	89
II/4.	Conclusion	95
II/5.	Bibliography	97

CHAPTER III: HYDROPHOBISATION OF TANNIN-BASED FOAMS 101

III/1.	Introduction	103
III/2.	Experimental	105
III/2.1.	Foam preparation	105
III/2.2.	Hydrophobisation process	108
III/2.3.	Foam characterisation	110
III/2.3.1	Morphological characterisation	111
III/2.3.2	Elemental analysis	112

III/2.3.3	Fourier-transform infrared (FTIR) spectroscopy	113
III/2.3.4	Contact angle measurements	114
III/2.3.5	Surface energy determination	116
III/2.3.6	Water vapour sorption	117
III/2.3.7	Thermal conductivity	119
III/3.	Results and discussion	120
III/3.1.	Foam characteristics	120
III/3.2.	Organosilane grafting observed by FTIR	122
III/3.3.	Surface properties	124
III/3.4.	Water vapour sorption	128
III/3.5.	Thermal conductivity	135
III/4.	Conclusion	138
III/5.	Bibliography	139
 CHAPTER IV: OPTIMISATION OF BLOWING AGENT-FREE AND FORMALDEHYDE-FREE TANNIN-BASED FOAMS		145
IV/1.	Introduction	147
IV/2.	Experimental	148
IV/2.1.	Foam preparation	148
IV/2.2.	Identification of the most relevant ingredients of the foam's formulation	149
IV/2.3.	Experimental design	151
IV/2.4.	Characterisation of tannin-furanic foams	155
IV/2.4.1	Apparent density, skeletal density and porosity	155
IV/2.4.2	Thermal conductivity	155
IV/2.4.3	Mechanical properties	156
IV/3.	Results and discussion	158
IV/3.1.	Foams' properties	158
IV/3.2.	Results of experimental design and related statistical analysis	160
IV/3.3.	Analysis of response surface methodology (RSM)	163
IV/3.4.	Optimisation of the formulation	165

IV/4. Conclusion	167
IV/5. Bibliography	168
CHAPTER V: FLAMMABILITY OF TANNIN-BASED FOAMS	171
V/1. Introduction	173
V/2. European fire testing of building products	175
V/3. Experimental	178
V/3.1. Foam preparation	178
V/3.2. Foam properties	182
V/3.2.1 Cone calorimetry studies	183
V/3.2.2 Pyrolysis combustion flow calorimetry (PCFC)	184
V/3.2.3 Thermogravimetric analysis coupled with Fourier transform infrared spectroscopy (TGA-FTIR)	186
V/4. Results and discussion	187
V/4.1. Cone calorimetry studies	187
V/4.2. Pyrolysis combustion flow calorimetry (PCFC)	192
V/4.3. Thermogravimetric analyses coupled to Fourier Transform Infrared Spectroscopy (TGA-FTIR)	199
V/5. Conclusion	206
V/6. Bibliography	207
CHAPTER VI: NEW METHODS FOR MECHANICAL CHARACTERISATION OF TANNIN-BASED FOAMS	211
VI/1. Introduction	213
VI/2. Experimental	215
VI/2.1. Foams preparation	215
VI/2.2. Mechanical properties characterisation	216
VI/2.2.1 Classical, destructive, method	216
VI/2.2.2 Non-destructive method	219

VI/3. Results and discussion	223
VI/3.1. Destructive mechanical compression	224
VI/3.2. Quasistatic mechanical analysis	228
VI/3.3. Comparison of destructive method (with and without plates) vs non-destructive one (QMA)	231
VI/4. Conclusion	234
VI/5. Bibliography	235
CONCLUSIONS ET PERSPECTIVES	239
LIST OF FIGURES	245
LIST OF TABLES	251
LIST OF WORKS	253
ABSTRACT	258
RÉSUMÉ	258

Résumé de la thèse

Ce travail s'inscrit dans un contexte sociétal dans lequel les biens de consommation dérivés de la pétrochimie sont devenus une menace pour notre environnement. La demande de pétrole pour les applications énergétiques et chimiques augmente d'année en année, et cependant cette ressource fossile est de plus en plus limitée. La société en général, et la communauté scientifique en particulier, sont de plus en plus conscientes de ce problème qui, avec d'autres aspects tels que le changement climatique ou la pollution, aboutit à la nécessité absolue de développer de nouvelles technologies et des matériaux plus respectueux avec l'environnement.

Dans cet esprit, de nouveaux solides poreux biosourcés multifonctionnels pour applications énergétiques et environnementales doivent être davantage développés, notamment, et c'est le sujet central de cette thèse, dans le domaine de l'isolation thermique du bâtiment. Il y est en effet question de proposer de nouvelles méthodes de caractérisation et d'optimisation de mousses isolantes à base de tanin, des matériaux principalement renouvelables et d'origine naturelle, dans le but de pouvoir remplacer à terme les autres mousses pétrosourcées dominant actuellement le marché de l'isolation.

L'objectif de la thèse était alors de faire des avancées significatives sur le long chemin qui part de la mise au point d'un nouveau matériau au laboratoire à sa possible commercialisation sur un marché de grande ampleur. De par leur caractère biosourcé, les mousses de tannin ont une place à prendre et un public à trouver, sous réserve que leurs performances et leur coût soient en adéquation. Il était donc nécessaire de réaliser des études plus poussées que celles qui avaient été faites jusqu'alors, notamment en termes d'optimisation des formulations, de recherches de nouveaux procédés de moussage, et de nouvelles méthodes de caractérisations.

Ce travail a été réalisé dans l'équipe 402 « Matériaux Biosourcés » de l'Institut Jean Lamour (IJL – UMR CNRS 7198), hébergée dans les locaux de l'Ecole Nationale Supérieure des Techniques et Industries du Bois (ENSTIB), à l'Université de Lorraine. Les fonds correspondants ont été acquis au travers du projet FUI (fonds unique interministériel) « BRIIO – BiosouRced InsulatiON », financé par la banque publique d'investissement (BPI). Les partenaires de ce projet

étaient deux entreprises françaises associées à deux organismes de recherche : Université de Lorraine et CNRS. La description du contenu de chaque chapitre est abordée ci-dessous.

Chapitre I: Etat de l'art

Ce premier chapitre décrit d'abord le contexte sociétal dans lequel s'inscrit la thèse, notamment en ce qui concerne les ressources et les problèmes environnementaux actuels, puis évoque l'état du marché des matériaux d'isolation thermique. Il en a été déduit le besoin de produire des matériaux d'origine naturelle tels que les mousses de tanin présentées ici. Dans ce but, et de manière à effectuer une recherche scientifique utile et efficace, toutes les informations associées aux mousses de tanin ont aussi été recueillies et analysées dans ce premier chapitre bibliographique. L'origine et la nature des tanins, leur processus d'extraction, leur réactivité, les différents procédés de moussage qui donnent naissance à des mousses rigides, et les principales propriétés de ces mousses à ce jour, sont quelques-uns des points qui y sont développés.

En bref, les tanins sont des composés polyphénoliques naturels (Fig. 1) dotés d'une excellente réactivité qui les rend sujets à plusieurs types de réactions chimiques, notamment autocondensation ou réticulation par des composés comme les aldéhydes, l'hexaméthylène-tétramine ou l'alcool furfurylique. Ces processus de polymérisation sont à la base de la formation de mousses rigides à base de tanins.

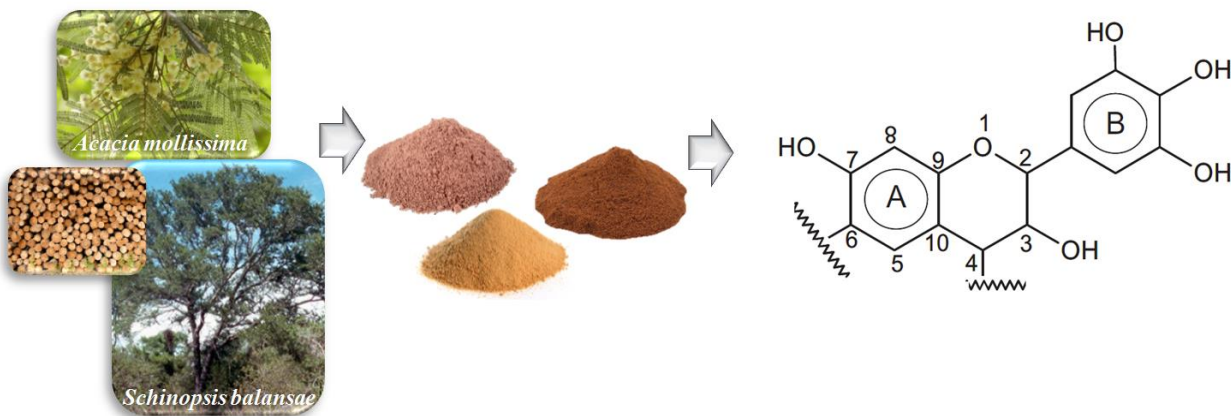


Fig. 1. Exemples de plantes à partir desquelles le tanin est extrait, les extraits correspondants, et l'unité flavonoïde majoritaire dans les tanins condensés de mimosa (*Acacia mollissima*).

Dans ses grandes lignes, la préparation des premières mousses de tanin a eu lieu il y a environ vingt ans. Depuis lors, mais surtout au cours des dernières années, de nombreuses formulations originales ont été développées, utilisant de nouvelles méthodes de moussage et de nouveaux ingrédients dans le but d'obtenir des mousses de tanin avec de meilleures propriétés ou avec des caractéristiques différentes. Les toutes premières mousses de tannin avaient ainsi été développées par moussage physique d'une résine tannin-alcool furfurylique-formaldéhyde avec un agent gonflant. Le formaldéhyde utilisé dans cette formulation permet un fort durcissement du matériau, mais sa volatilité en fait un produit potentiellement dangereux qui peut être relâché lentement dans l'atmosphère. Cela a motivé la recherche de nouvelles mousses de tanin sans formaldéhyde ou en utilisant d'autres aldéhydes non volatils et beaucoup moins toxiques. Une autre grande étape dans l'amélioration des mousses de tanins a été l'élimination de l'agent gonflant organique dans la formulation, qui était aussi un risque pour la santé et l'environnement et qui était aussi extrêmement inflammable. De plus, de nouvelles méthodes de fabrication de mousses de tanin ont été mises au point, comme le battage mécanique d'une formulation liquide contenant un tensioactif, donnant lieu à une mousse liquide qui est ensuite durcie en étuve à 85°C pendant 24 h pour obtenir une mousse solide, dite « meringue ».

A l'heure actuelle, plusieurs familles de mousses à base de tanins sont connues, elles-mêmes obtenues à partir de nombreuses formulations. C'est ainsi que ces matériaux sont très versatiles et peuvent présenter une large gamme de caractéristiques en fonction de la méthode de moussage et des ingrédients de leurs formulations. En général, il s'agit de matériaux solides cellulaires avec des propriétés telles que légèreté, résistance mécanique similaire à celle d'autres mousses commerciales pétrochimiques, excellente résistance au feu, caractère bon marché et renouvelable, facilité de préparation, et très faible conductivité thermique. Toutes ces qualités dans le contexte général actuel font de ces nouveaux matériaux des candidats très prometteurs pour des applications dans le bâtiment ou les transports. Cependant, ils ont également des faiblesses qui doivent être considérées avec grand soin afin de pouvoir concurrencer les matériaux actuels sur le marché de l'isolation thermique. C'était aussi l'objet de cette thèse que d'étudier ces insuffisances et le moyen de les surmonter.

Chapitre II: Analyse de stabilité et optimisation de mousses de tannin de type « meringue »

Un nouveau type de mousse de tannin, obtenu par une méthode récemment mise au point de battage mécanique de solutions aqueuses de tannin, agent réticulant et tensioactif, a été soigneusement étudié en ce chapitre. Ces mousses liquides ont été analysées en termes de stabilité et de procédé de polymérisation en utilisant une méthode d'analyse de la lumière rétrodiffusée, dans le but de les transformer en mousses rigides, appelées « meringues ». La technique, utilisant un analyseur optique basé sur des mesures de diffusion multiple de la lumière, s'est révélée véritablement adaptée pour détecter les différents phénomènes de déstabilisation tels que drainage, sédimentation, et croissance et coalescence des bulles qui ont lieu dans les mousses liquides. Un exemple de différences (ΔBS , %) entre les profils de lumière rétrodiffusée en fonction du temps d'une mousse liquide de tannin à 60°C et son profil à $t = 0$, en fonction de la position dans la hauteur de la mousse et obtenu par l'analyseur optique Turbiscan, est donné en Fig. 2. Il est possible d'y observer les différents phénomènes de déstabilisation qui se produisent dans une mousse liquide de tannin.

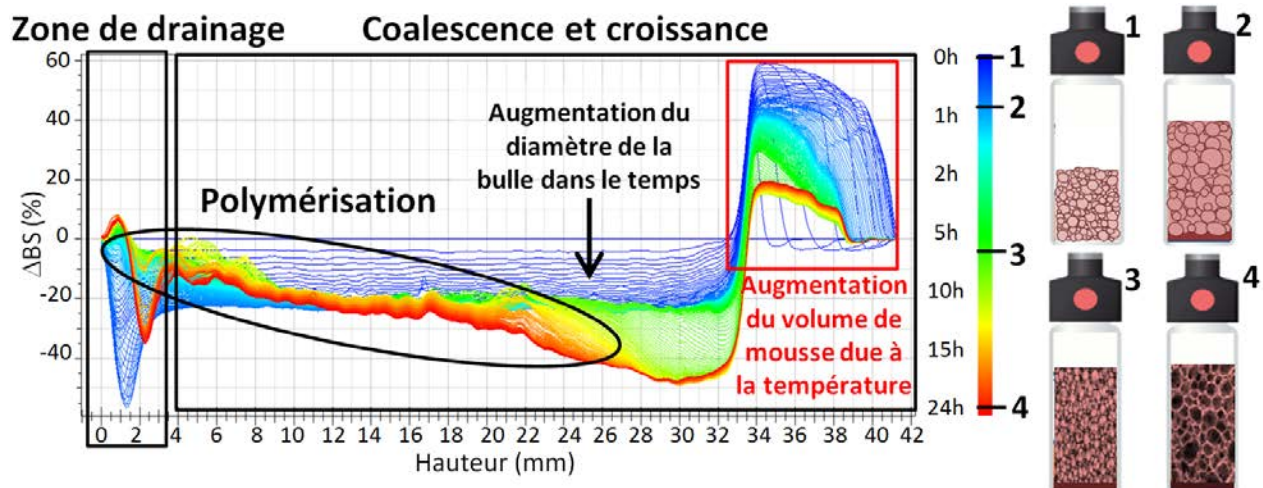


Fig. 2. Profil typique de différence de lumière rétrodiffusée par des mousses liquides de tannin, mesuré par l'analyseur optique Turbiscan.

La méthode a également permis de séparer les processus de façon à ce que chacun d'eux puisse être étudié indépendamment en fonction : du temps d'agitation pour former la mousse, de

la quantité de tensioactif, de la présence d'agent de réticulation, et de la température de durcissement. Les diamètres moyens des bulles ont aussi été déterminés en fonction du temps.

Les résultats ont indiqué que la dynamique des bulles était liée au taux de drainage et qu'il y avait un couplage important entre le drainage et les phénomènes de coalescence et croissance. A composition fixée, le temps d'agitation optimal conduisant à la mousse la plus expansée et la plus stable et, à temps d'agitation fixé, la quantité optimale de tensioactif conduisant à la mousse liquide la plus stable, ont été identifiés. D'autre part, on a constaté que la température avait un impact majeur sur la déstabilisation, mais qu'un chauffage était nécessaire pour obtenir facilement de la mousse rigide avec une structure poreuse fixe donnée. De plus, une température plus élevée entraîne une polymérisation plus rapide et donc une réduction du temps pendant lequel la mousse se déstabilise.

Enfin, la même méthode a été utilisée avec succès pour étudier le processus de polymérisation qui a lieu dans les mousses liquides chauffées. Des informations très importantes ont pu être obtenues, en particulier les vitesses de déstabilisation, les variations de taille moyenne des bulles et le début de la polymérisation, ainsi que l'ordre de réaction et l'énergie d'activation, ce qui permet de comprendre la conversion des mousses liquides en « meringues » de tanin. Il a été ainsi démontré que ce type d'analyse optique est tout à fait pertinent pour optimiser les formulations et les conditions de moussage dans le but de récupérer des mousses rigides après polymérisation, ayant une structure homogène donnée qui pourrait être utile pour diverses applications telles que l'isolation thermique ou l'absorption acoustique.

Chapitre III: Hydrophobisation des mousses de tanin

Des mousses à base de tanin ont été hydrophobisées dans le but de diminuer leur sensibilité à l'humidité. Ce traitement d'hydrophobisation a été effectué car de nombreuses études au cours des dernières années ont confirmé que la conductivité thermique des matériaux poreux thermiquement isolants dépend fortement de l'humidité ambiante. L'efficacité des matériaux poreux isolants est en effet réduite en proportion de leur capacité à ad/ab-sorber l'eau. Les mousses à base de tanin sont donc directement concernées par cet aspect en raison de leurs propriétés d'isolation prometteuses et de leur caractère intrinsèquement hydrophile. Cette

hydrophilie est due à la présence d'une grande quantité de groupes hydroxyles (-OH), qui peuvent se lier très facilement aux molécules d'eau (revoir la molécule de tanin en Fig. 1).

Deux formulations différentes de mousse à base de tanin, « meringue » et « standard », de densités apparentes et de textures poreuses similaires, ont alors été préparées puis hydrophobisées par greffage covalent de silanes portant trois différents types de groupes fonctionnels. Les échantillons non traités et hydrophobisés ont tous été soigneusement caractérisés par spectroscopie FTIR, mesures d'angle de contact et calculs correspondants d'énergie de surface, sorption de l'eau, et mesures de conductivité thermique en fonction de l'humidité relative.

Les deux types de mousses ont été hydrophobisés avec succès. En effet, après traitement, les matériaux ont montré une excellente déperlance de l'eau au niveau macroscopique en raison d'un angle de contact considérablement plus élevé et d'une diminution correspondante de l'énergie de surface, principalement par la disparition de la composante polaire. Cependant, l'hydrophobisation n'a pas totalement empêché la sorption de la vapeur d'eau, qui a seulement légèrement diminué par rapport aux matériaux non traités. Ceci est probablement dû à ce que l'agent greffé sur la mousse a produit une couche hydrophobe en extrême surface, rendant compte du caractère macroscopique observé pour l'eau liquide, mais n'a pas pu éviter la pénétration au niveau microscopique des molécules de vapeur dans le réseau de polymère. Ainsi, les molécules d'eau, qui sont très petites, peuvent encore diffuser dans la résine de tanin et interagir avec les groupes hydroxyles résiduels en volume. La Fig. 3 illustre de manière schématique une structure possible de la mousse après le processus de greffage, qui explique les résultats observés d'une manière cohérente.

En conséquence, la conductivité thermique augmente toujours avec l'humidité relative, mais moins que pour les mousses non traitées. Ainsi, le traitement d'hydrophobisation le plus efficace a permis de limiter l'augmentation de la conductivité thermique à la moitié de ce qui a été mesuré pour la mousse non traitée, donnant ainsi à ces matériaux un meilleur potentiel d'isolation thermique en conditions humides.

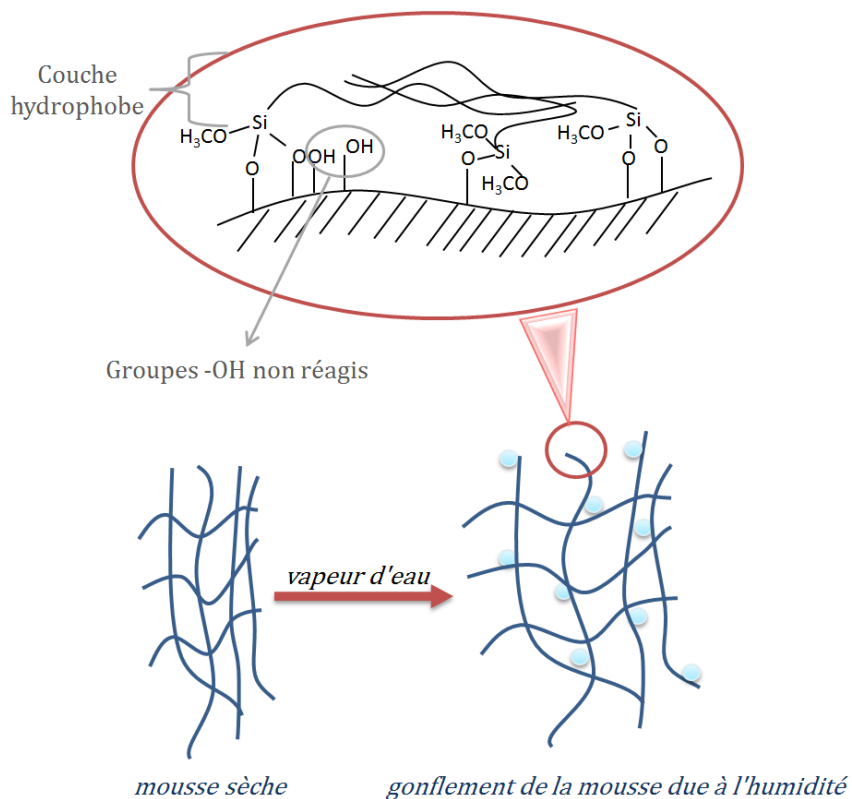


Fig. 3. Schéma possible de la mousse greffée à base de tanin dans un environnement humide.

Chapitre IV: Optimisation des mousses de tanin exemptes d'agent moussant et de formaldéhyde

Dans ce chapitre, des mousses furaniques de tanin ont été préparées à base de formulations exemptes de formaldéhyde, d'agent moussant et d'isocyanate, en tant qu'alternatives plus respectueuses de l'environnement pour remplacer les mousses synthétiques d'isolation thermique actuelles. Obtenir des formulations liquides appropriées, avec des composés non toxiques et/ou d'origine naturelle, et qui forment des mousses rigides avec des propriétés convenables est difficile en raison des nombreuses contraintes de nature chimique et de leurs conséquences sur les matériaux finaux. En effet, si le moussage est plus rapide que la polymérisation, la mousse va s'effondrer avant durcissement. Cependant, si elle réagit trop vite elle n'aura pas le temps de développer une porosité optimale.

De plus, il est également très important de connaître l'effet que les principaux ingrédients produisent sur les propriétés finales des mousses. Le principal but de ce chapitre a alors été

d'obtenir les meilleurs isolants thermiques avec la plus grande résistance mécanique possible. Étant donné que les deux propriétés sont antagonistes, car une faible conductivité thermique nécessite une porosité élevée quand de bonnes propriétés mécaniques nécessitent une faible porosité, un compromis entre isolation thermique et résistance mécanique était donc nécessaire. Pour atteindre cet objectif, un ensemble de mousses à base de tanin a été préparé et analysé en utilisant, pour la première fois avec ce type de matériaux, un plan d'expériences avec analyse statistique des résultats.

Grâce à un nombre limité d'expériences suggérées par une conception rationnelle des formulations, les réponses expérimentales – conductivité thermique, module élastique et résistance à la compression – ont été modélisées. Il a ainsi été possible de prédire leurs valeurs en fonction des proportions relatives des trois ingrédients principaux de la formulation – tanin, alcool furfurylique et catalyseur – pour obtenir des mousses suffisamment isolantes thermiquement tout en restant mécaniquement convenables. Les formulations optimales correspondent contiennent une grande quantité d'alcool furfurylique, une quantité modérée de tanin et une faible quantité de catalyseur. La Fig. 4 schématise l'étude effectuée, et montre deux des trois propriétés modélisées.

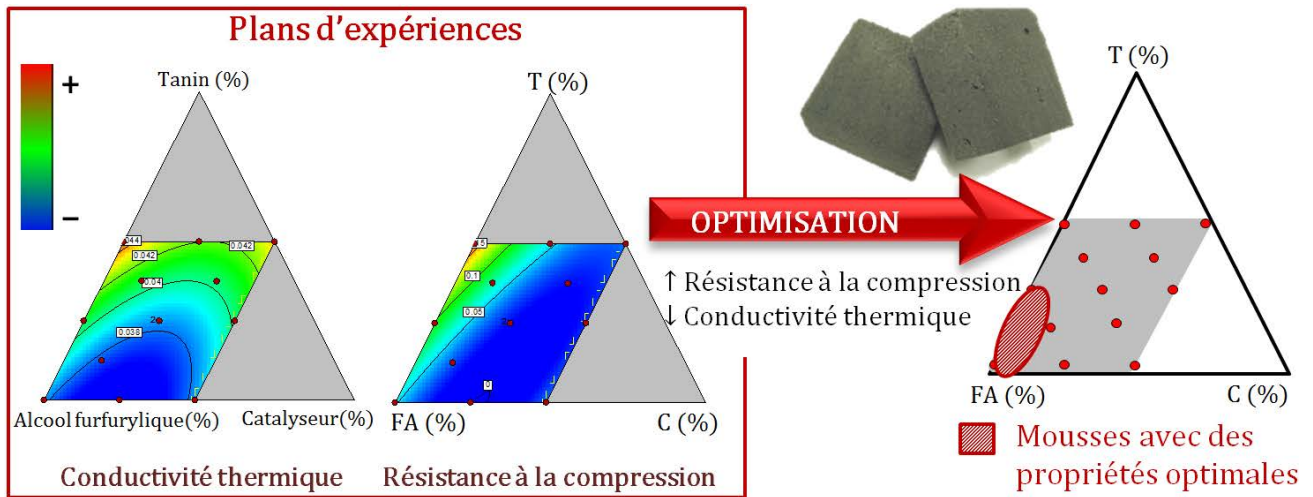


Fig. 4. Représentation graphique de l'effet des quantités de tanin, alcool furfurylique et catalyseur sur la conductivité thermique et la résistance à la compression, et visualisation des mousses aux propriétés optimales dans le diagramme ternaire. Les valeurs numériques des réponses augmentent du bleu au rouge.

La pertinence du plan d'expériences et de son modèle a aussi été testée grâce à la préparation de mousses ayant les propriétés attendues de conductivité thermique, de module élastique et de résistance à la compression. Les résultats ont montré que les valeurs correspondantes étaient en excellent accord avec celles prédites par le modèle. En conséquence, ce dernier s'est révélé être un outil très utile pour développer des mousses furaniques de tanin avec les caractéristiques mécaniques et thermiques convenables pour leur industrialisation.

Chapitre V: Comportement au feu des mousses de tanin

Aujourd'hui, l'amélioration du comportement ignifuge des matériaux d'isolation thermique est un défi majeur pour étendre leurs domaines d'utilisation, et parce que les exigences de sécurité sont de plus en plus sévères. Les propriétés de réaction au feu des premières formulations de mousses à base de tanin ont été étudiées il y a quelques années, et ces mousses présentent une excellente retardance qui, ajoutée à leur caractère renouvelable, de faible coût et de respect de l'environnement, en font des matériaux très attractifs. Cependant, de nombreuses autres formulations avec de nouveaux ingrédients et de nouvelles méthodes de moussage ayant été développées récemment, il a été nécessaire de reconduire en profondeur ce type d'étude, objet du présent chapitre. D'ailleurs, le caractère inflammable ou non d'un matériau n'est pas une grandeur directement mesurable, et une étude exhaustive des paramètres les plus influents sur le comportement anti-feu des mousses est nécessaire pour pouvoir améliorer et « contrôler » leurs propriétés vis-à-vis du feu.

Les mousses de tanin utilisées pour étudier leur inflammabilité ont été soigneusement sélectionnées afin d'analyser l'effet des teneurs en tensioactif, plastifiant, alcool furfurylique et agent réticulant, ainsi que les effets de la méthode de moussage, de la température de durcissement, et du type de tanin. Après avoir effectué ces analyses, il a été constaté que la retardance au feu des mousses est principalement due à la composition aromatique de la matrice polymérique, qui forme un réseau macromoléculaire résistant à la chaleur avec une faible perte de masse au cours de sa décomposition thermique. Cela a été mis en évidence par la bonne corrélation entre le comportement thermogravimétrique en atmosphère inerte et la libération de chaleur mesurée par calorimétrie de flux de combustion.

D'autre part, il a été observé que l'inflammabilité des mousses à base de tanin dépend fortement de leur formulation et pas tant de leurs propriétés structurales. Tous les composés et additifs pour changer les caractéristiques des mousses ont donc une grande influence sur les propriétés au feu du matériau. En effet, en fonction de la présence de tensioactifs et d'additifs et, plus important encore, de la teneur initiale en eau des formulations, le comportement des mousses pendant un incendie peut être très différent. La quantité d'eau initiale dans les mousses est particulièrement importante car la vaporisation de l'eau affaiblit la structure, ce qui facilite la dégradation thermique de la mousse. Ainsi, la réduction de la teneur en eau dans la formulation peut améliorer les performances des mousses de tanin soumises au feu. D'un autre côté, dans l'analyse de mousses identiques avec différents types de tanins, les mousses montrent une inflammabilité très similaire qui est vraiment intéressante du point de vue de la fabrication. Cela signifie que les mousses peuvent être préparées à partir d'une ressource considérablement plus disponible que ne l'est actuellement le tanin de mimosa, majoritairement utilisé dans cette thèse. Les courbes de débit calorifique mesuré par calorimétrie de flux, montrées en Fig.5, ont mis en évidence les principaux processus de dégradation thermique observés dans les mousses, selon leur formulation. Les pics de dégradation ont été attribués à différentes origines, et on peut voir comment le débit calorifique augmente avec la présence de tensioactifs et de plastifiants, et avec la quantité d'eau comme mentionné précédemment.

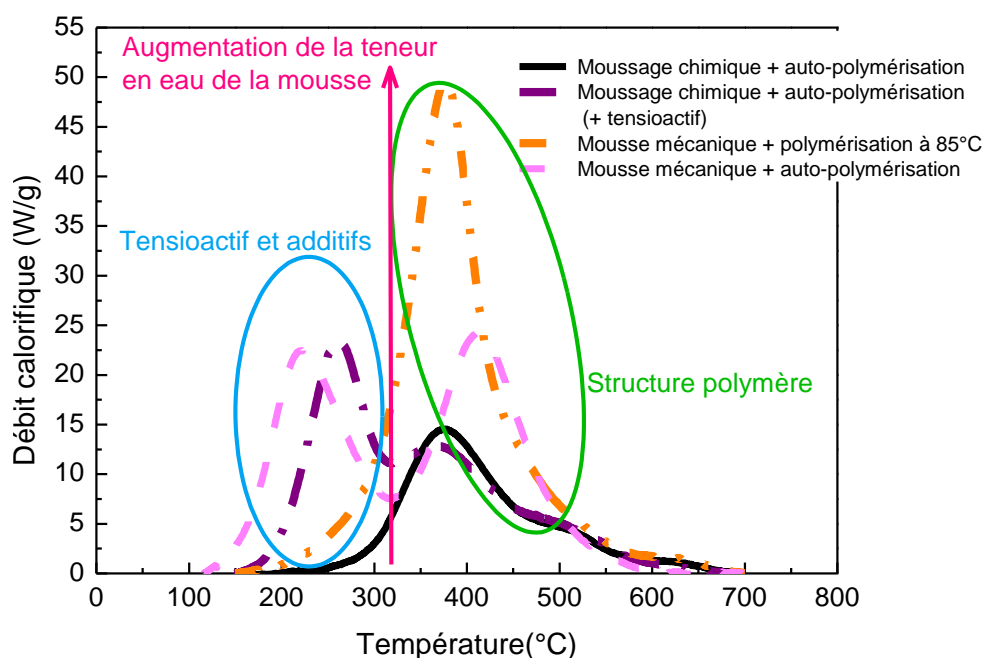


Fig.5. Courbes de débit calorifique mesuré par calorimétrie de flux à $1 \text{ K}\cdot\text{s}^{-1}$.

En général, on a constaté que les mousses rigides organiques à base de tanins présentent, dans toutes leurs variantes, une excellente retardance. Les résultats correspondants ont été comparés à ceux des principaux matériaux isolants actuellement commercialisés tels que le polystyrène expansé et la mousse de polyuréthane – qui ont une inflammabilité relativement élevée, le plus souvent accompagnée par la production de gaz corrosifs hautement toxiques et de fumée pendant la combustion – et les mousses phénoliques, confirmant que l'isolation à base de mousses de tanin présente un meilleur comportement en cas d'incendie.

Chapitre VI: Nouvelles méthodes pour la caractérisation mécanique des mousses de tanin

Ce chapitre est consacré à la caractérisation mécanique de différentes mousses à base de tanin. Au cours des dernières années, de nouvelles méthodes expérimentales ont été proposées pour caractériser les paramètres d'élasticité des matériaux poreux et pour trouver une technique unique de caractérisation. Cependant, cela n'est pas directement applicable à des matériaux comme nos mousses, qui peuvent présenter des propriétés mécaniques allant de dures et fragiles à semi-rigides, voire purement élastiques, selon leur formulation.

Ce travail a donc principalement été axé sur la détermination des propriétés d'une large sélection de mousses de tanin avec des caractéristiques mécaniques très différentes, en utilisant deux techniques distinctes: (i) le procédé classique de compression mécanique, dynamique et destructif, qui peut être réalisé avec et sans plaques collées aux faces de l'échantillon soumises à la sollicitation, et (ii) une nouvelle technique d'analyse mécanique quasi-statique et non-destructive, basée sur l'analyse de la réponse de l'échantillon à des vibrations de basse fréquence. Cette dernière technique a également été utilisée pour déterminer des paramètres tels que le coefficient de Poisson et le facteur de perte, qui n'avaient jamais été mesurés jusqu'à présent pour des mousses de tannin, et qui pourraient être très intéressants du point de vue de la modélisation des mousses pour explorer d'autres applications comme l'isolation acoustique.

L'analyse des mousses selon la méthode classique, avec et sans plaques collées aux faces du matériau soumis à la compression, a montré que lier ainsi les extrémités de l'échantillon aux plaques est un point essentiel pour la détermination du module des mousses fragiles. En effet, elle

induit une meilleure répartition de la charge dans la section de la mousse, et conduit à l'effondrement soudain de l'ensemble du matériau au lieu d'une rupture progressive. En revanche, l'effet du collage de plaques rigides sur les mousses élastiques-plastiques est à peine perceptible, et des résultats similaires sont obtenus avec ou sans plaques collées. Aussi, quel que soit le type de mousse, la même valeur de résistance à la compression a été obtenue si les expériences sont réalisées avec ou sans plaques.

Les valeurs du module d'élasticité mesuré par la nouvelle méthodologie ont été comparées à celles de la méthode de compression mécanique destructive. Une très bonne corrélation a été observée entre le module obtenu par la technique quasi-statique et celui obtenu par compression dynamique sans plaques. Cependant, les résultats de la nouvelle technique n'étaient pas en accord avec la compression avec plaques, plus spécifiquement en ce qui concerne le module élastique des mousses fragiles (voir Fig. 6). On a effectivement observé que, bien que la mousse soit correctement fixée entre les deux plateaux dans la nouvelle méthode, la répartition de la charge n'était pas assez homogène à travers la section des mousses fragiles et, tout comme la compression sans plaques collées, aucun module élastique représentatif du matériau n'a pu être obtenu.

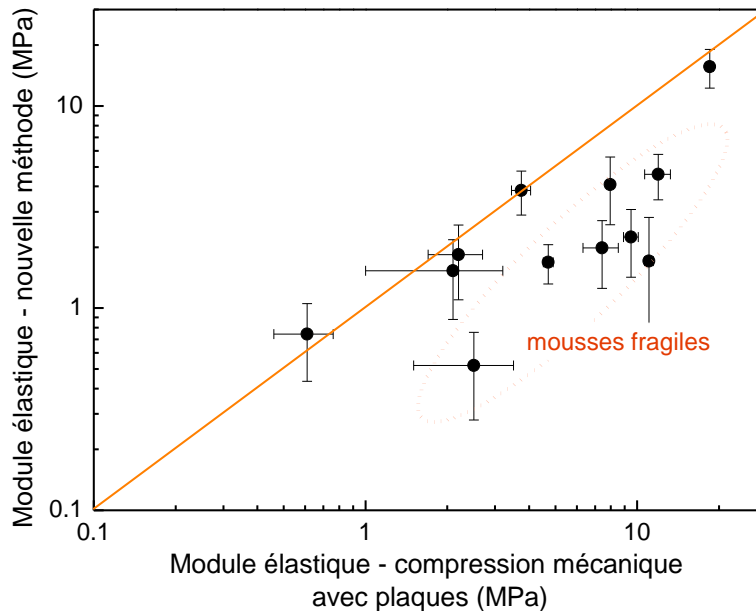


Fig. 6. Comparaison des modules élastiques obtenus par la nouvelle méthode (non destructive) et par celle (destructive) de compression mécanique destructive avec plaques collées.

En conclusion, le moyen le plus sûr de caractériser les propriétés mécaniques d'un matériau poreux cellulaire est d'utiliser une combinaison de méthodes. La nouvelle technique non destructive et la compression mécanique sans plaques sont bien appropriées pour des mousses ayant des caractéristiques élastiques-plastiques. Cependant, elles ne conviennent pas aux mousses fragiles qui doivent avoir leurs faces opposées collées à des plaques rigides pour assurer une répartition homogène de la charge dans toute leur section.

Les principales conclusions et quelques perspectives viennent enfin clore le mémoire. Nous croyons que les études menées dans cette thèse ont apporté des progrès majeurs dans les recherches sur les mousses de tanin, en permettant notamment d'évaluer les performances et de mieux comprendre les propriétés de ces matériaux prometteurs, respectueux de l'environnement, principalement à base de produits naturels et avec un procédé de production relativement écologique. Nous espérons ainsi favoriser leur possible mise sur le marché.

Une liste des travaux scientifiques auxquels ce travail a déjà donné lieu, ainsi que d'autres développés dans le même temps en lien avec des matériaux dérivés de tannin de natures différentes, peut être trouvée en toute fin du manuscrit.

Introduction générale

Nous ne pouvons plus ignorer que nous vivons dans une société où la demande en pétrole pour l'énergie et les applications chimiques croît et se développe toujours davantage, année après année, sans signe d'essoufflement. C'est ainsi que les produits pétroliers ont envahi notre quotidien, ce qui ne pourra pas continuer indéfiniment car les réserves de cette ressource fossile sont en voie d'épuisement.

Dans ce contexte dominé par la nécessité absolue d'économiser les combustibles fossiles et de réduire notre dépendance à eux, combiné à d'autres problèmes environnementaux majeurs comme le réchauffement climatique et la pollution de l'air et des eaux, un intérêt croissant de la communauté scientifique pour la recherche d'une chimie durable est né, avec de plus en plus d'alternatives crédibles aux produits pétrochimiques sur la base de matières premières renouvelables. La société aussi semble avoir commencé à prendre conscience de l'écologie, et à accompagner favorablement la production de produits compatibles avec l'environnement.

Plus concrètement, le monde de l'isolation thermique et de l'isolation du bâtiment en général est en train de changer. Alors que jusqu'à présent seuls comptaient le coût et l'efficacité des matériaux, il y a à l'heure actuelle une tendance croissante dans ce marché à évaluer d'autres paramètres tels que la performance environnementale, avec une isolation écologique pour un habitat sain. Les isolants écologiques sont devenus plus importants en raison de leurs caractéristiques renouvelables, de leur faible énergie grise associée, de leur innocuité, de leur faible coût, de leur facilité d'accès, de leur absence ou de leur moindre contenu en ressources fossiles, etc. Certains matériaux isolants thermiques tels que le liège, la ouate de cellulose, la fibre de bois ou même la laine, notamment, sont déjà sur le marché et sont des alternatives « vertes » aux – jusqu'à présent – incontournables isolants comme la mousse de polyuréthane ou le polystyrène extrudé, certes plus performants thermiquement dans l'absolu.

Dans cet esprit d'innovation technologique favorisant l'émergence de nouveaux matériaux biosourcés et multifonctionnels, des mousses de tanin dérivés à plus de 90% à partir de substances naturelles ont été développées. Ces mousses polymères sont constituées à plus de 50% en masse de tanins condensés, i.e., de composés végétaux de nature phénolique extraits

principalement d'écorces de bois, et présentant des propriétés chimiques qui leur donnent un grand potentiel dans la synthèse de nouveaux polymères.

Depuis quelques années, différentes méthodes pour préparer des mousses à base de tanin ont été développées et étudiées. La plupart des études réalisées avec ces mousses se sont focalisées sur leurs principales propriétés. Et de fait ces mousses solides, en raison de leur structure cellulaire associée à une faible densité, d'un fort pouvoir isolant thermique et d'une excellente résistance au feu, entre autres, constituent a priori une alternative très intéressante aux mousses phénoliques synthétiques commerciales et aux polyuréthanes dans diverses applications.

Les travaux de cette thèse ont été réalisés dans le cadre du projet FUI (fonds unique interministériel) « BRIIO – BiosouRced InsulatiON », financé par la banque publique d'investissement (BPI). Les partenaires de ce projet sont une ETI (Entreprise de Taille Intermédiaire) qui pilote le projet, et une PME (Petite et Moyenne Entreprise), toutes deux françaises et associées à deux organismes de recherche : Université de Lorraine et CNRS. L'objectif du projet BRIIO était la fabrication d'un nouveau produit pour l'isolation thermique des bâtiments avec des matériaux biosourcés peu valorisés jusqu'à présent et économiquement attractifs, susceptibles d'être mis sur le marché à court ou moyen terme. Ce nouveau produit, dans notre cas des mousses de tanin, permettrait ainsi de répondre à toutes les demandes du marché : performances, prix, moindres impacts environnementaux sur le cycle de vie complet, facilité de mise en œuvre, faible densité, valorisation de ressources naturelles, etc.

Afin d'atteindre ces objectifs, il a été nécessaire d'étudier les mousses de tannins du point de vue de leur application, et d'imaginer les problèmes qui pourraient être rencontrés lors de leur utilisation. D'une manière générale, quelques-uns des points faibles qui ont été étudiés et analysés tout au long de la thèse sont leur affinité pour l'eau, qui rend leurs propriétés sensibles aux conditions ambiantes, ainsi que leurs propriétés mécaniques qui doivent être améliorées sans pour autant compromettre leur conductivité thermique. Par ailleurs, les propriétés au feu d'une nouvelle génération de mousses obtenue par foisonnement à l'air d'une formulation liquide, ainsi que la manière dont les différents paramètres de synthèse affectent les mousses rigides finales afin d'en optimiser la formulation, ont été abordées.

La thèse est ainsi structurée de la manière suivante. Le premier chapitre est un état de l'art qui rappelle le contexte actuel des matériaux d'isolation thermique, et qui donne toutes les informations utiles concernant les tanins ainsi qu'une synthèse résumant ce qui est connu à propos des mousses dérivées. Le second chapitre décrit la réalisation de mousses solides par durcissement de mousses liquides, ainsi que l'étude des paramètres qui affectent la stabilité de ces mousses liquides et leur impact sur la mousse rigide finale. Les propriétés hygroscopiques des mousses et un moyen de les rendre plus hydrophobes sont ensuite décrits dans le troisième chapitre. Dans le quatrième chapitre, des mousses tanin-alcool furfurylique exemptes de formaldéhyde, d'agent moussant et d'isocyanate ont été préparées, et leurs propriétés ont été optimisées pour obtenir des matériaux qui soient à la fois bien isolants thermiquement et suffisamment résistants mécaniquement. Le cinquième chapitre est consacré aux propriétés au feu des mousses, en étudiant soigneusement comment les différents aspects de la formulation affectent les différents paramètres caractérisant la tenue au feu de ces matériaux. Enfin, une méthode non destructive de mesure des propriétés mécaniques des mousses est présentée dans le dernier chapitre, et comparée avec la méthode classique pour laquelle une variante est proposée, conduisant à des valeurs bien plus représentatives du module de compression.

Etant donné que la thèse a été réalisée dans le cadre d'un projet où des entreprises françaises sont impliquées, certains des résultats sont confidentiels et n'ont donc pas été présentés. En d'autres termes, un travail bien supérieur a été réalisé mais seuls les résultats ayant un intérêt académique n'interférant pas avec les développements industriels en cours ont été rapportés ici. Finalement, après la conclusion, une liste des publications, parues et soumises, et des communications, orales ou écrites, est fournie.

Chapter I: State of the art

I/1. Global context

I/1.1. Energy, resources and environmental issues

Polymers derived from petroleum chemistry have been part of our everyday life since their development towards the middle of the 20th century. The demand of oil for energy and chemical applications is growing year after year, especially with the demand from emerging countries. According to the estimations done by International Energy Agency (*Publication: WEO-2016 Special Report Energy and Air Pollution, 2016*), the bulk of the known reserves will be consumed by the end of the 21st century. The discovery of new deposits, notably in the form of shale gas, might delay this deadline, but this does not exclude the fact that fossil energy will be more and more limited (Brecha, 2013).

The need to reduce our dependence on fossil fuels is therefore proved. The scientific community is thus turning massively towards the development of new technologies and materials that are more environment-friendly. Moreover, in recent decades there has been a growing desire for ecological development throughout the world, with the protection and preservation of the environment as a final motivation. There has been a real renewed interest in all actions that can be taken in the direction of eco-responsible approaches. The development of renewable energies has grown and research began integrating natural products into industrial processes.

In this exposed overall context dominated by the need of saving fossil resources, reducing greenhouse gas emissions and limiting the carbon footprint of industrialists, chemists develop alternatives to petrochemical products using biomass as raw material. In this spirit, new multifunctional biosourced porous solids for energy and environmental applications have been developed. That is particularly the case of tannin-based foams, with the specific objective of considerably reducing or even completely replacing foams based on petroleum derivatives currently used by-products of natural and renewable origin.

As far as elastic foams are concerned, commercial products are mainly made of polyurethanes but there are natural alternatives, in particular, latex which is increasingly developing on the market. On the other hand, in the case of rigid foams, practically no natural product is offered in

substitution for synthetic products. Rigid tannin foams are thus a technological innovation at the forefront in this sector (Celzard et al., 2015).

I/1.2. Current market of insulating materials

Thermal insulation refers to materials, methods and processes used to reduce the rate of heat transfer. Insulators do not allow heat to pass through easily and therefore heat is retained. The more heat flow resistance insulation provides to the building, the lower are heating and cooling costs. Properly insulating buildings not only reduce costs but also improves comfort.

Heat is transferred from one material to another by conduction, convection and/or radiation. Materials used for thermal insulation of buildings are selected because they are poor conductors of heat. Moreover, there are a number of other properties that are required to ensure that a material will perform well as both thermal insulator and construction material such as compressive strength, density, shrinkage, temperature limits, toxicity, fire retardance, moisture and corrosion resistance, and durability in general.

In general, there are three main groups of thermal insulation material on the market: biosourced (cellulose, cork, straw, sheep's wool, wood fibre, etc.), inorganic (glass mineral wool, foamed glass, aerogel, etc.) and synthetic-oil based (expanded polystyrene, extruded polystyrene, rigid polyurethane, phenolic foam, etc.). Details are provided in Fig. I-1. Moreover, other considerations are interesting in thermal insulation materials such as indoor air quality impacts, life cycle costs, recycled content, embodied energy, and ease of installation. Some insulation strategies require professional installation, while homeowners can easily handle others. As it stands, there are advantages and disadvantages associated with each type of insulation product available on the market and there is no one-size-fits-all answer. For many buildings, choosing an alternative to sprayed polyurethane foam will mean increasing the thickness of the insulator if the thermal performances of the used material are lower. Moreover, from an energy-saving point of view, there are only a few products that insulate as effectively and seal as tightly as fresh polyurethane foams. Replacing the latter by less performing materials may require higher volumes, but air quality, sustainability and recyclability are also important questions that have to be considered in green building.

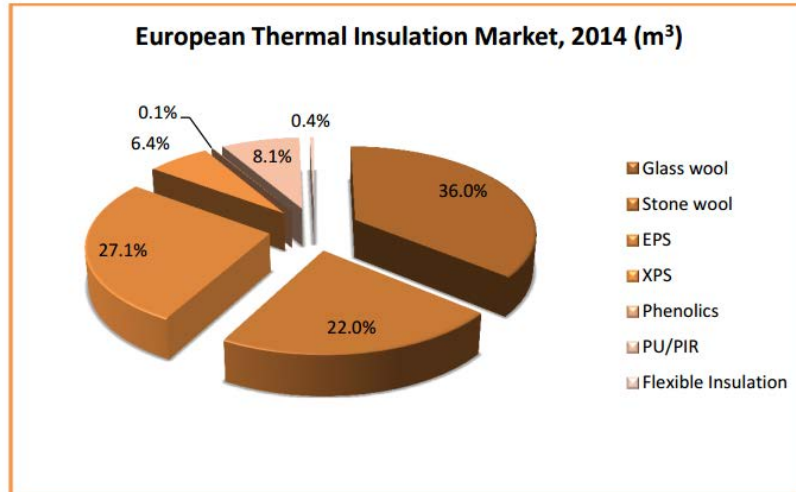


Fig. I-1. Status of the European thermal insulation market in 2014.

In the last decades, the search for renewable and environment-friendly materials for thermal insulation applications attracted much industrial and academic interest. Green materials based on bioresources are developed and used in a way that protects the environment and conserves natural resources trying to get rid of plastics made from fossil fuels and toxic chemicals, as it was pointed previously. In addition, more attention is being given to the recyclability or biodegradability of those products and industry wastes.

Such research for sustainable materials from renewable resources also concerns acoustic insulation. Nowadays, building materials are expected to perform several functions and to be sustainable. For example, materials are supposed to satisfy structural, thermal and acoustical standards, the latter involving both sound absorption and sound insulation. This enables an interesting gain of space in the buildings, in comparison to the use of several materials put aside each other, as well as a gain of time and money during the construction (Glé et al., 2011). This is the reason why new materials such as tannin-based foams have been – and still are – investigated (Amaral-Labat et al., 2013a; Celzard et al., 2015; Lacoste et al., 2015; Yang et al., 2003).

Rigid foams based on condensed tannin have attracted a considerable attention in the industry of acoustic and insulation materials, especially in the latter, due to their composition based predominantly (up to 98%) on renewable, environment-friendly raw materials, extreme lightness, mechanical strength not very far from the ones of other petrochemical commercial foams,

acoustic insulating properties, great thermal and fire resistance, lower cost and ease of preparation (Celzard et al., 2015). All these qualities make these new materials serious ecological and biosourced, thermal insulation alternatives for buildings. After pyrolysis, these foams can also be converted into vitreous carbon with a quite high carbon yield, around 50%, retaining the same structure, and whose chemical resistance makes them usable as filters for molten metals and corrosive fluids, while their electrical conductivity also allows them to be used as porous electrodes (Szczyrek et al., 2013; Tondi et al., 2009a).

I/2. Natural precursor of rigid foams - Tannin

I/2.1. Definition and extraction

Tannins are natural polyphenolic materials contained in many species throughout the plant kingdom, where they play an important role in protection from predation of insects, fungi and even herbivores due to their astringent nature (Hemingway and Laks, 2012). They are found in almost any part of the plant, from roots to leaves, bark to unripe fruit; however, they are mainly stored in different zones of the plants depending on the species (Gross et al., 2012).

Examples of tannin-rich plants are quebracho (*Schinopsis balansae*) where the tannin is dispersed through all the trunk of the tree; mimosa (*Acacia mollissima*) and pine (*Pinus radiata*) where the highest concentration is in the tree barks; tara (*Caesalpinia Tinctoria*) where tannin is extracted from the fruit skin; and chestnut (*Castanea sativa*) extracted from the wood of the Mediterranean typical tree (Arbenz and Avérous, 2015). The examples are shown in Fig. I-2.

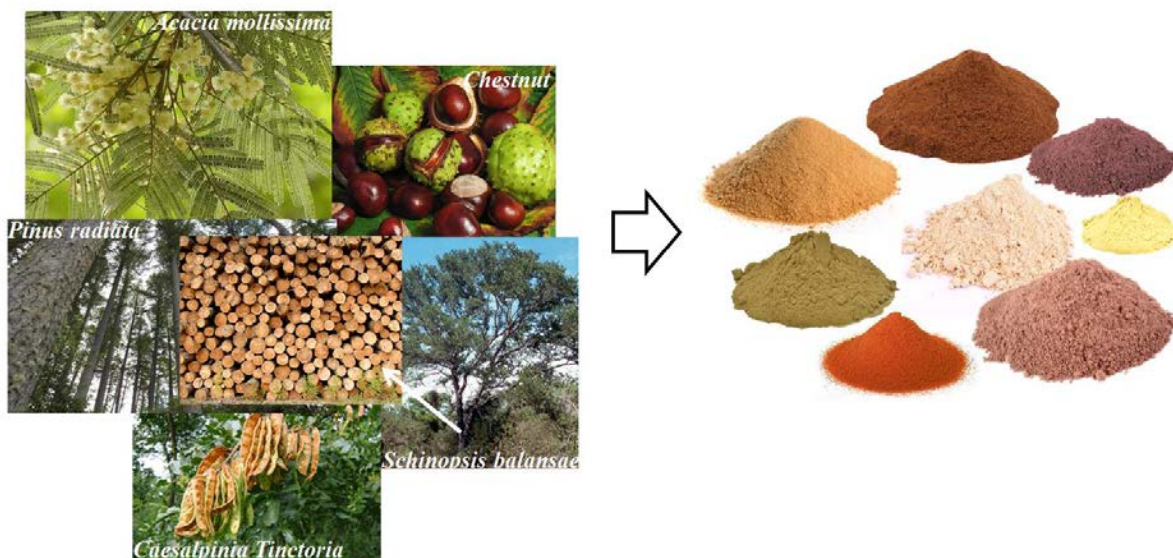


Fig. I-2. Some examples of tannin-rich plants and corresponding tannin extracts.

Plant preparation and extraction processes have a great influence on tannin extract composition. Phenolic compounds can be extracted from fresh, frozen or dried plant and there is no single protocol for extracting tannin from all plants. The procedures used for tannins are widely variable and usually based on solvents. The industrial methods habitually use a system of autoclaves with boiling water in order to solubilise the tannin contained in the plant and extracting it (Sealyfisher and Pizzi, 1992). Water can be used alone although sometimes some organic solvents are used with or without water or some alkaline solutions to increase the extraction efficiency (Cork and Krockenberger, 1991; Gironi and Piemonte, 2011; Hayouni et al., 2007; Yang et al., 2009). Afterwards, the solution is generally decanted (this step is not required for mimosa tannin) and concentrated by evaporation, generally spray-drying, until obtaining the desired concentration. Finally, the tannin is atomised to obtain a dry powder. Mimosa tannin produces this way typically contains about 80 – 82% flavonoid polyphenols, 4 – 6% of water, 1% of amino and imino acids, the remainder being monomeric and oligomeric carbohydrates, in generally broken pieces of hemicelluloses. The colour changes depending on several factors, for instance, the older is the bark, the darker is the colour of tannin (Arbenz and Avérous, 2015; Feng et al., 2013; Matturro et al., 2006).

I/2.2. Classification and structure

Tannins were classified depending on their chemical structures by Freudenberg in 1920 (Gross, 1999). This classification groups them into three major classes: hydrolysable, condensed and complex tannins, see Fig. I-3. Hydrolysable tannins are subdivided into gallotannins and ellagitannins.

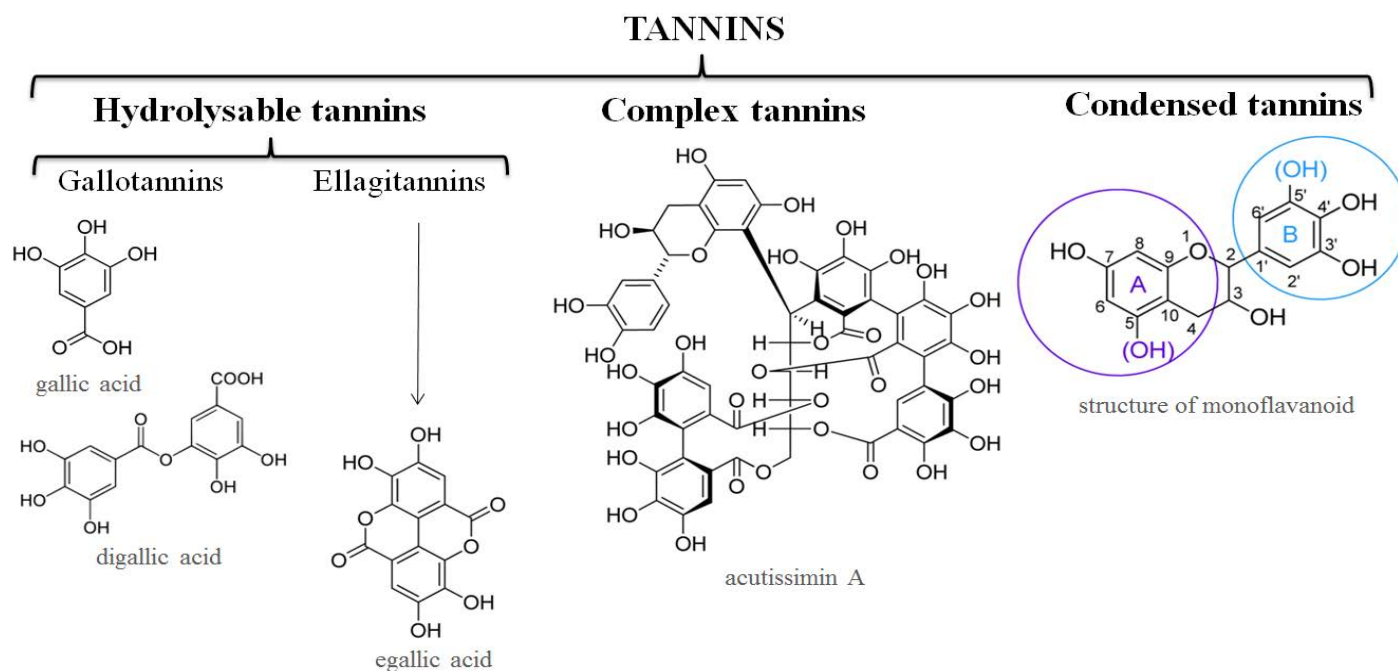


Fig. I-3. Tannin classification and examples of structures.

Hydrolysable tannins are composed of simple phenolic compounds such as gallic, digallic, and ellagic acids, and various monosaccharides such as glucose which hydrolyse easily with acids or bases (Pizzi, New York : M. Dekker, c1994). This kind of tannins is mainly used in the tanning industry although its use is quite limited due of its low reactivity. The most used are tannins of chestnut and tara.

Condensed tannins are polyflavonoids, polymers of up to a few tens of flavonoid units linked by C-C bonds; these molecules are therefore not easily hydrolysable. The flavonoid units are constituted by a heterocyclic ring linking two phenolic rings, A-ring and B-ring. They have different reactivity depending on the presence or not of OH in positions 5 and 5'. These various

configurations generate two possibilities for each ring and four corresponding monoflavonoids: profisetinidin, prorobinetinidin, procyanidin and prodelphinidin (Pizzi, 1982) (see Fig. I-4).

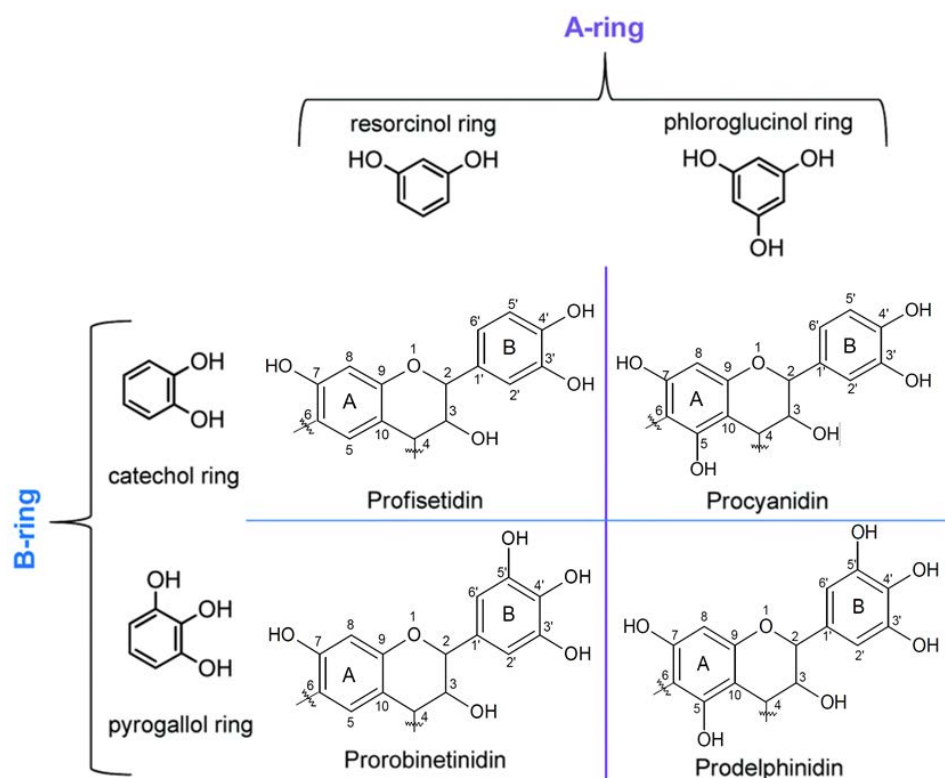


Fig. I-4 Structures of the two possibilities of each phenolic ring and the flavonoid units present in the condensed tannins (Arbenz and Avérous, 2015).

According to the type of tannins considered, the monoflavonoids are present in different proportions. For example, quebracho tannin is composed of between 20 and 30% of prorobinetinidin and of between 70 and 80% of profisetinidin. Mimosa tannin instead is composed predominantly of between 50 and 70% of type prorobinetinidin and only of between 15 and 25% of type profisetinidin (Pasch et al., 2001).

Finally, there is also another kind of particular tannins called complex tannins that consist of ellagitannin units (hydrolysable tannins of ellagic acid type) linked to flavonoid units. Their structures are rather complex and may be linked to other types of polyols (Khanbabaee and Ree, 2001).

I/2.3.Reactivity

The type of connection between the various flavonoid units and its reactivity with other molecules depend on the nature of the rings. The reactivity is an important characteristic to take into account because it is directly connected to their potential applications. Knowing the proportions of these flavonoid units makes it possible to predict how tannins will react.

In general, nucleophilic centres of the A-ring are generally more reactive than those of the B-ring. The inter-flavanoid linkage is mainly either C4-C8 or C4-C6. In the case of profisetinidin and prorobinetinidin the linkage is primarily C4-C6. In the case of procyanidin and prodelphinidin the linkage is mostly C4-C8. Procyanidin is the most reactive polyflavonoid. The degree of polymerisation of the tannins and the nature of the latter (linear or branched) depend on the plant species from which they were extracted. Generally, the degree of polymerisation of condensed tannins is around 4-5 and, for instance, the polyflavonoids of mimosa tannin consist of 2 to 11 monoflavonoids. For pine tannins, there are up to 30 monomers for an average degree of polymerisation of between 4 and 5. For quebracho tannins, the average polymerisation degree is 6 - 7 (Meikleham et al., 1994).

Tannins have a high reactivity and can, therefore, undergo several kinds of structural modifications (Arbenz and Avérous, 2015). Thus, tannins can give rise to new building blocks of great interest for synthesising new polymers. Some of these modifications are related to the heterocycle such as hydrolysis, heterocyclic ring opening (Pizzi, 1989) or sulfonation (Pizzi, 1979), others are related to hydroxyl groups such as acylation (Nicollin et al., 2013) or esterification (Luo et al., 2013), and others are related to the reactivity of nucleophilic sites and their reactions with aldehydes, hexamine or furfuryl alcohol, amongst others.

The polymerisation of tannin is mainly due to the reactivity of its nucleophilic sites. Such reactivity with aldehydes, hexamine and furfuryl alcohol is detailed below.

I/2.3.1 Reactions with aldehydes

Formaldehyde is the most commonly used aldehyde in tannin-based resins for adhesive and foam preparation. With condensed tannins, formaldehyde reacts mainly with the A-ring in the

free nucleophilic sites C6 and C8 to form methylene bridges. The B-ring is far less reactive, and therefore only poorly participates in strong acidic or basic environments (Roux et al., 1975).

The reaction between the A-ring and the formaldehyde is carried out in the form of two simultaneous reactions: the formation of methylene bridges ($-\text{CH}_2-$) (Fig. I-5) and the formation of dimethylethers bridges ($-\text{CH}_2\text{OCH}_2-$) which, due to their instability, recombine themselves in methylene bridges. This reaction leads to the creation of a crosslinked three-dimensional network decreasing the molecular mobility. The latter, together with the size of the molecules, the configuration and the lack of flexibility, create an incompletely polymerised and, therefore, a weak structure (Pizzi and Mittal, 2003). This reaction of formaldehyde with tannin is also very dependent on pH, which controls the rate of the reactions (Meikleham and Pizzi, 1994).

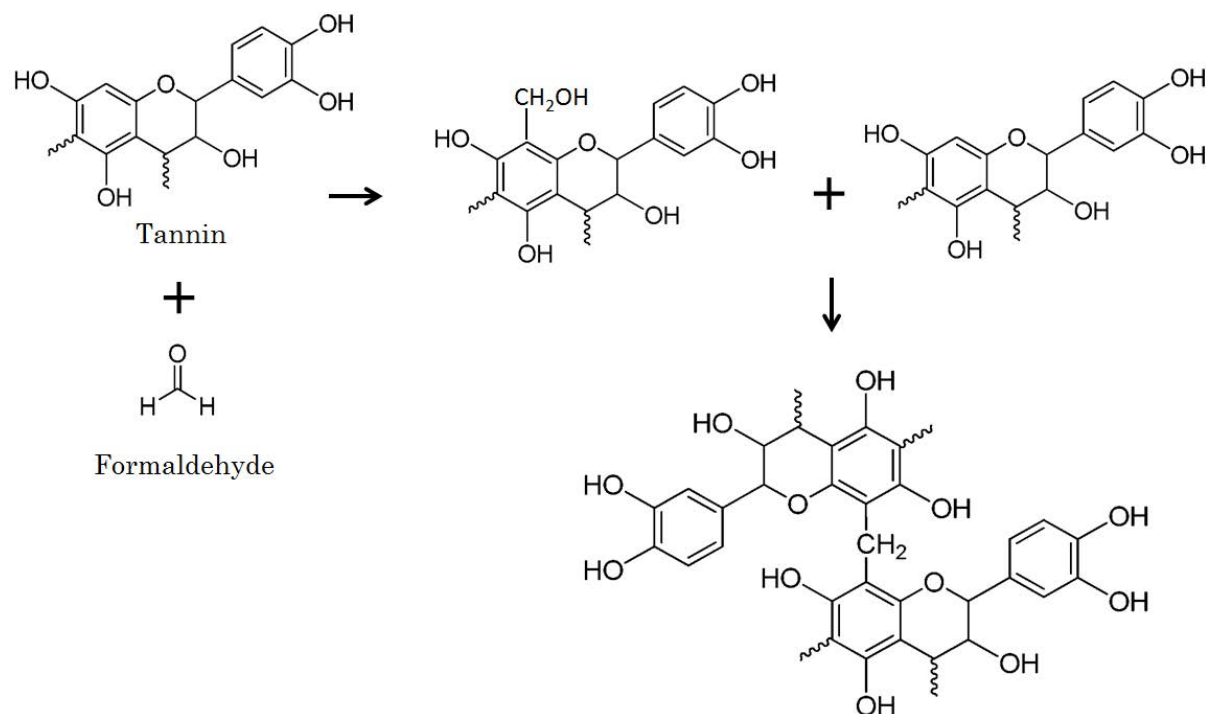


Fig. I-5. Reaction between tannin and formaldehyde.

In order to reduce the problem of incomplete polymerisation, crosslinking agents such as aldehydes with bifunctional characteristics such as acetaldehyde, isobutyraldehyde or furfuraldehyde have been sometimes used to allow the establishment of bonds between sites too distant to be connected by a bridge of methylene type (Rossouw et al., 1980).

In the preparation and curing of tannin-based resins with applications in different areas, formaldehyde is the most used aldehyde. However, it has been reclassified by the International Agency for Research on Cancer (IARC) from Group 2 (probably carcinogenic to humans) to Group 1 (carcinogenic to humans) (“IARC CLASSIFIES FORMALDEHYDE AS CARCINOGENIC TO HUMANS,” 2004). This has encouraged research for reducing and even eliminating formaldehyde emissions during the last years. In this field, the most innovative technologies are based on the formulation of materials without the addition of formaldehyde or with the addition of hardeners that do not emit formaldehyde because the latter is sequestered within the system.

The two most optimal and widely used aldehydes for replacing formaldehyde are glyoxal and glutaraldehyde. Both indeed have several important advantages with respect to formaldehyde. Their toxicity is so low that they are even been used for dentifrice applications (Edward, 1970). Their biodegradable nature makes them be quickly transformed by bacteria or fungi. In addition, they are not volatile, unlike formaldehyde, thereby eliminating the possibility of harmful gas emission during use. The main disadvantage, especially for glutaraldehyde, is their lower reactivity with phenol compared to that observed with formaldehyde (Ballerini et al., 2005; Rossouw et al., 1980). However, it was found that glyoxal can completely substitute formaldehyde to prepare tannin foams with good properties for insulation, whereas glutaraldehyde is less suitable for the purpose because of its lower reactivity with pine tannins (Lacoste et al., 2013b).

The reactivity of condensed flavonoid tannins towards an aldehyde used as crosslinker is the most common way to characterise the reactivity of the tannin (Pizzi, New York : M. Dekker, c1994). Usually, the method consists in measuring the gelling time, i.e., the time required to get a gel texture, as a function of pH once the aldehyde has been added (Garnier et al., 2002).

1/2.3.2 Reactions with hexamine

Hexamethylenetetramine, also called hexamine, is a heterocyclic organic compound of raw formula $(\text{CH}_2)_6\text{N}_4$. This white crystalline compound prepared industrially by combining

formaldehyde and ammonia (Eller et al., 2000) is highly soluble in water and in polar organic solvents, and has been thoroughly studied as a substitute to toxic formaldehyde.

Hexamine under acidic conditions is decomposed into formaldehyde and ammonia whereas, under alkaline conditions, it decomposes into formaldehyde and trimethylamine (Kamoun et al., 2003). However, when reacting with species of high reactivity such as the polyphenols with nucleophilic sites (tannins), it is possible to avoid the production of formaldehyde from hexamine since the reaction that occurs through intermediates is faster than the decomposition of hexamine in ammonia and formaldehyde (Pichelin et al., 1999). This reaction has been studied by ^{13}C -NMR, showing that the decomposition of hexamine occurs through a variety of intermediates that derivate in very reactive and unstable imines and amino-imino methylene bases that react with tannin, forming amino-methylene bridges (Kamoun et al., 2003; Pichelin et al., 2006, 1999). Thus, two tannin units are connected by one benzylamine bridge (Fig. I-6).

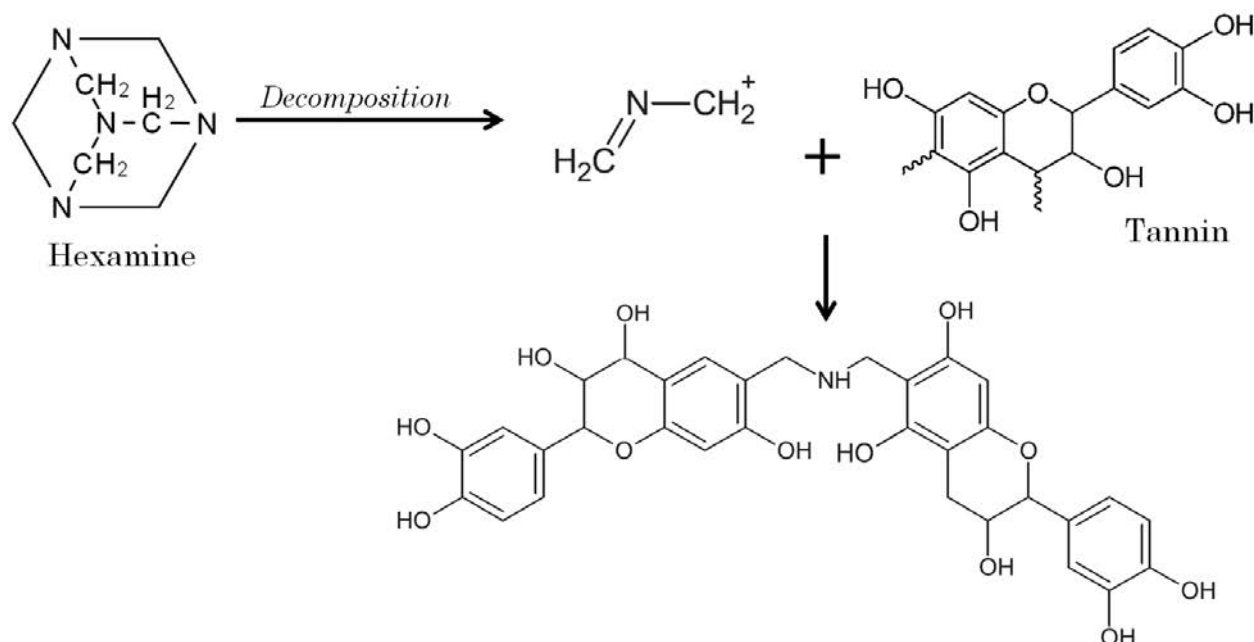


Fig. I-6. Example of crosslinking of tannin through benzylamine bridges by reaction with an amino-imino methylene base obtained by decomposition of hexamine in the presence of tannins (Pichelin et al., 1999).

The effect of the pH on the process is significant, not only for the decomposition of hexamine but also for the tannin reactivity (Peña et al., 2009). That factor is important because, for instance,

hexamine decomposition is faster at high pH than the reaction with tannin which would lead to the formation of formaldehyde.

Based on this, the use of hexamine as a tannin hardener is a major environmental advance, mainly due to the low emission of formaldehyde and because it has been successfully used as a crosslinker for the fabrication of boards that meet the specifications required for the formaldehyde emission (Pizzi et al., 1995). Rigid foam (Szcurek et al., 2014) and polyHIPEs (Szcurek et al., 2015) were also prepared from tannin – hexamine formulations.

1/2.3.3 Reactions with furfuryl alcohol

Furfuryl alcohol is a bio-sourced heterocyclic alcohol derived from hemicellulose (Fig. I-7). It combines a low aromaticity and the reactivity of an alcohol. It is obtained industrially by high pressure and catalytic hydrogenation of furfural with catalysts such as Co-Mo-B (Chen et al., 2002) and Cu-MgO (Nagaraja et al., 2003). Furfural is, in turn, extracted by hydrolysis of sugars (pentoses from hemicelluloses) from various agricultural by-products such as corncobs, oat, wheat bran, and sawdust (Basta and El-Saied, 2003; Ge et al., 2016; Hu et al., 2012). It is therefore considered a natural product.

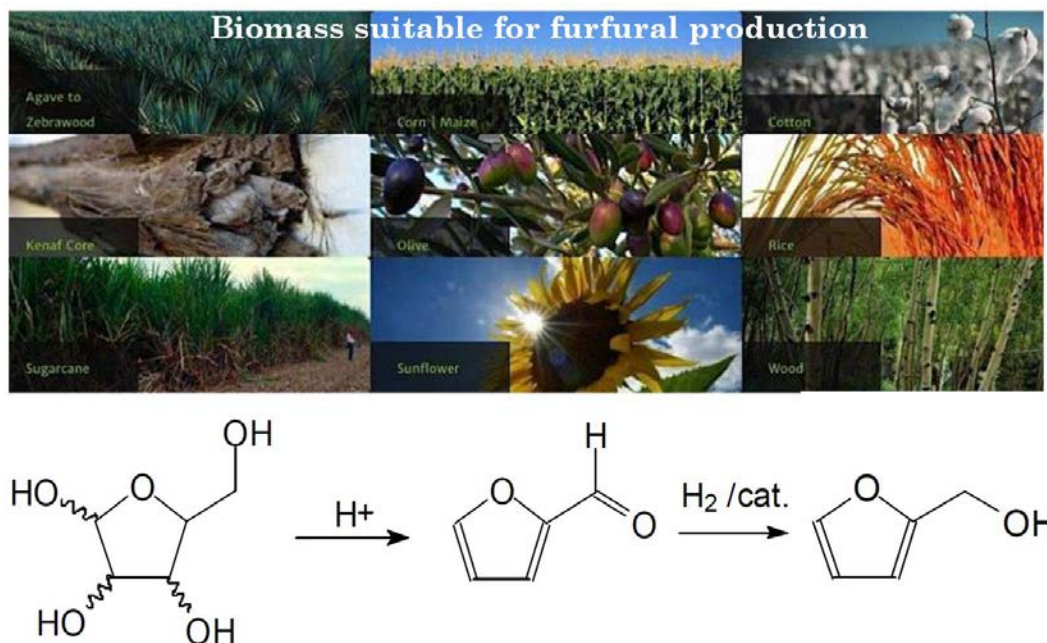


Fig. I-7. Production of furfuryl alcohol from pentoses.

Furfuryl alcohol is well-known for its autocondensation reaction in acid medium, which is highly exothermic and self-sustaining until complete conversion to polyfurfuryl alcohol (Fig. I-8). Such polycondensation is assumed to involve two steps, the linear growth of the chains and the chain crosslinking (Choura et al., 1996). Those reactions give linear, branched or three-dimensional structures according to the catalytic conditions (Kandola et al., 2015).

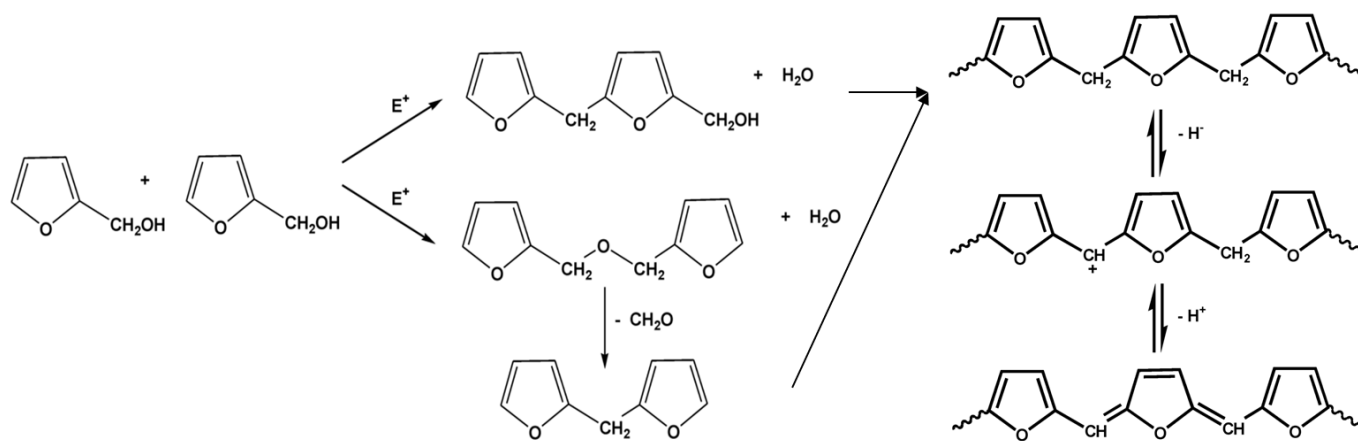


Fig. I-8. Reactions proposed for the polycondensation and chain extension of furfuryl alcohol resins in the presence of acids and other electrophiles (Choura et al., 1996; Dunlop and Peters, 1953).

Furfuryl alcohol can also react with tannin to give intermediates for further synthesis with formaldehyde for example. The study of the reactions between furfuryl alcohol and tannins was carried out by Foo and Hemingway (Foo and Hemingway, 1985) in acid medium – necessary for the reaction of furfuryl alcohol mainly with itself – and at 100°C. After separation and purification, two flavonoids were obtained with C8 and C6 substitutions with better yield for C8 position (Fig. I-9).

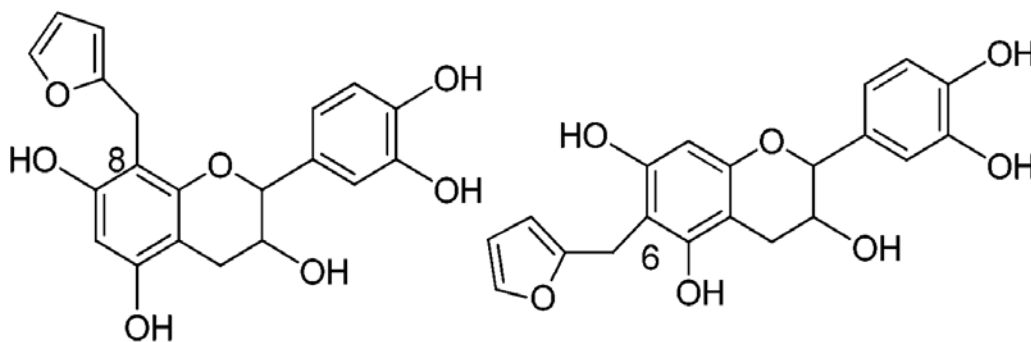


Fig. I-9. Reaction products between tannin and furfuryl alcohol (Arbenz and Avérous, 2015).

Finally, some studies have shown how furfuryl alcohol is also able to react with formaldehyde to give 2,5-bis (hydroxymethyl) furan (Fig. I-10). The latter is commonly used, mixed with tannin, as a reactive species to improve the crosslinking (Pizzi et al., 2008).

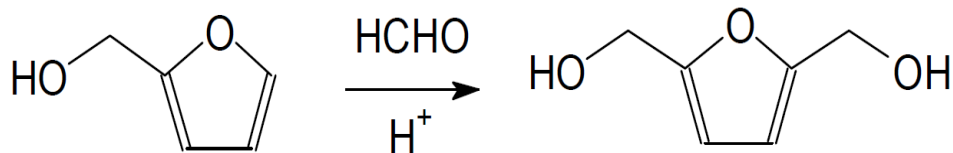


Fig. I-10. Reaction of furfuryl alcohol with formaldehyde.

In the production of a resin based on tannins, furfuryl alcohol and formaldehyde, all the reactions described above may occur at the same time and create a highly crosslinked complex three-dimensional structure due to: (i) the polycondensation of tannins with formaldehyde, (ii) the self-condensation of furfuryl alcohol in acid medium, and (iii) the reaction of furfuryl alcohol on ring A of the tannins, supplemented by (iv) the reaction of formaldehyde with furfuryl alcohol. Such combination is used to produce standard rigid tannin-based foams (Tondi et al., 2009b).

I/2.4. Economic aspect and applications

Tannin is the fourth most abundant component of vascular plant tissue, after cellulose, hemicellulose, and lignin. Thus, tannin greatly contributes to define the specificities of bulk organic matter, including colour, astringency, and reactivity (Hernes et al., 2001). In terms of geography, the tannin market can be segmented into North America, Latin America, Europe, Africa and Asia Pacific. Europe holds the largest share of the market, over the past few years, due to its immensely developed wine industry.

Nowadays, condensed tannins are the most abundant on the market and constitute more than 90% of the worldwide production of commercial tannins (Stokke et al., 2013). In particular, the most important ones are mimosa (*Acacia mollissima*), quebracho (*Schinopsis balansae* and *lorenzii*) and maritime pine (*Pinus pinaster*) tannins. The production of mimosa and quebracho tannin is about 60 000 tonnes/year and their prices are rather low, estimated from 1 500 to 2 300 €/ton. In contrast, maritime pine tannin production is much lower and this tannin is only available

at quite high purity, hence its much higher price, 29 000 €/ton. Therefore, the use of mimosa and quebracho tannin as materials precursor is ideal due to their availability on the market and their reasonable cost.

The great advantages of tannins are their high availability, solubility in water, alcohol and acetone, combined with the fact that they are not very toxic by ingestion or inhalation. Indeed, their high reactivity, different but still qualitatively comparable to that of synthetic and more expensive phenol molecules as explained in the previous section, is a good indication of their great economic potential.

The main industrial application of tannins is found in the textile and leather industries, where tanning is carried out thanks to their high reactivity with protein in animal skin (Covington, 2009; Haslam, 1997). However, beyond these classical applications, they are also used in other minor fields of industry such as dyes agents (Pisitsak et al., 2016), cosmetic / pharmaceutical / nutraceutical industry (Ferri et al., 2016; Henke et al., 2017; Lin et al., 2016; Stojiljkovic et al., 2016), pollutant bio-adsorption (Bacelo et al., 2016), and in the oenological industry as regulator of the tannin content present in the wines (Baker and Ross, 2014; Harbertson et al., 2012), amongst others. Moreover, they were successfully applied for manufacturing several kinds of adhesive resins used in the production of panels and particleboards (Pizzi, 1982; Pizzi and Merlin, 1981) for furniture and building.

They can also be used for producing high-added value materials such as rigid foams (Celzard et al., 2015; Szczurek et al., 2014) and gels (aerogels, xerogels or cryogels) (Amaral-Labat, 2013; Amaral-Labat et al., 2013b; Szczurek, 2011) with acoustical, insulating, or pollutant removal applications amongst others. All these materials can also be pyrolysed under an inert atmosphere and their derived carbons (Amaral-Labat et al., 2013a; Szczurek, 2011; Szczurek et al., 2013, 2011) can be used for adsorption, catalytic and energy storage purposes. The research work of the present thesis is focused in the study of rigid tannin-based foams with special applications in thermal insulation.

I/3. Tannin foams

I/3.1. Generalities about foams

Foams are porous structures consisting of empty cells surrounded by a condensed phase. The drastic differences in nature between gases filling the cells and liquids or solids as the condensed phase make foams unique combinations that have special properties for a number of applications. The range of such applications is further broadened, depending on whether the porosity is closed or open. For instance, the presence of a cellular structure can regulate flow velocity, dissipate disturbance, and enlarge mass transfer area. Metal foams, polymeric foams, paper foams, and ceramic foams are examples that have been developed.

It is hard to go a day without coming across some sorts of foams. The foams are present in many products in everyday life such as the majority of cakes and desserts, shaving cream or cappuccino and they are used in a wide variety of applications such as packaging for transport, furniture (cushions and mattresses) or insulating materials (whether thermal, electrical, or acoustic). Their specific properties are also exploited for some highly specialised applications.

Foams are systems with habitually complex behaviour according to their liquid, solid but soft or rigid nature, their ordered or disordered, or open vs. closed, structure. Rigid ones are rare in nature but widespread in the modern economy; in general, they are produced from the polymerisation/curing of liquid foams.

I/3.1.1 Solid foams

Solid foams are a class of materials generally characterised by their lightness and "alveolar" structure which guarantee their interest from an applicative point of view. They can be categorised from many perspectives depending on the material (thermoplastic and thermoset), physical properties (flexible and rigid), structure (closed cell and open cell), cell size, density, dimension, etc. One of the most important distinctions between solid foams is based on the interconnectivity of the cells: closed-cell foams and open-cell foams. In closed-cell foam, the gas forms discrete pockets, each one completely surrounded by the solid material while in open-cell foam, the gas pockets connect with each other. There are of course many intermediate situations

(more or less closed cells with perforated walls), but these are the most common denominations because they correspond to two distinct types of foams with different properties and applications.

The foams can be described according to the periodic arrangement of their cells. The first studies on the distribution and shape of different cells in a static foam structure were carried out in the 1980's (Thomson, 1887). The Kelvin conjecture proposed a periodic organisation consisting of a compact stack of tetrakaidecahedron cells (Fig. I-11(a)). For about a century, this partition was considered to be the closest to the actual structure of the foams because it minimises the total contact area per unit volume. However, more recently, Weaire and Phelan (Weaire and Phelan, 1994) discovered a structure that is more compact and made it possible to understand that, for a given amount of material and a given volume, the cells are organised according to a structure constituted by two types of polyhedron. The volume of a foam is thus constituted by 75% of tetrakaidecahedra (polyhedra formed by 12 pentagons and 2 hexagons) and by 25% of dodecahedra (12 pentagons) as shown in Fig. I-11(b).

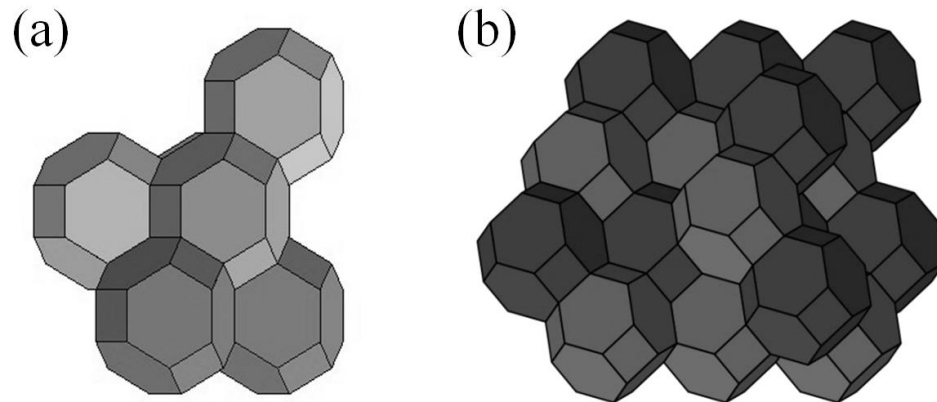


Fig. I-11. Schematic arrangement of foams: a) ideal: made only of tetrakaidecahedra; b) real: 75% tetrakaidecahedra and 25% dodecahedra.

These representations are only theoretical and approximate foams with an ideal structure, which is almost never the case. Indeed, according to the method of preparation, the foams can have very different structures with strong polydispersity in terms of cell sizes, or even a very marked anisotropy (elongated cells in the direction of foaming, for example).

The formation of a rigid foam depends on the physicochemical variables related to the process, such as viscosity, crosslinking speed, gas to liquid ratio, temperature, pressure, amount

and nature of surfactants, etc. which in turn have a large influence on the stability of the precursor liquid foams which is subjected to forces of gravity, capillarity and displacement. As a result, a system comprising a gas dispersed in a liquid is produced that results in a rigid foam. The process is divided, in general, in three main stages (Lee and Ramesh, 2004; Minogue, 2000):

1. Induction. The resin with all or most of the components involved in the foam preparation is prepared and some isolated bubbles are formed. The most widely used precursor systems for producing rigid foams are based on rather complex liquid formulations, otherwise, the rupture of the bubbles will immediately occur. It is, therefore, necessary, in order to obtain good rigid foams, that some other components are present. Thus, the catalyst must be carefully selected, as well as the additives for better controlling the process or the final additional properties to the foam, and/or blowing agents, capable of carrying out the dispersion of gas throughout the fluid polymer phase and stabilise the resultant foam.

2. Expansion/foaming. The proportion of gas becomes significant and many bubbles form, causing the expansion of the foam with bubbles separated by thin films which are still liquid. Such foaming can be mechanical, chemical, physical or mixed (combining some of them). The first type of foaming is achieved by introduction of gases by mechanical stirring, microwave, etc. in a polymer system which either cures by catalyst or by heating (or both), thus trapping bubbles in the polymer matrix (Choe et al., 2016; Merle et al., 2016; Szczurek et al., 2014). The second and third types of foaming involve a release of gas by use of a foaming agent. The latter can be produced by simple reactions between reactants, by thermal decomposition of chemical blowing agents by heating or exothermic reaction (Basso et al., 2013a), by volatilisation of gases produced during the exothermic polymerisation reaction (Tondi et al., 2009c), or by expansion of a dissolved gas in the resin by reducing the system pressure (Kumar et al., 2013), amongst others. The foaming process is one of the most important steps determining the final morphology of the foam. The number and distribution of bubbles can affect immensely the orientation and properties of the final rigid foam.

3. Polymerisation and stabilisation of the polymer. The macromolecular chains react to form a three-dimensional structure around the bubbles. This step is critical for the stability

of the future rigid foam. Indeed, if it occurs too early, the cellular microstructure does not have time to develop to form a proper foam. On the other hand, if it begins too late, the structure risks to collapse due to the drainage and coalescence of bubbles. It is, therefore, necessary to find an optimum between these related mechanisms. Once the foam is formed and mechanically stabilised, the gel point of the polymer is exceeded; the foam can then dry, completing the entire crosslinking process.

In general, many parameters are needed to fully control and understand foams. The physics involved in the formation, stabilisation and in the subsequent characterisation of foams' properties are important concepts to master from a practical point in view of the elaboration of the materials developed during this thesis.

I/3.2. Introduction to tannin foams

Tannin-based foams are, as repeatedly stated, environment-friendly materials composed predominantly (up to 98%) of natural products. Fig. I-12 show how these materials look like. In addition to their biosourced composition, those cellular solids have a considerable interest on the market due to their remarkable properties such as lightness, mechanical strength similar to that of other petrochemical commercial foams, fire resistance, lower cost, ease of preparation and exceptionally low thermal conductivity. All these qualities in the current overall context make these new materials serious candidates that are worth studying, improving and optimising in order to compete with other non-renewable products.



Fig. I-12. Standard tannin-based foams.

The first tannin foams were developed using a tannin-furfuryl alcohol-formaldehyde resin (Meikleham and Pizzi, 1994) which has been modified over the time to produce a range of materials, among them solvent-free and formaldehyde-free foams with similar features (Basso et al., 2013a, 2011; Celzard et al., 2015; Szczurek et al., 2014). Thus, their application research has been extended to rigid foams for thermal (Celzard et al., 2015) and acoustic (Lacoste et al., 2015) insulation, for floral foams (Basso et al., 2016) and even, after pyrolysis, to derived vitreous carbon with other applications (Amaral-Labat et al., 2013a; Celzard et al., 2012; Jana et al., 2014; Letellier et al., 2015; Szczurek et al., 2013). As a result of these researches, tannin-based foams have been, and still are, an interesting and quite active research topic.

I/3.3. Formulations of tannin foams

As stated above, tannin foams can be formed from many different formulations, which have been modified and improved over time. Several thermoset resins can be prepared from flavonoid tannins through different reactions (explained in detail in Section 2.3. *Reactivity*): tannin-autocondensation (occurring at low or high pH or in the presence of a catalyst), crosslinking with aldehydes (formaldehyde, but also non-volatile and much less-toxic aldehydes such as glyoxal or glutaraldehyde) or with other molecules such as furfuryl alcohol and hexamethylenetetramine, for example, in order to get high-quality biosourced foams. It is also possible to make tannin co-react with other natural (e.g. lignin or albumin) or synthetic (e.g. phenol and resorcinol) molecules, and to add some other components such as plasticiser (polyethylene glycol (PEG) or glycerol), isocyanate polymers (pMDI) or fillers such as nanotubes in order to develop foams with better and/or different features. A schematic summary of all foams formulations that exist until now, slightly chronologically ordered, is shown in Fig. I-13.

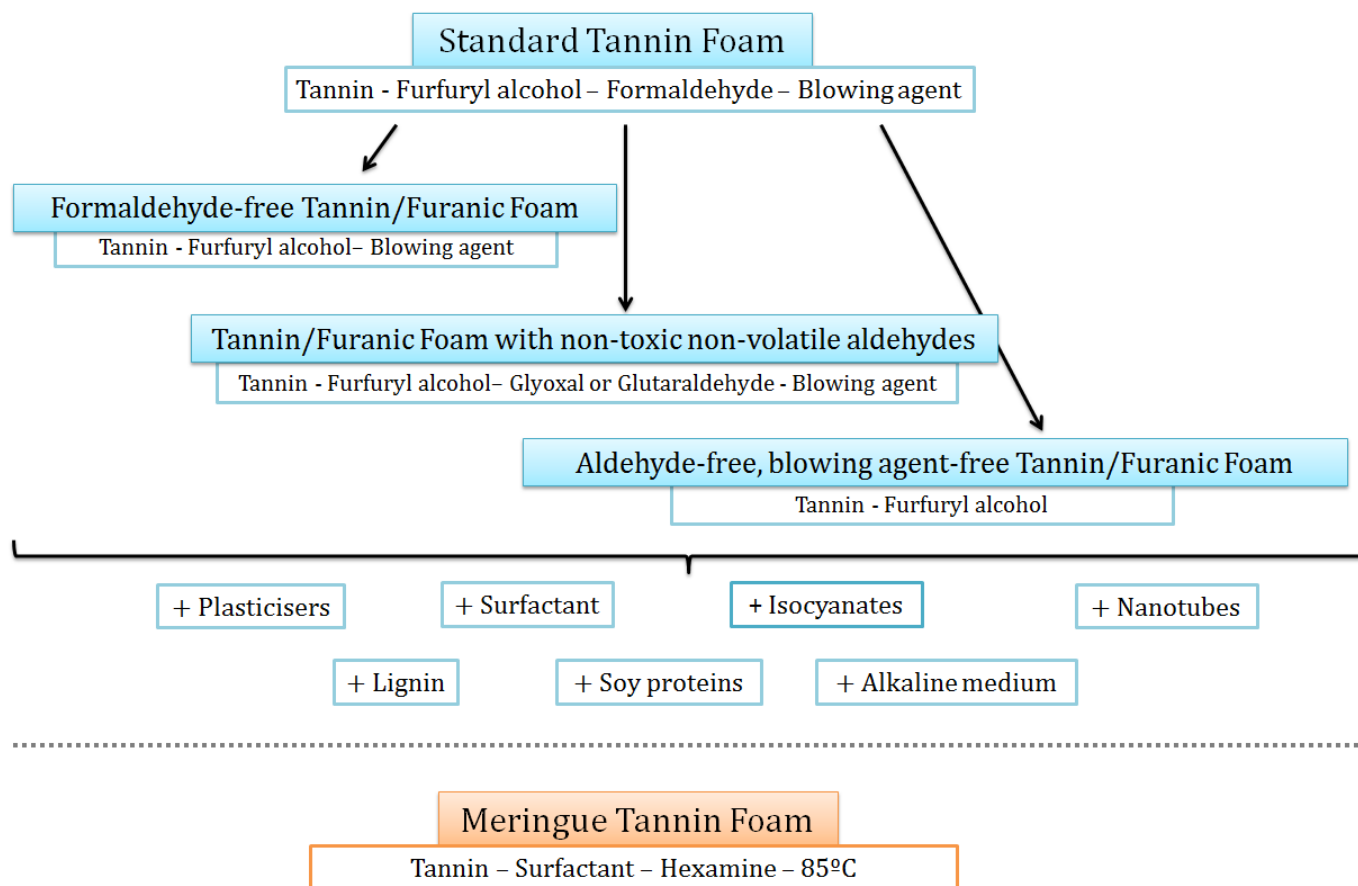


Fig. I-13. Scheme explaining how different tannin-based foam families could be prepared so far.

The first tannin-based foams, called thereafter **Standard Tannin Foams**, were developed by physical foaming using a tannin-furfuryl alcohol-formaldehyde resin (Meikleham and Pizzi, 1994). This kind of foam was prepared as follow: furfuryl alcohol (5.2 g), formaldehyde 37% water solution (3.7 g) and water (3.0 g) were mixed with 15 g of tannin extract under mechanical stirring; when the mixture became homogeneous, diethylether (foaming agent: variable amount between 0.75 and 2.5 g) and then para-toluene-4-sulphonic acid (pTSA, catalyst) 65% water solution (6.0 g) were added and mixed for 10 s. The foam was obtained by exothermic autocondensation of furfuryl alcohol and polycondensation of the polyflavonoid tannin with furfuryl alcohol which induced the increase of the local temperature, thereby boiling the foaming agent and hence expanding the foam. There was also self-condensation of tannin and the reaction of tannin with formaldehyde that allowed a better curing of the foam formed and increased the mechanical strength of the polymer. During expansion, polymerisation of the resin continued

until its complete hardening, which was also accelerated by the induced temperature. Under ambient conditions of pressure and temperature, the foam expanded in less than one minute (Fig. I-14). That kind of formulation has been carefully described in several research works (Meikleham and Pizzi, 1994; Tondi et al., 2009c, 2008).

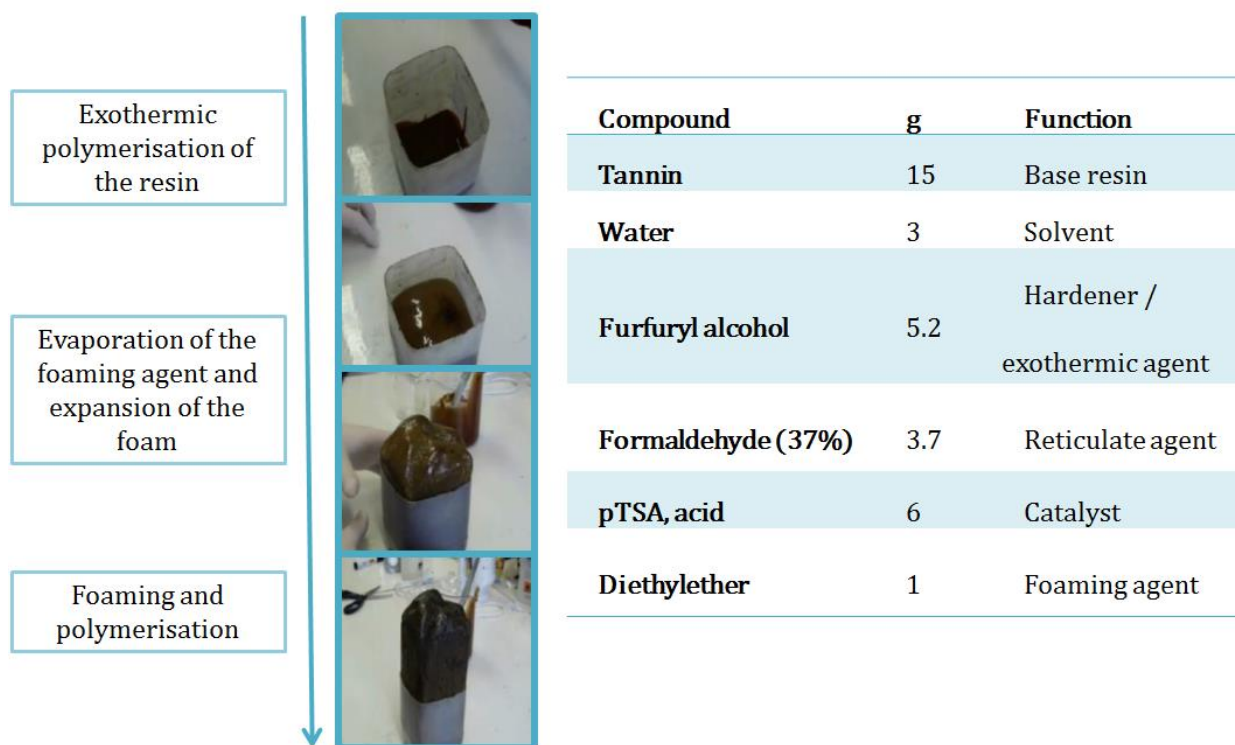


Fig. I-14. Foaming process and composition of a standard tannin foam.

The formaldehyde used in the tannin formulation allows a fast and strong hardening of the material after foaming, however, its volatility and flammability make it a potentially dangerous chemical which might be slowly released into the atmosphere. That motivated the research of tannin foams without formaldehyde. Basso et al (Basso et al., 2011) elaborated pine **tannin/furanic rigid foams without formaldehyde** which presented better thermally insulating properties but lower mechanical resistance under compression than standard tannin foams (Lacoste et al., 2013a).

With the objective of developing formaldehyde-free foam of competitive mechanical properties, a new approach was carried out using non-toxic and non-volatile aldehydes as hardeners: **glyoxal or glutaraldehyde**. It was found that glyoxal could completely substitute

formaldehyde to prepare foams with good properties whereas glutaraldehyde was not so suitable for that purpose because of its lower reactivity with some kinds of tannins (Lacoste et al., 2013b).

The second important step in the improvement of tannin-based foams was the elimination of organic blowing agent in the formulation which was considered essential until that moment to obtain foams. The total removal of such health and environmental threat was carried out for the first time in 2013 (Basso et al., 2013a), although they still contained a little amount of isocyanate which is also dangerous for the health. **Tannin/furanic foams totally free of formaldehyde and blowing agent** were 98% renewable materials foams, thus even more environment-friendly. For getting them, the amount of furfuryl alcohol was increased to amplify the heat release and thereby prevent the formed foam from collapsing due to late curing. Indeed, the hardening depends on the temperature, and if it increases fairly quickly, the resin solidifies faster. They presented equal thermal insulation and fire resistance, as well as similar stress–strain characteristics as those of tannin/furanic foams containing formaldehyde and organic blowing agents.

The addition of small doses of other components in order to lead to new foams with different properties was also carefully studied in the past. On the one hand, the addition of polyethylene glycol 400 (PEG400) or others glycols or glycol ethers as emulsion/dispersion agents eased the mixing of the other components of the formulation by reducing the viscosity of the initial mixture and by allowing a better homogenisation of the temperature within the mixture. Thus, the increase in temperature, the crosslinking and the expansion took place more slowly (Basso et al., 2013a). They also acted as **plasticisers** helping to obtain flexible tannin foams, unlike all other rigid tannin foams prepared before (Li et al., 2012b). Those plasticisers were selected due to their high boiling temperature that avoids their evaporation, coupled to their low toxicity. On the other hand, the addition of small amount of **isocyanates** (Basso et al., 2013a) or multiwalled **carbon nanotubes** (Li et al., 2013) improved the compressive strength and the impact resistance of the tannin/furanic foams.

Finally, one of the last refinements that have been realised in the preparation of tannin/furanic foams was the addition of **surfactant** into the formulation. Surfactants were used in the formulation of foams to reduce the surface energy necessary for bubble stabilisation. It was also observed that during the foaming process the surfactant promoted the expansion. The

incorporation of a non-ionic surfactant led to smaller cells and to a more homogeneous cell size distribution and, moreover, increased the degree of elasticity of the foams (Basso et al., 2015, 2013b).

For all those kinds of tannin-furanic foams it is really necessary to take into account that, when the proportions of these components are varied, the proportion of the rest of the reagents must be carefully adjusted to obtain well-developed, homogeneous foams. Otherwise, the latter can suffer either structural collapse, due to lack of dissipation of the heat generated by the exothermic reaction, or insufficient porosity development. It is also very important to control the environment in which the foam is formed, in particular, the ambient temperature and the mould in which the foam has to expand. These additional parameters can determine the final properties of the material (shape, density, cell size, etc.). Thus, the same formulation can lead to a final foam of low or high density, with consequently more or less mechanical and/or thermal properties, depending on the conditions in which it was formed.

After all those modifications, a new way of producing tannin-based foams was considered in which the objective was to prepare a liquid foam at room temperature through purely mechanical means and, once formed, curing it in an oven at moderate temperature. For curing, hexamethylenetetramine (simply referred to as hexamine) was tried in acid medium as a crosslinker. Previously, only a few trials had been carried out to get foams with the polymerisation of tannin with hexamine, and all of them were made in alkaline conditions (Basso et al., 2014). That new way of producing tannin-based foams is described in detail elsewhere (Szczurek et al., 2014). This method was inspired from the preparation of meringues from egg whites, and the corresponding materials were thus called **Tannin Meringue Foams**. In the present case, liquid and stable foam was obtained from an aqueous solution of tannin to which surfactant, crosslinker and catalyst were added, see Fig. I-15. Such a simple, fast and cost-effective method allowed obtaining, after curing the liquid foam in an oven at 85°C during 24 h, new cellular thermoset materials. These new materials had properties and characteristics which were easy to control, and close to those of more traditional foams.

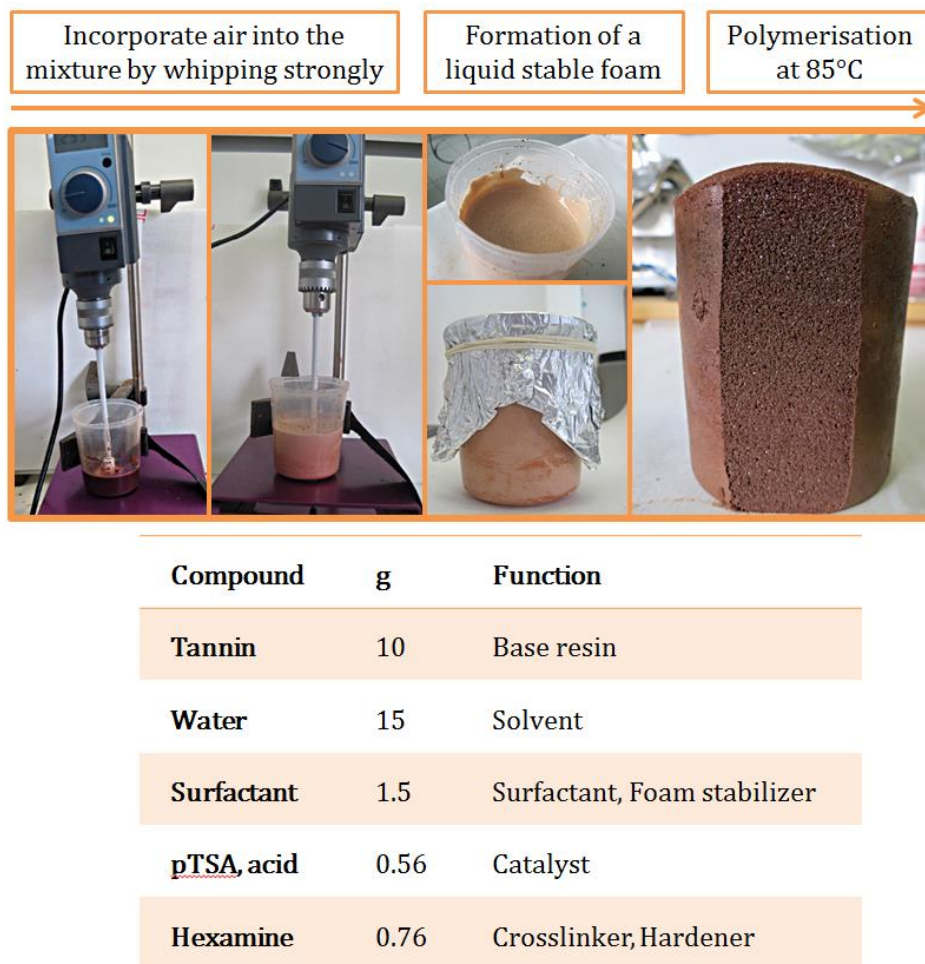


Fig. I-15. Foaming process and composition of a tannin meringue foam.

All the different formulations explained above constitute the base on which different species and families of tannin-based foams can be prepared at present. The nature of the tannin could be successfully changed in those formulations, from mimosa to quebracho and pine tannins, having different chemical structures. Changing the nature of the tannin was not obvious at all since, for example, the reactivity of pine tannin is six to seven times higher than that of mimosa tannin. However, developing new formulations from alternative tannins opened the route to cheaper materials, which can be prepared from a considerably more available resource.

In general, it has been found that foams cannot be made from any formulations and/or under any conditions. Some formulations never give foams because the resin remains in the liquid state, others harden without expanding or too poorly so that they form a too dense material, and there

are even others for which hardening and expansion occur in such chaotic mode that the result is non-homogeneous. Hence the importance of carefully selecting all the components present in the formulation and the conditions under which they are made.

I/3.4. Structure and main physical properties of tannin foams

The macroscopic properties of the foams directly depend on their density and cellular structure in terms of cell morphology (sizes, shapes, distribution and orientation) and inter-connectivity (presence of membranes called windows and sizes of interconnections), as well on the intrinsic properties of the solid and gas of which they are made. The properties of the polymers forming the solid network of the foam condition the mechanical, thermal and electrical properties, among others, of the foams themselves.

At the macroscopic scale, the foam is considered homogeneous and the most representative parameter is the relative density, defined as the ratio of the apparent density (mass/volume of a representative sample) to the density of the solid constituting the solid backbone. Unlike apparent densities, the relative densities of foams of different chemical compositions can be compared with each other. The relative density is related to the porosity. Those parameters are relatively easy to obtain and affect in a global manner all the properties of the foams.

Tannin foams can have a wide range of characteristics depending on the way of foaming and the components used in their formulation. For that reason, it is necessary to characterise the tannin foams in order to better understand their physical properties and to determine their possible application. The characterisation can concern very different quantities such as density, porosity, structure (cell size, tortuosity, anisotropy, etc.), thermal conductivity, fire behaviour, acoustic properties or mechanical properties, for example.

I/3.4.1 Structure

The structure of a foam is defined by several parameters such as total porosity (related to the relative density), cell morphology (dimensions, polydispersity, shapes), mutual arrangement of cells (orientations, anisotropy), cells interconnectivity and structure of struts and membranes.

Tannin foams can be produced in a broad range of density, depending on the method of preparation and their compounds. As for any type of foam, the intrinsic parameters of the resin such as viscosity, reactivity of the components (type of tannins, proportions of reactive hydroxyl groups, molar ratio of tannin / hardener, polymerisation kinetics, surfactants) as well as external parameters such as stirring speed, heating temperature, and type of mould all influence the final density of the foam. Density is a fundamental parameter for tannin foams because the properties of solid foams strongly depend on it.

In standard tannin foams, the density was inversely proportional to the amount of foaming agent. Given that the blowing agent evaporates completely, the volume of bubbles was strictly proportional to the mass it introduced in the formulation (Zhao et al., 2010). In tannin/furanic foams without blowing agent, it was more difficult to control the density with the amount of furfuryl alcohol as the self-condensation of furfuryl alcohol is a parameter that is quite difficult to manage. And on the other hand, tannin-based meringues have bulk densities whose values strongly depend on the initial tannin concentration.

The ranges of density and porosity of tannin foams are very broad. Standard mimosa tannin foams have an average density of 0.055-0.075 g·cm⁻³ (Tondi et al., 2009c) but with the development of new formulations it is possible to produce tannin foams with very low densities close to 0.030 g·cm⁻³ (Basso et al., 2011), very high densities close to 1.3 g·cm⁻³ in foams modified with isocyanates (Li et al., 2012a), and series of foams such as tannin-based meringues that present a broad range of densities of 0.03-0.18 g·cm⁻³ by themselves (Szcurek et al., 2014). In spite of the wide variety of tannin foams, the skeletal density of tannin-based resin is always similar, 1.45 ± 0.05 g·cm⁻³, whatever the formulation (Amaral-Labat et al., 2013b; Szcurek et al., 2014; Tondi and Pizzi, 2009; Zhao et al., 2010).

Scanning electron microscope imaging and mercury porosimetry are two of the most well-known techniques that allow observing the structure of the foams and determining the average size of cells, windows and edges. In tannin foams, the average pore diameter can range from 100 to 1500 µm depending on the formulation. Additional structural and morphological information can also be acquired by 3D X-ray micro-computed tomography that provides an accurate three-dimensional representation of the internal structure of the foams. Such technique has been used to measure total porosity, closed porosity, grain size and tortuosity of different tannin foams in

several works (Basso et al., 2013b; Szczurek et al., 2014). Fig. I-16 shows an example of the structure of a meringue tannin foam.

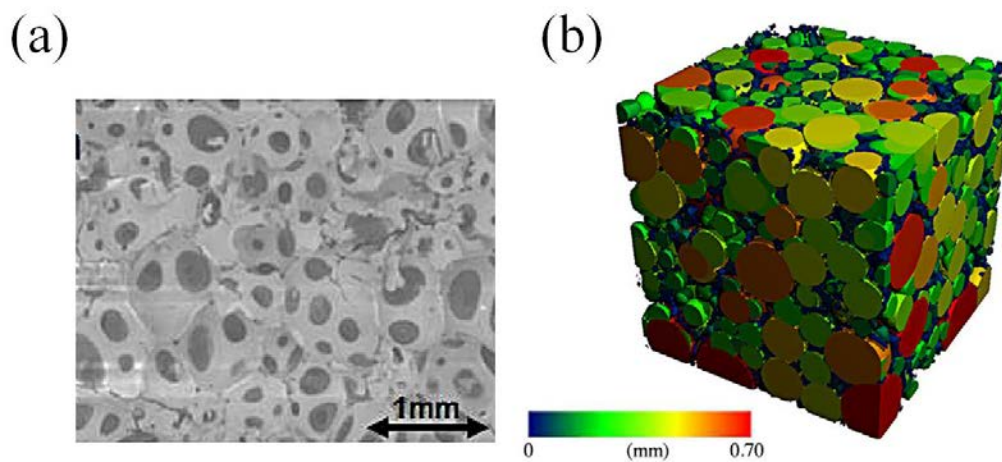


Fig. I-16. Meringue tannin foam: a) a detail of its surface observed by scanning electron microscopy (SEM); b) its complementary image obtained by 3D X-ray micro-computed tomography (the colour coded the size distribution).

The aforementioned techniques can also reveal if there is some inhomogeneity in the foam. Tannin foams obtained by vertical rising normally present some gradient of both density and anisotropy inherent to the foaming process. The anisotropy decrease from the bottom to the top of the foam and the radial changes in cell morphology are negligible (Zhao et al., 2010). Such anisotropy is insignificant in formulations having a little amount of surfactant (tannin/furanic and meringue foams) helping to get more homogeneous structure and bubble size.

I/3.4.2 Mechanical properties

Cellular materials such as tannin-based foams have a very singular mechanical behaviour due to the structure of their porosity. The mechanical properties can be studied in compression, tension, bending or shearing, and in the form of uniaxial or multiaxial stresses. When the foams are used for their mechanical properties, they are generally used for their good compressive strength depending on their density, and especially for their ability to absorb shocks. A foam compression test produces a stress curve as a function of deformation, describing its behaviour in a general way. The foams can show different types of behaviour depending on the nature of the

constituting material: elastomer, elastoplastic and brittle (Gibson and Ashby, 1997). An example of compression curves of tannin foams with different behaviours can be observed in Fig. I-17.

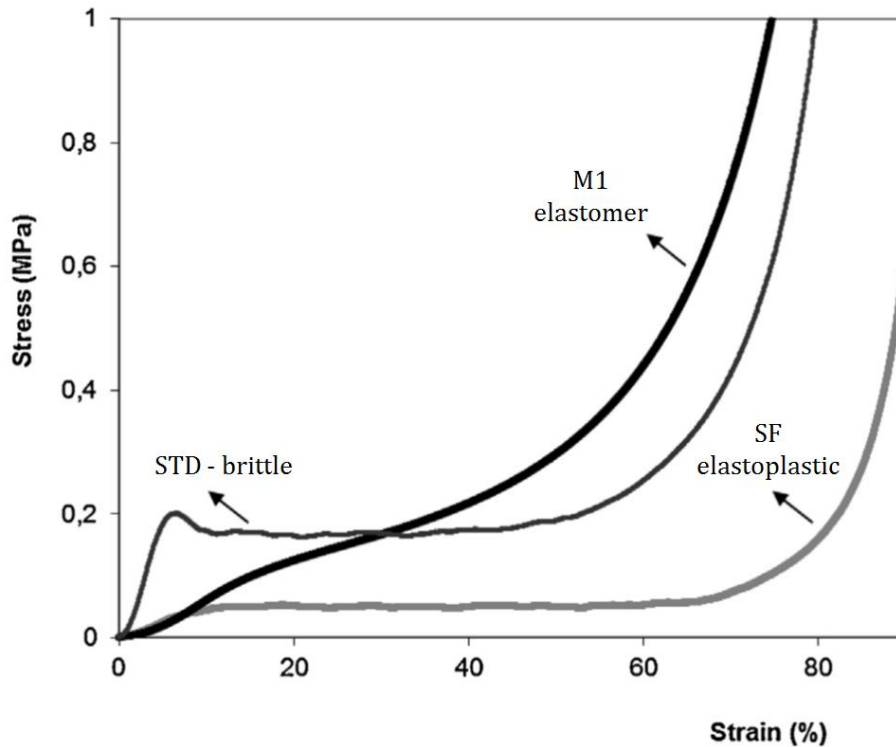


Fig. I-17. Comparative mechanical resistance of a standard foam – STD (with formaldehyde and a blowing agent), a SF foam (without formaldehyde but with a blowing agent) and a foam M1 without formaldehyde and without a blowing agent (Basso et al., 2013a).

The original tannin-based foams, standard tannin foam, present a brittle fracture. However, with the development of new formulations, the new families of tannin-based foams can be less brittle and more elastic. Nowadays, they can present all possible mechanical properties from semi-rigid to purely soft and elastic, allowing their use in a wide range of applications (Celzard et al., 2015).

I/3.4.3 Thermal properties

It has been observed that rigid tannin-based foams are excellent thermal insulation materials that can be used for building insulation. Their thermal conductivity obviously depends on the formulations but can drop within the range 0.038–0.053 W/(m·K) for densities of 0.04–0.16

$\text{g}\cdot\text{cm}^{-3}$ (Celzard et al., 2015; Tondi et al., 2009c). These tannin-based foams can also be used directly as core of sandwich panels (Zhou et al., 2013).

The thermal conductivity of these foams is comparable to that of cork, glass wool or synthetic foams derived from petroleum such as polyurethane and phenolic foams. Indeed, the thermal conductivity of the rigid polyurethane foam is $0.025 \text{ W}/(\text{m}\cdot\text{K})$ (Tseng et al., 1997); of the phenolic foam is between 0.018 and $0.035 \text{ W}/(\text{m}\cdot\text{K})$ (Carvalho et al., 2003) and that of the expanded polystyrene is $0.036 \text{ W}/(\text{m}\cdot\text{K})$.

1/3.4.4 Acoustic properties

Open-celled tannin/furanic foams prepared using two different types of tannins have been tested for acoustic absorption. They were shown to give good sound absorption/acoustic insulation characteristics at medium and high frequencies ($1000 - 4000 \text{ Hz}$) with coefficients of acoustic absorption of $0.85-0.97$. They present lower acoustic absorption coefficient at lower sound frequencies, namely between 250 and 500 Hz , which is a usual behaviour of porous solids, but still presenting respectable coefficient values of $0.40-0.60$ which depends on the open porosity and the thickness. Compared to classical acoustic absorption materials (open-celled polyurethane foam or melamine foam), tannin/furanic foams have the same typical behaviour of lightweight porous materials. The more open is the material structure, the better is its sound absorption. Then the porosity is, as expected, a key parameter in sound absorption for tannin / furanic foams. Their good acoustic performances make them biosourced acoustic absorbing alternatives with respect to those currently available on the market (Lacoste et al., 2015).

1/3.4.5 Fire behaviour

One of the most important and valuable characteristics of tannin foams, apart from being biosourced, is their retardance to fire (Meikleham and Pizzi, 1994). All tannin-based foams analysed so far are flame resistant and self-extinguishing. Such inherent behaviour originates from the chemical structure of the cured resin, based on many aromatic rings of high binding energy, which are able to form a stable and impervious char having a poor thermal conductivity. Moreover, when the foam is exposed to a strong heat flux, its loss of mass is minimal, which

explains its low flammability. Finally, the huge amount of radiant heat that is required for maintaining the combustion explains its high self-extinguishing capacity (Celzard et al., 2011).

The analysed tannin-based rigid foams, without the addition of flame retardants, have higher fire retardance than commercial phenolic foams, epoxy foams and polyurethane foams of similar density. Very long ignition time, around 100s for a heat flux of 50 kW/m², and very low heat release rate are the main features of such cellular organic materials (Celzard et al., 2011; Tondi et al., 2009c). Those values are very interesting if we compare them with some commercial phenolic, epoxy and polyurethane foams with estimated ignition times of 6s, 2s (Aquad et al., 2007) and 4s (Lorenzetti et al., 2012), respectively.

1/3.4.6 Liquid sorption properties

Tannin and phenolic foams have, in general, a very good affinity with water and polar solvents (Tondi and Pizzi, 2009). The properties of the absorption of different liquids (butanol, xylenes, alkanes, sunflowers oil) have been slightly studied with the aim of detecting new applications or limitations in the use of tannin foams. The results showed that water is the liquid most absorbed by tannin-based foams. The absorption of other liquids was not only much weaker than that of water but saturated rapidly, while the water absorption was practically linear until complete pore filling was achieved (Tondi et al., 2009c). These behaviours were essentially explained on the basis of polarity, viscosity and molecular size of the liquids involved. Especially, extremely small, mobile and polar molecules such as H₂O strongly interact with the high number of hydroxyl groups present everywhere on the foam surface, based on flavonoid units (Pasch et al., 2001). Less polar molecules intrude the porosity much slower than water due to the lower interaction with the surface. Besides, bigger molecules probably cannot permeate throughout pore walls and a higher viscosity may also contribute to a lower uptake, just like in the case of oil.

This affinity of tannin foams for water allows them to be used as floral foams (Basso et al., 2016). It was just necessary to use solvent-free, formaldehyde-free foams with a completely open porosity and using alkaline catalysts to ensure that the foams were not too acidic. However, such hydrophilic character is a disadvantage in other applications. It indeed makes them very sensitive to the environmental humidity, compromising their properties of thermal insulation. Thermal

properties such as thermal conductivity, specific heat and thermal diffusivity have been found to increase with the moisture content of the material, leading to much less insulating materials (Abdou and Budaiwi, 2013; Jerman and Černý, 2012; Yu et al., 2015).

1/3.4.7 Bio-adsorbent

Adsorption has been proved to be an efficient process to remove pollutants from aqueous solutions. Tannin-based materials are biosorbents with very promising applications in wastewater treatment that is, nowadays, the spotlight due to the promotion of environmental and economic sustainability. Tannin-based materials, tannin foams among them, seem to have a natural affinity to uptake some heavy metals, dyes, surfactants and pharmaceutical compounds from contaminated waters (Bacelo et al., 2016).

Tannin foams can adsorb up to 2.94 mg Cu²⁺/g and 3.62 mg Pb²⁺/g of foam. The type of tannins used have little influence on the adsorption capacity, but the cellular structure is very significant (Tondi et al., 2009b). In addition, tannin-based foams have a high adsorption capacity of anionic and cationic pollutants such as methylene blue, pharmaceutical products or surfactants, having properties comparable to commercial absorbents (Sánchez-Martín et al., 2013a, 2013b). That effect was all the more marked as the quantity of furfuryl alcohol was minimal. In spite of the interesting results obtained with the type of tannin foams analysed, all the possibilities that these materials have as natural adsorbents have not been deeply evaluated yet.

I/4. Objective of the thesis

Tannin-based foams are promising materials for replacing foams of petrochemical origin because of their biosourced origin, low cost, good thermal insulation performance, excellent fire retardance and high pyrolytic carbon yield. However, they also have some weaknesses that need to be improved in order to be able to compete on the market with insulating and/or fire-resistant commercialised foams such as polyurethane, polystyrene or phenolic foams.

The improve of the mechanical properties of the foams without compromise their thermal conductivity, their water affinity that makes their properties sensible to the ambient conditions, lack of information about the fire properties of the new generation of foams, the information on how the different parameters affect final rigid foams in order to optimise the formulation, etc. are some of the weakness points of the tannin foams that need some research work.

The objectives of this thesis were, therefore, to study the following points with a view to improving them:

Studying the stability of liquid Meringue foams, establishing relationships between the foams' structure and some basic parameters such as the amount of surfactant, stirring time or temperature (key on the crosslinking process that ends with rigid foam) - **Chapter II**

Studying the behaviour of tannin-based foams in the presence of humidity and their modification for turning their hydrophilic character into a more hydrophobic - **Chapter III**

Developing “green” tannin-based foams totally free of blowing agent, formaldehyde or isocyanate, and with valuable and optimal thermal insulation and mechanical properties - **Chapter IV**

Studying the flammability of the new generation foams, analysing the influence of the formulation of the fire properties of the foam and comparing them with other materials with similar application - **Chapter V**

Comparing different method of mechanical characterisation of the foam and calculating new interesting parameters never recorded before on tannin-based foams - **Chapter VI**

I/5. Bibliography

- Abdou, A., Budaiwi, I., 2013. The variation of thermal conductivity of fibrous insulation materials under different levels of moisture content. *Constr. Build. Mater.* 43, 533–544. doi:10.1016/j.conbuildmat.2013.02.058
- Amaral-Labat, G., 2013. Gels poreux biosourcés: production, caractérisation et applications (Thèse de doctorat). Ecole Nationale Supérieure des Technologies et Industries du Bois, Epinal, France.
- Amaral-Labat, G., Gourdon, E., Fierro, V., Pizzi, A., Celzard, A., 2013a. Acoustic properties of cellular vitreous carbon foams. *Carbon* 58, 76–86. doi:10.1016/j.carbon.2013.02.033
- Amaral-Labat, G., Grishechko, L.I., Fierro, V., Kuznetsov, B.N., Pizzi, A., Celzard, A., 2013b. Tannin-based xerogels with distinctive porous structures. *Biomass Bioenergy* 56, 437–445. doi:10.1016/j.biombioe.2013.06.001
- Arbenz, A., Avérous, L., 2015. Chemical modification of tannins to elaborate aromatic biobased macromolecular architectures. *Green Chem.* 17, 2626–2646. doi:10.1039/C5GC00282F
- Auad, M.L., Zhao, L., Shen, H., Nutt, S.R., Sorathia, U., 2007. Flammability properties and mechanical performance of epoxy modified phenolic foams. *J. Appl. Polym. Sci.* 104, 1399–1407. doi:10.1002/app.24405
- Bacelo, H.A.M., Santos, S.C.R., Botelho, C.M.S., 2016. Tannin-based biosorbents for environmental applications – A review. *Chem. Eng. J.* 303, 575–587. doi:10.1016/j.cej.2016.06.044
- Baker, A.K., Ross, C.F., 2014. Wine finish in red wine: The effect of ethanol and tannin concentration. *Food Qual. Prefer.* 38, 65–74. doi:10.1016/j.foodqual.2014.05.014
- Ballerini, A., Despres, A., Pizzi, A., 2005. Non-toxic, zero emission tannin-glyoxal adhesives for wood panels. *Holz Als Roh- Werkst.* 63, 477–478. doi:10.1007/s00107-005-0048-x
- Basso, M.C., Giovando, S., Pizzi, A., Celzard, A., Fierro, V., 2013a. Tannin/furanic foams without blowing agents and formaldehyde. *Ind. Crops Prod.* 49, 17–22. doi:10.1016/j.indcrop.2013.04.043
- Basso, M.C., Giovando, S., Pizzi, A., Lagel, M.C., Celzard, A., 2014. Alkaline Tannin Rigid Foams. *J. Renew. Mater.* 2, 182–185. doi:10.7569/JRM.2013.634137
- Basso, M.C., Lagel, M.-C., Pizzi, A., Celzard, A., Abdalla, S., 2015. First Tools for Tannin-Furanic Foams Design. *Bioresources* 10, 5233–5241.
- Basso, M.C., Li, X., Fierro, V., Pizzi, A., Giovando, S., Celzard, A., 2011. Green, formaldehyde-free, foams for thermal insulation. *Adv. Mater. Lett.* 2, 378–382. doi:10.5185/amlett.2011.4254
- Basso, M.C., Pizzi, A., Al-Marzouki, F., Abdalla, S., 2016. Horticultural/hydroponics and floral natural foams from tannins. *Ind. Crops Prod.* 87, 177–181. doi:10.1016/j.indcrop.2016.04.033
- Basso, M.C., Pizzi, A., Celzard, A., 2013b. Dynamic Monitoring of Tannin-based Foam Preparation: Effects of Surfactant. *Bioresources* 8, 5807–5816.
- Basta, A.H., El-Saied, H., 2003. Furfural production and kinetics of pentosans hydrolysis in corn cobs. *Cellul. Chem. Technol.* 37, 79–94.
- Brecha, R., 2013. Ten Reasons to Take Peak Oil Seriously. *Sustainability* 5, 664–694. doi:10.3390/su5020664

- Carvalho, G. de, Pimenta, J.A., Santos, W.N. dos, Frollini, E., 2003. Phenolic and Lignophenolic Closed Cells Foams: Thermal Conductivity and Other Properties. *Polym.-Plast. Technol. Eng.* 42, 605–626. doi:10.1081/PPT-120023098
- Celzard, A., Fierro, V., Amaral-Labat, G., Pizzi, A., Torero, J., 2011. Flammability assessment of tannin-based cellular materials. *Polym. Degrad. Stab.* 96, 477–482. doi:10.1016/j.polymdegradstab.2011.01.014
- Celzard, A., Szczurek, A., Jana, P., Fierro, V., Basso, M.-C., Bourbigot, S., Stauber, M., Pizzi, A., 2015. Latest progresses in the preparation of tannin-based cellular solids. *J. Cell. Plast.* 51, 89–102. doi:10.1177/0021955X14538273
- Celzard, A., Tondi, G., Lacroix, D., Jeandel, G., Monod, B., Fierro, V., Pizzi, A., 2012. Radiative properties of tannin-based, glasslike, carbon foams. *Carbon* 50, 4102–4113. doi:10.1016/j.carbon.2012.04.058
- Chen, X., Li, H., Luo, H., Qiao, M., 2002. Liquid phase hydrogenation of furfural to furfuryl alcohol over Mo-doped Co-B amorphous alloy catalysts. *Appl. Catal. Gen.* 233, 13–20. doi:10.1016/S0926-860X(02)00127-8
- Choe, J., Kim, M., Kim, J., Lee, D.G., 2016. A microwave foaming method for fabricating glass fiber reinforced phenolic foam. *Compos. Struct.* 152, 239–246. doi:10.1016/j.compstruct.2016.05.044
- Choura, M., Belgacem, N.M., Gandini, A., 1996. Acid-Catalyzed Polycondensation of Furfuryl Alcohol: Mechanisms of Chromophore Formation and Cross-Linking. *Macromolecules* 29, 3839–3850. doi:10.1021/ma951522f
- Cork, S.J., Krockenberger, A.K., 1991. Methods and pitfalls of extracting condensed tannins and other phenolics from plants: Insights from investigations on Eucalyptus leaves. *J. Chem. Ecol.* 17, 123–134. doi:10.1007/BF00994426
- Covington, A.D., 2009. *Tanning Chemistry: The Science of Leather*. Royal Soc Chemistry, Cambridge.
- Dunlop, A.P., Peters, F.N., 1953. *The Furans*. Reinhold Publ. Corp.
- Edward, E., 1970. Oral Compositions Containing Non-Toxic, non-Volatile Aliphatic Aldehyde. US3497590 (A).
- Eller, K., Henkes, E., Rossbacher, R., Höke, H., 2000. Amines, Aliphatic, in: *Ullmann's Encyclopedia of Industrial Chemistry*. Wiley-VCH Verlag GmbH & Co. KGaA.
- Feng, S., Cheng, S., Yuan, Z., Leitch, M., Xu, C. (Charles), 2013. Valorization of bark for chemicals and materials: A review. *Renew. Sustain. Energy Rev.* 26, 560–578. doi:10.1016/j.rser.2013.06.024
- Ferri, M., Bin, S., Vallini, V., Fava, F., Michelini, E., Roda, A., Minnucci, G., Bucchi, G., Tassoni, A., 2016. Recovery of polyphenols from red grape pomace and assessment of their antioxidant and anti-cholesterol activities. *New Biotechnol.* 33, 338–344. doi:10.1016/j.nbt.2015.12.004
- Foo, L.Y., Hemingway, R.W., 1985. Condensed Tannins: Reactions of Model Compounds with Furfuryl Alcohol and Furfuraldehyde. *J. Wood Chem. Technol.* 5, 135–158. doi:10.1080/02773818508085184
- Garnier, S., Pizzi, A., Vorster, O.C., Halasz, L., 2002. Rheology of polyflavonoid tannin-formaldehyde reactions before and after gelling. II. Hardener influence and comparison of different tannins. *J. Appl. Polym. Sci.* 86, 864–871. doi:10.1002/app.10990
- Ge, Z., Tian, W., Zhang, K., Chen, M., Qin, S., Chen, X., Liu, W., 2016. Preparation of Cellulose and Synthesis of 5-Hydroxymethyl Furfural from Agricultural Waste Cottonseed Hull. *Appl. Eng. Agric.* 32, 661–667. doi:10.13031/aea.32.11013

- Gibson, L.J., Ashby, M.F., 1997. *Cellular Solids: Structure and Properties*. Cambridge University Press.
- Gironi, F., Piemonte, V., 2011. Temperature and solvent effects on polyphenol extraction process from chestnut tree wood. *Chem. Eng. Res. Des.* 89, 857–862. doi:10.1016/j.cherd.2010.11.003
- Glé, P., Gourdon, E., Arnaud, L., 2011. Acoustical properties of materials made of vegetable particles with several scales of porosity. *Appl. Acoust.* 72, 249–259. doi:10.1016/j.apacoust.2010.11.003
- Gross, G.G., 1999. 3.20 - Biosynthesis of Hydrolyzable Tannins A2 - Barton, Sir Derek, in: Nakanishi, K., Meth-Cohn, O. (Eds.), *Comprehensive Natural Products Chemistry*. Pergamon, Oxford, pp. 799–826.
- Gross, G.G., Hemingway, R.W., Yoshida, T., 2012. *Plant Polyphenols 2: Chemistry, Biology, Pharmacology, Ecology*. Springer Science & Business Media.
- Harbertson, J.F., Parpinello, G.P., Heymann, H., Downey, M.O., 2012. Impact of exogenous tannin additions on wine chemistry and wine sensory character. *Food Chem.* 131, 999–1008. doi:10.1016/j.foodchem.2011.09.101
- Haslam, E., 1997. Vegetable tannage: Where do the tannins go? *J. Soc. Leather Technol. Chem.* 81, 45–51.
- Hayouni, E.A., Abedrabba, M., Bouix, M., Hamdi, M., 2007. The effects of solvents and extraction method on the phenolic contents and biological activities in vitro of Tunisian *Quercus coccifera* L. and *Juniperus phoenicea* L. fruit extracts. *Food Chem.* 105, 1126–1134. doi:10.1016/j.foodchem.2007.02.010
- Hemingway, R.W., Laks, P.E., 2012. *Plant Polyphenols: Synthesis, Properties, Significance*. Springer Science & Business Media.
- Henke, A., Dickhoefer, U., Westreicher-Kristen, E., Knappstein, K., Molkentin, J., Hasler, M., Susenbeth, A., 2017. Effect of dietary Quebracho tannin extract on feed intake, digestibility, excretion of urinary purine derivatives and milk production in dairy cows. *Arch. Anim. Nutr.* 71, 37–53. doi:10.1080/1745039X.2016.1250541
- Hernes, P.J., Benner, R., Cowie, G.L., Goñi, M.A., Bergamaschi, B.A., Hedges, J.I., 2001. Tannin diagenesis in mangrove leaves from a tropical estuary: a novel molecular approach. *Geochim. Cosmochim. Acta* 65, 3109–3122. doi:10.1016/S0016-7037(01)00641-X
- Hu, L., Zhao, G., Hao, W., Tang, X., Sun, Y., Lin, L., Liu, S., 2012. Catalytic conversion of biomass-derived carbohydrates into fuels and chemicals via furanic aldehydes. *Rsc Adv.* 2, 11184–11206. doi:10.1039/c2ra21811a
- IARC CLASSIFIES FORMALDEHYDE AS CARCINOGENIC TO HUMANS [WWW Document], 2004. . Int. Agency Res. Cancer - World Health Organization. URL <https://www.iarc.fr/en/media-centre/pr/2004/pr153.html>
- Jana, P., Fierro, V., Pizzi, A., Celzard, A., 2014. Biomass-derived, thermally conducting, carbon foams for seasonal thermal storage. *Biomass Bioenergy* 67, 312–318. doi:10.1016/j.biombioe.2014.04.031
- Jerman, M., Černý, R., 2012. Effect of moisture content on heat and moisture transport and storage properties of thermal insulation materials. *Energy Build.* 53, 39–46. doi:10.1016/j.enbuild.2012.07.002
- Kamoun, C., Pizzi, A., Zanetti, M., 2003. Upgrading melamine-urea-formaldehyde polycondensation resins with buffering additives. I. The effect of hexamine sulfate and its limits. *J. Appl. Polym. Sci.* 90, 203–214. doi:10.1002/app.12634

- Kandola, B.K., Ebdon, J.R., Chowdhury, K.P., 2015. Flame Retardance and Physical Properties of Novel Cured Blends of Unsaturated Polyester and Furan Resins. *Polymers* 7, 298–315. doi:10.3390/polym7020298
- Khanbabaee, K., Ree, T. van, 2001. Tannins: Classification and Definition. *Nat. Prod. Rep.* 18, 641–649. doi:10.1039/B101061L
- Kumar, G.S.V., Mukherjee, M., Garcia-Moreno, F., Banhart, J., 2013. Reduced-Pressure Foaming of Aluminum Alloys. *Metall. Mater. Trans. A* 44, 419–426. doi:10.1007/s11661-012-1398-8
- Lacoste, C., Basso, M.-C., Pizzi, A., Celzard, A., Ella Ebang, E., Gallon, N., Charrier, B., 2015. Pine (*P. pinaster*) and quebracho (*S. lorentzii*) tannin-based foams as green acoustic absorbers. *Ind. Crops Prod.* 67, 70–73. doi:10.1016/j.indcrop.2014.12.018
- Lacoste, C., Basso, M.C., Pizzi, A., Laborie, M.-P., Celzard, A., Fierro, V., 2013a. Pine tannin-based rigid foams: Mechanical and thermal properties. *Ind. Crops Prod.* 43, 245–250. doi:10.1016/j.indcrop.2012.07.039
- Lacoste, C., Basso, M.C., Pizzi, A., Laborie, M.-P., Garcia, D., Celzard, A., 2013b. Bioresourced pine tannin/furanic foams with glyoxal and glutaraldehyde. *Ind. Crops Prod.* 45, 401–405. doi:10.1016/j.indcrop.2012.12.032
- Lee, S.-T., Ramesh, N.S., 2004. *Polymeric Foams: Mechanisms and Materials*. CRC Press.
- Letellier, M., Macutkevic, J., Paddubskaya, A., Plyushch, A., Kuzhir, P., Ivanov, M., Banys, J., Pizzi, A., Fierro, V., Celzard, A., 2015. Tannin-Based Carbon Foams for Electromagnetic Applications. *Ieee Trans. Electromagn. Compat.* 57, 989–995. doi:10.1109/TEMC.2015.2430370
- Lin, D., Xiao, M., Zhao, J., Li, Z., Xing, B., Li, X., Kong, M., Li, L., Zhang, Q., Liu, Y., Chen, H., Qin, W., Wu, H., Chen, S., 2016. An Overview of Plant Phenolic Compounds and Their Importance in Human Nutrition and Management of Type 2 Diabetes. *Molecules* 21, 1374. doi:10.3390/molecules21101374
- Li, X., Basso, M.C., Fierro, V., Pizzi, A., Celzard, A., 2012a. Chemical Modification of Tannin/Furanic Rigid Foams by Isocyanates and Polyurethanes. *Maderas-Cienc. Tecnol.* 14, 257–265. doi:10.4067/S0718-221X2012005000001
- Li, X., Pizzi, A., Cangemi, M., Fierro, V., Celzard, A., 2012b. Flexible natural tannin-based and protein-based biosourced foams. *Ind. Crops Prod.* 37, 389–393. doi:10.1016/j.indcrop.2011.12.037
- Li, X., Srivastava, V.K., Pizzi, A., Celzard, A., Leban, J., 2013. Nanotube-reinforced tannin/furanic rigid foams. *Ind. Crops Prod.* 43, 636–639. doi:10.1016/j.indcrop.2012.08.008
- Lorenzetti, A., Modesti, M., Gallo, E., Schartel, B., Besco, S., Roso, M., 2012. Synthesis of phosphinated polyurethane foams with improved fire behaviour. *Polym. Degrad. Stab.* 97, 2364–2369. doi:10.1016/j.polymdegradstab.2012.07.026
- Luo, C., Grigsby, W.J., Edmonds, N.R., Al-Hakkak, J., 2013. Vegetable oil thermosets reinforced by tannin-lipid formulations. *Acta Biomater.* 9, 5226–5233. doi:10.1016/j.actbio.2012.08.048
- Matturro, G., Danesi, P., Festuccia, A., Mustacchi, C., 2006. Process and plant to extract and concentrate tannins from wood and from other natural products. WO1999021634 A1.
- Meikleham, N.E., Pizzi, A., 1994. Acid-and alkali-catalyzed tannin-based rigid foams. *J. Appl. Polym. Sci.* 53, 1547–1556.
- Meikleham, N.E., Pizzi, A., Stephanou, A., 1994. Induced accelerated autocondensation of polyflavonoid tannins for phenolic polycondensates. I. ¹³C-NMR, ²⁹Si-NMR, X-ray, and

- polarimetry studies and mechanism. *J. Appl. Polym. Sci.* 54, 1827–1845. doi:10.1002/app.1994.070541206
- Merle, J., Birot, M., Deleuze, H., Mitterer, C., Carré, H., Bouhtoury, F.C.-E., 2016. New biobased foams from wood byproducts. *Mater. Des.* 91, 186–192. doi:10.1016/j.matdes.2015.11.076
- Minogue, E., 2000. An in-situ study of the nucleation process of polyurethane rigid foam formation (doctoral). Dublin City University. School of Chemical Sciences.
- Nagaraja, B.M., Siva Kumar, V., Shasikala, V., Padmasri, A.H., Sreedhar, B., David Raju, B., Rama Rao, K.S., 2003. A highly efficient Cu/MgO catalyst for vapour phase hydrogenation of furfural to furfuryl alcohol. *Catal. Commun.* 4, 287–293. doi:10.1016/S1566-7367(03)00060-8
- Nicollin, A., Zhou, X., Pizzi, A., Grigsby, W., Rode, K., Delmotte, L., 2013. MALDI-TOF and ¹³C NMR analysis of a renewable resource additive—Thermoplastic acetylated tannins. *Ind. Crops Prod.* 49, 851–857. doi:10.1016/j.indcrop.2013.06.013
- Pasch, H., Pizzi, A., Rode, K., 2001. MALDI-TOF mass spectrometry of polyflavonoid tannins. *Polymer* 42, 7531–7539. doi:10.1016/S0032-3861(01)00216-6
- Peña, C., Caba, K. de la, Retegi, A., Ocando, C., Labidi, J., Echeverria, J.M., Mondragon, I., 2009. Mimosa and chestnut tannin extracts reacted with hexamine in solution. *J. Therm. Anal. Calorim.* 96, 515. doi:10.1007/s10973-007-8352-9
- Pichelin, F., Kamoun, C., Pizzi, A., 1999. Hexamine hardener behaviour: effects on wood glueing, tannin and other wood adhesives. *Holz Als Roh- Werkst.* 57, 305–317. doi:10.1007/s001070050349
- Pichelin, F., Nakatani, M., Pizzi, A., Wieland, S., Despres, A., Rigolet, S., 2006. Structural beams from thick wood panels bonded industrially with formaldehyde-free tannin adhesives. *For. Prod. J.* 56, 31–36.
- Pisitsak, P., Hutakamol, J., Thongcharoen, R., Phokaew, P., Kanjanawan, K., Saksang, N., 2016. Improving the dyeability of cotton with tannin-rich natural dye through pretreatment with whey protein isolate. *Ind. Crops Prod.* 79, 47–56. doi:10.1016/j.indcrop.2015.10.043
- Pizzi, A., 1989. *Wood Adhesives: Chemistry and Technology---Volume 2.* CRC Press.
- Pizzi, A., 1982. Condensed tannins for adhesives. *Ind. Eng. Chem. Prod. Res. Dev.* 21, 359–369. doi:10.1021/i300007a005
- Pizzi, A., 1979. Sulfited Tannins for Exterior Wood Adhesives. *Colloid Polym. Sci.* 257, 37–40. doi:10.1007/BF01539014
- Pizzi, A. (Antonio), New York : M. Dekker, c1994. *Advanced wood adhesives technology.* M. Dekker, New York.
- Pizzi, A., Meikleham, N., Dombo, B., Roll, W., 1995. Autocondensation-based, zero-emission, tannin adhesives for particleboard. *Holz Als Roh- Werkst.* 53, 201–204. doi:10.1007/BF02716424
- Pizzi, A., Merlin, M., 1981. A new class of tannin adhesives for exterior particleboard. *Int. J. Adhes. Adhes.* 1, 261–264. doi:10.1016/0143-7496(81)90075-0
- Pizzi, A., Mittal, K.L., 2003. *Handbook of Adhesive Technology, Revised and Expanded.* CRC Press.
- Pizzi, A., Tondi, G., Pasch, H., Celzard, A., 2008. Matrix-assisted laser desorption/ionization time-of-flight structure determination of complex thermoset networks: Polyflavonoid tannin–furanic rigid foams. *J. Appl. Polym. Sci.* 110, 1451–1456. doi:10.1002/app.28545
- Publication: WEO-2016 Special Report Energy and Air Pollution, 2016. . International Energy Agency.

- Rossouw, D. du T., Pizzi, A., McGillivray, G., 1980. The kinetics of condensation of phenolic polyflavonoid tannins with aldehydes. *J. Polym. Sci. Polym. Chem. Ed.* 18, 3323–3343. doi:10.1002/pol.1980.170181201
- Roux, D.G., Dannel, Ferreira, Hundt, Hans K. L., Malan, Elfranco, 1975. Structure, stereochemistry, and reactivity of natural condensed tannins as basis for their extended industrial application, in: *Applied Polymer Symposia. Presented at the Proc. Cellul. Conf., 8th*, pp. 335–353.
- Sánchez-Martín, J., Beltrán-Heredia, J., Delgado-Regaña, A., Rodríguez-González, M.A., Rubio-Alonso, F., 2013a. Adsorbent tannin foams: New and complementary applications in wastewater treatment. *Chem. Eng. J.* 228, 575–582. doi:10.1016/j.cej.2013.05.009
- Sánchez-Martín, J., Beltrán-Heredia, J., Delgado-Regaña, A., Rodríguez-González, M.A., Rubio-Alonso, F., 2013b. Optimization of tannin rigid foam as adsorbents for wastewater treatment. *Ind. Crops Prod.* 49, 507–514. doi:10.1016/j.indcrop.2013.05.029
- Sealyfisher, V., Pizzi, A., 1992. Increased Pine Tannins Extraction and Wood Adhesives Development by Phlobaphenes Minimization. *Holz Als Roh- Werkst.* 50, 212–220. doi:10.1007/BF02663290
- Stojiljkovic, D., Arsic, I., Tadic, V., 2016. Extracts of wild apple fruit (*Malus sylvestris* (L.) Mill., Rosaceae) as a source of antioxidant substances for use in production of nutraceuticals and cosmeceuticals. *Ind. Crops Prod.* 80, 165–176. doi:10.1016/j.indcrop.2015.11.023
- Stokke, D.D., Wu, Q., Han, G., 2013. Adhesives Used to Bond Wood and Lignocellulosic Composites, in: *Introduction to Wood and Natural Fiber Composites*. John Wiley & Sons Ltd, pp. 169–207.
- Szczurek, A., 2011. Nouveaux gels organiques et carbonés dérivés de composés phénoliques naturels et synthétiques (Thèse de doctorat). Institut Jean Lamour, Nancy ; Vandoeuvre-lès-Nancy ; Metz, France.
- Szczurek, A., Amaral-Labat, G., Fierro, V., Pizzi, A., Masson, E., Celzard, A., 2011. The use of tannin to prepare carbon gels. Part I: Carbon aerogels. *Carbon* 49, 2773–2784. doi:10.1016/j.carbon.2011.03.007
- Szczurek, A., Fierro, V., Pizzi, A., Stauber, M., Celzard, A., 2014. A new method for preparing tannin-based foams. *Ind. Crops Prod.* 54, 40–53. doi:10.1016/j.indcrop.2014.01.012
- Szczurek, A., Fierro, V., Pizzi, A., Stauber, M., Celzard, A., 2013. Carbon meringues derived from flavonoid tannins. *Carbon* 65, 214–227. doi:10.1016/j.carbon.2013.08.017
- Szczurek, A., Martinez de Yuso, A., Fierro, V., Pizzi, A., Celzard, A., 2015. Tannin-based monoliths from emulsion-templating. *Mater. Des.* 79, 115–126. doi:10.1016/j.matdes.2015.04.020
- Thomson, S.W., 1887. LXIII. On the division of space with minimum partitional area. *Philos. Mag. Ser. 5* 24, 503–514. doi:10.1080/14786448708628135
- Tondi, G., Fierro, V., Pizzi, A., Celzard, A., 2009a. Tannin-based carbon foams. *Carbon* 47, 1480–1492. doi:10.1016/j.carbon.2009.01.041
- Tondi, G., Oo, C.W., Pizzi, A., Trosa, A., Thevenon, M.F., 2009b. Metal adsorption of tannin based rigid foams. *Ind. Crops Prod.* 29, 336–340. doi:10.1016/j.indcrop.2008.06.006
- Tondi, G., Pizzi, A., 2009. Tannin-based rigid foams: Characterization and modification. *Ind. Crops Prod.* 29, 356–363. doi:10.1016/j.indcrop.2008.07.003
- Tondi, G., Pizzi, A., Pasch, H., Celzard, A., Rode, K., 2008. MALDI-ToF investigation of furanic polymer foams before and after carbonization: Aromatic rearrangement and surviving furanic structures. *Eur. Polym. J.* 44, 2938–2943. doi:10.1016/j.eurpolymj.2008.06.029

- Tondi, G., Zhao, W., Pizzi, A., Du, G., Fierro, V., Celzard, A., 2009c. Tannin-based rigid foams: A survey of chemical and physical properties. *Bioresour. Technol.* 100, 5162–5169. doi:10.1016/j.biortech.2009.05.055
- Tseng, C., Yamaguchi, M., Ohmori, T., 1997. Thermal conductivity of polyurethane foams from room temperature to 20 K. *Cryogenics* 37, 305–312. doi:10.1016/S0011-2275(97)00023-4
- Weaire, D., Phelan, R., 1994. A counter-example to Kelvin's conjecture on minimal surfaces. *Philos. Mag. Lett.* 69, 107–110. doi:10.1080/09500839408241577
- Yang, H.-S., Kim, D.-J., Kim, H.-J., 2003. Rice straw–wood particle composite for sound absorbing wooden construction materials. *Bioresour. Technol.* 86, 117–121. doi:10.1016/S0960-8524(02)00163-3
- Yang, L., Jiang, J.-G., Li, W.-F., Chen, J., Wang, D.-Y., Zhu, L., 2009. Optimum extraction Process of polyphenols from the bark of *Phyllanthus emblica* L. based on the response surface methodology. *J. Sep. Sci.* 32, 1437–1444. doi:10.1002/jssc.200800744
- Yu, D.U., Shrestha, B.L., Baik, O.D., 2015. Thermal conductivity, specific heat, thermal diffusivity, and emissivity of stored canola seeds with their temperature and moisture content. *J. Food Eng.* 165, 156–165. doi:10.1016/j.jfoodeng.2015.05.012
- Zhao, W., Pizzi, A., Fierro, V., Du, G., Celzard, A., 2010. Effect of composition and processing parameters on the characteristics of tannin-based rigid foams. Part I: Cell structure. *Mater. Chem. Phys.* 122, 175–182. doi:10.1016/j.matchemphys.2010.02.062
- Zhou, X., Pizzi, A., Sauget, A., Nicollin, A., Li, X., Celzard, A., Rode, K., Pasch, H., 2013. Lightweight tannin foam/composites sandwich panels and the coldset tannin adhesive to assemble them. *Ind. Crops Prod.* 43, 255–260. doi:10.1016/j.indcrop.2012.07.020

Chapter II: Stability analysis and optimisation of meringue tannin-based foams

II/1. Introduction

Tannin-based foams were formerly obtained by physical, chemical, or mixed physical-chemical foaming, until a new simple way was suggested in 2014 (Szczurek et al., 2014) as introduced in Chapter I. They were named **Meringue Tannin Foams**. This new method simply consists in whipping until stiff an aqueous solution of tannin, crosslinker and surfactant, and polymerising the resultant froth in an oven. Structural, mechanical and thermal characterisation evidenced that these new rigid foams present features similar to those made by conventional foaming from self-blowing formulations. This finding turns this formulation into one of the most promising ones until now, but it is also among the most unknown and therefore deserves further researches.

So far, all published works dealing with those tannin-based foams mainly focused on the properties and performances of the final rigid materials, whether in the form of thermoset polymer foams or derived carbon foams (Szczurek et al., 2014, 2013a, 2013b), but studies of the precursor liquid foams were never carried out. Such studies are very important especially in this kind of foams where the rigid foam is created by the polymerisation of a formerly liquid foam, unlike other formulations for which foaming and crosslinking take place almost at the same time. For this reason, a better and systematic understanding of the stability of liquid tannin-based foams and of the polymerisation processes by which those liquid foams harden before they can collapse or destabilise is required, with the aim of optimising the formulations, controlling their structure and *in fine* developing new materials.

Therefore, the objective of the present work was to provide information on how meringue liquid foams evolve with time and to see whether some relationships can be established between the foams' structure and some basic parameters such as the amount of surfactant, stirring time or temperature. Especially, the temperature is a crucial parameter to be investigated because, in addition to its major effect on the liquid foam stability, it triggers the crosslinking process that ends with rigid foam.

Over the years, several methods have been employed to measure the stability of liquid foams. Some methods are based, for example, on volumetric determinations such as the half-life of the foam, i.e., the time required for reducing the foam volume to half of its original value (Dickinson

and Izgi, 1996), on electrical conductivity measurements (Kato et al., 1983), or on image analysis (Guillerme et al., 1993). However, most of these methods only provide partial information, so that combining several techniques is required (Lioumbas et al., 2015; Wang et al., 2016a). Furthermore, most of the time, none is really appropriate to the case of very stable and/or opaque liquid foams as tannin-based foams can be. Moreover, the destabilisation of liquid foam may occur from the combination of different phenomena such as liquid drainage, gas diffusion (coarsening), coalescence, creaming and/or sedimentation, most of them being coupled with each other, and hence these phenomena can be very difficult to separate (Carrier and Colin, 2003; Vera and Durian, 2002; Wang et al., 2016b).

In the present study, the stability of tannin-based liquid foams has been determined using a recently developed optical analyser (Turbiscan Tower from Formulaction, L'Union, France). It is based on a light-scattering detection method which has been successfully used to study the stability of emulsions (Choi et al., 2014; Degrand et al., 2016; Palazolo et al., 2005), foams (Martínez-Padilla et al., 2015, 2014; Rouimi et al., 2005; Sceni and Wagner, 2007) and concentrated dispersions (Goscianska et al., 2016; Li et al., 2008; Mengual et al., 1999). This method allows acquiring full information on the whole process of foam destabilisation through the simultaneous detection of all phenomena that may happen in any colloidal system, e.g. particle migration (creaming, sedimentation) and/or changes of particle size (coalescence, coarsening). The main advantage of such kind of optical analysis is its ability to detect these phenomena much earlier and more precisely than by naked eye, especially in the case of concentrated and opaque systems such as tannin-based foams. Moreover, it is a non-destructive method, and no sample dilution is needed which allows the direct measurement of the tannin-based liquid foam.

Herein, a useful contribution to the multiple light-scattering detection analysis is offered. Not only the stability of tannin-based liquid foams was investigated, but also was the formation of derived rigid foams through tests carried out at different temperatures. To the best of our knowledge, there are no other studies so far having applied this kind of optical analysis to foams heated at different polymerisation temperatures. Only a few studies have reported the changes of structure of suspensions (Dudášová et al., 2009; Wisniewska, 2010) and emulsions (Xu et al., 2013) as a function of temperature, but no reaction took place in these systems.

II/2. Experimental

II/2.1. Foam preparation

Meringue tannin-based liquid foams were prepared by mechanical whipping of aqueous solutions of tannin, crosslinker (unless otherwise specified), catalyst and surfactant, according to the method detailed in Chapter I and elsewhere (Szcurek et al., 2014). Tannin is the main component of the foam and the type of tannin used for the preparation of the foam is very important. In this case, raw Mimosa bark extract, known as FINTAN OP on the market and kindly supplied by company Silva Team (San Michele Mondovi, Italy), was used. Briefly, the industrial extraction process of this tannin was carried out as follow: fresh Mimosa bark (*Acacia Mearnsii*) was leached in a sodium bisulphite aqueous solution at 70°C, the resultant solutions were concentrated and, then, spray-dried to yield a light-brown powder containing 80–82 wt. % of phenolic flavonoid materials, 4–6 wt. % of water, 1 wt. % of amino acids and other components such as monomeric and oligomeric carbohydrates consisting of broken pieces of hemicellulose. The phenolic content was a mixture of 70% of prorobinetinidin and 25% of profisetinidin, generally composed of two up to ten flavonoid units to produce tannin of a average degree of polymerization of 4-5 (Pizzi, New York : M. Dekker, c1994).

In a typical experiment, 20 g of tannin were carefully dissolved in 30 g of lab-made bi-distilled water until a homogeneous brown solution was obtained. Subsequently, 1.42 g of hexamethylenetetramine (hexamine) in powder and 1.12 g of solid para-toluene sulphonic acid (pTSA), both supplied by Merck, were added as crosslinker and polymerisation catalyst, respectively, to the tannin solution. The blend was then stirred at 300 rpm for 10 min with a digital mixer equipped with a three-bladed Teflon-lined stirring rod. In the next step, different amounts of non-ionic surfactant, a polyethylene sorbitol ester called Tween 80® and supplied by Sigma Aldrich, ranging from 1 to 5 g, were added and then the rotation speed of the blade was increased to 2000 rpm to start the frothing process (Fig. II-1). Various whipping times were used in order to incorporate different fractions of air in the liquid and hence to obtain foams having different densities. The whole process took place at room temperature, and the temperature of the foam did not increase during whipping.



Fig. II-1. Preparation of a liquid meringue tannin-based foam.

Each sample was identified by its amount of surfactant, whipping time and temperature of stability assay. For instance, the sample called 3g-20min-25°C corresponds to a tannin-based liquid formulation prepared as explained above, using 3 g of surfactant whose addition was followed by whipping for 20 minutes at 2000 rpm and by stability analysis in the device at 25°C. If the sample needs any other additional information, the latter was added after the temperature in the label, e.g. 3g-20min-25°C-without hexamine to clarify that the foam did not contain hexamine.

II/2.2. Foam capacity

The foaming capacity or volume fraction of air, θ_{air} (%), was determined immediately at the end of the frothing step and calculated from Eq. (II-1), where V_{foam} is the final volume reached at the end of the stirring time, and V_{liquid} is the initial volume of the liquid resin (~ 40 mL).

$$\theta_{air} = \frac{V_{foam} - V_{liquid}}{V_{foam}} \times 100 \quad (\text{II-1})$$

For measuring its volume, the liquid foam was prepared in a graduated glassware beaker.

II/2.3. Foam stability

II/2.3.1 Basics of the optical analyser

Foam stability was determined using the Turbiscan Tower optical analyser (Formulation, France). Each liquid foam prepared as detailed above was transferred immediately after whipping into a special sample holder, a cylindrical glass vial of height and internal diameter of about 55 and 25 mm, respectively, open at both ends (see Fig. II-2(a)). The cylindrical glass was used as a “cookie cutter” so that no effect on foam’s structure was expected, nor was actually observed. It was, therefore, dipped for about 4 cm into the fresh, thick and viscous liquid foam, and then quickly closed at both ends (Fig. II-2(b)). The exterior of the tube was carefully cleaned before inserting the vial in the analyser, previously conditioned at a desired, fixed temperature.

The stability of the foams was analysed based on transmission (T) and backscattering (BS) profiles as responses to pulses applied by a near-infrared ($\lambda = 850$ nm) laser diode. The setup works as follows, see Fig. II-2(c). After the emitted photons are scattered many times by objects in suspension (here bubbles), the T detector receives the light emerging out of the foam, i.e., at 180° from the incident beam, and the BS detector receives the light scattered backwards at 45° from the incident beam. The transmitted and backscattered light intensities are measured as a function of time along the full height of the sample by scanning it up-and-down, and the corresponding profiles are represented graphically. In the present case, the samples were opaque all over the experiments and, therefore, only BS data were analysed with the Turbiscan’s software. The mobile detection head scanned the sample tube along its vertical axis every 2 min during 24 h. For each scan, T (negligible in our case) and BS data were acquired every $20 \mu\text{m}$ along sample’s height.

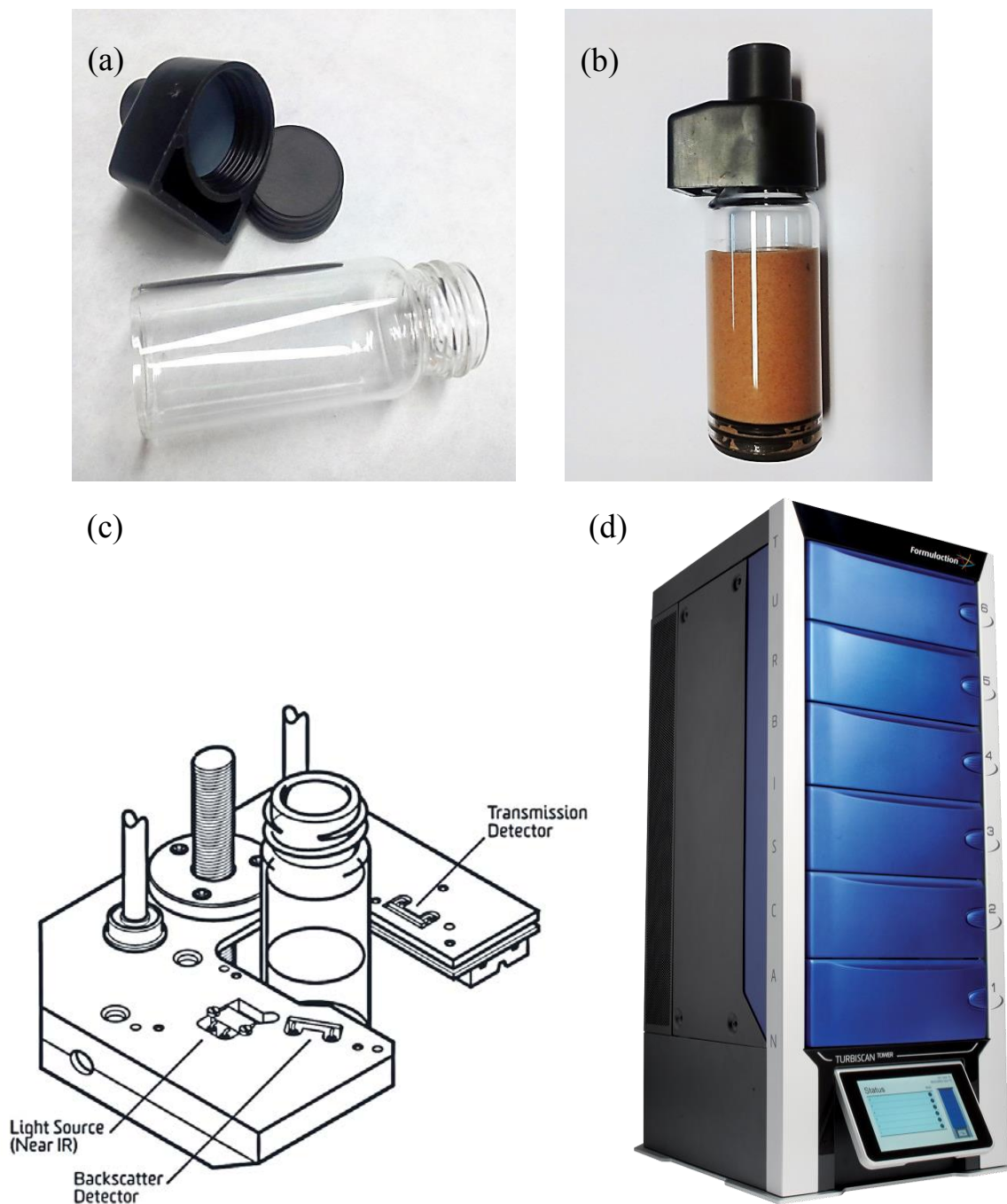


Fig. II-2. Views of the Turbiscan setup: (a) open, empty sample holder; (b) liquid tannin-based foam in the closed sample holder; (c) scheme of the sample environment in the Turbiscan device, showing light source and detectors; (d) Turbiscan Tower analyser, admitting up to 6 samples.

From the backscattered (BS) profiles, Turbiscan's software allows monitoring the average size of the air bubbles as a function of time, provided that the refractive indexes of both continuous and dispersed phases, as well as the volume fraction of air, are known. The calculation is based

on the direct relationship between the BS value and the photon mean free path throughout the foam which, in turn, depends on both gas volume fraction and bubble mean diameter (Mengual et al., 1999). For the calculation of the refractive index of the continuous phase, a solution of tannin, pTSA, hexamine and surfactant in water, with or without hexamine, was investigated with an Abbe refractometer (Carl Zeiss 22394, Germany). After the measurements, which led to the same value of 1.49 for the index of the continuous phase with and without hexamine, the index of the dispersed phase (air) was fixed at 1.00. Despite the difficulty of obtaining precise values for the diameter of bubbles in foams within which various phenomena of destabilisation may take place, including sedimentation, it has been proved that this kind of optical analysis is able to give information about how the average bubble diameter of liquid foams changes with time, the values of which are in good agreement with results from microscopy studies (Rouimi et al., 2005).

II/2.3.2 Assessment of foams' destabilisation phenomena

For better detecting the various destabilisation phenomena that may occur in the present liquid meringue foams as a function of time, the BS profiles were analysed in Delta (Δ) mode. In this mode, one of the profiles (by default, the very first one) is used as a reference corresponding to the initial state of the foam. This profile was then subtracted to all the other ones, thus emphasising the changes. When some destabilisation phenomenon takes place in the foam, the delta backscattering (Δ BS) varies along the height of the foam but also as a function of time. If the foam was completely stable, no change of Δ BS would be observed.

The main instabilities that can be encountered in liquid meringue foams at room temperature can be observed in the typical Δ BS profiles shown in Fig. II-3. These profiles are presented as examples for helping understanding the rest of the study. Thus, Fig. II-3 displays the raw Δ BS data of two tannin-based liquid foams as a function of time (corresponding to different colours of the curves, from blue at instant 0 to red at 24h) and as a function of foam height (corresponding to the horizontal axis). Both foams were prepared from the same formulation using 3 g of surfactant and 40 min of whipping, but just differed by the presence or not of crosslinker (hexamine).

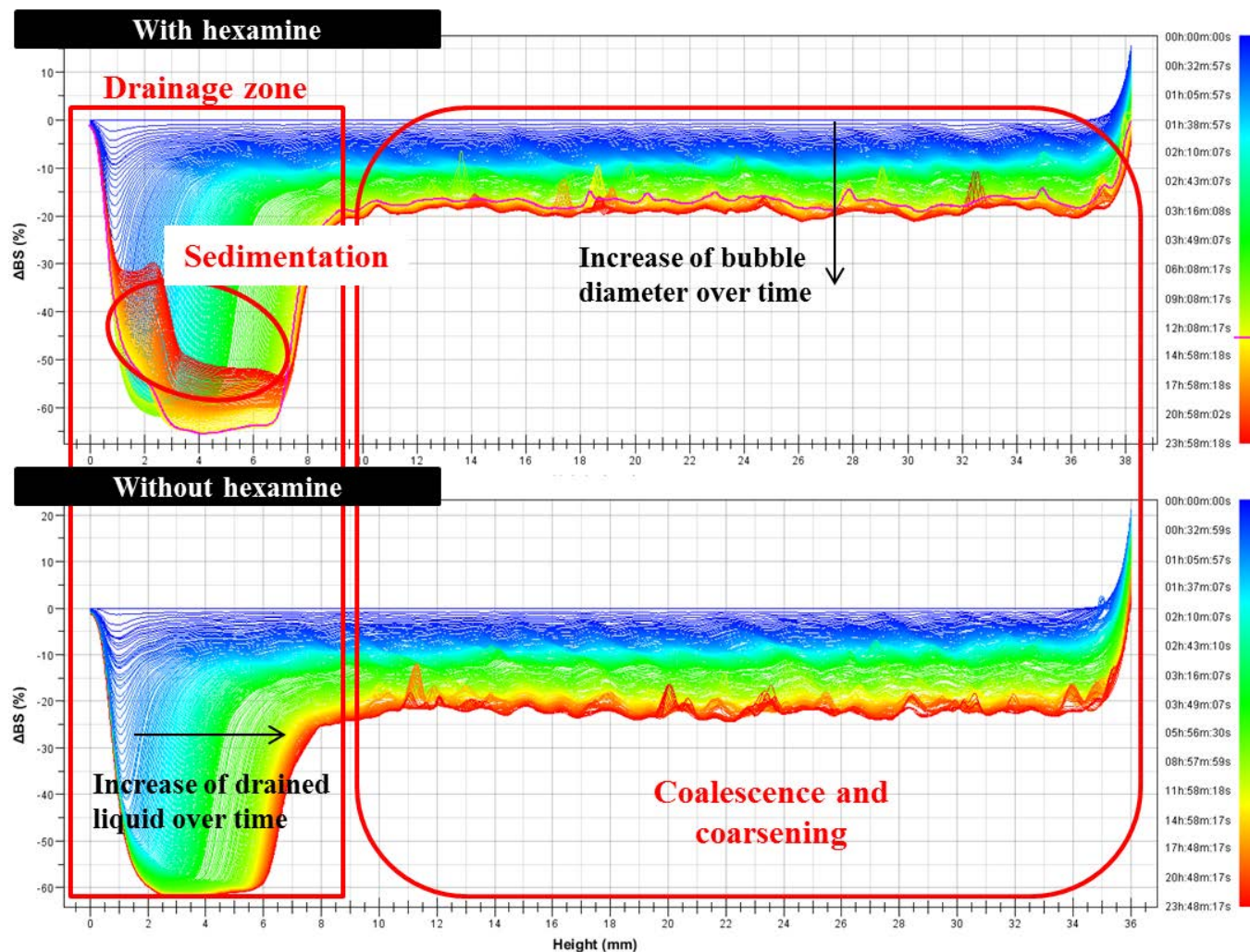


Fig. II-3. Typical Δ -backscattering profiles of tannin-based liquid foams recorded by the optical analyser: top = with crosslinker (hexamine); bottom = without crosslinker.

The drainage of fluid can be identified at the bottom of the sample holder (here typically at less than 8 mm of height from the bottom) by a negative peak of Δ BS that becomes deeper and broader with time. The opaque continuous phase indeed moves downwards over time, driven by gravity and/or capillary forces. As a result, Δ BS decreases with storage time and shows a marked negative peak (Mengual et al., 1999). A second phenomenon can be detected in the rest of the glass tube, corresponding to the increase of bubble diameter. Such bubble growth is controlled by two mechanisms: (i) coarsening, due to the diffusion of gas across liquid films from higher pressure (small) bubbles to lower pressure (large) ones; and (ii) coalescence, due to some ruptures of the thin liquid film separating two adjacent cells. The resultant increase of average

bubble size induces a progressive decrease in the Δ -backscattering profile because of the correspondingly lower number of light-scattering objects, as reported for similar systems in the past (Rouimi et al., 2005; Sceni and Wagner, 2007). Finally, a third phenomenon, sedimentation, can also be observed at room temperature but only in the formulation containing crosslinker (see the top part of Fig. II-3).

Sedimentation originates from the reactions between crosslinker and tannin molecules, producing a thermoset polymer whose higher density with respect to the aqueous medium induces an increase of Δ BS. When the foam is maintained at room temperature, the polymerisation reactions are very slow and thus occur to a very low extent, so that the foam remains liquid. The as-formed resin is then free to fall down slowly towards the bottom of the sample holder, leading to the observed sedimentation in the corresponding area (Mengual et al., 1999). In the following, the onset of polymerisation was then identified with the moment at which Δ BS begins to increase.

Taking into account all the aforementioned mechanisms and events that occur over time, the destabilisation of tannin-based liquid foams could be described as follows. Initially, bubble growth and liquid drainage induced a progressive drop of Δ BS signal all over the sample height, such drop being more important at the bottom of the liquid foam (drainage zone) than in the upper part (coalescence and coarsening zone). At the same time, the thermoset resin formed by polymerisation of tannin molecules, in low amount at room temperature, and the subsequent sedimentation produced the increase of Δ BS in the bottom area.

The way those different kinds of instabilities can be affected by the presence of crosslinker (hexamine) and, more importantly, by changes of experimental parameters such as surfactant amount and whipping time were thus first investigated at room temperature. For that purpose, drainage rate, onset of sedimentation/polymerisation and average bubble size were calculated. In addition, similar assays were carried out at different temperatures for studying the stability of liquid foams during crosslinking.

The kinetics of destabilisation in the bottom of the foam was calculated by fitting a sigmoidal model, Eq. (II-2), to the data of drained liquid volume, V , measured as a function of time. Such sigmoidal behaviour of free drainage profiles has indeed been reported in the past in various foam systems (Baeza et al., 2004; Lioumbas et al., 2015; Martínez-Padilla et al., 2015; Raharitsifa et

al., 2006; Sceni and Wagner, 2007). Eq. (II-2) uses three adjustable parameters: V_{max} , being the maximum drainage volume; m , describing the sigmoidal character of the curve (the higher m the more sigmoidal the curve); and $t_{1/2}$, being the time required to reach half of the maximum volume of the drainage (Carp et al., 1997).

$$V = \frac{V_{max} \cdot t^m}{t_{1/2}^m + t^m} \quad (\text{II-2})$$

The volume of liquid drained as a function of time was calculated from the height of liquid at the bottom of the tube of known diameter, and corresponding to the width of the negative Δ BS peak seen for example in the left part of Fig. II-3.

II/3. Results and discussion

II/3.1. Foaming capacity

The foaming capacity of tannin-based formulations, prepared as explained in section II/2.1 with crosslinker and different amounts of surfactant, and after different stirring times at 2000 rpm and at room temperature, is shown in Fig. II-4. It represents the volume fraction of air in the liquid foams produced by whipping ~ 40 mL of the formulation as a function of time. It is clearly seen that the foaming capacity depends both on whipping time and on surfactant content. The foaming capacity always increased with the surfactant concentration in the limited range investigated here. However, only small differences were observed when comparing formulations based on 4 or 5 g of surfactant: the foaming capacity was indeed practically not modified, suggesting that adding even higher amounts of surfactant would not change anything and, therefore, that the maximum useful concentration of surfactant was nearly reached (Schramm, 2005). In contrast, and whatever the formulation, the ability to incorporate air increased with stirring time until an optimum was reached around 20 min, beyond which the foam destabilised and started losing part of its air content. This phenomenon is well-known and has been extensively studied especially in the food industry, for example with egg white foams (Stadelman, W. J. et al., 1995).

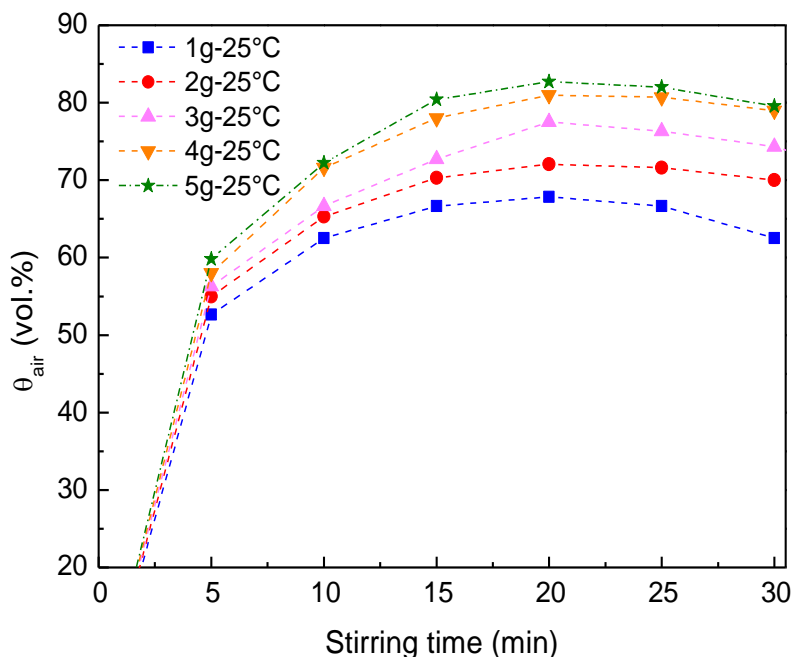


Fig. II-4. Foaming capacity at 25°C of liquid formulations (30 g of water, 20 g of tannin, 1.42 g of hemaxine and 1.12 g of pTSA) prepared with different amounts of surfactant as a function of stirring time. The dotted lines are just guides for the eye.

The values presented in Fig. II-4 were quite reproducible and give very important information about the foaming of the system, which is essential in the analysis of liquid foam stability. The fraction of air that is present in a given volume of foam is indeed expected to affect strongly destabilisation phenomena such as drainage or growth rate of bubble size. In addition, the foaming capacity of the initial liquid formulation is also directly related to the density of the final rigid foam resulting from its polymerisation. In other words, the foaming capacity directly impacts the properties of the final cellular materials, as such properties depend on both porous volume and porous structure (Schramm, 2005).

II/3.2. Foam stability

As explained before, the effect of the presence of a crosslinker and of the three following experimental parameters were investigated: *time of whipping*, *amount of surfactant* and *temperature*. Whatever the formulation, all foams were metastable systems and presented the typical features shown in Fig. II-3. Each destabilisation mechanism was treated separately by

dividing the Δ -backscattering profiles into different zones. The progress of drainage and the occurrence of sedimentation were investigated at the bottom of the cylindrical glass tube, i.e., at sample heights ranging from 0 to 11 mm, and the evolution of bubble size was determined in the middle part of the sample holder, i.e., at heights ranging from 14 to 29 mm wherein this phenomenon is better detected and observed alone. On the other hand, the whole Δ BS profile was employed for estimating the average bubble diameter as a function of time. Doing so, errors were minimised as the corresponding calculation is indeed based on the fraction of air of the whole foam. All curves of drainage volume vs. time followed the expected sigmoidal shape (see next subsections), since the drainage was high at the beginning but slowed down over time, and hence Eq. (II-2) fitted very well all the experimental data, with $R^2 > 0.99$.

II/3.2.1 Effect of crosslinker

A comparative study of liquid meringue foams with and without crosslinker (hexamine) was carried out to better understand the effect of this essential component on the formation and stability of the liquid foam. The main function of the hexamine is undoubtedly to react with tannin molecules upon heating, thus turning the foam from liquid to rigid. However, it is also interesting to learn how this reagent is involved in the formation of the metastable initial liquid foam in order to be able to control the whole system. The polymerisation process at different temperatures, finally leading to a rigid foam, will be studied extensively further in this chapter.

A liquid foam prepared as described in Subsection II/2.1, having a fixed formulation: 20 g of tannin, 30 g of water, 1.42 g of hexamine, 1.12 g of pTSA and 3 g of surfactant, was prepared after 40 min of whipping and analysed in the optical device at 25°C. A similar foam without hexamine was also prepared and investigated in the same conditions. Foaming capacity of both foams increased with stirring time until reaching a maximum of 79 vol.% of air incorporated, beyond which the foam capacity began to decrease slowly (Fig. II-5(a)) as shown previously in Fig. II-4. The main difference found in the foaming capacity of the foams was the stirring time required to reach the maximum air incorporated which was achieved slightly earlier in foams without hexamine.

After 40 min of stirring, the stability of the foams was studied by Turbiscan. At this point, the foam without hexamine showed a volume fraction of air slightly higher (70 vol.%) than the foam with hexamine (67 vol.%). The results extracted from the analyses in the Turbiscan showed that the decrease of backscattering in the bottom of the sample was a bit higher in the foam with hexamine (Fig. II-5(b)) indicating the ability of hexamine to improve the drainage; probably due to its higher fraction of liquid. Moreover, the presence of hexamine caused the appearance of sedimentation, detected by a change of trend in the Δ BS profile at the sample bottom, which was absent in foams without hexamine, see Fig. II-5(b), supporting the description given in the section II/2.3.2.

The Δ BS as a function of time in the middle of the sample, wherein the influence of drainage of sedimentation is less pronounced, gave information on foam destabilisation due to coalescence and coarsening of the bubbles. The rate at which bubbles grow is indeed a function of, amongst others, liquid viscosity, diffusivity of the gas, pressure inside the bubbles, and external pressure under which the growth is allowed to occur. Both curves initially decreased sharply, see Fig. II-5(c), but the corresponding slope progressively tended towards zero at high times, a typical behaviour also observed elsewhere (Martínez-Padilla et al., 2015; Sceni and Wagner, 2007). This behaviour was explained by the theory of Amon and Denson according to which bubbles expanding very close to each other cannot grow infinitely, because only a finite supply of gas is available for growth (Amon and Denson, 1984). During the first 4 hours, both foams exhibited a similar behaviour and, afterwards, the decrease of Δ BS was much less pronounced for foams containing hexamine. Such higher stabilisation was partly due to the slightly lower air volume fraction at the same amount of surfactant stabilising the system (Rouimi et al., 2005), and also due to the creation of a more stable and fixed structure caused by the interaction between hexamine and tannin molecules.

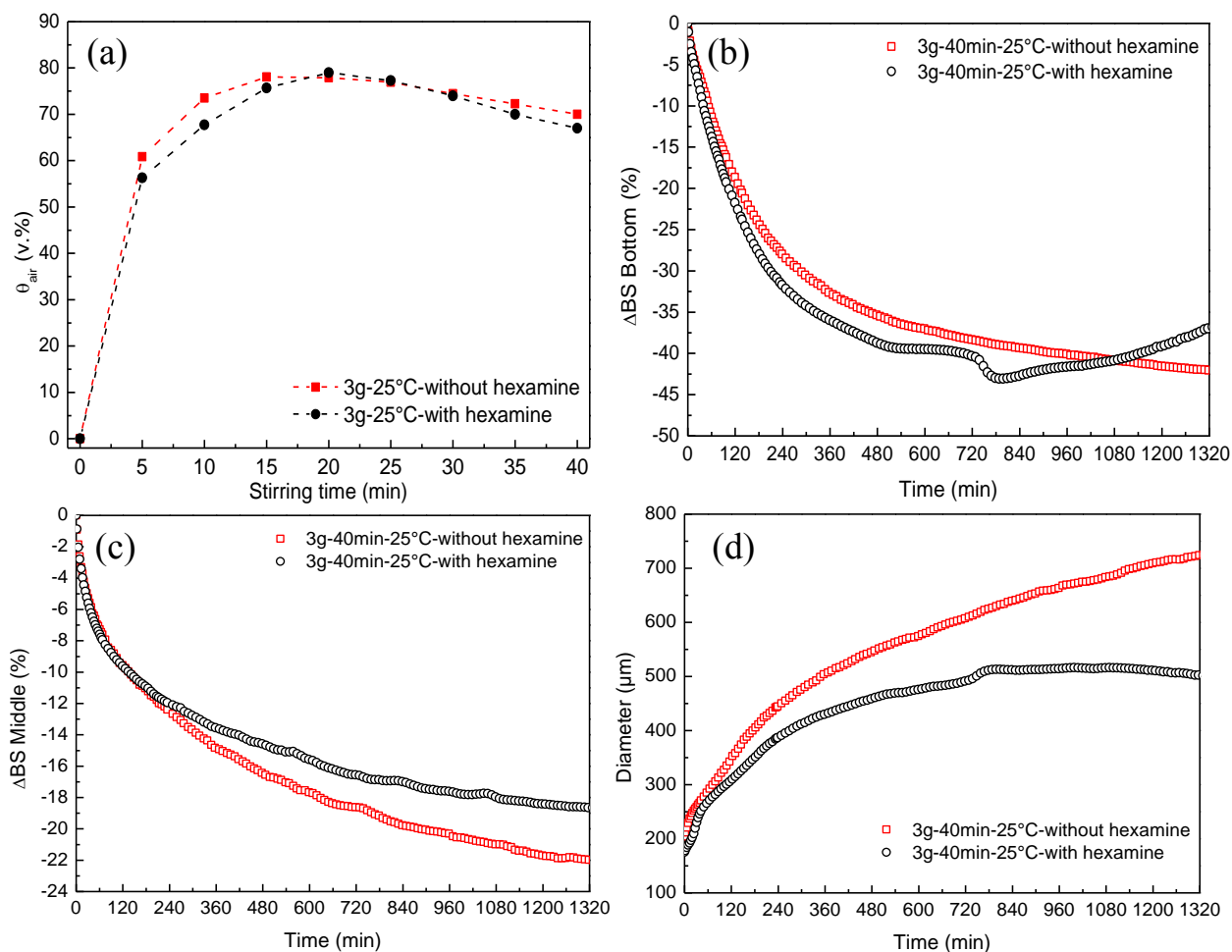


Fig. II-5. Effect of the presence of crosslinker (hexamine) on: (a) foaming capacity as a function of stirring time; (b) drainage and sedimentation at the sample's bottom; (c) coalescence and coarsening in the middle of the foam; and (d) average bubble diameter. The typical uncertainties on these curves are $\leq 5\%$.

Finally, the average bubble size as function of time, see Fig. II-5(d), showed that the bubble size progressively increased with the ageing of the foam. Such increase of the mean bubble diameter was more moderate in foams with hexamine, for which the bubbles achieved a stable state after 12 hours unlike what happened in the foam without hexamine where the stabilization was reached much later than 24 hours. Moreover, the bubbles were smaller in foams with hexamine than in foams without hexamine. Thus, it can be concluded that the hexamine promotes the formation of a network joining the molecules, even at room temperature when the reaction is very limited, fixing the structure and helping in the stability of the liquid foam.

After these studies of the role of hexamine on the stability of liquid foams, all the remaining tests were carried out with hexamine, which is essential for getting solids foams. The work focused on the effect of parameters such as the time of whipping and amount of surfactant that can modify the features of the final rigid foam. In addition, the study was completed by analysing the effect of temperature and monitoring the polymerisation reactions in the Turbiscan device.

II/3.2.2 Effect of stirring time

Four liquid foams having a fixed formulation: 20 g of tannin, 30 g of water, 1.42 g of hexamine, 1.12 g of pTSA and 3 g of surfactant, were prepared at different times of whipping: 10, 20, 30 and 40 min, and analysed in the optical device at 25°C in order to study the effect of the stirring time on the characteristics and stability of the liquid foams. The corresponding air fractions, onsets of sedimentation, and adjustable parameters derived from fits to the drainage curves by Eq. (II-1) are gathered in Table II-1.

Table II-1. Effect of stirring time on: onset of sedimentation, foaming capacity and sigmoidal model parameters for liquid drainage.

Sample	Onset of sedimentation	θ_{air} (vol. %)	Liquid drainage			
			V_{max} (mL)	$t_{1/2}$ (min)	m (-)	R^2
3g-10min-25°C	9h58min	67.7	3.52	105.74	1.55	0.998
3g-20min-25°C	10h17min	79.0	1.86	255.24	1.91	0.999
3g-30min-25°C	10h48min	75.0	2.33	224.03	1.80	0.999
3g-40min-25°C	12h58min	67.0	3.48	171.44	1.50	0.999

Foaming capacity increased with stirring time until reaching 79 vol.% of incorporated air after 20 min, beyond which it decreased slowly as formerly presented in Fig. II-4 and Fig. II-5(a). The maximum drainage volume (V_{max} , see Table II-1), derived from the fits to the drainage curves shown in Fig. II-6(a), presented a clear minimum for the formulation 3g-20min-25°C, i.e., for the one containing the highest fraction of air. This result is logical as this foam presents the lowest

amount of liquid to drain. The latter was also associated with the highest time $t_{1/2}$ for draining half of this volume. Regarding the effect of stirring time, it was found to have an important influence on drainage. Comparing the samples with a similar fraction of air but different times of whipping, i.e., 3g-10min-25°C and 3g-40min-25°C, it was observed that despite having similar V_{max} values, $t_{1/2}$ was significantly higher (lower drainage rate) in the foam submitted to longer whipping. This finding may be explained by the formation of a more homogeneous and stable system at higher stirring times, in which the drainage was, therefore, slower. Similar effects of whipping time were observed with apple juice foams (Raharitsifa et al., 2006). The drainage curves were more sigmoidal when the fraction of air increased, see again Fig. II-6(a), hence the corresponding increases in the values of m .

The onset of sedimentation was detected in the change of trend of ΔBS profile at the sample bottom, see Fig. II-6(b). The slow separation of tannin-based resin from the liquid phase indeed induced an increase of backscattered light intensity. Table II-1 shows that the onset of sedimentation was delayed when the whipping time increased. This may be again attributed to an increase of liquid foam homogeneity and, as a result, to a lower amount of precipitated solid in agreement with the observed decrease of drainage rate.

The time-dependence of ΔBS in the middle of the sample, i.e., wherein the influence of drainage is less pronounced, gave information on foam destabilisation due to coalescence and coarsening processes as introduced before. Initially, the curves decreased sharply, see Fig. II-6(c), but the corresponding slope progressively tended towards zero at high times, which is a typical behaviour explained by the theory of Amon and Denson (Amon and Denson, 1984) and observed in others research works (Martínez-Padilla et al., 2015; Sceni and Wagner, 2007). The destabilisation at the half-height of the sample was directly proportional to the fraction of air in the foam: at a constant amount of surfactant, higher gas volume fractions tended to destabilise the system faster (Rouimi et al., 2005). The bubbles were indeed less hydrated in foams with lower liquid fraction and the pressure was lower, favouring the coarsening (Saint-Jalmes and Langevin, 2002; Sceni and Wagner, 2007).

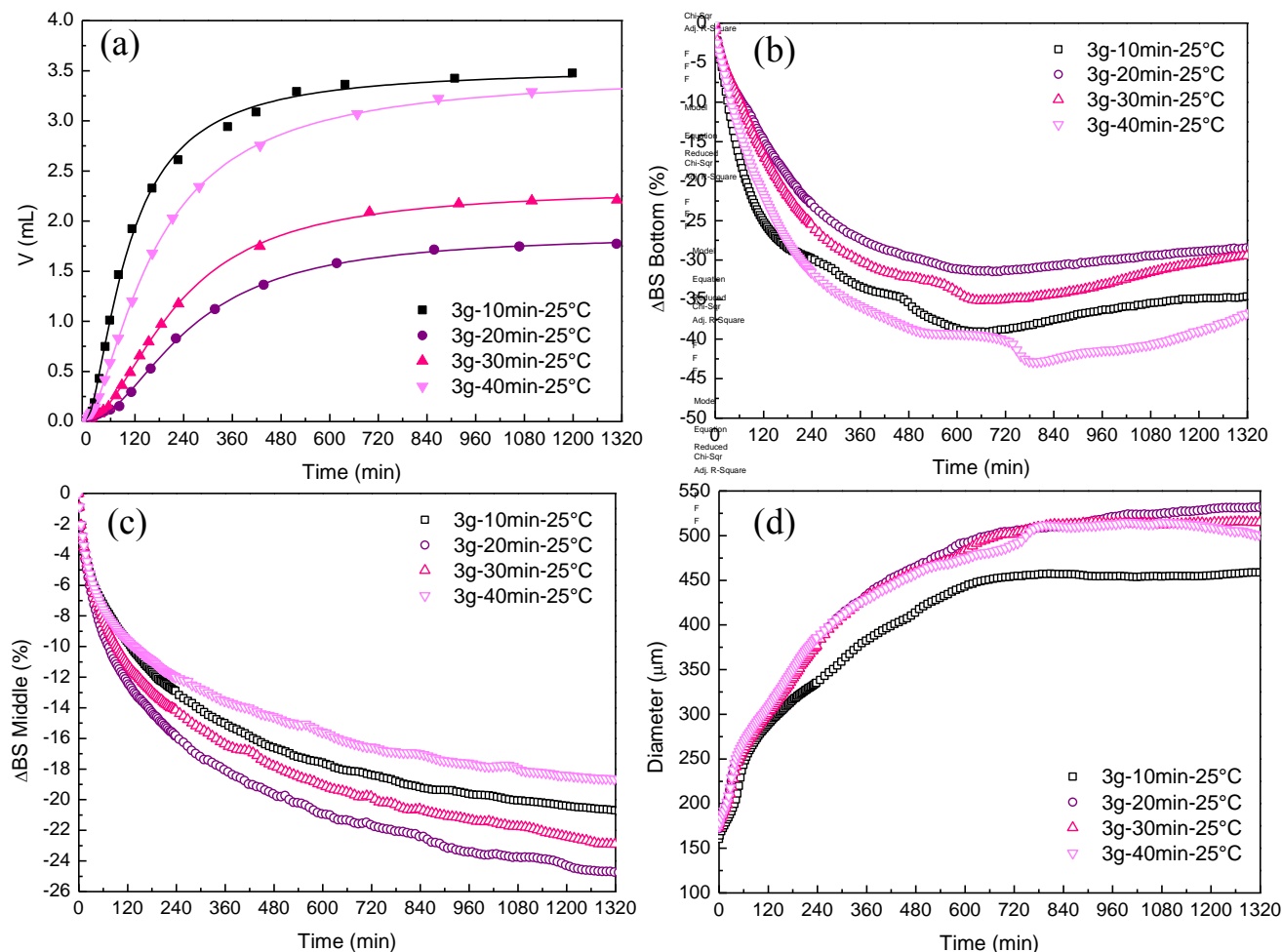


Fig. II-6. Effect of whipping time on: (a) volume of drained liquid; (b) drainage and sedimentation at the sample's bottom; (c) coalescence and coarsening in the middle of the foam; and (d) average bubble diameter.

Finally, the average bubble size in the foam, see Fig. II-6(d), progressively increased with the ageing of the foam as reported elsewhere (Raharitsifa et al., 2006). A roughly linear and very similar increase for all liquid foams was observed during the first 3h of the test. Then, the average diameter of the sample whipped for the shortest time, 3g-10min-25°C, increased slower than the others, which all behaved the same. It can be concluded from the latter results that stirring time did not have a significant effect on the final bubble diameter once the foam achieved the maximum foaming capacity. This finding explains and confirms the results of pore structure analysis formerly reported for meringue rigid foams prepared from comparable formulations presented here (Szcurek et al., 2014).

II/3.2.3 Effect of surfactant amount

The same analytical procedure was applied to a series of five different foams prepared as described in subsection II/2.1, but using various amounts of surfactant: 1, 2, 3, 4, and 5 g and a constant whipping time of 30 min. 30 min was chosen as a good compromise between the optimum whipping time for getting the highest volume fraction of air (as deduced from Fig. II-4), and a resultant low drainage rate (as explained in the previous subsection when discussing the data of Table II-1). The drainage of the liquid by gravity or capillary action through the films separating bubbles from each other was again successfully fitted by the sigmoidal model, see Fig. II-7(a), and the parameters were gathered in Table II-2. An increase of surfactant content significantly decreased the maximum drained volume (V_{max}) and increased the time to reach half of this volume ($t_{1/2}$) accordingly, indicating the ability of more surfactant to improve foam's stability by decreasing the drainage. The foam with the highest amount of surfactant presented the lowest volume fraction of liquid (see again Fig. II-4 and Table II-2), also decreasing the drainage as previously shown in the studies of stirring time effect. Moreover, the lower drainage in foams having high surfactant concentrations was also attributed to an increase of viscosity of the continuous phase (Martínez-Padilla et al., 2015; Raharitsifa et al., 2006) as well as to the drying of the foam, which caused a more stable structure since the Plateau border walls became more rigid and opposed drainage (Lioumbas et al., 2015).

Increasing the surfactant amount had no significant impact on the sigmoidal character of the curves, as the parameter m only slightly changed without clear trend unlike what was observed for whipping time, for which a higher fraction of air led to higher m . The sample 3g-30min-25°C was the one leading to the most sigmoidal curve; in other words, its drainage was the slowest at the beginning and was the fastest to stabilise after the increase. Such behaviour is interesting for foams able to harden quickly, as the initial structure of the liquid foam is indeed more likely to be maintained after polymerisation.

Table II-2. Effect of surfactant amount on: onset of sedimentation, foaming capacity and sigmoidal model parameters for liquid drainage.

Sample	Onset of sedimentation	θ_{air} (vol. %)	Liquid drainage			
			V_{max} (mL)	$t_{1/2}$ (min)	m (-)	R^2
1g-30min-25°C	20h00min	62.0	4.67	140.22	1.55	0.999
2g-30min-25°C	13h48min	70.2	3.93	164.07	1.61	0.999
3g-30min-25°C	10h48min	75.0	2.54	226.41	1.80	0.999
4g-30min-25°C	7h46min	79.1	1.34	279.58	1.68	0.986
5g-30min-25°C	7h24min	79.9	1.04	279.58	1.49	0.996

The decrease of backscattering in the bottom of the sample by drainage and sedimentation was much lower for higher amounts of surfactant, see Fig. II-7(b). More surfactant indeed produced a lower volume of drained liquid in which sedimentation occurred earlier (Table II-2) and was also less visible.

Δ -backscattering profiles in the middle of the foam height (Fig. II-7(c)), together with the changes of average bubble diameter (Fig. II-7(d)), are among the most important results for studying the effect of surfactant amount on the stability of tannin-based foams. As shown in Fig. II-7(c), all foams exhibited a similar behaviour during the first 30 minutes but, afterwards, the destabilisation kinetics were somehow different and revealed that the most stable foams were the ones prepared with 2 and 3g of surfactant. The corresponding Δ BS curves, therefore, did not follow the same trend as found above when studying the effect of stirring time, for which the destabilisation of bubbles was directly related to the fraction of air within the foam. But in the present case, the formulations of higher foaming capacity were those containing more surfactant, unlike in the previous case for which the surfactant concentration was constant. Therefore, depending on the parameter under study, the trends can be different and reveal the existence of optimum values for each experimental parameter taken separately.

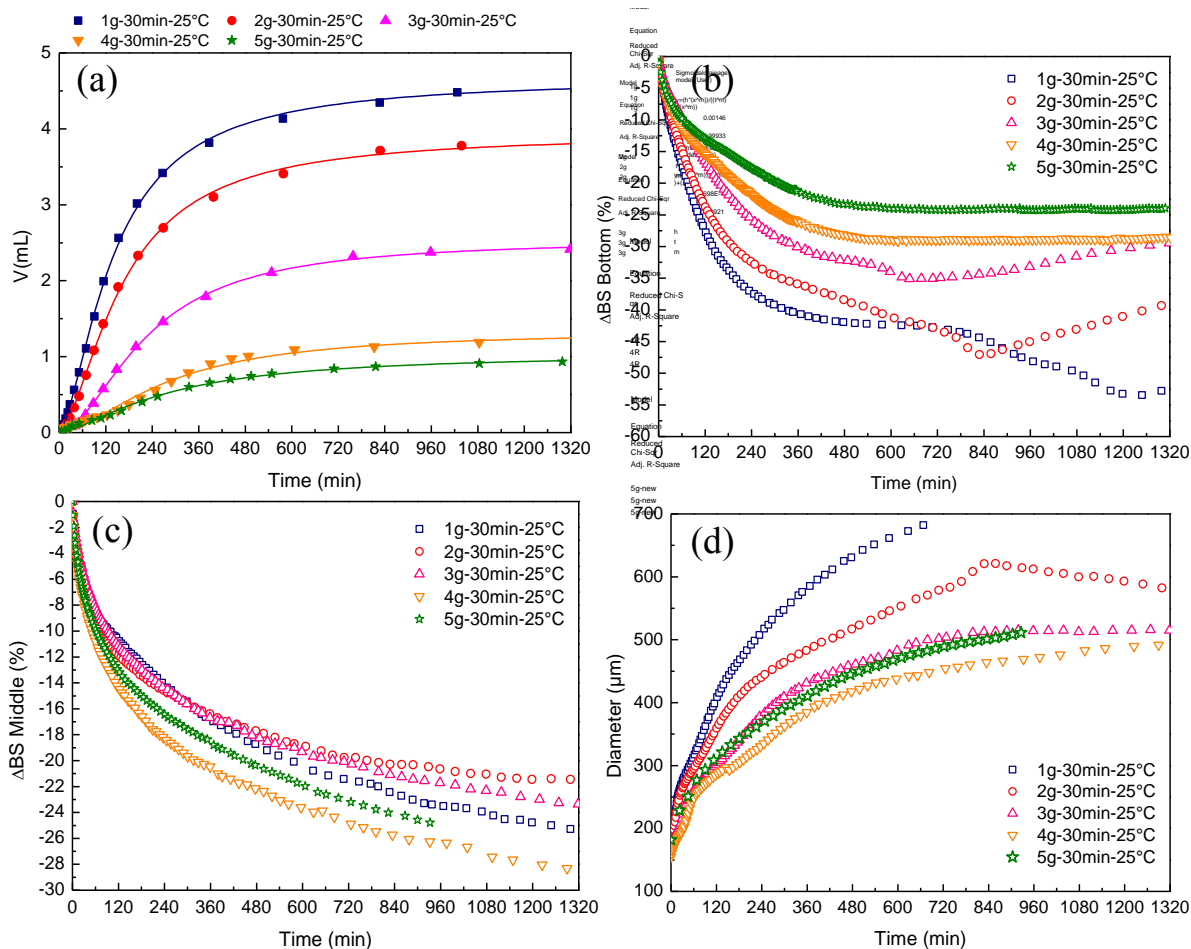


Fig. II-7. Effect of surfactant amount on: (a) volume of drained liquid; (b) drainage and sedimentation at the sample's bottom; (c) coalescence and coarsening in the middle of the foam; and (d) average bubble diameter.

The mean diameter of the bubbles was also quite dependent on the surfactant concentration, see Fig. II-7(d), and globally decreased with the amount of surfactant. Formulations prepared with 3, 4 and 5 g of surfactant presented approximately the same bubble size over the time. Even though 4g-30min-25°C and 5g-30min-25°C samples contained the highest amount of surfactant, they were finally not more stable and their bubbles were not smaller than those of 3g-30min-25°C. This result is consistent with the instability of these foams observed in Fig. II-7(c).

So far, the phenomena of drainage and coalescence in tannin-based liquid foams were investigated above almost separately. However, it has been shown by many studies (Carrier and Colin, 2003; Hilgenfeldt et al., 2001; Magrabi et al., 2001, 1999; Vera and Durian, 2002) that

bubble dynamics in liquid foams is closely related to drainage rate and foam stability, and that there is a coupling between drainage and coalescence-coarsening. The influence of surfactant amount on the interrelations between such phenomena is not very well-known. More surfactant not only accelerated foam drying, leading faster to fixed and stable structures with less drainage as shown in Table II-2, but also increased coarsening and coalescence (Fig. II-7(c)). Higher fractions of air in the foam, in addition to the correspondingly smaller bubble size, on average, made bubbles be more closely packed with thinner Plateau borders. This situation favoured the coalescence of bubbles because the interface between them is a thin liquid film, in which the pressure is higher than that in Plateau borders. This pressure difference forces liquid to flow towards the Plateau borders, causing a further thinning of the films and favouring coalescence and coarsening (Schramm, 2005).

Overall, the formulation 3g-30min-25°C might contain the optimum surfactant concentration as it showed a good compromise between the different destabilisation events. This formulation indeed exhibited a high foaming capacity that allowed a moderate drainage, although formulations richer in surfactant (4g-30min-25°C and 5g-30min-25°C) presented lower drainage. Moreover, among the liquid foams of lowest bubble diameter, 3g-30min-25°C was the most stable. For that reason, 3g-30min-25°C was taken as a reference in the next subsection for studying the effect of temperature on liquid foams crosslinking, with the aim of getting rigid foams with practical applications such as thermal insulation.

II/3.2.4 Effect of temperature

Four identical formulations based on 20 g of tannin, 30 g of water, 1.42 g of hexamine, 1.12 g of pTSA and 3 g of surfactant were prepared and whipped for 30 min at room temperature. The resultant liquid foams were then immediately transferred to the optical analyser preheated at different temperatures: 25°C, 40°C, 60°C and 80°C, and within which they were investigated during 24h. The temperature was expected to affect destabilisation events such as drainage rate and bubble growth and, at the same time, to accelerate the reaction between tannin and hexamine and to finally result in a rigid foam (Szczyrek et al., 2015).

Fig. II-8 shows Δ -backscattering profiles at the four investigated temperatures. All exhibited the same destabilisation phenomena already described in subsection II/2.3.2. However, the

relative importance of some of these events was modified with temperature, and a new zone on the right side of the graphs of Fig. II-8, which did not exist at 25°C, appeared. This zone, shown in a red box and which was present only above room temperature, was due to the increase of foam volume produced by the higher temperature inside the analyser and lasted until the set point was reached. The moment at which the set point was met by the whole foam was detected from the horizontal axis of the Δ BS curves showing the end of the foam expansion. As a result of heating, the volume fraction of air in the liquid foam increased with temperature. The corresponding parameters are gathered in Table II-3.

Table II-3. Effect of temperature on: final fraction of air in the foam, onset of polymerisation, and time required to reach the set point.

Sample	Time to reach constant temperature (min)	θ_{air} final (vol. %)	Onset of polymerisation
3g-30min-25°C	-	75.0	10h48min
3g-30min-40°C	38	79.0	2h37min
3g-30min-60°C	18	86.5	34min
3g-30min-80°C	16	90.7	11min

At the same time, the rest of destabilisation phenomena (drainage, sedimentation, coalescence and coarsening) took place in the foams. Out of those phenomena, drainage was the main one (the corresponding peak was also broader) at lower temperatures, whereas the increase of Δ BS related to sedimentation was low but increased with temperature. The latter finding confirms that sedimentation was due to the formation of solid resin by reaction between tannin and hexamine, known to be favoured by higher temperature. Thus, the increase of Δ BS at room temperature was only detected in the bottom, due to the sedimentation of the few molecules polymerised. However, as the temperature increased, more resin formed and polymerisation occurred to a higher extent, thus was not only detected in the sample bottom. At 80°C, polymerisation was practically the only phenomenon that took place in the foam after a few minutes because, as explained above, polycondensation reactions were quite fast at this temperature so that the structure of the foam quickly became stationary, preventing phenomena such drainage or bubble growth.

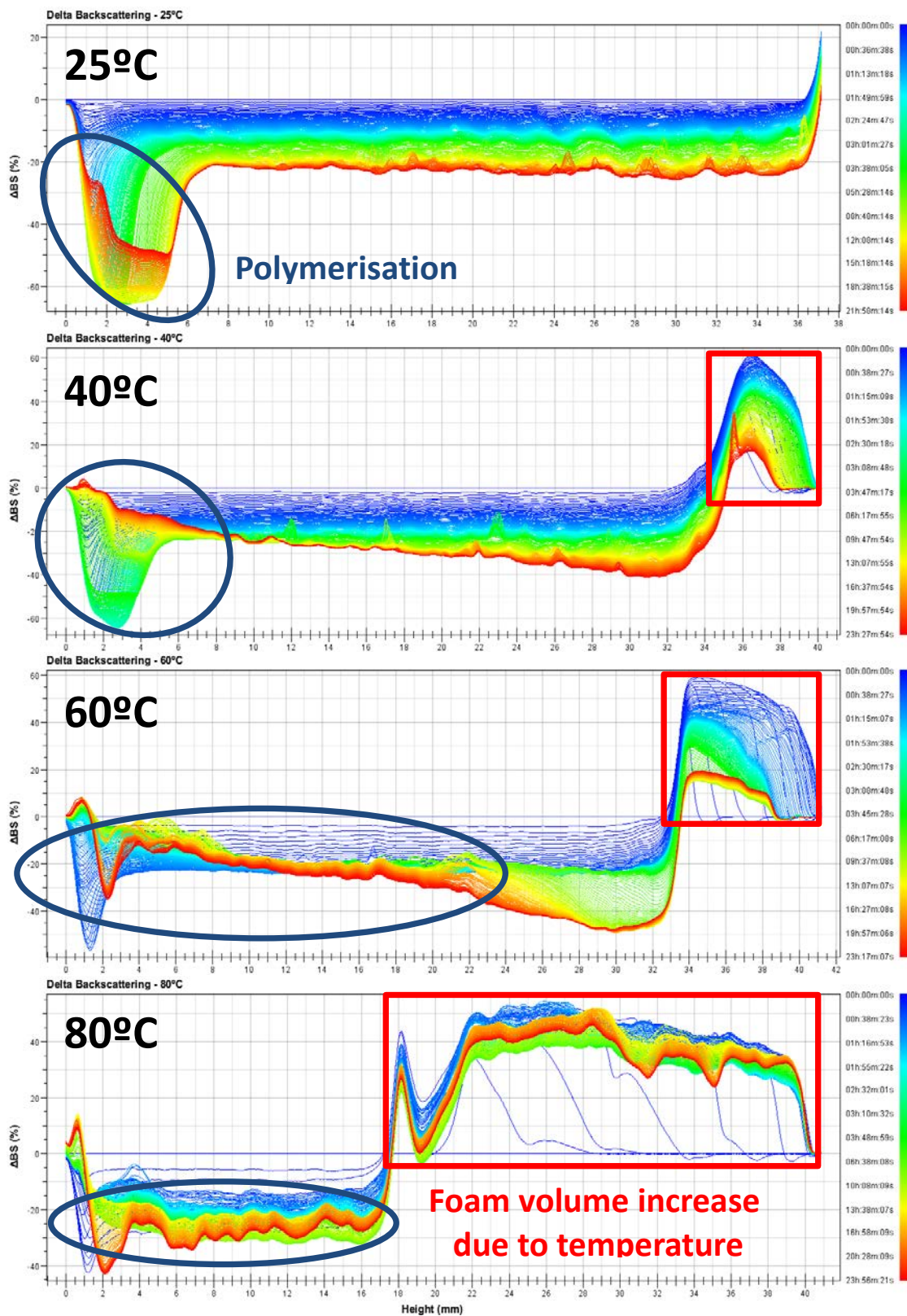


Fig. II-8. Δ -backscattering profiles of foams evaluated by the analyser at 25, 40, 60 and 80°C

The destabilisation curves corresponding to the bottom of the foams are displayed in Fig. II-9(a), and presented the behaviour described above. Initially, ΔBS decreased as the volume of liquid drained in the bottom of the tube increased, and the drainage peak became deeper and broader. The decrease of ΔBS was much more pronounced in foams submitted to higher temperatures, which means that the temperature had a strong influence on the drainage rate, increasing the latter. A rise in temperature indeed increases thermal motions, thereby enhancing the molecular collision rate, and also reduces the viscosity, thus increasing the drainage rate as long as the foam remains liquid (Schramm, 2005). In a second step, and after a given time depending on the temperature, polymerisation occurred as noticed by the upward change of slope of the ΔBS curve (Fig. II-9(a)). This turnaround point, given in Table II-3 as a list of onsets of polymerisation, happened earlier and was more marked at higher temperatures. In summary, increasing the temperature first increased the drainage rate of the foam as long as the latter remained liquid, but such effect was limited by polymerisation which quickly fixed the structure of the foam when the latter became solid.

The temperature also had an important impact on Δ -backscattering curves in the middle part of the foam height (see Fig. II-9(b)) and, therefore, on the bubble growth. The lower viscosity and the thermal motions induced by heating increase the probability of coalescence and coarsening, as observed by a more pronounced decrease of ΔBS curves in the middle part of the samples. As a consequence, the average bubble diameter (see Fig. II-9(c)) increased faster when the temperature increased, and the moment at which it suddenly stopped increasing was more clearly observed. Such critical time corresponds to the onset of polymerisation, leading to a fixed foam structure at 80°C within which the liquid phase vanished. Therefore, as the light-scattering method was no more relevant and led to non-reliable data, the corresponding curves in Fig. II-9(a-c) were truncated accordingly above the hardening point.

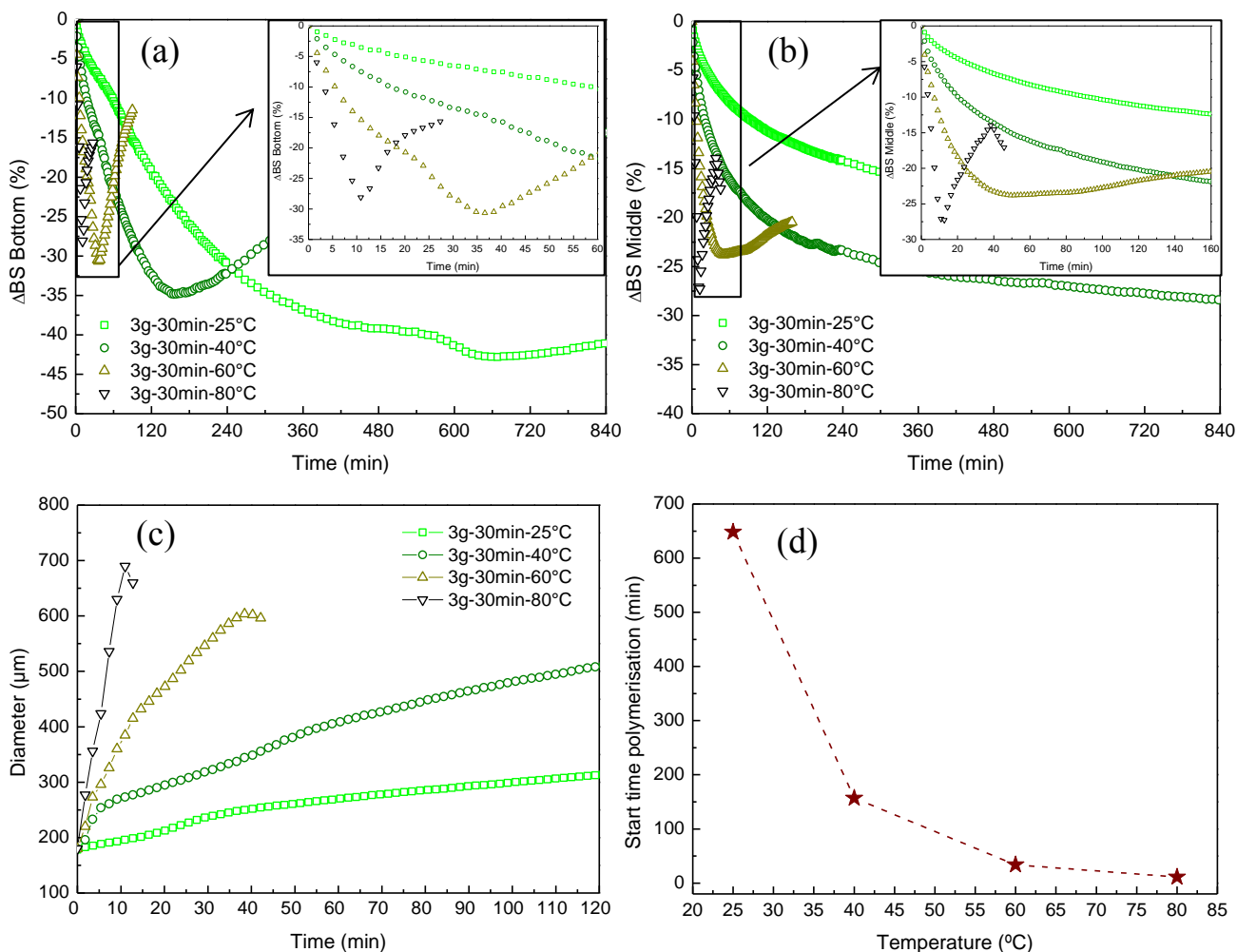


Fig. II-9. Effect of temperature on liquid foams as a function of time: (a) drainage and polymerisation at the sample's bottom; (b) coalescence and coarsening in the middle of the foam; (c) variation of average bubble diameter; and (d) starting point of polymerisation.

It is important to recall that, despite the foam heated at 80°C evidenced significant destabilisation at the beginning due to the hot environment in which it was placed, there was no more destabilisation after 10 min and the structure of foam became fixed. As a result, this foam quickly stabilised with a mean bubble size of around 680 μm. This value is rather consistent with the cell sizes reported elsewhere for tannin-based rigid foams of similar formulation and prepared in similar conditions (Szcurek et al., 2014). Thus, a very important parameter to investigate in the framework of foam stability studies is the time of reaction between tannin and hexamine as it has a significant impact on the final rigid foam structure.

A more detailed study of the kinetics of liquid foam hardening was then carried out. The purpose was to get more knowledge of the processes governing the curing of tannin-based resins, thereby helping to improve the quality of the final products. Polyphenolic resins such as those based on tannin are complex systems in which the activation energies may change depending on the progress of the polymerisation (Pérez et al., 2009; Riccardi et al., 2002). The onset of polymerisation derived from the Δ BS profiles decreased *a priori* exponentially as the temperature increased (see Table II-3 whose last column is presented graphically in Fig. II-9(d)), so that Arrhenius equation (Eq. (II-3)) was assumed to describe the temperature-dependence of the kinetic constant of polymerisation. It reads:

$$k = Ae^{-\frac{E_a}{RT}} \quad (\text{II-3})$$

where k is the kinetic constant of polymerisation, T is the absolute temperature, A is a pre-exponential factor, E_a is the activation energy of the reaction, and R is the universal gas constant ($8.314 \text{ J mol}^{-1} \text{ K}^{-1}$). Herein, the kinetic constant was simply calculated as the inverse of the onset of polymerisation. This implicitly assumes first-order kinetics, which is indeed the most likely in processes producing a solid from reactions in the liquid phase (Laidler, K. J., 1987), as their kinetics indeed depends on the concentration of only one reactant.

Arrhenius law, which is widely used for determining the rate of chemical reactions and for calculating the corresponding activation energy (Laidler, K. J., 1987) indeed perfectly applied to the present case as it can be seen in Fig. II-10, in which Eq. (II-3) was linearised as follows:

$$\ln(k) = \frac{-E_a}{R} \left(\frac{1}{T}\right) + \ln(A) \quad (\text{II-4})$$

Application of Eq. (II-4) led to the following expression: $\ln(k) = - (7818.65 \pm 327.95) / T + (15.74 \pm 1.02)$ with a correlation coefficient (R^2) of 0.995. The activation energy, E_a , was thus $65 \pm 2.7 \text{ kJ mol}^{-1}$. This value is within the range reported for phenolic resins in general: $55 - 167 \text{ kJ mol}^{-1}$ (Domínguez et al., 2010; Pérez et al., 2009; Wang et al., 2005). This finding supports the definition of the kinetic constant of polymerisation as the inverse of initial polymerisation time, the latter being identified with the increase of Δ BS. The light-scattering technique used here, therefore, appears accurate enough and quite suitable for investigating polymerisation reactions and kinetics. Therefore, all the parameters related to the preparation of rigid foams from the

polymerisation of liquid foams, whether they deal with reaction kinetics or with the destabilisation phenomena expected in this kind of systems, can be derived from light-scattering experiments. Such collection of data will be useful to optimise both formulations and curing processes for obtaining rigid foams with desired specifications for various applications.

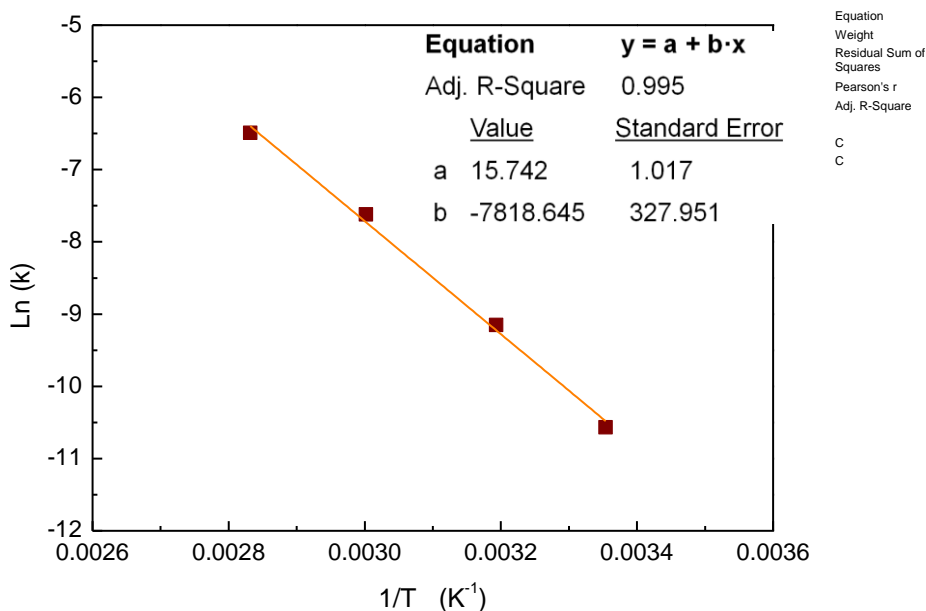


Fig. II-10. Application of Eq. (II-4) to the data of Fig. II-9(d), accounting for the polymerisation of tannin in liquid foam formulations.

II/4. Conclusion

In this part of the thesis, liquid foams obtained by mechanical whipping of aqueous solutions of tannin, crosslinker and surfactant were investigated in terms of stability and polymerisation process using a backscattered light detection method, with the aim of converting them into rigid foams. The technique, using an optical analyser based on multiple light-scattering measurements, proved to be actually suitable to detect the different destabilisation phenomena, namely drainage, sedimentation, coarsening and coalescence, that take place in liquid foams, and to investigate how parameters such as presence of crosslinker, whipping time, amount of surfactant and temperature affected them. The results, based on changes of backscattered light only (as no light was transmitted in the present case), indicated that bubble dynamics was related to drainage rate and that there was an important coupling between drainage and coalescence-coarsening

phenomena. The optimal stirring time leading to the highest and most stable foaming and the optimal surfactant amount leading to the most stable liquid meringue foam were identified to be 30 min and 3g of surfactant, respectively. On the other hand, the temperature was found to have a major impact on destabilisation, but heating was required for readily obtaining rigid foam with a given, fixed porous structure.

Finally, the same method was successfully used to investigate the polymerisation process that takes place in the heated liquid foams. As far as we are aware, this had never been carried out before. Very important information could be obtained, especially rates of separate destabilisation phenomena, changes of average bubble size and onset of polymerisation, as well as order of reaction and activation energy, helping to understand the conversion of liquid foams into rigid ones. Compared to more traditional methods for investigating liquid foams, the analysis of the backscattered light provided more accurate and complete information about this kind of systems. Fig. II-11 shows an instructive schematic overview of all the study carried out on meringue tannin-based foams using the Turbiscan optical analyser.

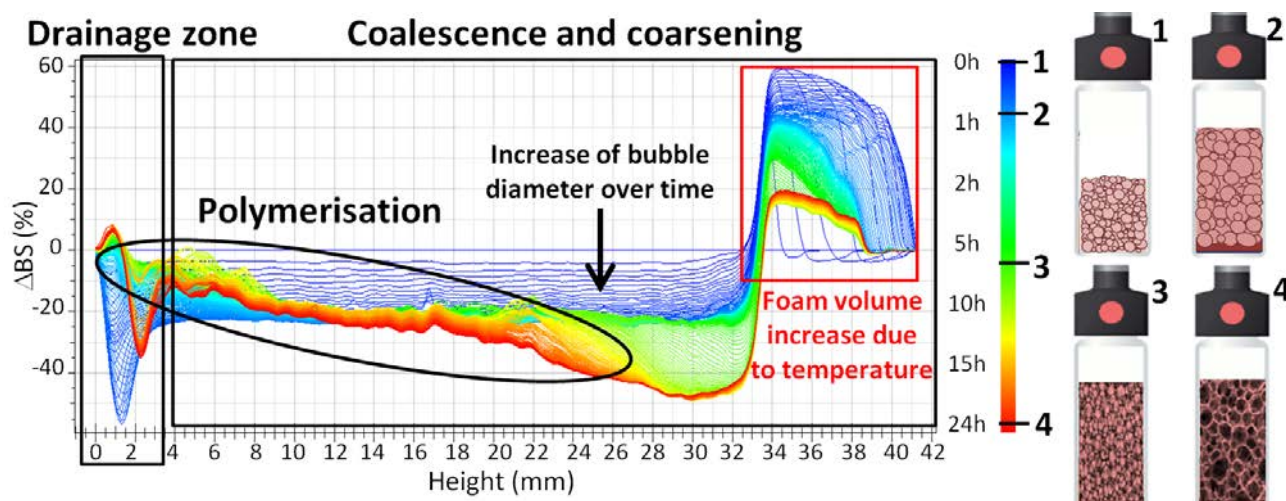


Fig. II-11. General scheme of the study using the Turbiscan analyser.

Meringue tannin foams have potential use, after crosslinking, as thermal insulators and acoustic absorbers. It has been already demonstrated that hardening tannin-based liquid foams or foaming tannin-based liquid formulations produce materials having very similar structures and physical properties (Szczurek et al., 2014). As these rigid foams were shown to present quite

good performances for thermal (Celzard et al., 2015) and acoustic (Lacoste et al., 2015) insulation, the same is expected with the present foams. Moreover, now, after this study, we are able to create rigid foams with the desired final characteristics by using the appropriate stirring time and/or amount of surfactant; which open up the range of potential applications.

II/5. Bibliography

- Amon, M., Denson, C., 1984. A Study of the Dynamics of Foam Growth - Analysis of the Growth of Closely Spaced Spherical Bubbles. *Polym. Eng. Sci.* 24, 1026–1034. doi:10.1002/pen.760241306
- Baeza, R., Sanchez, C.C., Pilosof, A.M.R., Patino, J.M.R., 2004. Interfacial and foaming properties of prolylenglycol alginates: Effect of degree of esterification and molecular weight. *Colloids Surf. B Biointerfaces* 36, 139–145. doi:10.1016/j.colsurfb.2004.04.005
- Carp, D.J., Bartholomai, G.B., Pilosof, A.M.R., 1997. A Kinetic Model to Describe Liquid Drainage from Soy Protein Foams over an Extensive Protein Concentration Range. *LWT - Food Sci. Technol.* 30, 253–258. doi:10.1006/fstl.1996.0173
- Carrier, V., Colin, A., 2003. Coalescence in draining foams. *Langmuir* 19, 4535–4538. doi:10.1021/la026995b
- Celzard, A., Szczurek, A., Jana, P., Fierro, V., Basso, M.-C., Bourbigot, S., Stauber, M., Pizzi, A., 2015. Latest progresses in the preparation of tannin-based cellular solids. *J. Cell. Plast.* 51, 89–102. doi:10.1177/0021955X14538273
- Choi, S.J., Won, J.W., Park, K.M., Chang, P.-S., 2014. A New Method for Determining the Emulsion Stability Index by Backscattering Light Detection: ESI Determination by Backscattered Light. *J. Food Process Eng.* 37, 229–236. doi:10.1111/jfpe.12078
- Degrad, L., Michon, C., Bosc, V., 2016. New insights into the study of the destabilization of oil-in-water emulsions with dextran sulfate provided by the use of light scattering methods. *Food Hydrocoll.* 52, 848–856. doi:10.1016/j.foodhyd.2015.08.021
- Dickinson, E., Izgi, E., 1996. Foam stabilization by protein-polysaccharide complexes. *Colloids Surf. Physicochem. Eng. Asp.* 113, 191–201. doi:10.1016/0927-7757(96)03647-3
- Domínguez, J.C., Alonso, M.V., Oliet, M., Rojo, E., Rodríguez, F., 2010. Kinetic study of a phenolic-novolac resin curing process by rheological and DSC analysis. *Thermochim. Acta* 498, 39–44. doi:10.1016/j.tca.2009.09.010
- Dudášová, D., Flåten, G.R., Sjöblom, J., Øye, G., 2009. Study of asphaltenes adsorption onto different minerals and clays: Part 2. Particle characterization and suspension stability. *Colloids Surf. Physicochem. Eng. Asp.* 335, 62–72. doi:10.1016/j.colsurfa.2008.10.041
- Goscianska, J., Olejnik, A., Nowak, I., Marciniak, M., Pietrzak, R., 2016. Stability analysis of functionalized mesoporous carbon materials in aqueous solution. *Chem. Eng. J.* 290, 209–219. doi:10.1016/j.cej.2016.01.060
- Guillerme, C., Loisel, W., Bertrand, D., Popineau, Y., 1993. Study of Foam Stability by Video Image-Analysis - Relationship with the Quantity of Liquid in the Foams. *J. Texture Stud.* 24, 287–302. doi:10.1111/j.1745-4603.1993.tb01285.x

- Hilgenfeldt, S., Koehler, S.A., Stone, H.A., 2001. Dynamics of coarsening foams: Accelerated and self-limiting drainage. *Phys. Rev. Lett.* 86, 4704–4707. doi:10.1103/PhysRevLett.86.4704
- Kato, A., Takahashi, A., Matsudomi, N., Kobayashi, K., 1983. Determination of Foaming Properties of Proteins by Conductivity Measurements. *J. Food Sci.* 48, 62–65. doi:10.1111/j.1365-2621.1983.tb14788.x
- Lacoste, C., Basso, M.-C., Pizzi, A., Celzard, A., Ella Ebang, E., Gallon, N., Charrier, B., 2015. Pine (*P. pinaster*) and quebracho (*S. lorentzii*) tannin-based foams as green acoustic absorbers. *Ind. Crops Prod.* 67, 70–73. doi:10.1016/j.indcrop.2014.12.018
- Laidler, K. J., 1987. *Chemical Kinetics*, 3rd ed. Harper & Row.
- Lioumbas, J.S., Georgiou, E., Kostoglou, M., Karapantsios, T.D., 2015. Foam free drainage and bubbles size for surfactant concentrations below the CMC. *Colloids Surf. Physicochem. Eng. Asp.* 487, 92–103. doi:10.1016/j.colsurfa.2015.09.050
- Li, P., Yang, D., Lou, H., Qiu, X., 2008. Study on the stability of coal water slurry using dispersion-stability analyzer. *J. Fuel Chem. Technol.* 36, 524–529. doi:10.1016/S1872-5813(08)60033-X
- Magrabi, S.A., Dlugogorski, B.Z., Jameson, G.J., 2001. Free drainage in aqueous foams: Model and experimental study. *AIChE J.* 47, 314–327. doi:10.1002/aic.690470210
- Magrabi, S.A., Dlugogorski, B.Z., Jameson, G.J., 1999. Bubble size distribution and coarsening of aqueous foams. *Chem. Eng. Sci.* 54, 4007–4022. doi:10.1016/S0009-2509(99)00098-6
- Martínez-Padilla, L.P., García-Mena, V., Casas-Alencáster, N.B., Sosa-Herrera, M.G., 2014. Foaming properties of skim milk powder fortified with milk proteins. *Int. Dairy J.* 36, 21–28. doi:10.1016/j.idairyj.2013.11.011
- Martínez-Padilla, L.P., García-Rivera, J.L., Romero-Arreola, V., Casas-Alencáster, N.B., 2015. Effects of xanthan gum rheology on the foaming properties of whey protein concentrate. *J. Food Eng.* 156, 22–30. doi:10.1016/j.jfoodeng.2015.01.018
- Mengual, O., Meunier, G., Cayre, I., Puech, K., Snabre, P., 1999. Characterisation of instability of concentrated dispersions by a new optical analyser: the TURBISCAN MA 1000. *Colloids Surf. Physicochem. Eng. Asp.* 152, 111–123. doi:10.1016/S0927-7757(98)00680-3
- Palazolo, G.G., Sorgentini, D.A., Wagner, J.R., 2005. Coalescence and flocculation in o/w emulsions of native and denatured whey soy proteins in comparison with soy protein isolates. *Food Hydrocoll., Food Colloids 2004 (Harrogate)* 19, 595–604. doi:10.1016/j.foodhyd.2004.10.022
- Pérez, J.M., Oliet, M., Alonso, M.V., Rodríguez, F., 2009. Cure kinetics of lignin–novolac resins studied by isoconversional methods. *Thermochim. Acta* 487, 39–42. doi:10.1016/j.tca.2009.01.005
- Pizzi, A. (Antonio), New York : M. Dekker, c1994. *Advanced wood adhesives technology*. M. Dekker, New York.
- Raharitsifa, N., Genovese, D.B., Ratti, C., 2006. Characterization of Apple Juice Foams for Foam-mat Drying Prepared with Egg White Protein and Methylcellulose. *J. Food Sci.* 71, E142–E151. doi:10.1111/j.1365-2621.2006.tb15627.x
- Riccardi, C.C., Astarloa Aierbe, G., Echeverría, J.M., Mondragon, I., 2002. Modelling of phenolic resin polymerisation. *Polymer* 43, 1631–1639. doi:10.1016/S0032-3861(01)00736-4

- Rouimi, S., Schorsch, C., Valentini, C., Vaslin, S., 2005. Foam stability and interfacial properties of milk protein–surfactant systems. *Food Hydrocoll., Food Colloids 2004 (Harrogate)* 19, 467–478. doi:10.1016/j.foodhyd.2004.10.032
- Saint-Jalmes, A., Langevin, D., 2002. Time evolution of aqueous foams: drainage and coarsening. *J. Phys. Condens. Matter* 14, 9397. doi:10.1088/0953-8984/14/40/325
- Sceni, P., Wagner, J.R., 2007. Study on sodium caseinate foam stability by multiple light scattering. *Food Sci. Technol. Int.* 13, 461–468. doi:10.1177/1082013207087815
- Schramm, L.L., 2005. *Emulsions, Foams, and Suspensions: Fundamentals and Applications*. Blackwell Science Publ, Oxford.
- Stadelman, W. J., Newkirk, D., Newby, L., 1995. *Egg Science and Technology*, Fourth Edition, 4th ed.
- Szczurek, A., Fierro, V., Pizzi, A., Celzard, A., 2013a. Mayonnaise, whipped cream and meringue, a new carbon cuisine. *Carbon* 58, 245–248. doi:10.1016/j.carbon.2013.02.056
- Szczurek, A., Fierro, V., Pizzi, A., Stauber, M., Celzard, A., 2014. A new method for preparing tannin-based foams. *Ind. Crops Prod.* 54, 40–53. doi:10.1016/j.indcrop.2014.01.012
- Szczurek, A., Fierro, V., Pizzi, A., Stauber, M., Celzard, A., 2013b. Carbon meringues derived from flavonoid tannins. *Carbon* 65, 214–227. doi:10.1016/j.carbon.2013.08.017
- Szczurek, A., Martinez de Yuso, A., Fierro, V., Pizzi, A., Celzard, A., 2015. Tannin-based monoliths from emulsion-templating. *Mater. Des.* 79, 115–126. doi:10.1016/j.matdes.2015.04.020
- Vera, M.U., Durian, D.J., 2002. Enhanced drainage and coarsening in aqueous foams. *Phys. Rev. Lett.* 88, 088304. doi:10.1103/PhysRevLett.88.088304
- Wang, J., Laborie, M.-P.G., Wolcott, M.P., 2005. Comparison of model-free kinetic methods for modeling the cure kinetics of commercial phenol–formaldehyde resins. *Thermochim. Acta* 439, 68–73. doi:10.1016/j.tca.2005.09.001
- Wang, J., Nguyen, A.V., Farrokhpay, S., 2016a. Effects of surface rheology and surface potential on foam stability. *Colloids Surf. Physicochem. Eng. Asp.* 488, 70–81. doi:10.1016/j.colsurfa.2015.10.016
- Wang, J., Nguyen, A.V., Farrokhpay, S., 2016b. A critical review of the growth, drainage and collapse of foams. *Adv. Colloid Interface Sci.* 228, 55–70. doi:10.1016/j.cis.2015.11.009
- Wisniewska, M., 2010. Influences of polyacrylic acid adsorption and temperature on the alumina suspension stability. *Powder Technol.* 198, 258–266. doi:10.1016/j.powtec.2009.11.016
- Xu, B., Kang, W., Wang, X., Meng, L., 2013. Influence of Water Content and Temperature on Stability of W/O Crude Oil Emulsion. *Pet. Sci. Technol.* 31, 1099–1108. doi:10.1080/10916466.2010.551812

Chapter III: Hydrophobisation of tannin-based foams

III/1. Introduction

The effectiveness of a thermal insulation material depends on its thermal conductivity and its ability to maintain its thermal characteristics over an extended period of time. During the past years it has been confirmed by many investigators that thermal properties such as thermal conductivity, specific heat and thermal diffusivity of thermally insulating porous materials are dependent on both temperature and moisture content (Abdou and Budaiwi, 2013; Jerman and Černý, 2012; Lacoste et al., 2014; Yu et al., 2015). Such thermal properties were found to increase with temperature, but within a limited range related to the characteristic climatic conditions in which the materials have to be used. The observed changes of thermal properties were, therefore, not dramatic as far as only temperature was involved. On the contrary, the dependence on moisture content – itself related to relative humidity – was far more important, affecting especially the insulation materials. The effectiveness of those materials at higher moisture content was indeed reduced in proportion to the moisture content level. The impact of operating temperature and moisture content on insulation thermal conductivity varies with the type of insulation depending on the composition, properties and internal structure of the materials used. From this point of view, the material studied in this thesis, i.e., tannin-based foams are really concerned by this question, due to their promising insulation properties (Basso et al., 2011; Szczurek et al., 2014; Tondi and Pizzi, 2009) and the high hydrophilic character (Tondi and Pizzi, 2009) pointed out in Chapter I of the thesis.

The study of the behaviour of tannin-based foams in the presence of humidity and their modification for turning their hydrophilic character into a more hydrophobic one, i.e., for lowering their affinity for humidity, are really important points to work on. Tannin foams originally have a highly hydrophilic character due to the presence of a huge amount of hydroxyl (–OH) groups (Pasch et al., 2001), which can bind very easily to water molecules. These materials were also shown to be able to absorb several times their own weight of liquid water when soaked inside (Tondi et al., 2009; Zhao et al., 2010a). For limiting this problem, hydrophobisation of tannin foams has been considered in two very recent works. In the first one (Tondi and Petutschnigg, 2015a), tannin foams were heat-treated by infrared with various incident powers for decreasing the surface content of hydroxyl groups and in the second one

(Rangel et al., 2016), tannins were grafted with fatty chains, and then the as-modified materials were used to prepare foams. However, although clear trends in the decrease of hydrophobicity of the foams were found in the two studies, the effect was very limited. It was therefore wondered whether grafting organosilanes, some of them based on perfluoroalkyl chains far more hydrophobic than fatty chains, and taking the place of hydroxyl groups if used in excess, would be a more efficient solution.

It is indeed well known that organosilanes can be covalently grafted on various surfaces for giving them hydrophobic character (Abidi et al., 2007; Akamatsu et al., 2001; Cohen et al., 1992; Cosnier et al., 2005; Fadeev and Yaroshenko, 1996; Krajewski et al., 2004; Picard et al., 2001; Takei et al., 1997). Grafting is generally performed by reaction between $-OH$ surface groups and alkoxy groups of organosilane compounds as presented in Fig. III-1 (Castro et al., 1996; Picard et al., 2001; Schondelmaier et al., 2002). Successive reactions, for instance, second silylation with the first layer or condensation involving two neighbouring groups from different grafted molecules may also occur as reported elsewhere (Cohen et al., 1992; Cosnier et al., 2005; Derouet et al., 1998), leading to a layer of organosilane compound at the surface of the materials and making the latter hydrophobic, or at least much less hydrophilic. As the surface chemistry of tannin-based materials is mainly based on $(-OH)$ groups, the same kind of hydrophobisation process could be expected.

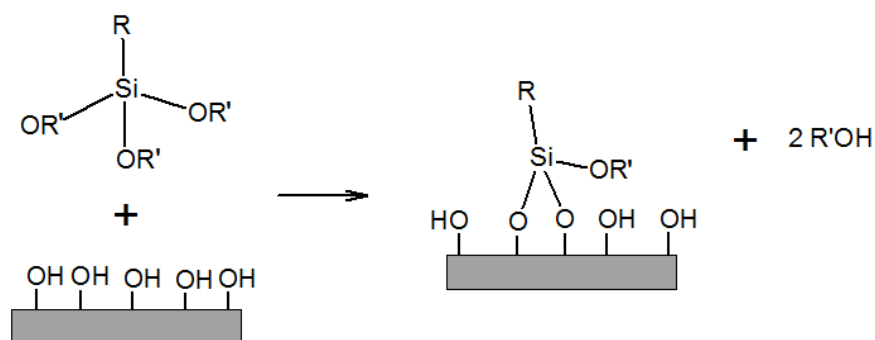


Fig. III-1. Schematic representation of the grafting process of organosilane compounds on a material surface bearing hydroxyl groups.

Thus, the aim of this part of the thesis was to prepare organosilane-grafted tannin-based foams and to quantify the efficiency of such hydrophobisation treatment by different components. Two

organic foams with very different formulations were used in the study in order to compare one with the other, and to obtain a representative idea of how hydrophobisation on tannin-based foams proceeds. The grafting of the foam was performed by use of different organosilanes RSi(OR')_3 , R being $\text{C}_8\text{F}_{17}\text{C}_2\text{H}_4$ or C_2H_3 and R' being CH_3 or C_2H_5 with the purpose of investigating the influence of functional (R) and alkoxy (R') groups on the hydrophobisation efficiency. These reagents were chosen because formerly shown to provide hydrophobic character to various surfaces (Abidi et al., 2007; Cosnier et al., 2005; Krajewski et al., 2004; Kujawa et al., 2014; Picard et al., 2001).

The work carried out hereafter is divided in an experimental part containing the foam preparation, the hydrophobisation process and a detailed description of the different techniques employed to quantify the efficiency of such treatment; a part of discussion of the results, and a part of final conclusions.

III/2. Experimental

III/2.1. Foam preparation

Two different foams were prepared and tested for carrying out this study (Fig. III-2). Both formulations were based on commercial Mimosa tannin, kindly supplied by SilvaChimica (Sant Michele Mondovi, Italy) and commercialised under the name “Fintan OP”. Its industrial extraction process and composition were described in detail in the Chapter II. The rest of components of the formulations and the foaming process of both foams were very different. In fact, the two most different tannin foams formulated so far: Standard-type and Meringue-type foam, were selected for the study.

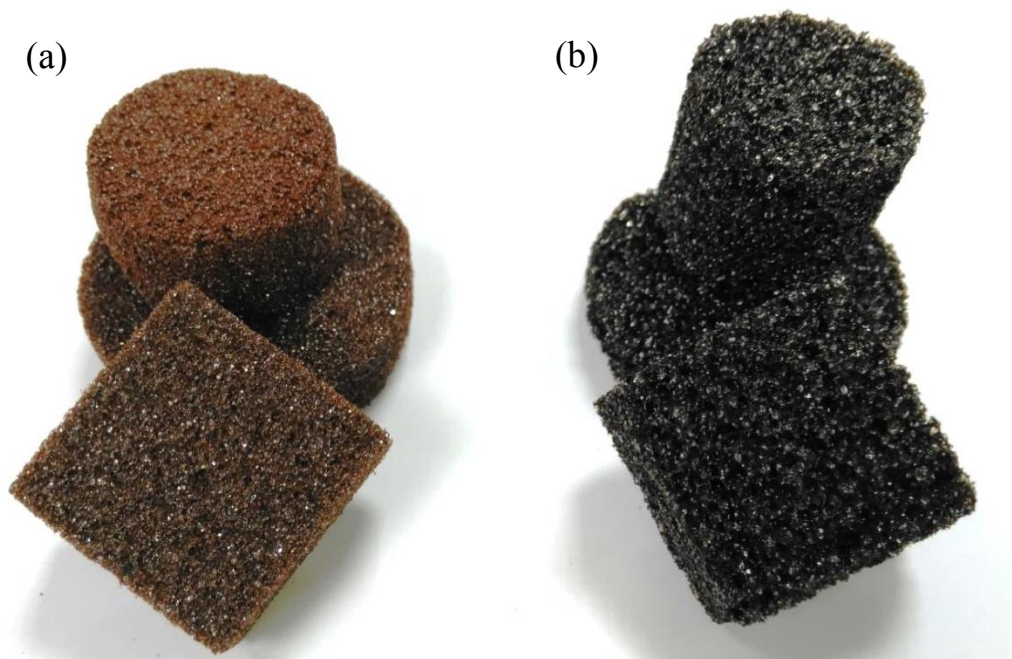


Fig. III-2. Tannin-based foams: (a) Meringue and (b) Standard.

The Standard-type foam is one of the pristine formulations from most others were derived in the past 10 years. It was obtained according to the method described in the “Chapter I/3.3. Formulations of tannin foams”, where a physical foaming due to the evaporation of the blowing agent in the resin undergoing polymerisation takes place (Zhao et al., 2010b). This foam (hereinafter referred to as “Standard”) was similar to the aforementioned Standard Tannin Foams but with a slight modification, the presence of polyethylene glycol as emulsifier. Initially water, polyethylene glycol, furfuryl alcohol and formaldehyde were added into a beaker, and mixed under mechanical stirring at 200 rpm during 2 min. After that, tannin was added and mixed during at least 5 min until obtaining a very homogenous blend. In the next step, the blowing agent, i.e., diethylether was added and stirring was continued during 40 s more at the same speed. Lastly, the 65 wt. % aqueous solution of para-toluene sulphonic acid used as catalyst was included into the mixture. The blend was stirred for another 20 s at higher speed (1000 rpm) and then, it was poured into a plastic container whose inner surface was covered with an aluminium foil beforehand. The whole was then introduced in a ventilated oven with a temperature of between 30 and 35°C before the foaming starts, and kept there for at least 10 minutes. Cooling, stabilisation and drying of the foam was carried out under a hood for about 24 hours before cutting the skin covering the surface and the base, which is generally non-homogeneous.

On the other hand, Meringue-type tannin-based foams (here referred to as “Meringue”) were prepared by polymerisation and hardening of the liquid, tannin-based, foam as described in detail at the beginning of Chapter II (Szczyrek et al., 2014). In our experiment, tannin, solid pTSA and hexamine in powder were carefully dissolved in water at room temperature until a homogeneous brown solution was obtained. The mixture was mechanically stirred with a Teflon-lined blade mixer at 500 rpm for 10 min. In the next step, surfactant was added and then the rotation speed of the blade was increased to 2000 rpm to begin the aeration of the solution gradually. After 30 min of stirring at 2000 rpm the material was protected with an aluminium sheet and transferred into a ventilated oven at 85 °C during 24 h, in which polymerisation was carried out. The specific meringue formulation used in this work was the one concluded to be optimal in the study carried out in Chapter II i.e. meringue tannin foams prepared with 3 g of surfactant and after 30 min of stirring.

After hardening, foams were dried at room temperature during one week. The corresponding formulations are given in detail in Table III-1. The analysis of these two foams by the techniques presented below in subsection III/2.3 allowed detecting if some of the components of the formulation or the foaming process have a positive or negative effect on the interaction of the foams with the moisture and on the grafting process.

Table III-1. Mimosa tannin-based foams formulations. All amounts are expressed in grams.

Ingredients	Standard-PEG foam	Meringue foam
Tannin	30	20
Water	6	30
PEG400 ¹	8	-
Furfuryl alcohol	10.5	-
Formaldehyde (37%)	7.4	-
Hexamine ²	-	1.42
Surfactant ³	-	3
pTSA ⁴	11 (65% aqueous solution)	1.12 (pure)
Diethylether	4	-

¹ Polyethylene glycol of molecular mass 380-420 g mol⁻¹

² Hexamethylenetetramine (also known as 1,3,5,7- tetraazaadamantane)

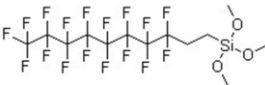
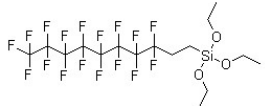
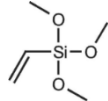
³ Tween® 80 (also known as Polyoxyethylenesorbitan (20) sorbitan monooleate or Polysorbate 80)

⁴ para-Toluenesulphonic acid (also known as 4-methylbenzenesulphonic acid)

III/2.2. Hydrophobisation process

Foam grafting was performed for both kinds of tannin foams with the three different reagents listed in Table III-2, all used as received without further purification. Those three reagents were chosen because a good hydrophobisation was obtained with them in materials such as cotton, silica and zirconia membranes or films, etc. (Abidi et al., 2007; Cosnier et al., 2005; Krajewski et al., 2004; Kujawa et al., 2014; Picard et al., 2001) and their different structure also allow studying the effect of the type of alkyl and functional chain in the efficiency of the process.

Table III-2. Description of hydrophobisation reagents.

Name	Formula	Structure	Notation	Supplier
1H,1H,2H,2H-perfluorodecyltrimethoxysilane	$C_8F_{17}C_2H_4Si(OCH_3)_3$		C8Me	SynQuest Laboratories
1H,1H,2H,2H-perfluorodecyltriethoxysilane	$C_8F_{17}C_2H_4Si(OCH_2CH_3)_3$		C8Et	Alfa Aesar
Vinyltrimethoxysilane	$C_2H_3Si(OCH_3)_3$		VTM	Alfa Aesar

The experiment was carried out by soaking around 2 g (i.e., approximately 30 cm³) of foam sample inside about 100 mL of the organosilane solution (see below for details of the solutions) during 3h, in which grafting reactions were assumed to occur according to the scheme shown in Fig. III-1. All reagents were added in large excess with respect to the hydroxyl groups supposed to be present in the tannin foam. This excess amount was calculated based on the assumption that all hydroxyl groups formerly existing in the flavonoid unit remained and were still available in the final foam. As the amount of tannin per gramme of final foam is known, and as Mimosa tannin is predominantly composed of prorobinetinidin (Pasch et al., 2001) which contains five –OH groups (see Fig. III-3), the number of hydroxyls per gramme of foam could be estimated. Then, it was considered that each grafting molecule was able to react with only one –OH group, even if organosilanes have three active sites. Finally, the corresponding theoretical amount of hydrophobised agent was multiplied by a factor 2. The main reason for using excess amounts is

the requirement of getting a surface fully saturated with hydrophobic chains, taking into account the fact that, given the expected heterogeneous distribution of hydroxyl groups in the foam, the probability of finding three nearest –OH neighbours able to react with one single organosilane molecule is probably low.

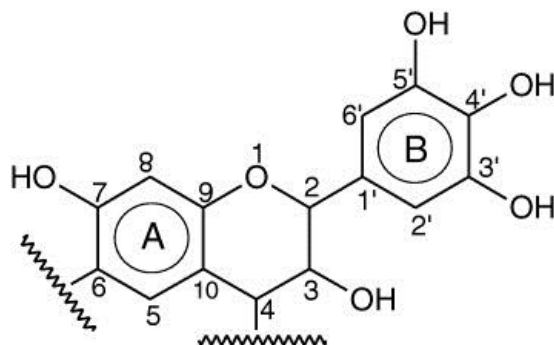


Fig. III-3. Prorobinetinidin, the main compound of Mimosa tannin.

The impregnation procedure was defined according to the reagent employed:

- C8Me was dissolved in dry methanol, and the reaction took place in a beaker under stirring at 400 rpm formerly installed in a vacuum bell jar at room temperature in order to remove the air inside the foam and facilitate its complete impregnation. The foam was installed in a protective grid inside the beaker with the solution in a manner that it was protected from shocks with the magnetic stirring and it was completely impregnated with the solution.
- C8Et was dissolved in dry ethanol at room temperature, and process was the same as described above.
- VTM was dissolved in pure toluene, and the reaction was performed under reflux at 110°C in a round-bottom flask equipped with a condenser as explained elsewhere (Cosnier et al., 2005).

After 3h, the hydrophobised Standard-PEG-type (S) and Meringue-type (M) samples were dried for 2h in a vacuum oven at 60°C and were labelled SC8Me, SC8Et, SVTM, MC8Me, MC8Et and MVTM depending on the chemical used: C8Me, C8Et and VTM, respectively.

III/2.3. Foam characterisation

The morphology of the untreated tannin-based foams was first characterised, then the effectiveness of the hydrophobisation process was investigated. The latter was evaluated through FTIR spectroscopy studies, and by considering the following characteristics and properties before and after treatment: contact angle and surface energy, water vapour sorption, and thermal conductivity. All tests (unless otherwise specified) were carried out in the same, controlled, relative humidity because of the major influence of the latter on such properties. Such influence was verified by measuring the contact angle of the two untreated foams at different relative humidities and noting that the results were different, as shown in Fig. III-4. For that purpose, the samples were completely dried for 2h at 60°C under vacuum in a first step and then conditioned for 24h in a humidity-controlled oven before testing.

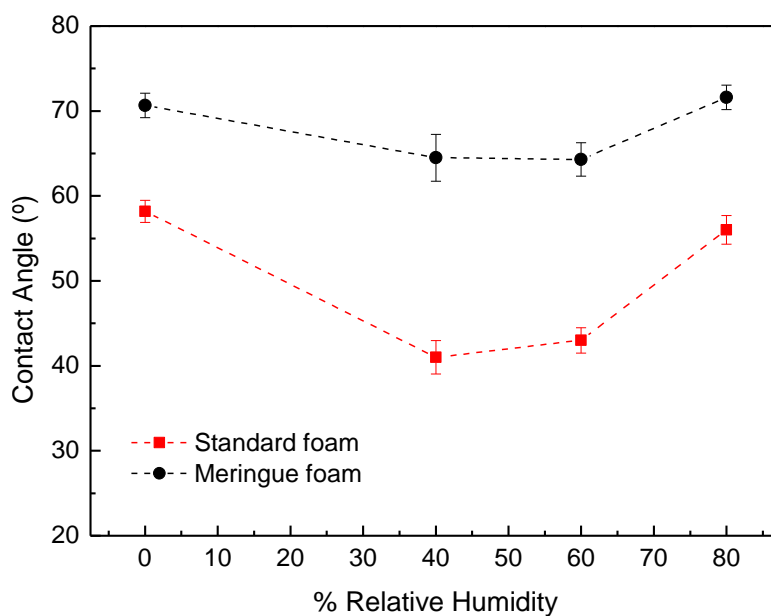


Fig. III-4. Water contact angle measured by Washburn method (see next section for details) at the surface of untreated foam samples formerly conditioned at various values of relative humidity.

Fig. III-4 clearly shows the big influence of the relative humidity on the resultant contact angle. In the present case, the contact angle presents a minimum at medium values of relative humidity. Although unexpected, the experiments were repeated several times and led to the same results. Moreover, the same behaviour has been already reported by other authors (Hołysz et al.,

2010; Mittal, 2008) working with strongly polar materials bearing hydroxyl functional groups at their surface, i.e., similar to tannin-based foams from this point of view.

III/2.3.1 Morphological characterisation

The most relevant and quantifiable parameters that can be measured on porous materials such as tannin foams, in term of morphological characterisation, are apparent density, relative density, porosity and cell size. The total porosity, Φ (dimensionless), was calculated according to Eq. (III-1), in which ρ_{ap} (g cm^{-3}) and ρ_s (g cm^{-3}) are the apparent density and the skeletal density of the foams, respectively:

$$\Phi = 1 - \frac{\rho_{ap}}{\rho_s} \quad (\text{III-1})$$

Here, ρ_{ap} , defined as the mass of the material divided by the total volume it occupies, was calculated by weighing a number of parallelepiped samples and measuring their dimensions with a calliper and ρ_s , the density of the solid from which the considered material is made of, was estimated by helium pycnometry using an Accupyc II 1340 (Micromeritics, USA) apparatus. So as to measure the skeletal density, all samples were ground into fine powder to be able to introduce as high amounts of material as possible in the sample holder of the pycnometer, but also to limit the contribution of any possible closed porosity. These powders were also dried overnight at 60°C under vacuum to avoid any influence of humidity on the results. The powder was then placed in a standard chamber of 10 cm^3 and the variation of helium pressure was measured with high accuracy, including 10 helium flushes in order to clean the volume chamber and to remove contaminants and gases that could eventually be found on the surface of the sample or in the room, followed by 30 analytical runs.

The average cell size of the foams was determined using a technique based on simple principles of stereology exposed by Underwood (Hilliard, 1967; Underwood, 1969). This method consists in counting the number of cells per unit length of straight lines drawn parallel to the principal directions of a number of scanning electron microscopy (SEM) pictures of the sample (see the example shown in Fig. III-5) and then, determining the average linear density of cells N_c . Such count was carried out by application of the ImageJ software on 3 to 4 SEM images of each

foam sample. If the cells are considered as perfect spheres as already suggested in the work of Gibson & Ashby (Gibson and Ashby, 1997) and in many other publications (Li et al., 2013; Martinez de Yuso et al., 2014; Szczurek et al., 2014), their equivalent diameters can be determined applying the following equation:

$$D_C = \frac{1.5}{N_C} \quad (\text{III-2})$$

where D_C is the average cell diameter. For each foam, the cells were then counted on at least 8 to 10 lines in each of the two directions of the 3 or 4 images analysed.

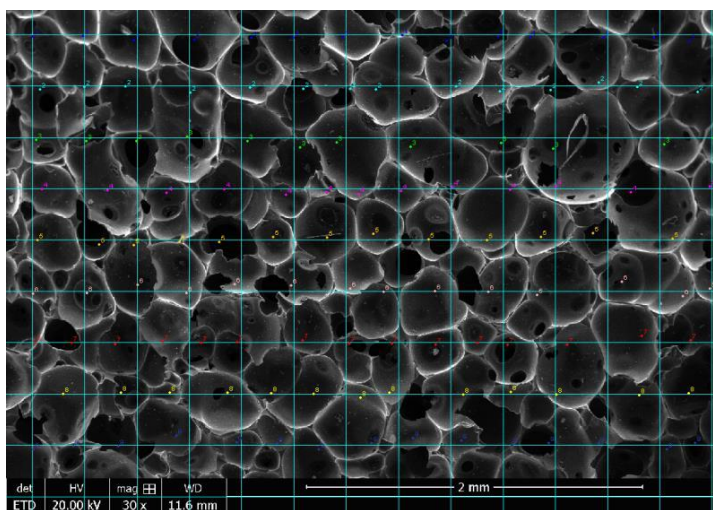


Fig. III-5. Determination of the mean linear cell density by counting the numbers of cells along lines of known length by the use of the « cell counter » tool of ImageJ software. The markers here correspond to the counts of the cells along the 9 horizontal lines, and the same is repeated along the vertical lines.

III/2.3.2 *Elemental analysis*

Elemental analysis is a technique that provides the total content of carbon (C), hydrogen (H), nitrogen (N) and sulphur (S) from any organic or carbonaceous material. In this study, this technique was performed, mainly, to check the oxygen content of the pristine foams and to detect the differences in composition between the 2 types of formulations investigated here. Thus, the ultimate composition of Standard-PEG and Meringue samples was determined by using a Vario EL Cube (Elementar, Germany) elemental analyser (Fig. III-6). The weight fractions of C, H, N and S were first determined from the gases obtained by burning a piece of the sample in an

excess of dioxygen at a temperature of approximately 1150°C. Gaseous CO₂ and H₂O were directly obtained, whereas N₂ and SO₂ were produced after reduction of NO_x and SO_x on hot copper. These four gases were then separated and quantified by a chromatographic column. As the oxygen amount present in the sample could not be determined in the same run, another piece of sample was burnt and the resultant CO₂ was reduced into CO which was then quantified, thereby leading to the oxygen fraction in the material.

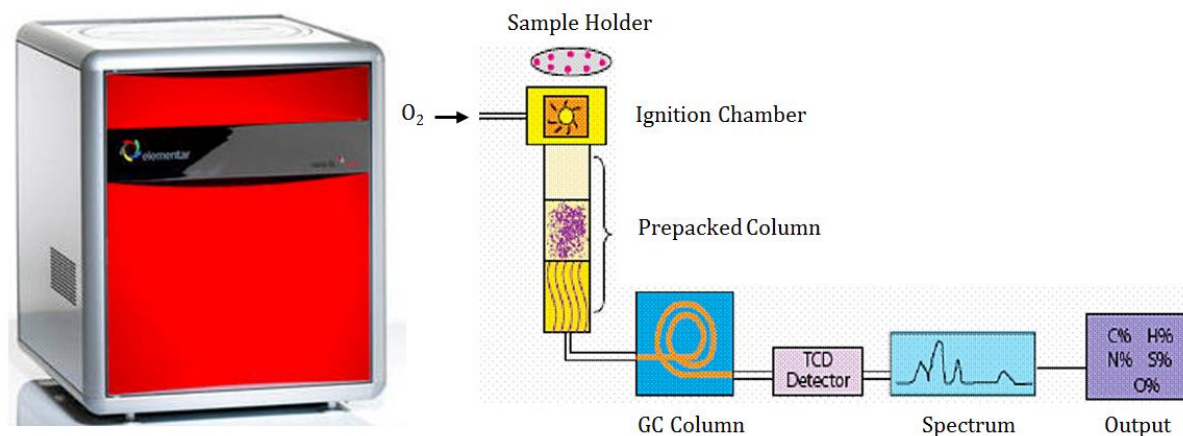


Fig. III-6. Vario EL Cube elemental analyser and diagram of the measurement.

III/2.3.3 Fourier-transform infrared (FTIR) spectroscopy

Spectroscopy is a helpful mean of investigating molecular structure and composition based on the study of the interaction of radiation with matter. The substance of interest is submitted to an electromagnetic radiation of known incident intensity and frequency, and the transmitted or scattered intensity and frequency are recorded. More exactly, spectra are recorded in the form of graphs showing the resultant intensity after interaction with matter, as a function of wavelength or wavenumber. The mid-infrared region (IR) extends from 4000 cm⁻¹ to 400 cm⁻¹. Functional groups and other specific groups of atoms usually absorb infrared radiation in a relatively narrow frequency range, regardless of the structure of the rest of the molecule. FTIR spectroscopy is thus a rather simple, commonly used, identification method of functional groups and other elements of molecular structure.

FTIR studies were carried out with a Brücker Equinox 55 spectrometer, on the basis of dry samples ground (1 mg), dispersed in – and pressed with – dry potassium bromide (150 mg). A blank sample of pure KBr was also prepared for the reference spectrum. The pellets were investigated in transmission mode from 400 to 4000 cm^{-1} (six scans per spectrum at a resolution of 2 cm^{-1}). A typical IR spectrum is represented as plot of transmittance (%T) versus wavenumber (cm^{-1}).

III/2.3.4 Contact angle measurements

The simplest technique for studying the wettability of a material consists in measuring the angle formed at the contact with a liquid droplet. However, in the case of porous materials, and especially for hydrophilic ones, it is necessary to take into account the possible capillary or pore wetting as the liquid may spontaneously penetrate the porosity during contact angle measurement. With the aim of limiting such source of errors, two different methods have been used to study the wettability of these foams:

(a) Sessile drop method was used for hydrophobised foams, for which no spontaneous water imbibition was expected, using a liquid-solid contact angle analyser (DSA100, Krüss, Germany). Droplets of liquids of 2 μL were placed on the sample with an automatic drop deposition system. The contact angles were measured with the Krüss software from the droplet images captured with a digital camera. The measurements were performed at 20°C and 40% relative humidity, repeated at least 10 times on different fresh surfaces of the foams and the results averaged. Moreover, each contact angle was obtained by measuring the angles on the left- and right-hand sides of each droplet and taking the average. An example of the measurement of the contact angle in an image captured by the camera can be seen in Fig. III-7(a).

(b) Washburn method was used for non-treated, hydrophilic, foams, using a force tensiometer (DCAT21, Dataphysics, Germany). The principle of this measurement is based on the capillary rise of water in powder beds (see scheme in Fig. III-7(b)). A vertically suspended glass tube closed at the bottom by a sintered-glass filter was attached to the fixing clamp of the tensiometer. Afterwards, the system was brought carefully into contact with the liquid and the variations of mass were recorded as a function of time. The use of reproducible packing of finely ground foam

powder in the tube was essential for obtaining reliable results. The experiments were also performed with a perfectly wetting liquid (hexane) for which contact angle is equal to zero in order to determine the geometric factor C of Washburn's modified equation (III-3), see below. Average values of two independent measurements of the contact angle at 20°C and 40% relative humidity were calculated. Washburn's modified equation provides the relationship between liquid penetration rate and contact angle (θ) according to:

$$t = \left(\frac{\eta}{C\rho^2\gamma_l \cos\theta} \right) M^2 \quad (\text{III-3})$$

where t is the contact time, M is the mass of liquid rising into the porous sample, η , ρ and γ_l are viscosity, density and surface tension of the liquid in contact, respectively, and C is a material's constant which depends on powder bed porosity (ε), equivalent pore radius (r_c) and powder packing radius (R) as given by Eq. (III-4):

$$C = \frac{r_c \varepsilon^2 (\pi R^2)^2}{2} \quad (\text{III-4})$$

For the determination of the contact angle, the linear part of the curve of the squared mass (M^2) vs. time was used. It was considered that, at the beginning of the test, the capillary rise was governed by inertial forces disturbing the linear variation of M^2 versus time (Quéré, 1997; Siebold et al., 2000) and, therefore, only data points recorded later than 0.5 s after the initial contact were taken into account for the calculations.

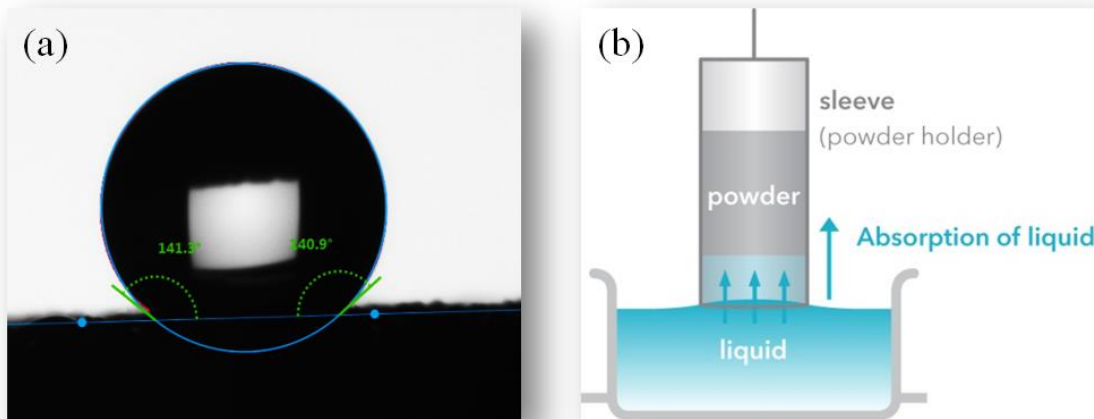


Fig. III-7. Details of contact angle measurements: (a) Sessile drop method and (b) Washburn method.

III/2.3.5 *Surface energy determination*

The surface free energy is another important factor for evaluating the wettability of the foams, and hence their hydrophobic/hydrophilic behaviour towards water. The surface energy of tannin foams was calculated based on contact angle measurements from sessile drop and Washburn methods. In the literature, the general equation describing the gas – liquid – solid triple point interface at equilibrium is called Young's equation (Young, 1805) and reads:

$$\gamma_s = \gamma_{sl} + \gamma_l \cos\theta \quad (\text{III-5})$$

where γ_s is the surface free energy of the solid, γ_{sl} is the solid-liquid interfacial tension, γ_l is the surface tension of the considered liquid, and θ is again the contact angle between the solid and the liquid.

There are several methods for analysing the surface free energy of solids based on the physical geometries of liquid droplets that differ in the way in which the interactions between the individual phases are interpreted. In the present study, the Owens, Wendt, Rabel and Kaelble (OWRK) method was applied to estimate the surface energy of the foam from the contact angle measured with several liquids. For doing so, the surface energy was divided into polar and dispersive parts, such as:

$$\gamma_s = \gamma_s^d + \gamma_s^p \quad (\text{III-6})$$

$$\gamma_l = \gamma_l^d + \gamma_l^p \quad (\text{III-7})$$

where γ_s^d and γ_l^d are the dispersive surface energy components of solid and liquid, respectively, and γ_s^p and γ_l^p are the corresponding polar parts.

The solid-liquid interfacial tension (γ_{sl}) can be calculated from the geometric mean of the contributions of the liquid and the solid, and reads:

$$\gamma_{sl} = \gamma_s + \gamma_l - 2 \left(\sqrt{\gamma_s^d \cdot \gamma_l^d} + \sqrt{\gamma_s^p \cdot \gamma_l^p} \right) \quad (\text{III-8})$$

Based on this approach, Owens, Wendt, Rabel, and Kaelble developed a linear equation (Kaelble, 1970; Owens and Wendt, 1969), in which the slope and the intercept are given by the square root of polar and dispersive components of the surface free energy, respectively:

$$\frac{\gamma_l(1+\cos\theta)}{2\sqrt{\gamma_s^d}} = \sqrt{\gamma_s^p} \sqrt{\frac{\gamma_l^p}{\gamma_l^d}} + \sqrt{\gamma_s^d} \quad (\text{III-9})$$

Thus, the measurement of contact angles of various test liquids having known surface tension and polar and dispersive components enables the determination of surface energy as a sum of polar and dispersive parts. As test liquids, polar liquids such as water and ethylene glycol and non-polar liquid such as diiodomethane have been chosen, whose surface tension and polar and dispersive parts are gathered in Table III-3.

Table III-3. Surface tension and corresponding polar and dispersive parts of liquids used for the determination of surface energy (Jańczuk and Białopiotrowicz, 1989).

Liquid	γ_l (mN m ⁻¹)	γ_l^p (mN m ⁻¹)	γ_l^d (mN m ⁻¹)
Water	72.8	51	21.8
Ethylene glycol	47.7	21.3	26.4
Diiodomethane	50.8	0	50.8

III/2.3.6 *Water vapour sorption*

The amount of vapour water adsorbed on a given material varies as a function of relative pressure and temperature. The curve formed at constant temperature by the plot of this sorbed quantity as a function of relative pressure is called isotherm. The hydrophilicity of any sorbent can also be quantitatively and qualitatively classified according to IUPAC based on the type of the sorption isotherms (Ng and Mintova, 2008). Basically, the water sorption isotherms are divided into seven types (Fig. III-8(b)). The isotherm type I is observed with very hydrophilic materials interacting with water, presenting a high water sorption capacity and fast saturation at low relative pressure (P/P_0). On the other hand, hydrophilic materials may also exhibit sorption isotherms of types II or IV, whereby a considerable sorption capacity of water at low P/P_0 and

high P/P_0 is measured. These two types of isotherms are the ones expected for untreated tannin-based foams. Additionally, the rare type VI step-like isotherm is also characteristic of hydrophilic sorbent having stepwise sorption. In contrast, sorption isotherms types III and V describe hydrophobic or poorly hydrophilic materials with low sorption at low P/P_0 and sometimes moderate sorption at medium P/P_0 , and suddenly high water sorption at P/P_0 close to 1. For highly hydrophobic sorbents, isotherm type VII can be observed, which gives a low sorption of water throughout the entire P/P_0 range.

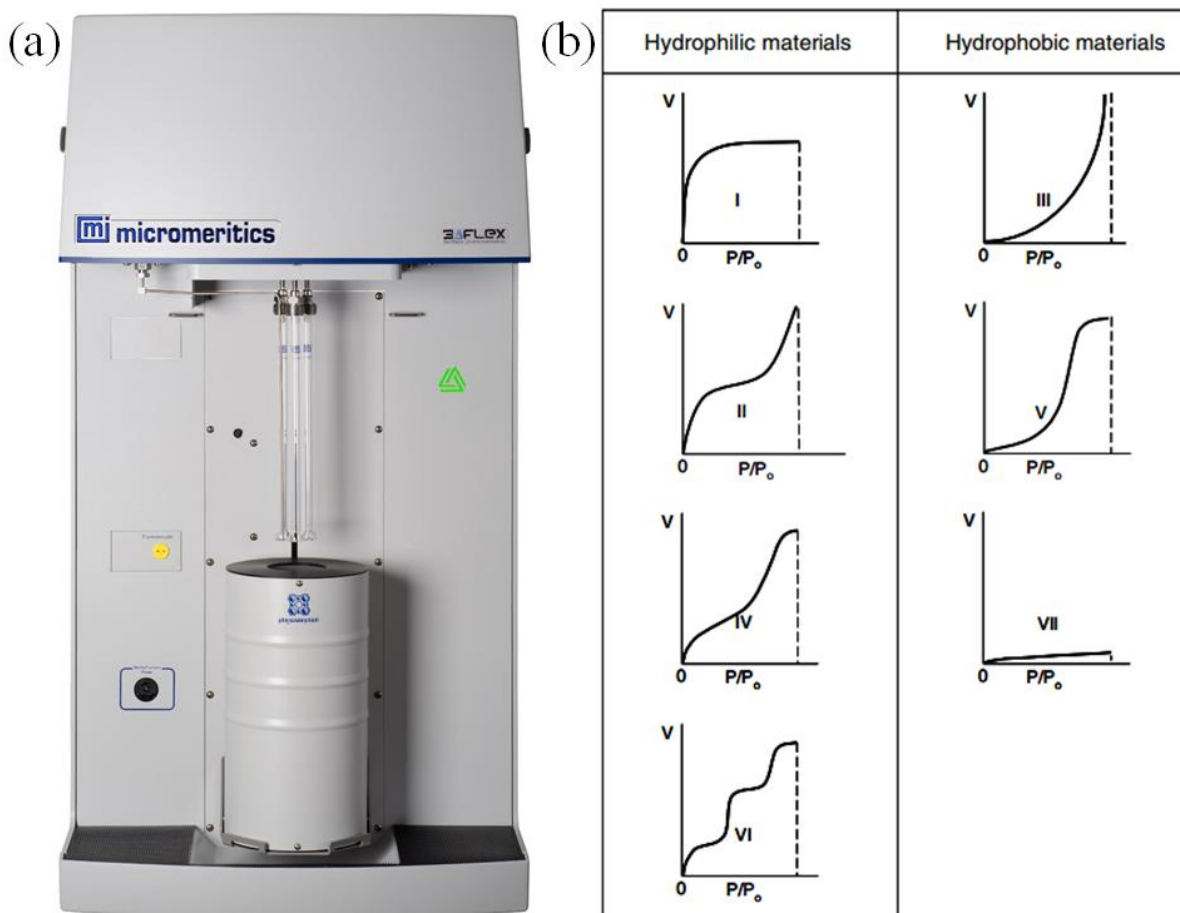


Fig. III-8. (a) 3Flex apparatus and (b) types of adsorption isotherms classified according to IUPAC (Ng and Mintova, 2008).

The two principal methods of measuring adsorption equilibrium are classified as volumetric/manometric and gravimetric, depending upon whether the amount of adsorbed gas is determined by means of experimental measured pressure or by direct measurement of the weight

gained by the adsorbent. Herein, the manometric method was used for obtaining the isotherms, in particular, the water vapour sorption-desorption isotherms were obtained with an automatic adsorption apparatus (3Flex, Micromeritics, USA) (Fig. III-8(a)). It is based on the measurement of the pressure drop after small amounts of water vapour are introduced in a sample holder of known volume at a given temperature. Sorption isotherms can, therefore, be obtained in the whole range of relative humidity and at a temperature which can be controlled. Prior to analysis, the samples were outgassed under secondary vacuum at 40°C for at least 72h. Afterwards, sorption measurements were performed by dosing water vapour at relative pressures (P/P_0) ranging from 0.01 to 0.9 at 20°C and measuring the water sorbed at equilibrium for each value of P/P_0 . Once $P/P_0 = 0.9$ was reached, desorption was monitored, and the corresponding sorbed volumes of water at equilibrium were measured in order to build the desorption branch of the isotherm. At least 60 points of water uptake (mass of water per unit mass of dry foam) vs relative pressure were recorded for each sorption-desorption isotherm. The equilibrium times were quite long so that the entire sorption-desorption process lasted for about ten days.

III/2.3.7 Thermal conductivity

The thermal conductivity test was performed by the transient plane source method with a thermal conductivity analyser (Hot Disk TPS 2500, ThermoConcept, France) at stable room temperature (21°C) and different values of relative humidity (0 – 90%). Thermal conductivity was calculated using the Hot Disk 6.1 software. The power employed for the analysis was 10mW and the sensor had radius of 6.403mm. Fig. III-9 shows some details of the device and of the probe.

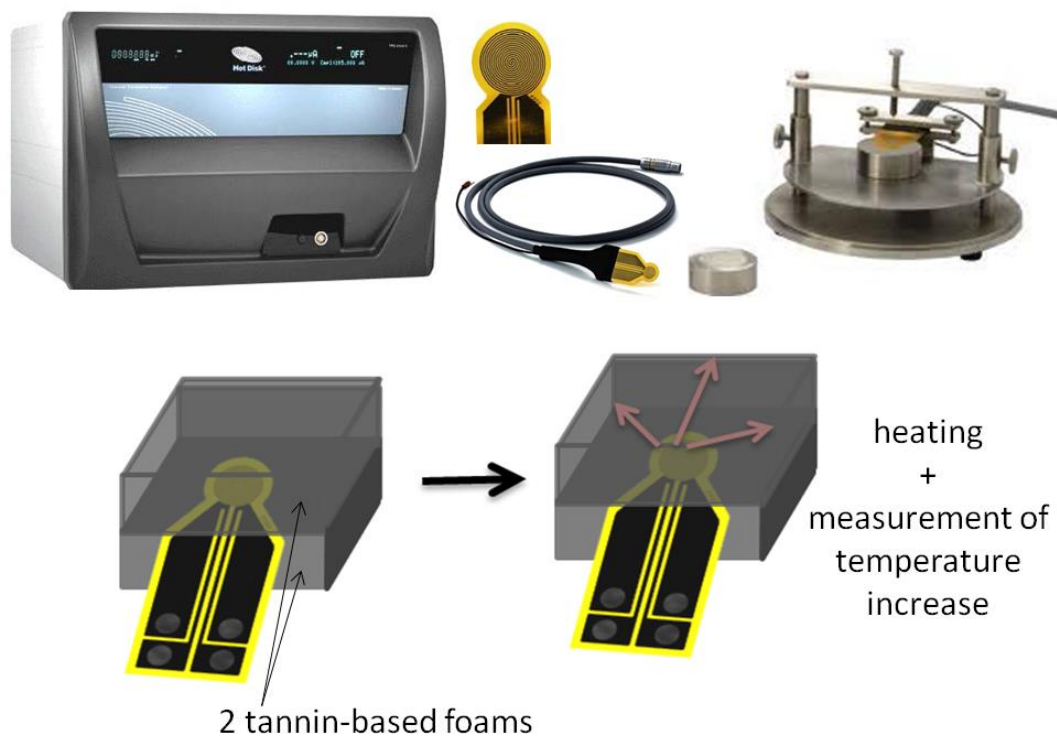


Fig. III-9. HotDisk TPS 2500 device and details of the probe.

The method is based on a transiently heated plane sensor that acts both as heat source and dynamic temperature sensor. The more insulating is the material, the more the local temperature increases even at very low heat outputs. On the contrary, a thermally conductive material requires higher heating capacities to cause a slight increase in temperature. This sensor consists of an electrically conducting pattern in the shape of a double spiral, which has been etched out of a thin nickel foil and sandwiched between two thin sheets of Kapton®. During the experiment, the hot disk sensor was fitted between two identical pieces of samples, having relevant sizes for considering them as semi-infinite media.

III/3. Results and discussion

III/3.1. Foam characteristics

The main features of the two tannin-based foams are given in Table III-4. It was observed that despite prepared in very different ways (physical foaming for standard foams (Standard) and for

meringue foams (Meringue)), both are very similar in terms of total porosity, as they present comparable values of bulk and skeletal density. The different formulations and ways of preparation, however, made the cell sizes rather different, the average cell diameter of standard sample being roughly two times higher than that of meringue foam.

Table III-4. Main features of the two studied tannin-based foam samples.

Property	Sample	
	Standard foam	Meringue foam
Bulk density (g cm ⁻³)	0.070	0.056
Skeletal density (g cm ⁻³)	1.55	1.50
Total porosity (%)	95.5	96.3
Cell size (µm)	~ 1400	~ 600

From the point of view of elemental composition (Table III-5), meringue foam was rather rich in nitrogen due to the use of hexamine as crosslinker. In contrast, the standard sample was rich in sulphur because more pTSA was used in the formulation. The level of other elements was, however, very comparable, especially in terms of oxygen content which may significantly account for differences of affinity towards water. The oxygen content in meringue foams was only slightly higher than in standard foams.

Table III-5. Ultimate analysis of the two studied tannin-based foams.

Ultimate analysis	Sample	
	Standard foam	Meringue foam
C (wt.%)	57.5	55.25
H (wt.%)	5.43	5.57
O (wt.%)	34.3	35.97
N (wt.%)	0.23	2.32
S (wt.%)	2.55	0.88

III/3.2. Organosilane grafting observed by FTIR

FTIR spectra of each pristine and grafted foam sample were recorded, with emphasis on the wavenumber region allowing detecting the presence of silane groups, as shown in Fig. III-10. This method can only confirm the presence of the organosilanes in the sample without explicitly proving their covalent grafting in the polymer of the foam. However, the latter reaction should have occurred in the same way as abundantly described in the literature (see again Fig. III-1 and related references), since it was proved to be very effective in the conditions that we have used. Moreover, it is very well known that the silanes are very reactive with hydroxyl groups and that our material is based on polyphenols, whose surface chemistry is precisely based on hydroxyl groups, so covalent grafting should have occurred indeed.

The more interesting absorption bands are the following. The spectral region between 1800 and 1300 cm^{-1} is strongly dominated by the aromatic structure of tannin-based thermoset polymers (Tondi et al., 2015; Tondi and Petutschnigg, 2015b). For instance, the strong peak at around 1610 cm^{-1} is typically attributed to C=C stretching in benzene ring. The spectral region between 1450 and 1370 cm^{-1} represents principally the bending of C-H groups attached to aromatic molecules. The region between 1550 and 1500 cm^{-1} is also dominated by heteroaromatic compounds and the band around 1720 cm^{-1} is assigned to carbonyl groups, mostly in the form of quinones that account for the typical red-brown colour of tannin-based resins.

The bands at 1240 cm^{-1} and 1205, 1153 and 1075 cm^{-1} , corresponding to stretching vibrations of the $\text{C}_x\text{F}_{2x+1}$ and $\text{Si}-\text{CH}_2\text{CH}_2\text{C}_x\text{F}_{2x+1}$ groups (Picard et al., 2001), respectively, appeared in foams treated with C8Me and C8Et, thereby indicating the presence of these compounds in the corresponding samples. Characteristic absorption peaks were also observed near 800 cm^{-1} in the foam treated with VTM, assigned to the presence of Si-CH from the vinyl group in silane (Ahmed et al., 2009; Cosnier et al., 2005), as expected.

The absence of significant peaks at 1092 and 1192 cm^{-1} in the spectra of VMT and C8Me, characteristic of the methoxy groups $\text{Si}-\text{O}-\text{CH}_3$, and of peaks at ~ 1100 cm^{-1} in those of C8Et, characteristic of $\text{Si}-\text{O}-\text{CH}_2\text{CH}_3$, indicate that silane grafting reactions occurred (Jiao et al., 2005). Only a small absorption band at 1092 cm^{-1} in the spectra of MVMT was seen, derived probably from some unreacted silane groups due to their use in excess and also probably due to steric impediment.

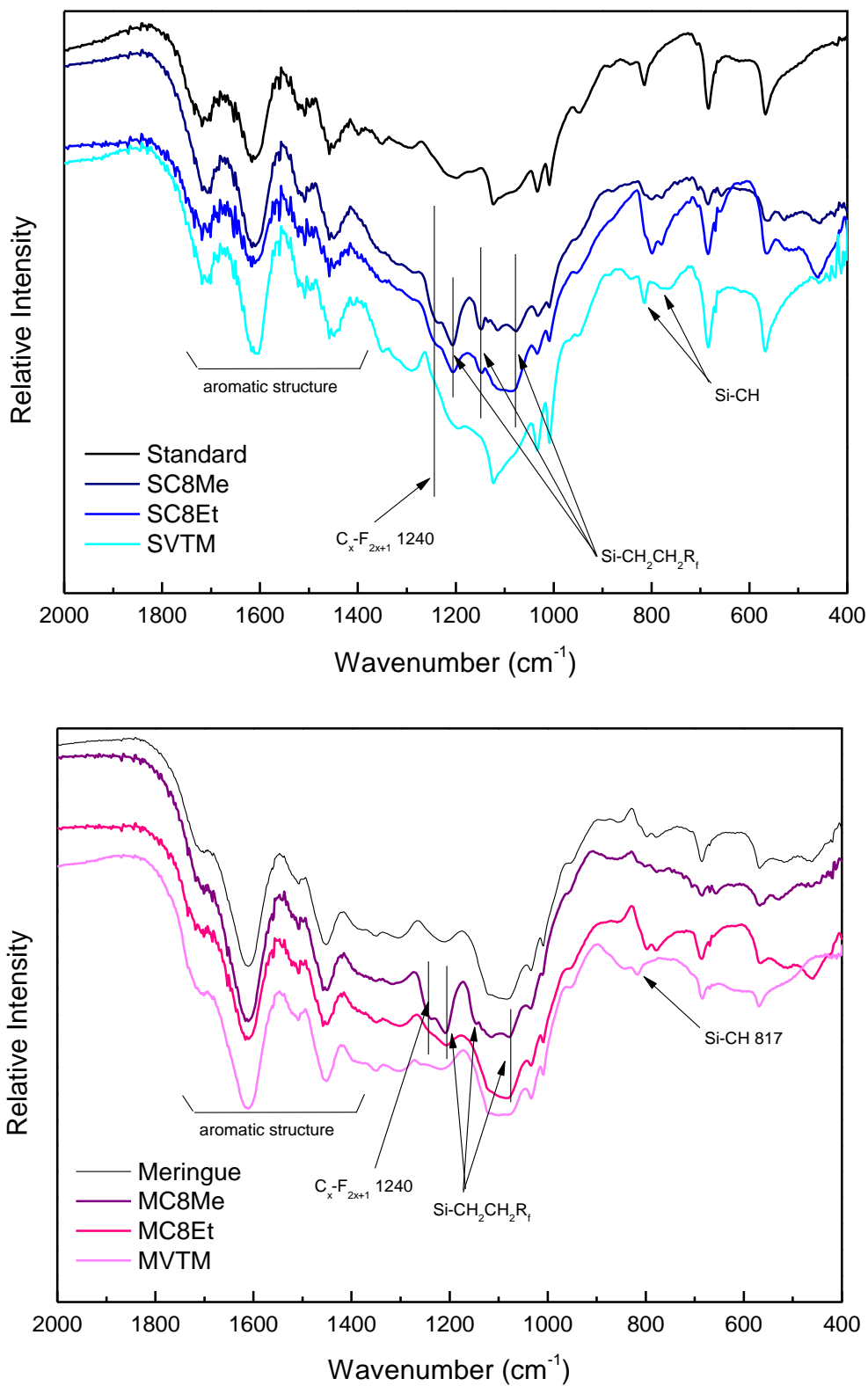


Fig. III-10. FTIR spectra of untreated and treated tannin foams based on standard (top) and meringue (bottom) formulations.

III/3.3. Surface properties

Measurements of contact angles of various test liquids were carried out at the surface of untreated and treated tannin foams in order to detect the expected improvement of the hydrophobic character of the foams. Such way of doing not only gave information about the wettability of raw and grafted tannin-based foams, but also allowed determining their surface free energy. All the results are reported in Table III-6.

Table III-6. Measured contact angles of various liquids on tannin-based foams, and calculated values of their total surface energy γ_s , as well as their dispersive γ_s^d and polar γ_s^p parts. All measurements were made at 20°C and 40% RH.^A

Sample	Mean contact angle (°)			Surface energy (mN·m ⁻¹)		
	Water	Ethylene glycol	Diiodomethane	γ_s	γ_s^d	γ_s^p
Standard	41.0 ± 1.9	0.0 ± 0.0	80.2 ± 1.2	57.8 ± 3.2	12.8 ± 0.7	45.0 ± 2.5
SC8Me	143.2 ± 1.5	129.3 ± 4.2	122.6 ± 3.9	2.8 ± 0.3	2.8 ± 0.3	0.0 ± 0.0
SC8Et	132.8 ± 2.5	139.2 ± 3.1	124.6 ± 4.3	2.3 ± 1.3	2.0 ± 0.9	0.3 ± 0.1
SVTM	134.0 ± 4.0	121.3 ± 4.3	109.9 ± 4.0	5.4 ± 0.4	5.4 ± 0.4	0.0 ± 0.0
Meringue	64.5 ± 2.8	2.1 ± 1.9	73.1 ± 2.4	41.2 ± 2.1	20.2 ± 0.2	21.0 ± 1.9
MC8Me	137.2 ± 2.7	136.9 ± 2.9	133.3 ± 2.9	1.3 ± 0.5	1.1 ± 0.4	0.2 ± 0.1
MC8Et	131.9 ± 3.9	130.7 ± 4.1	127.7 ± 4.4	2.1 ± 0.9	1.7 ± 0.6	0.4 ± 0.3
MVTM	132.9 ± 2.4	110.5 ± 3.2	73.2 ± 4.5	21.7 ± 2.3	19.9 ± 1.6	1.8 ± 0.7

^A Data are presented as means ± standard deviation.

The rather low contact angle of water on non-grafted materials results from the highly hydrophilic character of raw tannin-based foams as a consequence of the high amount of hydroxyls in their polymer structure. Such number of –OH groups allowed the grafting of hydrophobic chains and, as a result, the contact angle increased significantly. Interestingly, the formulation had a significant impact on the initial wettability of the raw materials at 40% RH, and standard foams were more hydrophilic (contact angle 41°) than meringue foams (contact angle 64.5°). No such differences were expected, and especially not that way because meringue

foam has slightly higher oxygen content as shown in Table III-5. The measurements were thus repeated to check the contact angles, but all led to the same value which suggests that some oxygen groups may not be easily available in meringue foam. It is also likely that the much more acidic formulation of the standard foam (see again Table III-1) made it more hydrophilic. Indeed, the observed behaviours cannot be attributed to differences in structure, as both samples were ground for applying Washburn's method. The sessile drop method could indeed not be used due to the hydrophilicity of the foams, as any drop placed at their surface would have been immediately absorbed, thus preventing any direct contact angle measurement.

After treatment, the contact angle of water on both kinds of materials converged toward the same, high, values in the range $130 - 140^\circ$, irrespective of the formulation. That fact supports the efficiency of the treatment, see Fig. III-11. This finding also proves that, although the number of $-OH$ groups, existing or accessible, in the foam was probably different at the beginning, all reagents were suitably used in excess, since the same contact angles were obtained for each hydrophobisation agent. Moreover, the cells of Standard and Meringue samples were interconnected and large enough for allowing an excellent impregnation of the foams by the organosilanes. This supposition was confirmed by cutting the samples through the middle, measuring the contact angle on the new surfaces created and obtaining always similar results.

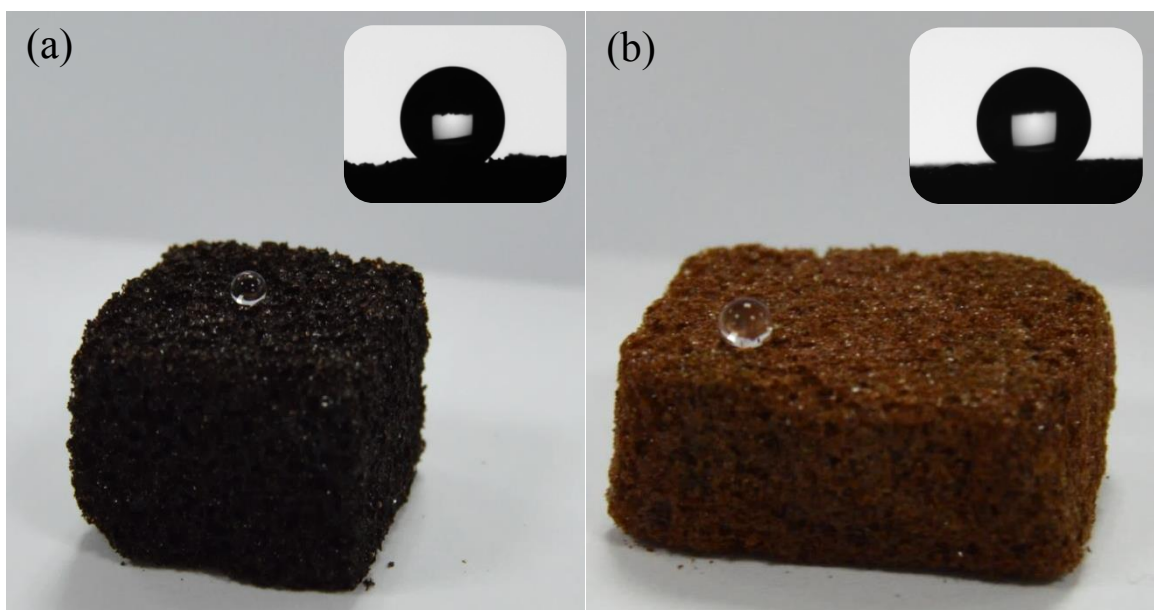


Fig. III-11. Top view of a droplet of water deposited on C8Me-grafted foams: (a) Standard; (b) Meringue.

Focusing on the data of surface energy, it was possible to confirm the above conclusions because raw Standard foam presented the highest value, as shown in Fig. III-12. Such foam is more hydrophilic than Meringue because of their significantly higher polar part, which is the main contribution to their surface energy. The latter dropped dramatically after chemical grafting, and especially the polar part vanished completely or almost. Such finding may be assumed to be due to the coating of the foam surface with a monomolecular layer of hydrophobic organosilane compounds (Schondelmaier et al., 2002).

The dispersive part also considerably decreased in most samples. However, in contrast with the polar part, the dispersive part was found to depend on the kind of reagent used, and especially on the nature of its functional group. Fluoroalkyl-silanes (C8Me and C8Et) reduced the dispersive part more than did alkenyl-silanes (VTM). For both kinds of Standard and Meringue foam formulations, C8Me was the reagent leading to the highest contact angle, although the difference with C8Et is probably not significant. VTM was found to be less efficient than the other hydrophobisation reagents in the case of meringue foam, since the surface energy did not decrease that much, with a resultant non-zero polar part. The fluorinated chains probably induced a more hydrophobic character to the foam than the vinyl group.

The obtained results are comparable and even better in terms of hydrophobic character than those of common, non-polar, industrial polymers such as PE or PTFE, which exhibit surface free energies of $32.82 \text{ mN}\cdot\text{m}^{-1}$ ($\gamma_s^p = 0.72 \text{ mN}\cdot\text{m}^{-1}$; $\gamma_s^d = 32.10 \text{ mN}\cdot\text{m}^{-1}$) and $21.77 \text{ mN}\cdot\text{m}^{-1}$ ($\gamma_s^p = 0.05 \text{ mN}\cdot\text{m}^{-1}$; $\gamma_s^d = 21.72 \text{ mN}\cdot\text{m}^{-1}$), respectively (Jańczuk and Białłopiotrowicz, 1989).

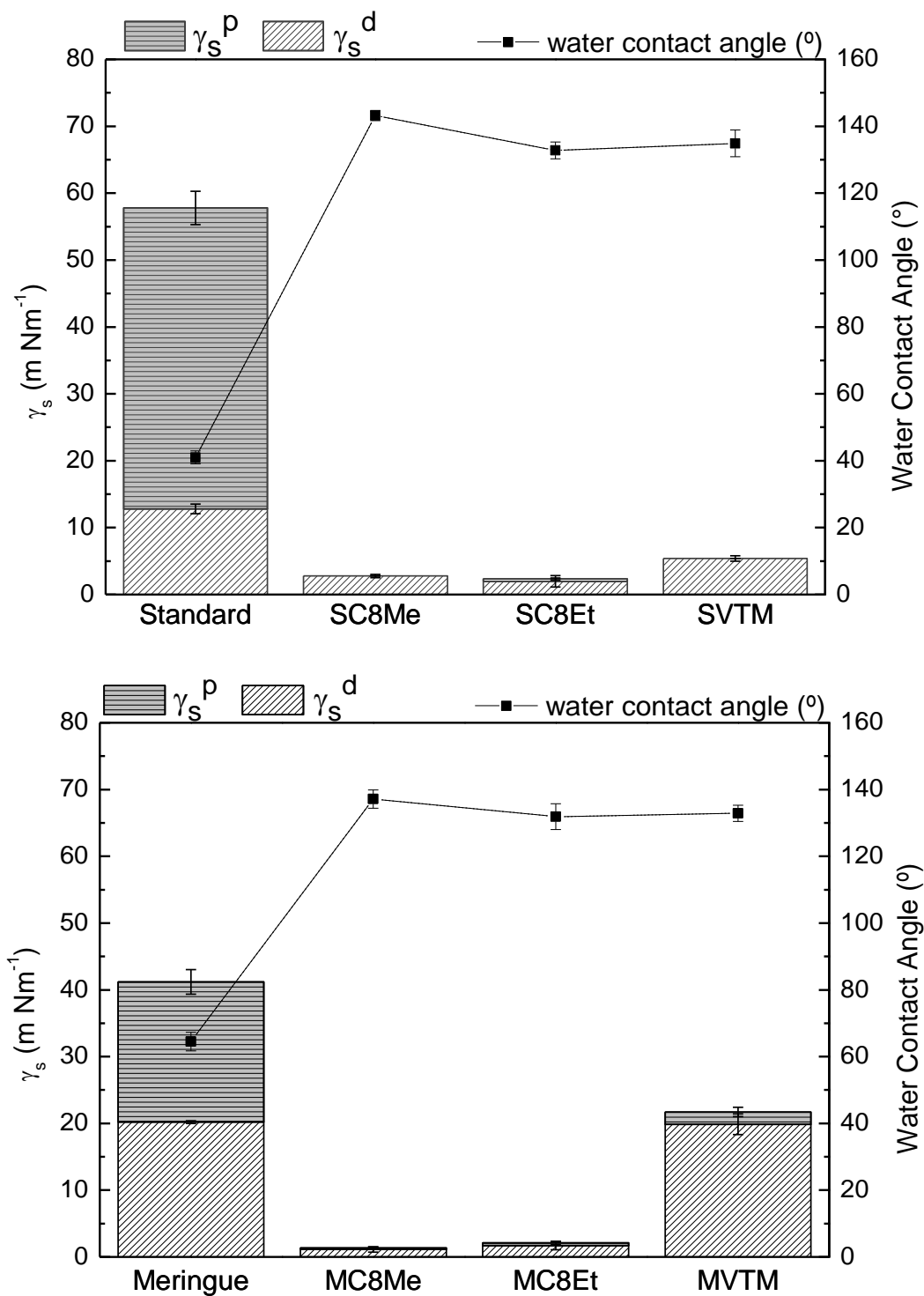


Fig. III-12. Surface energy and their dispersive and polar parts, determined using OWRK method with contact angle data from sessile drop and liquid penetration techniques, for raw and treated foams (top: standard, and bottom: meringue), and corresponding water contact angles.

III/3.4. Water vapour sorption

Despite treated foams unquestionably presented dramatically enhanced water repellence, with liquid water seeming to be no more able to penetrate the surface of the foam, checking their behaviour towards moisture sorption was necessary. Water sorption indeed proceeds through the gas phase, and water vapour may behave differently from liquid water.

Complete water vapour sorption - desorption isotherms for untreated Standard and Meringue tannin-based foams are shown in Fig. III-13. Two consecutive sorption/desorption cycles were carried out for Standard foam in order to prove the excellent reproducibility of the results. Both foams exhibited isotherms having a sigmoidal shape with a sharp increase in the region of higher relative pressures, which correspond exactly to type II of IUPAC classification (see again Fig. III-8(b)), as expected. The isotherms also showed a significant hysteresis cycle. These hysteresis cycles are quite common features for hydrophilic materials of natural origin, e.g. cellulose and lignocellulosic materials in general, amongst others (Hill et al., 2009; Popescu and Hill, 2013; Volkova et al., 2012), where the water vapour penetrates the polymer network of the material.

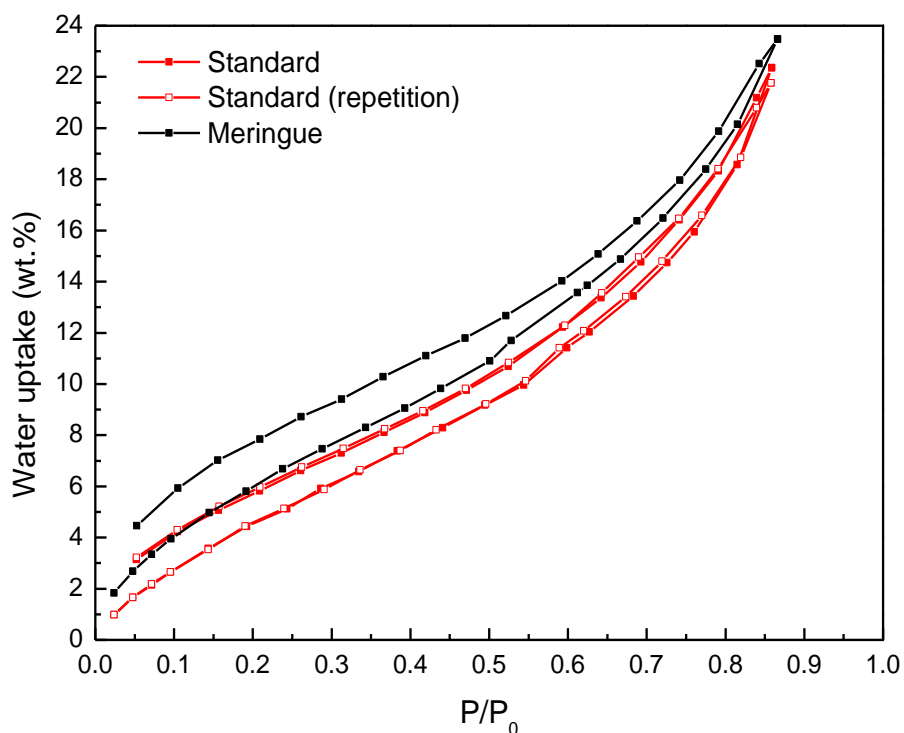


Fig. III-13. Sorption - desorption isotherms of water on pristine tannin-based foams.

The Meringue sample presented higher water uptake, in contrast to the results found previously with contact angle where it was demonstrated to be less hydrophilic than Standard foam. The result is consistent, however, with the correspondingly higher oxygen content of Meringue foam and with oxygen groups possibly poorly accessible from the surface, as suggested before. This finding clearly shows that water vapour does not behave as liquid water and supports the need of measuring water sorption in a range of relative humidity.

Fig. III-14 presents the sorption isotherms (desorption branches were not shown for clarity) of water on treated foams. After the hydrophobisation process, the amount of water adsorbed on the samples at any given relative pressure decreased whatever the hydrophobic reagents used. That decrease of water sorption was not as high as expected from the results of contact angle that evidenced very hydrophobic foams. A significant amount of water was still sorbed even when the foam was treated with the most efficient reagent, C8Me. Indeed, intrinsically hydrophobic synthetic foams tested in the same conditions were found to present far lower water sorption, typically 10 times less, see the inset in Fig. III-14.

The isotherms show that water sorption on treated foams strongly depends on the chemical used for hydrophobising them. For both kinds of samples, the foams processed with C8Et were the most similar to the initial non-treated foam. This finding suggests that the condensation reaction was more favoured when the reagent was a trimethoxysilane than when it was a triethoxysilane. A similar behaviour was also noticed elsewhere (Derouet et al., 1998) when grafting silica microparticles.

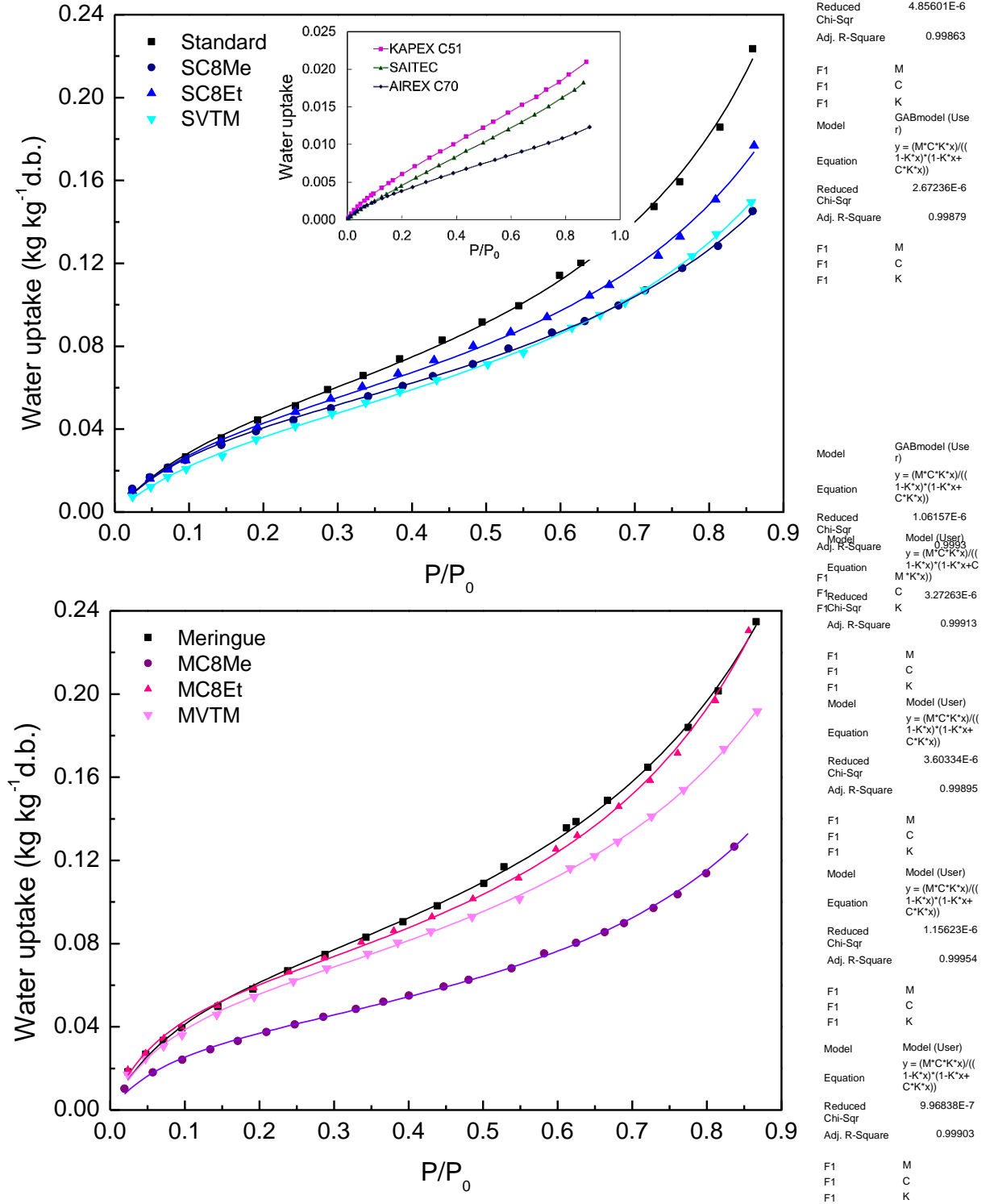


Fig. III-14. Sorption isotherms of water on pristine and treated foams on dry basis (d.b.) (top: standard foams; bottom: meringue foams). The inset shows the sorption behaviour of 3 structural PVC (Airex® C70) and polyurethane (Kapex® C51 and Saitec®) foam core materials for sandwich panels. The curves were calculated by Eq. (10).

In addition, Fig. III-14 again shows that there is no correlation between moisture uptakes and the formerly reported values of contact angle or surface energies when the materials were in contact with liquid water. Indeed, when in contact with water vapour, the foams still exhibited hydrophilic character and therefore should still present active sites for sorption. This effect has been already observed in the hydrophobisation of silica or glass surfaces (Belyakova and Varvarin, 1999; Forny et al., 2005; Takei et al., 1997). After hydrophobisation, water molecules, which are quite small, still are able to interact with the residual hydroxyl groups possibly remaining under far bigger grafted hydrophobic functional groups. Unreacted –OH groups could be present for different reasons, despite the significant excess of reagent introduced during the foam treatment, such as poor accessibility, steric impediment, secondary rehydration processes after treatment having regenerated some of them, etc. Consequently, the differences observed between results of water sorption and contact angle may be explained by the fact that the agent grafted on the foam produced a hydrophobic layer on the extreme surface, providing the observed macroscopic water repellent character, but could not prevent the deep penetration of water molecules at the microscopic level. Fig. III-15 illustrates in a schematic way a possible structure of the foam after the process of grafting that explains the present results in a consistent way.

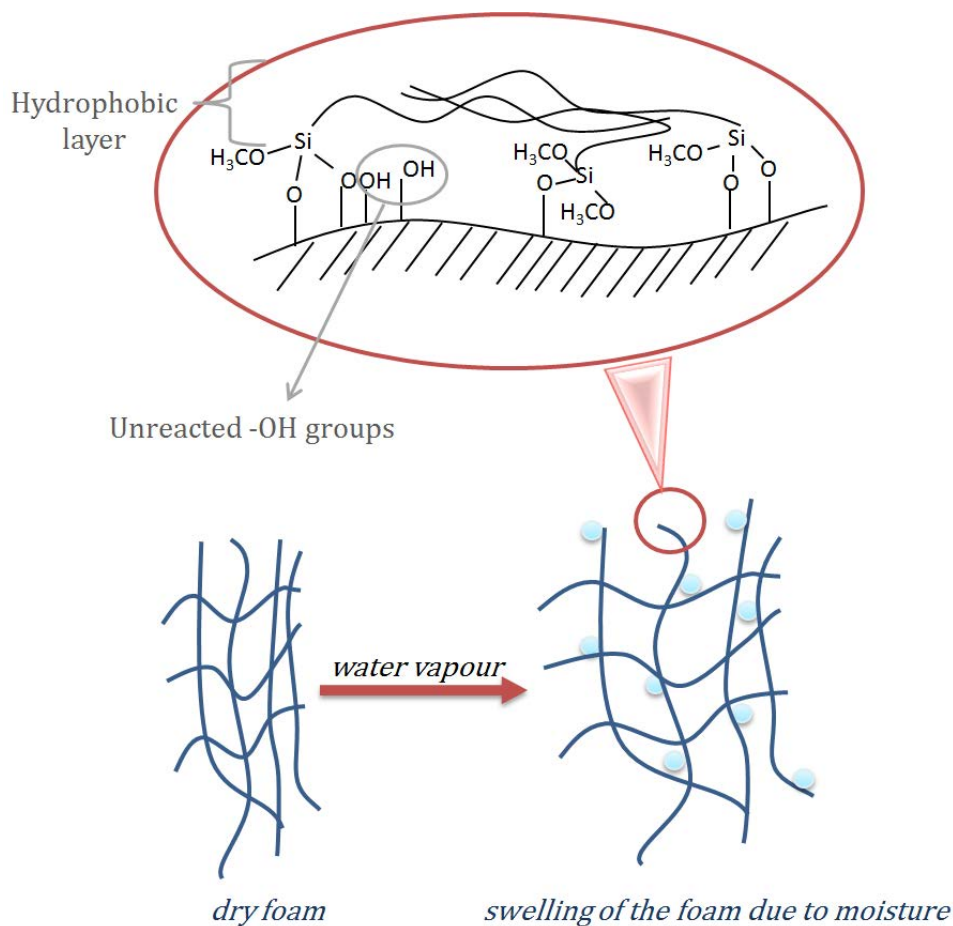


Fig. III-15. Schematic picture of grafted tannin-based foam in a moist environment.

Moreover, it has been observed (Letellier, 2015) that tannin-based foams are able to swell or shrink significantly, depending on the relative humidity (represented in Fig. III-15). This finding is most likely due to the diffusion of water molecules inside the bulk resin, changing the conformation of the polymer chains, acting as a plasticiser, and decreasing the rigidity of the polymer network as already known and observed for lignocellulosic materials (Champion et al., 2011; Passauer et al., 2012; Shamblin et al., 1998). Indeed, tannin-based foams dried in vacuum oven are much more brittle than those stored at 40% RH, and this effect is fully reversible (Letellier, 2015), suggesting the plasticising effect of water and hence its ability to migrate across the tannin-based resin. The corresponding, slow, diffusion process of water throughout the tannin-based polymer network would also explain why getting a full sorption – desorption cycle is so long and requires about 10 days. Additionally, this phenomenon has been postulated to be

related to the phenomenon of sorption hysteresis (Shamblin, Hancock, and Zografí 1998; Hill et al. 2012; Hill and Xie 2011), which might explain why the hysteresis loop is so broad.

In terms of quantitative amounts of sorbed water, no significant difference was observed from one formulation to another, both non-treated foams and the most efficiently hydrophobised ones sorbing ~ 23 wt. % and ~ 13 wt. % of water, respectively. However, for going deeper in the analysis, a sorption model was looked for. All data of Fig. III-14 were very adequately fitted with the Guggenheim-Anderson-de Boer (GAB) equation (van den Berg, 1984). The latter was selected because it is considered as the most versatile sorption model available in the literature. It indeed gives a very reliable description of the full range of water vapour sorption data for many raw and processed materials such as starches, foods, cellulose gums or natural leaves (Červenka et al., 2015; Chowdhury et al., 2006; Knani et al., 2014; Rodríguez-Bernal et al., 2015; Shittu et al., 2015; Timmermann and Chirife, 1991; Torres et al., 2012). Additionally, this model has many advantages over the others such as having a theoretical background since it is a refined extension of the well-known BET (Brunauer, Emmett and Teller) theory of physical adsorption. It postulates that the state of the sorbed molecules in the second and subsequent layers is equal, but different from that of the liquid-like state. This assumption introduces the parameter K , which measures this difference.

The GAB model was used in the following form (Samaniego-Esguerra et al., 1991):

$$MC = \frac{MC_0 H K (P/P_0)}{(1-K (P/P_0)) (1-K (P/P_0)+H K (P/P_0))} \quad (\text{III-10})$$

where M is the moisture content (kg/kg of dry solid) at a given water relative pressure P/P_0 , MC_0 is the monolayer moisture content (kg/kg of dry solid), H and K are the adsorption constants, which are related to the energies of interaction of the monolayer of sorbed molecules with individual sorption sites and with a multilayer of sorbed molecules, respectively. The GAB parameters estimated from the sorption isotherms can give useful information for understanding the physicochemical binding of water in the materials. They are gathered in Table III-7.

Table III-7. Sorption parameters derived from the application of the GAB equation (III-10) to the data of Fig. III-14. The correlation factor R^2 is also provided.

Sample	MC_0 (kg kg ⁻¹ d.b.)	H	K	R^2
Standard	0.0611 ± 0.0015	8.05 ± 0.64	0.853 ± 0.008	0.9988
SC8Me	0.0527 ± 0.0008	10.54 ± 0.49	0.759 ± 0.007	0.9989
SC8Et	0.0559 ± 0.0012	9.35 ± 0.63	0.805 ± 0.008	0.9937
SVTM	0.0527 ± 0.0008	7.36 ± 0.27	0.782 ± 0.005	0.9997
Meringue	0.0738 ± 0.0011	12.12 ± 0.67	0.802 ± 0.006	0.9992
MC8Me	0.0424 ± 0.0004	13.97 ± 0.56	0.808 ± 0.004	0.9991
MC8Et	0.0652 ± 0.0009	16.43 ± 1.06	0.841 ± 0.005	0.9991
MVTM	0.0647 ± 0.0007	14.45 ± 0.55	0.777 ± 0.004	0.9996

The monolayer moisture MC_0 is the water content corresponding to saturation of each of all primary sites by one single water molecule. It is, therefore, a measure of the hygroscopic characteristics of the surface of the foam and it is related to the chemical structure and to the composition of the foam (Torres et al., 2012). The fits to the isotherms show that non-treated foams have higher monolayer values than hydrophobised ones. This means that the amount of hydroxyl groups decreased after the hydrophobisation process, especially when C8Me was used.

On the other hand, the GAB parameter H is a measure of the binding strength of water molecules to primary active sites. The larger is the value of H , the larger is the sorption enthalpy of water in the first adsorbed layer. In most cases, the H values of hydrophobised foams were higher than those of raw materials. SVTM was the exception to the trend, and this should be related to the different curvature of the SVTM isotherm, which is the only one of the series which crosses another isotherm at a relative pressure far below the saturation (see again Fig. III-14(a)). In terms of sorption phenomenon, higher values of H mean that although fewer sorption sites were available because of the decrease of MC_0 , these sites had a higher binding energy. It can be seen that such water sorption energy is higher in meringue foams than in standard ones. This finding should be related to the higher oxygen content of Meringue foams already observed in Table III-4.

Finally, the parameter K measures the interactions between the multilayer sorbed molecules with the first adsorbed layer. This factor accounts for the properties of the adsorbed multilayer with respect to the bulk liquid and takes values intermediate between that corresponding to the molecules in the monolayer and that of the liquid water. In the present case, the K parameter appeared to be fairly constant for all foams, i.e., the interaction energies were practically the same for all materials. This finding is rather logical as water adsorbs on itself in all cases, whether the material was hydrophobised or not.

III/3.5. Thermal conductivity

Thermal conductivity measurements at different values of relative humidity were carried out in order to study the effect of the hydrophobisation treatment on the insulation properties of the materials. The results are presented in Fig. III-16, where it can be seen that the thermal conductivity always increased with relative humidity, as expected. However, hydrophobisation limited such increase in the domain of higher relative humidity, whereas the effect was rather poor below 60% RH. Whatever the % RH, the thermal conductivity of Meringue foam was always lower than that of Standard foam because of its slightly higher porosity and lower density (see again Table III-4).

For both kinds of non-treated tannin foams, the increase of thermal conductivity with relative humidity was very significant, as almost two times higher values were observed close to saturation with respect to the dry state. After hydrophobisation, the increase with % RH was more linear, hence the lower increase of conductivity at higher relative humidity, probably because condensation was hindered by the hydrophobicity of the surface molecular layer. A rather good agreement between Fig. III-14 and III-16 can also be observed, as the materials presenting the lowest water uptake were those for which the lowest conductivity increase was measured, especially SVTM and MC8Me.

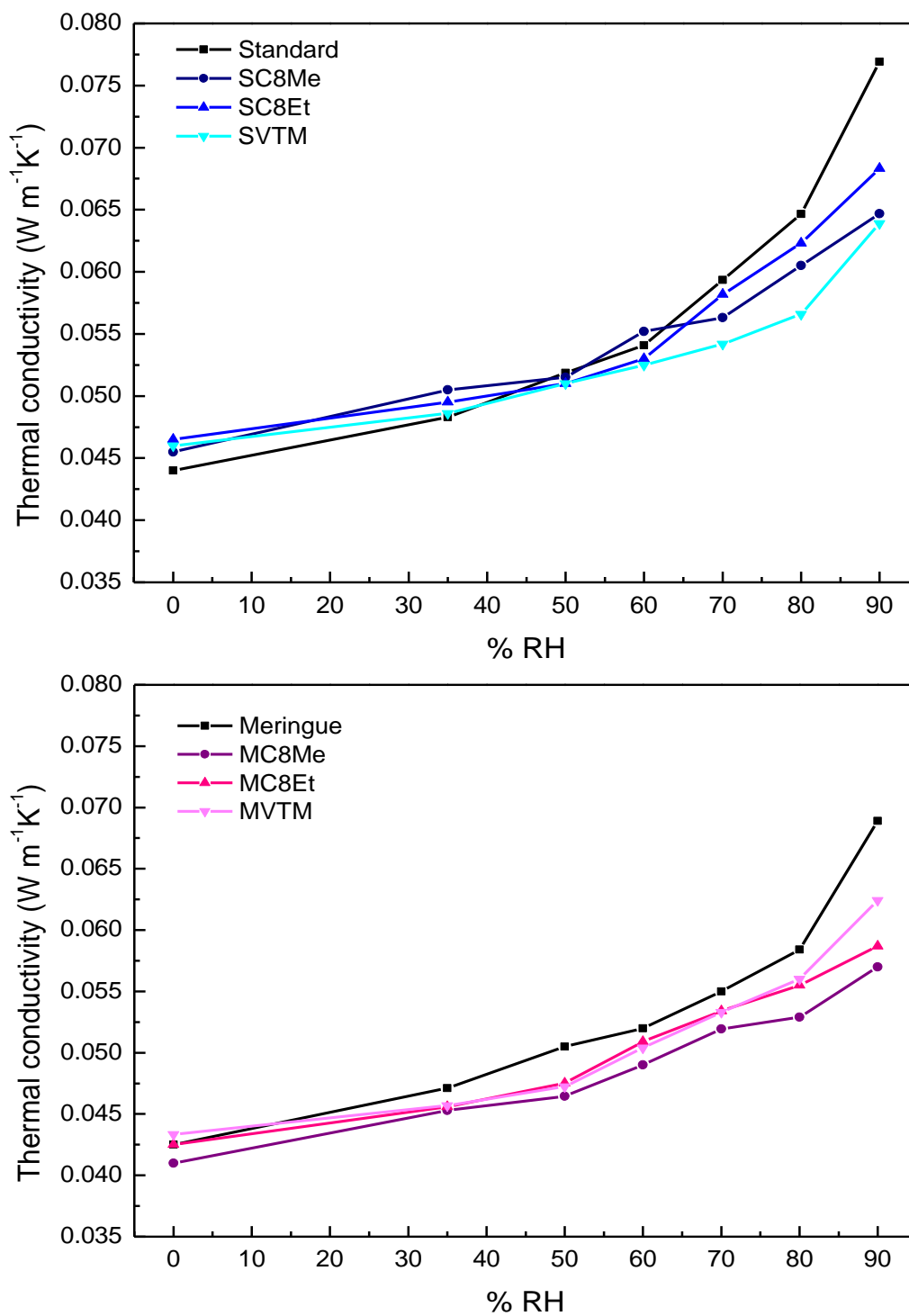


Fig. III-16. Thermal conductivity of pristine and treated tannin-based foams as a function of relative humidity (top: standard foams; bottom: meringue foams).

Combination of the data of Fig. III-14 and III-16 led to Fig. III-17, showing rather linear increases of thermal conductivity as a function of water uptake, whatever the initial formulation or the hydrophobisation agent. The nature of the treatment did not change the observed trends as all foams based on one given formulation presented the same increase of thermal conductivity, which was visibly controlled by the amount of sorbed water. Only formulation had an effect, producing different slopes, the meringue leading to a lower increase of thermal conductivity compared to the standard foam, $\sim + 2\%$ versus $\sim + 3\%$ per % of water uptake, respectively. The dotted lines shown in Fig. III-17, obtained by linear fitting of the experimental curves for each kind of foam, indeed presented slopes of 0.00088 and 0.00125, with correlation factors R^2 of 0.934 and 0.949, respectively. The naturally less hydrophilic Meringue sample was, therefore, less sensitive to relative humidity, as its insulating performances were less affected. As a consequence, the thermal conductivity of the most hydrophobic foams sample, MC8Me, which only sorbed 12.5 wt. % of water at 90% RH, increased by 37% from 0 to 90% of RH. All other materials presented higher increases, the highest one being obtained with the non-treated standard foam whose thermal conductivity increased by 74% when the RH increased from 0 to 90%.

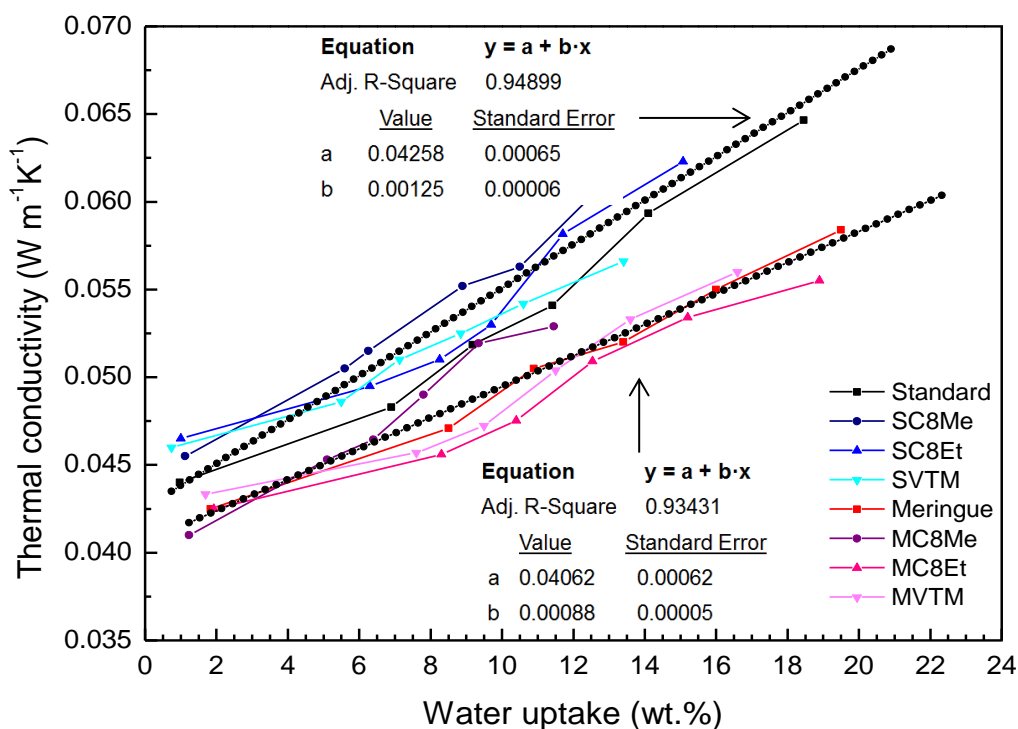


Fig. III-17. Thermal conductivity of pristine and treated tannin-based foams, as a function of water uptake. The dotted lines are just guides for the eye, evidencing two groups of samples, Meringue and Standard, having different slopes.

III/4. Conclusion

In the present work, two tannin-based foam formulations, called Standard and Meringue were prepared and hydrophobised by covalent grafting of silanes bearing various kinds of functional groups. Whereas the initial foam samples presented similar bulk densities and pore textures despite their different preparation processes (physical foaming and frothing of tannin-based thermoset polymers, respectively), the surface of Standard samples was significantly more hydrophilic and polar than Meringue samples. Such difference was attributed to the formulation and the poor accessibility of the oxygen groups in Meringue samples. Both foams were successfully hydrophobised; indeed, after treatment, the materials showed excellent macroscopic water repellence due to a considerably higher water contact angle and a corresponding decrease of surface energy, mainly due to the vanishing of the polar part.

Despite such macroscopic hydrophobic character, the hydrophobisation treatment could certainly not prevent moisture sorption, which was only slightly decreased with respect to non-treated materials. Such effect was assumed to be due to the high mobility of small water molecules, whose vapour could penetrate the bulk and strongly interact with it whereas liquid water was stopped by the extreme surface hydrophobic layer. This assumption explains the extremely long sorption-desorption processes. As a consequence, the thermal conductivity still increased with relative humidity, but less than for non-treated foams, and especially near the saturation where liquid water may condense. Thus, the most efficient hydrophobisation treatment was able to limit the increase of thermal conductivity at the half of what was measured for the non-treated foam.

This study provided us precious information about the behaviour of tannin-based foams under moisture condition. A complete hydrophobisation of tannin foam seems impossible since the moisture is able to penetrate the foam structure. Nevertheless, the treatment produced an important limitation in the increase of thermal conductivity, enabling those foams to remain as potential thermal insulation material.

Therefore, instead of trying to mimic synthetic foams already used for thermal insulation, tannin-based foams should be better considered as materials derived from natural resources, with different but still advantageous properties. In the past, most houses were poorly insulated but

were able to “breathe”. As a consequence, a lot of heat was lost, but the inside air quality was in many cases better than nowadays. On the positive side, current houses are generally much better insulated than before. However, the new hydrophobic materials such as polyurethane foams can have a negative influence on the indoor air quality, because the interior gets too humid and trapped moisture in the construction may create serious problems. Products such as the current tannin foams could offer the best of both worlds: a good thermal insulation combined with the ability to exhale excess humidity, because of its buffering capacity.

In fact, this kind of alternative insulation is growing significantly in the recent years. For instance, “BreatheTM insulation materials” are able to absorb and release moisture, helping to regulate internal moisture levels to enhance comfort and reduce the risk of condensation. This breathability is increasingly recognised by professionals from the construction sector as being an extremely useful function for maintaining a healthy and durable building. It is a nice alternative to conventional insulation, offering comparable performance with all the environmental benefits of a natural product (Swanson and Miller, 2008). There are nowadays several manufacturers such as “Isolina Flax Insulation Products” (“Isolina pellavaeriste esittely,” n.d.) and, as stated above, “BreatheTM Natural Fibre Insulation” (“Breathe Insulation | American Lime Technology Website,” n.d.) already commercialising products having such characteristics.

In essence, hydrophobised tannin-based foams showed a limited increase of thermal conductivity with the relative humidity but still maintained enough hydrophilic character for allowing them to “breathe”. Such features make this product a perfect candidate for the thermal insulation market.

III/5. Bibliography

- Abdou, A., Budaiwi, I., 2013. The variation of thermal conductivity of fibrous insulation materials under different levels of moisture content. *Constr. Build. Mater.* 43, 533–544. doi:10.1016/j.conbuildmat.2013.02.058
- Abidi, N., Hequet, E., Tarimala, S., 2007. Functionalization of Cotton Fabric with Vinyltrimethoxysilane. *Text. Res. J.* 77, 668–674. doi:10.1177/0040517507080621
- Ahmed, G.S., Gilbert, M., Mainprize, S., Rogerson, M., 2009. FTIR analysis of silane grafted high density polyethylene. *Plast. Rubber Compos.* 38, 13–20. doi:10.1179/174328909X387711

- Akamatsu, Y., Makita, K., Inaba, H., Minami, T., 2001. Water-repellent coating films on glass prepared from hydrolysis and polycondensation reactions of fluoroalkyltrialkoxysilane. *Thin Solid Films* 389, 138–145. doi:10.1016/S0040-6090(01)00901-4
- Basso, M.C., Li, X., Fierro, V., Pizzi, A., Giovando, S., Celzard, A., 2011. Green, formaldehyde-free, foams for thermal insulation. *Adv. Mater. Lett.* 2, 378–382. doi:10.5185/amlett.2011.4254
- Belyakova, L.A., Varvarin, A.M., 1999. Surfaces properties of silica gels modified with hydrophobic groups. *Colloids Surf. Physicochem. Eng. Asp.* 154, 285–294.
- Breathe Insulation | American Lime Technology Website [WWW Document], n.d. URL <http://www.americanlimetechnology.com/breathe-insulation/> (accessed 3.17.17).
- Castro, R.P., Cohen, Y., Monbouquette, H.G., 1996. Silica-supported polyvinylpyrrolidone filtration membranes. *J. Membr. Sci.* 115, 179–190. doi:10.1016/0376-7388(96)00019-1
- Červenka, L., Hloušková, L., Žabčíková, S., 2015. Moisture adsorption isotherms and thermodynamic properties of green and roasted Yerba mate (*Ilex paraguariensis*). *Food Biosci.* 12, 122–127. doi:10.1016/j.fbio.2015.10.001
- Champion, D., Loupiac, C., Simatos, D., Lillford, P., Cayot, P., 2011. Structural Relaxation During Drying and Rehydration of Food Materials—the Water Effect and the Origin of Hysteresis. *Food Biophys.* 6, 160–169. doi:10.1007/s11483-011-9204-5
- Chowdhury, M.M.I., Huda, M.D., Hossain, M.A., Hassan, M.S., 2006. Moisture sorption isotherms for mungbean (*Vigna radiata* L.). *J. Food Eng.* 74, 462–467. doi:10.1016/j.jfoodeng.2005.03.036
- Cohen, Y., Eisenberg, P., Chaimberg, M., 1992. Permeability of graft-polymerized polyvinylpyrrolidone-silica resin in packed columns. *J. Colloid Interface Sci.* 148, 579–586. doi:10.1016/0021-9797(92)90192-O
- Cosnier, F., Celzard, A., Furdin, G., Bégin, D., Marêché, J.F., Barrès, O., 2005. Hydrophobisation of active carbon surface and effect on the adsorption of water. *Carbon* 43, 2554–2563. doi:10.1016/j.carbon.2005.05.007
- Derouet, D., Forgeard, S., Brosse, J.-C., Emery, J., Buzare, J.-Y., 1998. Application of solid-state NMR (¹³C and ²⁹Si CP/MAS NMR) spectroscopy to the characterization of alkenyltrialkoxysilane and trialkoxysilyl-terminated polyisoprene grafting onto silica microparticles. *J. Polym. Sci. Part Polym. Chem.* 36, 437–453. doi:10.1002/(SICI)1099-0518(199802)36:3<437::AID-POLA8>3.0.CO;2-O
- Fadeev, A.Y., Yaroshenko, V.A., 1996. Wettability of porous silicas chemically modified with fluoroalkylsilanes according to data on water porosimetry. *Colloid J.* 58, 654–657.
- Forny, L., Pezron, I., Saleh, K., Guigon, P., Komunjer, L., 2005. Peculiar absorption of water by hydrophobized glass beads. *Colloids Surf. Physicochem. Eng. Asp.* 270-271, 263–269. doi:10.1016/j.colsurfa.2005.06.039
- Gibson, L.J., Ashby, M.F., 1997. *Cellular Solids: Structure and Properties*. Cambridge University Press.
- Hill, C.A.S., Norton, A., Newman, G., 2009. The water vapor sorption behavior of natural fibers. *J. Appl. Polym. Sci.* 112, 1524–1537. doi:10.1002/app.29725
- Hilliard, J.E., 1967. The Calculation of the Mean Caliper Diameter of a Body for Use in the Analysis of the Number of Particles Per Unit Volume, in: *Stereology*. Springer, Berlin, Heidelberg, pp. 211–215.
- Hołysz, L., Mirosław, M., Terpiłowski, K., Szcześ, A., 2010. Influence of relative humidity on the wettability of silicon wafer surfaces. *Ann. UMCS Chem.* 63, 223–239. doi:10.2478/v10063-009-0011-5

- Isolina pellavaeriste esittely [WWW Document], n.d. URL <http://www.isolina.com/> (accessed 3.17.17).
- Jańczuk, B., Białopiotrowicz, T., 1989. Surface free-energy components of liquids and low energy solids and contact angles. *J. Colloid Interface Sci.* 127, 189–204. doi:10.1016/0021-9797(89)90019-2
- Jerman, M., Černý, R., 2012. Effect of moisture content on heat and moisture transport and storage properties of thermal insulation materials. *Energy Build.* 53, 39–46. doi:10.1016/j.enbuild.2012.07.002
- Jiao, C., Wang, Z., Gui, Z., Hu, Y., 2005. Silane grafting and crosslinking of ethylene–octene copolymer. *Eur. Polym. J.* 41, 1204–1211. doi:10.1016/j.eurpolymj.2004.12.008
- Kaelble, D.H., 1970. Dispersion-Polar Surface Tension Properties of Organic Solids. *J. Adhes.* 2, 66–81. doi:10.1080/0021846708544582
- Knani, S., Aouaini, F., Bahloul, N., Khalfaoui, M., Hachicha, M.A., Ben Lamine, A., Kechaou, N., 2014. Modeling of adsorption isotherms of water vapor on Tunisian olive leaves using statistical mechanical formulation. *Phys. Stat. Mech. Its Appl.* 400, 57–70. doi:10.1016/j.physa.2014.01.006
- Krajewski, S.R., Kujawski, W., Dijoux, F., Picard, C., Larbot, A., 2004. Grafting of ZrO₂ powder and ZrO₂ membrane by fluoroalkylsilanes. *Colloids Surf. Physicochem. Eng. Asp.* 243, 43–47. doi:10.1016/j.colsurfa.2004.05.001
- Kujawa, J., Cerneaux, S., Kujawski, W., 2014. Characterization of the surface modification process of Al₂O₃, TiO₂ and ZrO₂ powders by PFAS molecules. *Colloids Surf. Physicochem. Eng. Asp.* 447, 14–22. doi:10.1016/j.colsurfa.2014.01.065
- Lacoste, C., Pizzi, A., Laborie, M.-P., Celzard, A., 2014. Pinus pinaster tannin/furanic foams: Part II. Physical properties. *Ind. Crops Prod.* 61, 531–536. doi:10.1016/j.indcrop.2014.04.034
- Letellier, M., 2015. Optimisation de mousses de carbone dérivées de tannin par l'étude et la modélisation de leurs propriétés physiques (Thèse de doctorat). Université de Lorraine, France.
- Li, X., Pizzi, A., Lacoste, C., Fierro, V., Celzard, A., 2013. Physical Properties of Tannin/Furanic Resin Foamed With Different Blowing Agents. *Bioresources* 8, 743–752.
- Martinez de Yuso, A., Lagel, M.C., Pizzi, A., Fierro, V., Celzard, A., 2014. Structure and properties of rigid foams derived from quebracho tannin. *Mater. Des.* 63, 208–212. doi:10.1016/j.matdes.2014.05.072
- Mittal, K.L., 2008. Contact Angle, Wettability and Adhesion. BRILL.
- Ng, E.-P., Mintova, S., 2008. Nanoporous materials with enhanced hydrophilicity and high water sorption capacity. *Microporous Mesoporous Mater.* 114, 1–26. doi:10.1016/j.micromeso.2007.12.022
- Owens, D.K., Wendt, R.C., 1969. Estimation of the surface free energy of polymers. *J. Appl. Polym. Sci.* 13, 1741–1747. doi:10.1002/app.1969.070130815
- Pasch, H., Pizzi, A., Rode, K., 2001. MALDI–TOF mass spectrometry of polyflavonoid tannins. *Polymer* 42, 7531–7539. doi:10.1016/S0032-3861(01)00216-6
- Passauer, L., Struch, M., Schuldt, S., Appelt, J., Schneider, Y., Jaros, D., Rohm, H., 2012. Dynamic Moisture Sorption Characteristics of Xerogels from Water-Swellable Oligo(oxyethylene) Lignin Derivatives. *Acs Appl. Mater. Interfaces* 4, 5852–5862. doi:10.1021/am3015179

- Picard, C., Larbot, A., Guida-Pietrasanta, F., Boutevin, B., Ratsimihety, A., 2001. Grafting of ceramic membranes by fluorinated silanes: hydrophobic features. *Sep. Purif. Technol.* 25, 65–69.
- Popescu, C.-M., Hill, C.A.S., 2013. The water vapour adsorption–desorption behaviour of naturally aged *Tilia cordata* Mill. wood. *Polym. Degrad. Stab.* 98, 1804–1813. doi:10.1016/j.polymdegradstab.2013.05.021
- Quéré, D., 1997. Inertial capillarity. *Europhys. Lett. EPL* 39, 533–538. doi:10.1209/epl/i1997-00389-2
- Rangel, G., Chapuis, H., Basso, M.C., Pizzi, A., Delgado-Sánchez, C., Fierro, V., Celzard, A., Gérardin, C., 2016. Improving water repellence and friability of tannin-furanic foams by oil-grafting flavonoid tannins. Submitted.
- Rodríguez-Bernal, J.M., Flores-Andrade, E., Lizarazo-Morales, C., Bonilla, E., Pascual-Pineda, L.A., Gutierréz-López, G., Quintanilla-Carvajal, M.X., 2015. Moisture adsorption isotherms of the borjón fruit (*Borojoa patinoi*. Cuatrecasas) and gum arabic powders. *Food Bioprod. Process.* 94, 187–198. doi:10.1016/j.fbp.2015.03.004
- Samaniego-Esguerra, C.M., Boag, I.F., Robertson, G.L., 1991. Comparison of regression methods for fitting the GAB model to the moisture isotherms of some dried fruit and vegetables. *J. Food Eng.* 13, 115–133. doi:10.1016/0260-8774(91)90014-J
- Schondelmaier, D., Cramm, S., Klingeler, R., Morenzin, J., Zilkens, C., Eberhardt, W., 2002. Orientation and Self-Assembly of Hydrophobic Fluoroalkylsilanes. *Langmuir* 18, 6242–6245. doi:10.1021/la0256533
- Shamblin, S.L., Hancock, B.C., Zografí, G., 1998. Water vapor sorption by peptides, proteins and their formulations. *Eur. J. Pharm. Biopharm.* 45, 239–247. doi:10.1016/S0939-6411(98)00006-X
- Shittu, T.A., Idowu-Adebayo, F., Adedokun, I.I., Alade, O., 2015. Water vapor adsorption characteristics of starch–albumen powder and rheological behavior of its paste. *Niger. Food J.* 33, 90–96. doi:10.1016/j.nifoj.2015.04.014
- Siebold, A., Nardin, M., Schultz, J., Walliser, A., Oppliger, M., 2000. Effect of dynamic contact angle on capillary rise phenomena. *Colloids Surf. Physicochem. Eng. Asp.* 161, 81–87. doi:10.1016/S0927-7757(99)00327-1
- Swanson, G., Miller, O., 2008. *A Biological Approach to Healthy Building Envelope Design and Construction, Breathing Walls.*
- Szczurek, A., Fierro, V., Pizzi, A., Stauber, M., Celzard, A., 2014. A new method for preparing tannin-based foams. *Ind. Crops Prod.* 54, 40–53. doi:10.1016/j.indcrop.2014.01.012
- Takei, T., Yamazaki, A., Watanabe, T., Chikazawa, M., 1997. Water Adsorption Properties on Porous Silica Glass Surface Modified by Trimethylsilyl Groups. *J. Colloid Interface Sci.* 188, 409–414. doi:10.1006/jcis.1997.4777
- Timmermann, E.O., Chirife, J., 1991. The physical state of water sorbed at high activities in starch in terms of the GAB sorption equation. *J. Food Eng.* 13, 171–179. doi:10.1016/0260-8774(91)90025-N
- Tondi, G., Link, M., Oo, C.W., Petutschnigg, A., 2015. A Simple Approach to Distinguish Classic and Formaldehyde-Free Tannin Based Rigid Foams by ATR FT-IR. *J. Spectrosc.* 2015, 1–8. doi:10.1155/2015/902340
- Tondi, G., Petutschnigg, A., 2015a. Hydrophobic tannin foams. *Int. Wood Prod. J.* 6, 148–150. doi:10.1179/2042645315Y.0000000007
- Tondi, G., Petutschnigg, A., 2015b. Middle infrared (ATR FT-MIR) characterization of industrial tannin extracts. *Ind. Crops Prod.* 65, 422–428. doi:10.1016/j.indcrop.2014.11.005

- Tondi, G., Pizzi, A., 2009. Tannin-based rigid foams: Characterization and modification. *Ind. Crops Prod.* 29, 356–363. doi:10.1016/j.indcrop.2008.07.003
- Tondi, G., Zhao, W., Pizzi, A., Du, G., Fierro, V., Celzard, A., 2009. Tannin-based rigid foams: A survey of chemical and physical properties. *Bioresour. Technol.* 100, 5162–5169. doi:10.1016/j.biortech.2009.05.055
- Torres, M.D., Moreira, R., Chenlo, F., Vázquez, M.J., 2012. Water adsorption isotherms of carboxymethyl cellulose, guar, locust bean, tragacanth and xanthan gums. *Carbohydr. Polym.* 89, 592–598. doi:10.1016/j.carbpol.2012.03.055
- Underwood, E.E., 1969. Stereology, or the quantitative evaluation of microstructures. *J. Microsc.* 89, 161–180.
- van den Berg, C., 1984. Desorption of water activity of foods for engineering purposes by means of the GAB model of sorption. *Eng. Foods* 1, 311–321.
- Volkova, N., Ibrahim, V., Hatti-Kaul, R., Wadsö, L., 2012. Water sorption isotherms of Kraft lignin and its composites. *Carbohydr. Polym.* 87, 1817–1821. doi:10.1016/j.carbpol.2011.10.001
- Young, T., 1805. An essay on the cohesion of fluids. *Philos. Trans. R. Soc. Lond.* 95, 65–87. doi:10.1098/rstl.1805.0005
- Yu, D.U., Shrestha, B.L., Baik, O.D., 2015. Thermal conductivity, specific heat, thermal diffusivity, and emissivity of stored canola seeds with their temperature and moisture content. *J. Food Eng.* 165, 156–165. doi:10.1016/j.jfoodeng.2015.05.012
- Zhao, W., Fierro, V., Pizzi, A., Du, G., Celzard, A., 2010a. Effect of composition and processing parameters on the characteristics of tannin-based rigid foams. Part II: Physical properties. *Mater. Chem. Phys.* 123, 210–217. doi:10.1016/j.matchemphys.2010.03.084
- Zhao, W., Pizzi, A., Fierro, V., Du, G., Celzard, A., 2010b. Effect of composition and processing parameters on the characteristics of tannin-based rigid foams. Part I: Cell structure. *Mater. Chem. Phys.* 122, 175–182. doi:10.1016/j.matchemphys.2010.02.062

Chapter IV: Optimisation of blowing agent-free and formaldehyde-free tannin-based foams

IV/1. Introduction

The first generation of tannin-furanic rigid foams presented good insulation and mechanical properties but they were produced with around 5% of formaldehyde, a recognised carcinogenic chemical, as well as with a highly flammable blowing agent (Tondi et al., 2009). Later on, new tannin-based foams without formaldehyde and without blowing agent was developed so as to produce “greener” materials based on up to 98% of natural resources. Such materials were obtained first by removing the formaldehyde (Basso et al., 2011), then through the development of self-blowing tannin-furanic formulations (Basso et al., 2013a). Although the latter still contained a little amount of isocyanate, another source of health hazard, such pioneering works opened the route to optimised greener formulations able to compete with other commercial foams on the market. All that information is more exhaustively explained in the section *I/3.3. Formulations of tannin foams* of the Chapter I.

Formulating liquid resins based on appropriate low-toxicity chemicals for achieving rigid foams with desired properties for a particular application is a difficult task. The precursor resin indeed needs to be well-balanced for obtaining foaming and crosslinking simultaneously, or so. For instance, too early or too late hardening with respect to foaming leads to either no foam or collapsed foam, respectively (Basso et al., 2013b). This is the reason why the foaming process of tannin-based foams has been investigated in-depth in the recent past with a dedicated method (Basso et al., 2013a, 2013b, 2013c). This method is capable of dynamically monitoring the main parameters controlling the foaming behaviour of any formulation such as temperature, polymerisation rate of the polymers, speed of expansion, etc., thereby giving a systematic understanding of the characteristics of the resultant rigid foams. However, the direct relationships between formulation and properties of those foams could not be studied very accurately and methodically so far, and only general trends were observed. As a consequence, accurate studies of the effect of ingredients of formaldehyde-free, blowing agent-free, tannin-based formulations on the properties of the final rigid foams are still missing.

The major objective of the work presented in this chapter was, therefore, to develop “green” tannin-based foams totally free of blowing agent, formaldehyde or isocyanate, and with valuable thermal insulation and mechanical properties. Decreasing the thermal conductivity of foams has

been a major focus in the search for better thermal insulation materials. However, such improvements are limited by the decrease of mechanical properties of the foams, due to the resultant, too high porosity (Lacoste et al., 2014; Tondi and Pizzi, 2009; Zhao et al., 2010). Reaching a compromise between thermal insulation and mechanical resistance thus appears to be necessary and, for this purpose, knowing and controlling how the different components of the foam formulation affect the final foam properties is essential. In order to reach this objective, tannin-based foams have to be prepared and analysed in a rational manner by using, for the first time with this kind of material, experimental design and related statistical analysis (Antony and Roy, 1998).

IV/2. Experimental

IV/2.1. Foam preparation

The foam formulations prepared in this study contained neither formaldehyde nor volatile organic blowing agents. The corresponding foams were produced as follows: a homogeneous solution made of furfuryl alcohol, ethylene glycol, water and tannin extract powder was first prepared under mechanical stirring for 50 s. A small proportion of glutaraldehyde and a mixture of two surfactants were then added and strongly stirred for approximately 30 s to ensure complete homogenisation. Lastly, the 65% aqueous solution of phenol-sulphonic acid catalyst was added while continuing stirring for 20 s after addition. The resultant mixture was then poured into a hard cardboard mould. After an induction time depending on the formulation, but typically ranging from approximately 30 to 460 s, spontaneous foaming and hardening occurred. The foams thus obtained were left to stabilise at room temperature for 72 h and then cut into specimens for testing. Table IV-1 presents a representative example of the composition of typical tannin-furanic foam prepared in the present work and Fig. IV-1 shows a material thus prepared after cutting it into samples of regular shape for studies.

In Table IV-1 and everywhere else in this chapter, the amounts of ingredients in the formulations of tannin-furanic foams have been provided in wt. % instead of absolute masses of

each. Doing so indeed gives a clearer idea of the proportions of the different components, but led to non-integer values of weight fractions (see again Table IV-1).



Fig. IV-1. Example of tannin-furanic foam samples prepared and tested in this work.

Table IV-1. Representative example of foam formulation.

Component	Function	%	
Tannin	Base of the resin	40.96	} 81.06 %
Furfuryl Alcohol	Hardener and exothermic agent	33.05	
Phenol-sulphonic acid (65% in water)	Catalyst	7.05	
Water	Solvent	8.38	} 18.94 %
Tegostab B8406	Surfactant	1.47	
Capstone 1470	Surfactant	1.48	
Ethylene glycol	Plasticiser	2.76	
Glutaraldehyde	Crosslinker	4.85	

IV/2.2. Identification of the most relevant ingredients of the foam's formulation

The tannin-furanic foams presented in this work were obtained thanks to the acid-catalysed exothermic polymerisation of tannin with furfuryl alcohol, together with the self-condensation of the furfuryl alcohol that leads to a significant heat release, producing both the hardening of the resin and the volatilisation of water vapour and other volatiles. Such production of gas expands

the resin by developing a high amount of porosity inside, whereas the thermoset resin progressively hardens at the same time, thereby leading to rigid foam that does not collapse as soon as these two phenomena take place concurrently.

The thermal conductivity and the mechanical properties of rigid foams are usually mainly governed by bulk density, which is not straightforwardly controlled in this kind of formulations free of blowing agent. Unlike what happens in former formulations of tannin-based foams where the density of the foams strictly depended on the amount of blowing agent (Zhao et al., 2010), predicting the final density is not easy in the present formulations since the effect of furfuryl alcohol is not so obvious. An increase of the amount of furfuryl alcohol indeed increases the heat generated by self-polymerisation and tends to decouple foaming from hardening (Basso et al., 2013b, 2013c). Thus, the important peak of temperature that is produced leads to a sudden foam expansion and to a high difference of temperature between the heart of the foam and the outer part, causing shrinkage. Furthermore, a too fast expansion is detrimental for the structure of the foam and thus for the final mechanical properties after hardening.

The effect of the amount of furfuryl alcohol is unquestionably linked to the amount of catalyst used in the system, because the catalyst is required for initiating the reaction. A high amount of one or both components may either lead to a violent and rapid foam expansion as explained above, or it can also happen that polymerisation occurs too quickly so that the foam does not have time to expand sufficiently. And, clearly, if there are not enough amounts of those components, the expansion and the polymerisation can also be incomplete.

On the other hand, the chemical structure of the polymer foam is mainly based on more or less polymerised tannin molecules. A higher concentration of tannin in the initial formulation is therefore expected to lead to foams having lower porosity, due to the corresponding increase of resin viscosity (Basso et al., 2013b; Szczurek et al., 2014), and hence to foams having higher mechanical properties but also higher thermal conductivity. Thus, it is essential to find the optimum concentration of this compound as one needs materials presenting both high compression resistance and as low thermal conductivity as possible. Actually, it was noticed elsewhere (Basso et al., 2015) that any modification in the formulation of tannin-based foams induces dramatic changes of curing/foaming behaviour, with major consequences on the characteristics of the final rigid foams.

The three aforementioned ingredients: furfuryl alcohol, catalyst and tannin, have therefore been considered herein as the most appropriate constituents to consider for carrying out the required optimisation work, not only because they are the major formulation components with a quite significant impact on the final foams, but also because their effect is the least predictable and the most difficult to control. Other components of the formulation, on the contrary, have a well-known effect on the foam which allowed fixing optimal values in previous studies. For instance, the main role of surfactant is improving the compatibility of the reactants and preventing the cell wall to become too thin and unstable during foaming (Basso et al., 2015, 2013b; Gardziella et al., 2000; Zhang et al., 1999), whereas the glutaraldehyde has been incorporated into the formulation in small proportion to favour slightly crosslinking and polymerisation (Lacoste et al., 2013; Szczurek et al., 2011).

Based on the general principles stated above, it was expected that “playing” with the amounts of each main ingredient would allow improving further the characteristics of the tannin-furanic foams in terms of thermal conductivity and mechanical properties. However, such trials should never be done by chance, and a methodology is required for doing as few but as representative trials as possible.

IV/2.3. Experimental design

The three most important parameters in the formulation of tannin-furanic foams are the amounts of tannin, furfuryl alcohol and catalyst, as stated before. Considering that the preparation of these foams involves complex physical and chemical processes, getting suitable foams with correct expansion requires using amounts of ingredients within appropriate ranges. For instance, too high fraction of furfuryl alcohol associated with too low fraction of catalyst never produces foam since the exothermic reaction of furfuryl alcohol never starts.

With the purpose of finding the optimum out of a huge number of possible formulations, the concepts of experimental design and statistical analysis have been applied. Experimental design is an important tool as it avoids blind tests and allows significant time and materials savings (Lundstedt et al., 1998). Moreover, once the most relevant parameters have been selected, and after the resultant materials have been prepared and analysed in terms of properties of interest, the experimental design also allows predicting the corresponding properties of any other

formulation within the range under study. This approach should be relevant for finding an optimum formulation that simultaneously minimises thermal conductivity and maximises mechanical resistance, which behave in opposite ways as a function of porosity.

Tannin, furfuryl alcohol and catalyst were then chosen as variable parameters, all other things being equal, whereas thermal conductivity, compressive strength and elastic modulus were chosen as response variables. The optimum proportions of those three components are hardly predicted directly from regular design methods because the proportions of the three components are linearly dependent on each other within a necessarily limited range of values (Lundstedt et al., 1998). In fact, in the present experiment, it is not the actual amount of each single ingredient that matters, but rather its proportion in relation to other ingredients. For making our system to become a uniform experimental design problem, the sum of all ingredients needs to be constant in order to get independent mixture parameters (Fang and Yang, 2000; Montgomery, 2008). This independence, in turn, affects the experimental region and brings a new particular condition on the generation of the model, in addition to the limited concentration range of each ingredient.

In order to ensure the formation of a proper polymer structure, the content of tannin and furfuryl alcohol should represent around 75 wt. % of the formulation. Several studies of formaldehyde-free tannin-furanic foams have shown that the appropriate tannin content commonly ranges from 36 to 45 wt. % (Basso et al., 2015, 2013a; Lacoste et al., 2013). Moreover, Basso suggested that the content of furfuryl alcohol should remain between 28 and 38 wt. %, otherwise the foam is neither stable nor homogeneous (Basso et al., 2011). And it was also observed that the catalyst content in similar foams was normally around 11 wt. % of the total content (Basso et al., 2015). Considering that the preparation of tannin-furanic foams is a complex physical and chemical process, and that the smallest change in the formulation may totally modify the foam structure, some preliminary experiments were carried out based on extreme ingredient fractions in order to define properly the boundaries of the study. It was, therefore, found that the appropriate range of tannin, furfuryl alcohol and catalyst content in this formulation was around 32 – 40 wt. %, 27 – 42 wt. % and 6 – 14 wt. %, respectively. According to the different experiences carried out when developing this new type of tannin-based foam, it was concluded that the sum of the amounts of tannin, furfuryl alcohol and catalyst should represent around 80 wt. % of the entire foam composition, whereas the remainder, close to 20 wt.

%, should be formed by a small amount of water, non-toxic and non-volatile crosslinker, surfactant and plasticiser/emulsifier (see again Table IV-1).

Once the aforementioned boundaries have been defined, the experimental design problem could be carried out. The precise relationships between the proportions of the three ingredients used in the problem are shown in Eq. (IV-1).

$$\left\{ \begin{array}{l} Y_i = f(A, B, C) \\ A + B + C = 81.06\% \\ 32.42\% \leq A \leq 40.53\% \\ 26.75\% \leq B \leq 42.56\% \\ 6.08\% \leq C \leq 13.78\% \end{array} \right\} \quad (\text{IV-1})$$

in which, A , B and C are the weight fractions of tannin, furfuryl alcohol and catalyst, respectively, and Y_i is the response, either thermal conductivity, compression strength or elastic modulus.

Experimental design is generally used to understand the effect of experimental parameters (here A , B and C) and their interaction, and to model the relationship between them and the response variables (Liang et al., 2001). The present study was, therefore, performed in totality using the Design-Expert 8.071 software. Eight experiment schemes uniformly distributed over the entire test range was the minimum necessary to get representative results. However, due to the complexity of the system and in order to improve the effectiveness of the approach, the number of trials was increased to 14 experiments uniformly distributed over the entire test range (see Table IV-2 and Fig. IV-2). The set of experiments carried out in this study thus included 8 factorial points, 4 middle boundary edges, one centre point and one repetition of the centre point experiment.

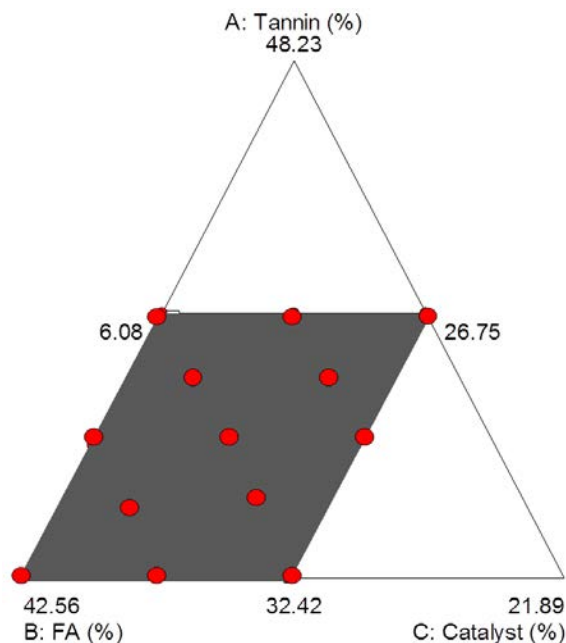


Fig. IV-2. Distribution of experimental design points in the investigated range of parameters *A* (tannin), *B* (furfuryl alcohol), and *C* (catalyst: 65 wt. % aqueous solution of phenol-sulphonic acid).

Table IV-2. Uniform experimental design scheme for the preparation of foams.

No.	Ingredients		
	Tannin (%) - <i>A</i>	Furfuryl alcohol (%) - <i>B</i>	Catalyst (%) - <i>C</i>
1	32.42	42.56	6.08
2	32.42	34.86	13.78
3	40.53	34.45	6.08
4	40.53	26.75	13.78
5	32.42	38.71	9.93
6	36.48	38.50	6.08
7	36.48	30.80	13.78
8	40.53	30.60	9.93
9	36.48	34.65	9.93
10	34.45	38.61	8.01
11	34.45	34.76	11.85
12	38.50	34.56	8.01
13	38.50	30.70	11.85
14	36.48	34.65	9.93

IV/2.4. Characterisation of tannin-furanic foams

All foams were cut into parallelepiped pieces of dimensions $3 \times 3 \times 1.5$ cm for investigating their structural and physical properties. The smallest dimension, 1.5 cm, corresponded to the vertical direction of the foams, i.e., along which expansion occurred before they turned rigid. All samples were characterised in terms of bulk density, porosity, thermal conductivity and mechanical properties, and the tests were performed in duplicate.

IV/2.4.1 Apparent density, skeletal density and porosity

The bulk density of the analysed foams, ρ_b ($\text{g}\cdot\text{cm}^{-3}$), defined as the mass of the material divided by the total volume it occupies, was simply obtained by weighing the aforementioned samples and calculating the average. The skeletal density, ρ_s ($\text{g}\cdot\text{cm}^{-3}$), is the density of the solid from which the considered material is made and was measured using helium pycnometry with an AccuPyc II 1340 automatic apparatus (Micromeritics, USA). The measurement was carried out with the same equipment and in the same conditions as described in *III/2.3.1 Morphological characterisation*. It means that the samples were crushed in a mortar and evacuated in vacuum at 60°C , so that possible errors due humidity or to closed porosity were avoided. From the experimental values of bulk and skeletal densities, the total porosity, θ (dimensionless), was calculated from the Eq. (IV-2):

$$\theta = 1 - \rho_r \quad (\text{IV-2})$$

where ρ_r is the relative density and reads $\rho_r = \rho_b / \rho_s$.

IV/2.4.2 Thermal conductivity

The thermal conductivity of each sample was measured by the transient plane source method with a thermal conductivity analyser (Hot Disk TPS 2500, ThermoConcept, France) at stable room temperature (21°C) and relative humidity (40% RH).

The basics of the method are described in *III/2.3.7 Thermal conductivity* wherein *Fig. III-9* showed some details of the device and of the probe. Briefly, the plane sensor was fitted between

two identical parallelepiped pieces of tannin-furanic foams and, from the temperature profile measured by one spiral after a heat pulse was delivered by the other spiral, the thermal conductivity was calculated by the Hot Disk 6.1 software.

IV/2.4.3 Mechanical properties

The mechanical tests were carried out at a constant compression rate of 0.0025 s^{-1} (approximately $2 \text{ mm} \cdot \text{min}^{-1}$) using an Instron 5944 universal testing machine equipped with a 2 kN load cell (Fig. IV-3). Just like for thermal conductivity measurements, the samples were analysed along the direction of foaming. Thus, the sample, in the form of a parallelepiped having dimensions $30 \times 30 \times 15 \text{ mm}$, was placed in the centre of the lower compression plate which is fixed. The second plate is mobile and compressed the foam with a low and constant speed. During the compression tests, deformation (strain, %) and load (stress, MPa) were continuously recorded. The stress was calculated dividing the load by the total cross-sectional area, and the strain or deformation was calculated from the cross-head displacement.



Fig. IV-3. Universal test machine INSTRON 5944 equipped with its compression plates.

The typical stress-strain curves of cellular materials usually present three distinct regions, namely:

- (i) The first linear region at low stresses corresponds to elastic deformation. It occurs at low stresses and up to 10% strain, on average. The initial slope in the linear region is the (compression) elastic modulus of the foam which, in the case of open cells foams, correspond to the elastic behaviour caused by cell wall bending (Gibson and Ashby, 2001). There is a maximum strain after this first stage, sometimes followed by a slight decrease before reaching the second region, i.e., a plateau.
- (ii) The second region correspond to a plateau corresponding to the more or less constant stress required for collapsing successive, more or less identical, cell layers. That plateau of compression is strongly dependent on the nature of the material, i.e., either elastomeric, elastic-plastic or brittle (Gibson and Ashby, 2001), see *Fig. I/17* in section *I/3.4.2. Mechanical properties* of Chapter I. In the case of elastic-plastic foams, the plateau stress is easily determined because its value varies very little over a broad deformation range. In the case of brittle foams, an average plateau is seen but with a strong scattering corresponding to the crack of cell layers. Meanwhile the elastic foams are characterised by the absence, strictly speaking, of a plateau, the stress increasing slightly and approximately linearly. In the cases where the plateau is clear, the stress average value is considered to be the compression strength. If instead the curve keeps rising and no horizontal plateau exists such as in elastic foams, the compressive strength is taken at the end of the first phase (elastic part).
- (iii) The last region is the densification of the foam. All the cell walls have then collapsed. The resultant fragments are compressed, and the stress rises sharply with further strain. A densification or maximum deformation is often determined as the intersection of the asymptote with the abscissa axis.

Based on such characteristic curves, the elastic modulus was defined below in this chapter as the slope of the linear, initial, part of the curve presenting the steepest slope, whereas the compressive strength was defined as the stress at the end of the elastic linear part.

IV/3. Results and discussion

IV/3.1. Foams' properties

The averaged properties of two specimens belonging to each of the 14 tannin-furanic foam formulations are given in Table IV-3. The results show that small differences in the concentration of some ingredients of the formulations led to significant differences in the final rigid foams. The bulk density of the latter indeed ranged from 0.022 to 0.069 g·cm⁻³. All foams presented high porosity, varying between 95 and 98 %, which is a non-negligible difference as far as thermal and mechanical properties are concerned (see below).

Table IV-3. Experimental results for the 14 foams' formulations.

No.	ρ_b (g·cm ⁻³)	ρ_s (g·cm ⁻³)	ρ_r	θ (%)	Compressive strength (MPa)	Elastic modulus (MPa)	Thermal Conductivity (W·m ⁻¹ ·K ⁻¹)
1	0.025	1.420	0.018	98.2	0.035	0.90	0.038
2	0.024	1.416	0.017	98.3	0.019	0.34	0.038
3	0.069	1.417	0.049	95.1	0.175	5.55	0.045
4	0.041	1.443	0.028	97.2	0.042	0.53	0.044
5	0.030	1.432	0.021	97.9	0.030	1.00	0.037
6	0.060	1.417	0.042	95.8	0.118	1.50	0.041
7	0.032	1.423	0.022	97.8	0.023	0.42	0.040
8	0.040	1.446	0.027	97.3	0.048	0.80	0.042
9	0.024	1.449	0.016	98.4	0.023	0.60	0.038
10	0.034	1.445	0.023	97.7	0.022	0.33	0.038
11	0.031	1.450	0.022	97.8	0.026	0.86	0.041
12	0.030	1.415	0.021	97.9	0.031	0.56	0.039
13	0.026	1.435	0.018	98.2	0.015	0.28	0.041
14	0.022	1.433	0.015	98.5	0.020	0.50	0.039

Thermal conductivity values of the foams, shown in Table IV-3, were low, supporting the use of this kind of material for insulating applications. Moreover, and as expected, the foams with the highest thermal conductivity were also those of lowest porosity and highest mechanical properties, on average. As for the latter, the present foams were elastic and did not crack easily

because rather flexible polymer chains were obtained, unlike what happens in the presence of formaldehyde which leads to highly friable materials. The shape of the compression curves shown in Fig. IV-4, wherein representative examples of some tannin-furanic foams prepared in this work can be seen, indeed suggests a typical elastic-plastic behaviour (Gibson and Ashby, 2001). When the density increased, a brittle character appeared as seen by the “noisy” aspect of the curve at the highest foam density, due to the redistribution of the compression after the fracture of some layers of cells, followed by the loading of the next cell layers.

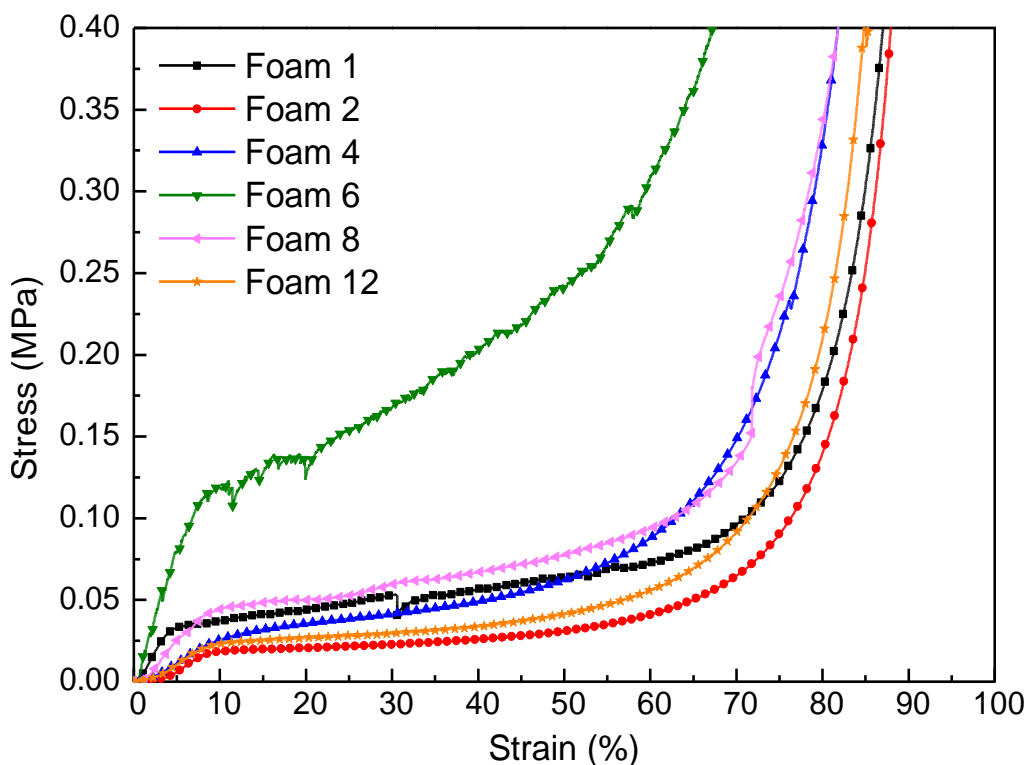


Fig. IV-4. Stress-strain curves of some tannin-based foams studied in this work.

Finally, Foams #9 and #14, prepared using exactly the same formulation in order to prove the repeatability of the foams, showed very similar properties indeed. Taking into account that the process is very complex and that the foams can present some point and surface defects, the results obtained from the foam characterisation were very repeatable. The density and porosity of the foam, and consequently the thermal conductivity, were quite similar; only low differences in mechanical properties were observed.

IV/3.2. Results of experimental design and related statistical analysis

The promising results reported in Table IV-3 with some tannin-furanic foams encouraged us to optimise the formulations further. Experimental design was thus employed to find some correlations between the main ingredients of the formulation and the resultant properties of the rigid foams. The responses in terms of thermal conductivity, compressive strength and elastic modulus of the tannin/furanic foams were modelled as a function of the weight fraction of tannin, furfuryl alcohol and catalyst in the formulation. A quadratic polynomial model was proposed by Design-Expert software, according to Eqs. (IV-3), (IV-4) and (IV-5):

$$\text{Thermal Conductivity} = 0.002304 \cdot A + 0.001015 \cdot B + 0.010291 \cdot C - 0.000047 \cdot A \cdot B - 0.000208 \cdot A \cdot C - 0.000141 \cdot B \cdot C \quad (\text{IV-3})$$

$$\text{Compressive Strength} = 0.035451 \cdot A + 0.005648 \cdot B + 0.2381 \cdot C - 0.000705 \cdot A \cdot B - 0.005368 \cdot A \cdot C - 0.002913 \cdot B \cdot C \quad (\text{IV-4})$$

$$\text{Elastic Modulus} = 1.720537 \cdot A + 0.501889 \cdot B + 6.143195 \cdot C - 0.047249 \cdot A \cdot B - 0.170622 \cdot A \cdot C - 0.056635 \cdot B \cdot C \quad (\text{IV-5})$$

The statistical evaluation of the proposed quadratic model developed for fitting thermal and mechanical properties was performed by analysis of variance (ANOVA). Error functions were defined to determine the significance of each parameter of the model and to assess the quality of the fits to the experimental data. Table IV-4 shows the results of ANOVA for Eqs. (IV-3)-(IV-5). The quality of the fits was expressed by the value of correlation coefficient (R^2), and its statistical significance was checked by Fisher's F-test (Fisher variation ratio) (Lundstedt et al., 1998).

The F-values 20.965, 8.506 and 5.176 gathered in Table IV-4 for thermal conductivity, compression strength and elastic modulus as responses, respectively, imply that the model is significant. On the other hand, the values of "Prob > F" less than 0.050 also indicate that model terms are significant (Fahimirad et al., 2017). Thus, AB is never significant and BC is not significant for the model of elastic modulus. The percentage of catalyst is the parameter having the highest influence on all the properties of rigid foams.

Table IV-4. ANOVA for Eqs. (IV-3)-(IV-5).

Source	Sum of Squares	Degree of freedom	Mean square	F-value	Prob > F
<i>ANOVA Thermal Conductivity</i>					
Model	7.0155E-05	5	1.4031E-05	20.9645751	0.00044197
Linear Mixture	5.4184E-05	2	2.7092E-05	40.4798856	0.00014218
<i>AB</i>	1.4941E-06	1	1.4941E-06	2.23248215	0.17878156
<i>AC</i>	1.2802E-05	1	1.2802E-05	19.1281726	0.00325984
<i>BC</i>	1.0925E-05	1	1.0925E-05	16.3229879	0.00493180
Residual	4.6849E-06	7	6.6927E-07		
Cor Total	7.4840E-05	12			
R-Squared	0.93743272				
<i>ANOVA Compressive strength</i>					
Model	0.02269210	5	0.00453842	8.50580542	0.00691837
Linear Mixture	0.01332719	2	0.00666360	12.4887655	0.00490779
<i>AB</i>	0.00033586	1	0.00033586	0.62946812	0.45359923
<i>AC</i>	0.00856403	1	0.00856403	16.0505052	0.00514842
<i>BC</i>	0.00467079	1	0.00467079	8.75389124	0.02114411
Residual	0.00373497	7	0.00053357		
Cor Total	0.02642707	12			
R-Squared	0.88871936				
<i>ANOVA Elastic modulus</i>					
Model	18.54315100	5	3.70863019	5.17577162	0.02635935
Linear Mixture	9.37954558	2	4.68977279	6.54505616	0.02496921
<i>AB</i>	1.51074795	1	1.51074795	2.10840282	0.18979375
<i>AC</i>	8.65133564	1	8.65133564	12.0738211	0.01033945
<i>BC</i>	1.76577668	1	1.76577668	2.46432142	0.16044884
Residual	5.01575673	7	0.71653668		
Cor Total	23.55890770	12			
R-Squared	0.85716687				

Furthermore, since higher R^2 corresponds to better fits, values close to 1 evidenced the reliability of Eqs (IV-3)-(IV-5). Herein, the R^2 was indeed found to be 0.9374, 0.8887 and 0.8572 for thermal conductivity, compressive strength and elastic modulus responses, respectively. The normal plots of the residuals for the responses are presented in Fig. IV-5, and

finding most points on the straight lines indicates a good agreement between experimental and calculated results.

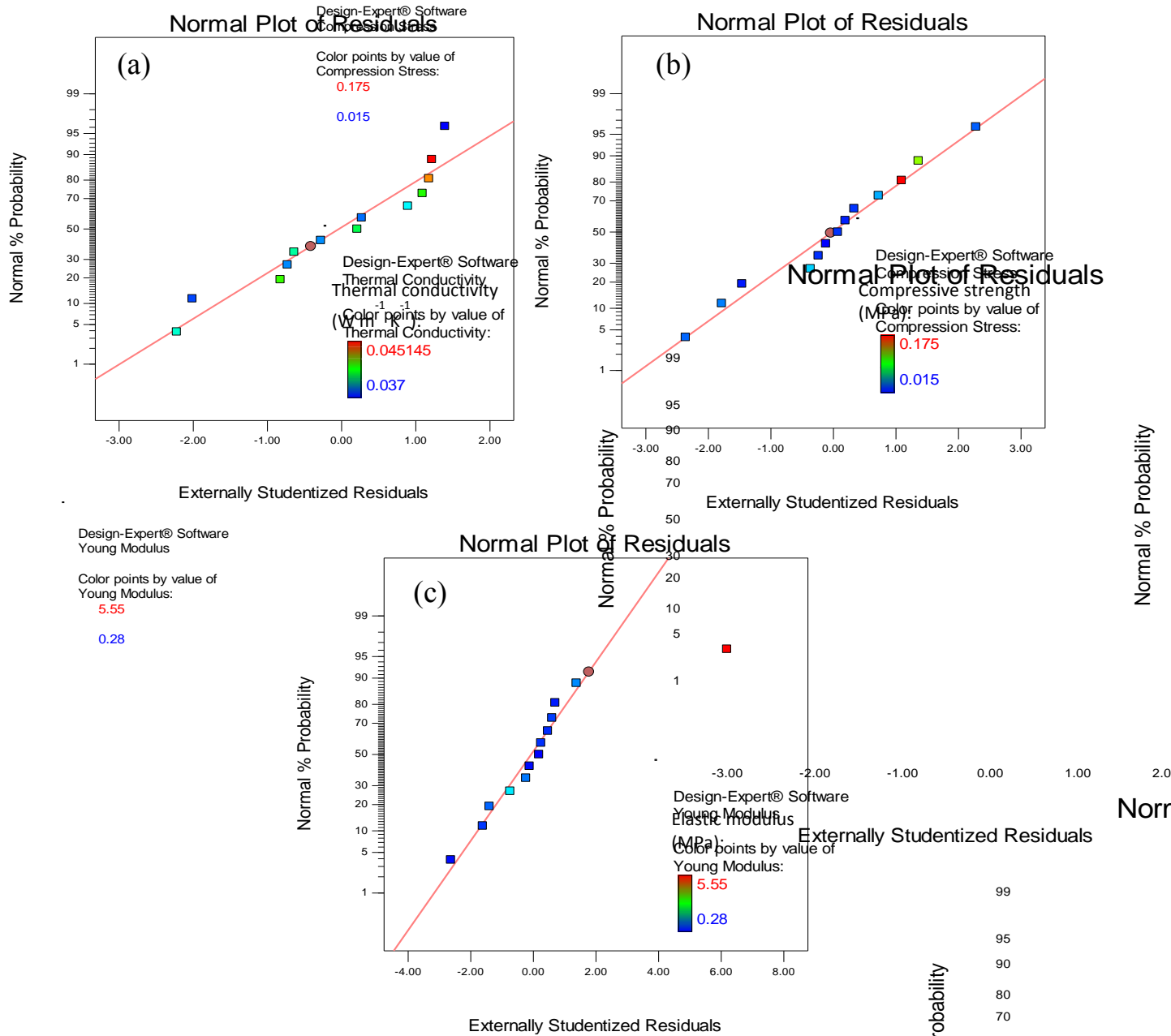


Fig. IV-5. Normal probability plot of residuals for: (a) thermal conductivity, (b) compression strength, and (c) elastic modulus. Numerical values of those properties increase from blue to red.

IV/3.3. Analysis of response surface methodology (RSM)

The relationship between the parameters and the responses is illustrated as contour plots and as three-dimensional response surface plots (Fig. IV-6) generated by the model. Thus, the impacts of the three main ingredients on the properties of the rigid foams are illustrated in Fig. IV-6(a), IV-6(b) and IV-6(c), respectively.

As shown in Fig. IV-6(a), the thermal conductivity increased with the amount of tannin in the formulation, thus supporting the discussion of subsection IV/2.3. It is also observed that when the amount of furfuryl alcohol was too low, the foam did not expand sufficiently, leading to foams with high density and, therefore, high thermal conductivity, which should be absolutely avoided. And indeed, since the investigated responses depend on porosity, the materials of higher thermal conductivity coincide with those of higher mechanical properties (compare Fig. IV-6(a) with IV-6(b) and IV-6(c)). Those foams were obtained with formulations containing low amounts of catalyst, large amounts of tannin and intermediate amounts of furfuryl alcohol.

On the other hand, the three-dimensional response surface plots show the formation of lightweight, insulating but mechanically weak foams when using a high amount of catalyst and a low amount of tannin. Consequently, in order to guarantee appropriate properties for using tannin-furanic foams as thermally insulating materials, it is absolutely necessary to find a compromise between thermal conductivity and mechanical properties through an optimal combination of ingredients.

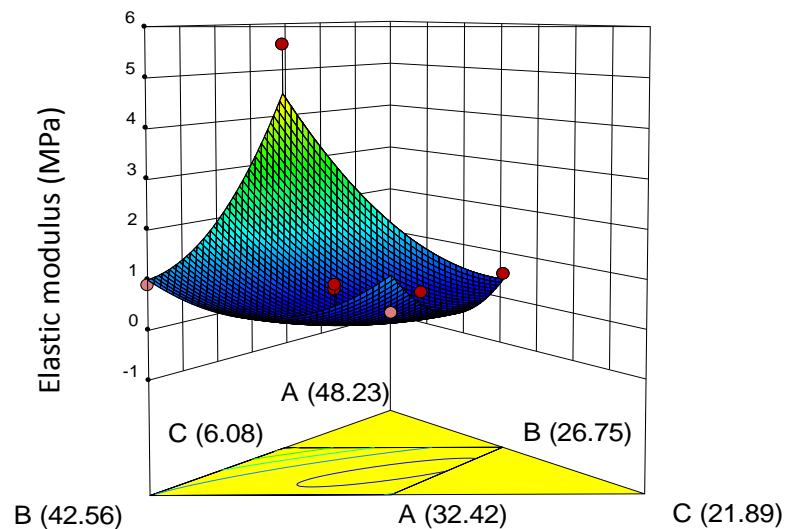
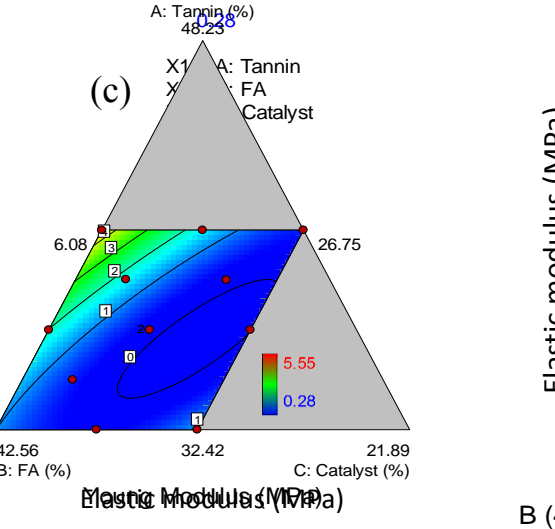
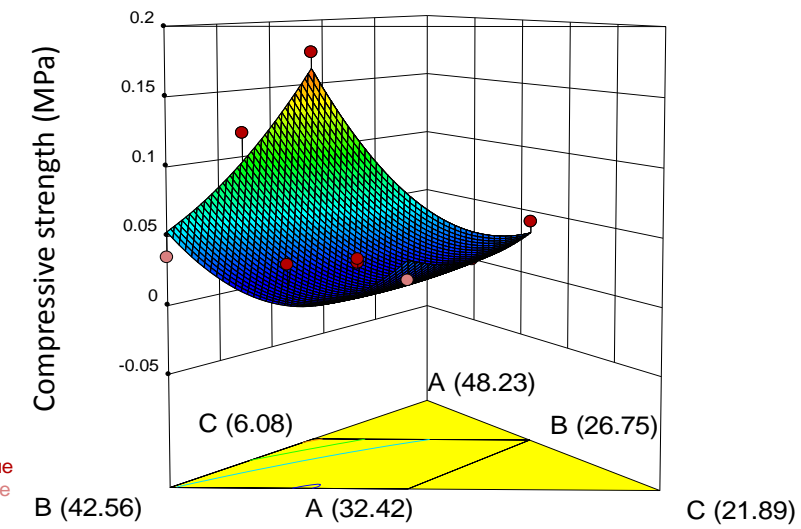
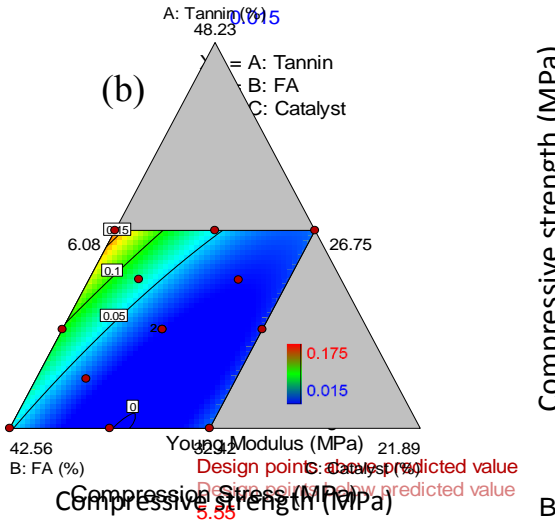
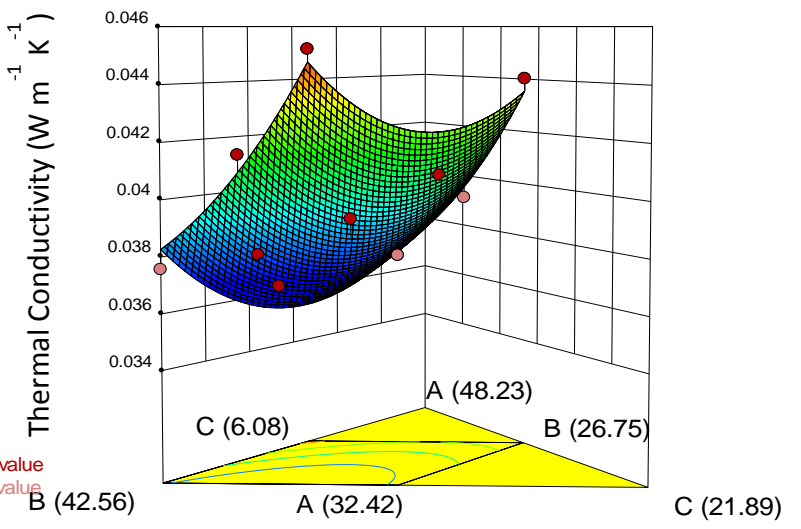
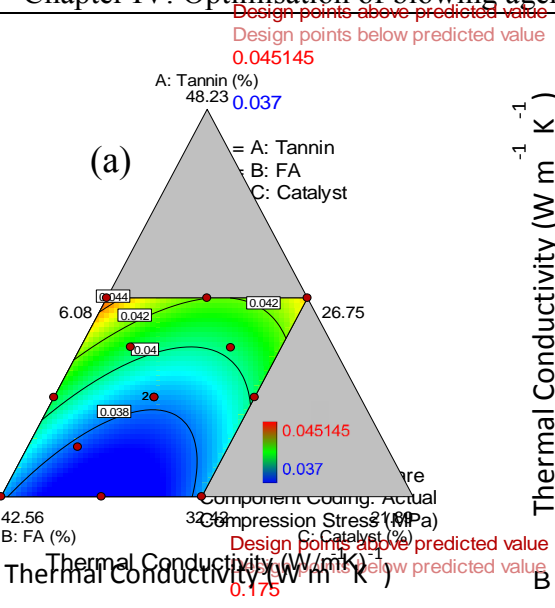


Fig. IV-6. Contour plots (first row, left) and surface plots (second row, right) of the effect of tannin, furfuryl alcohol and catalyst amounts on: (a) thermal conductivity; (b) compressive strength; (c) elastic modulus. Numerical values of the responses increase from blue to red.

IV/3.4. Optimisation of the formulation

The quadratic model obtained for determining the properties of the foams as a function of the fraction of main ingredients should allow defining an optimal formulation. The latter is essentially a compromise between insulating and mechanical properties that are practically antagonistic. Fig. IV-7 thus presents a plot of thermal conductivity versus compressive strength, both calculated from the model by using small discrete increments of wt. % of the three main ingredients. Compressive strength was chosen here instead of elastic modulus for the optimisation analyses, because it is the most significant mechanical property from a practical point of view and, moreover, both strength and modulus qualitatively vary in the same way.

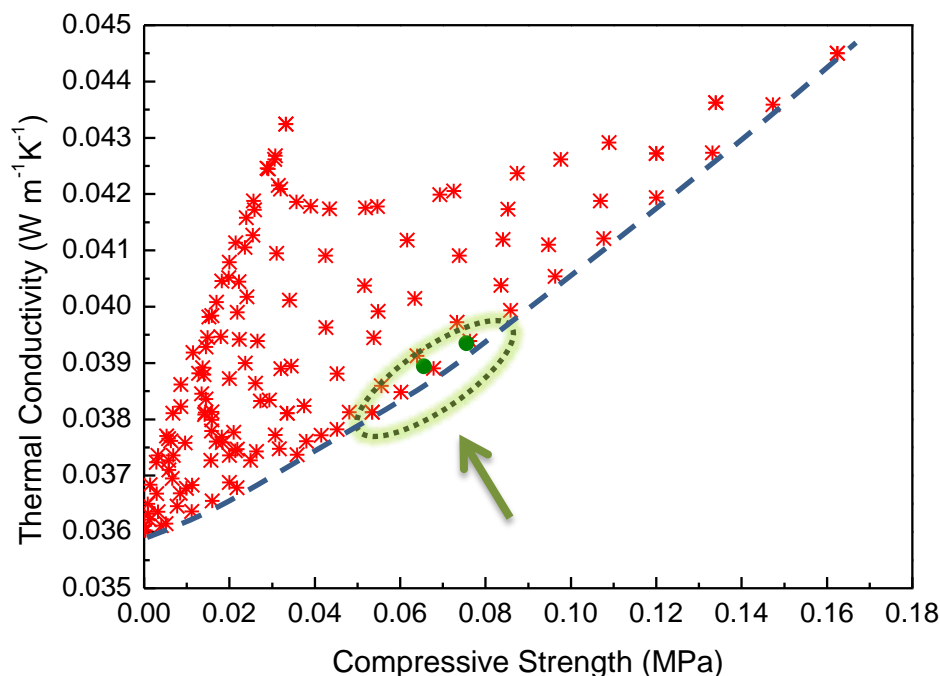


Fig. IV-7. Thermal conductivity versus compressive strength calculated by application of Eqs. (IV-3)-(IV-5), using compositions inside the ranges given in Eq. (IV-1). The best compromise between low thermal conductivity and high mechanical properties is highlighted by the dotted contour, and the two green points inside the dotted contour are the formulations employed to prove the relevance of the model. The dashed line is just a guide for the eye, indicating the lower boundary of thermal conductivity that can be expected with this kind of materials.

The area inside the contour in Fig. IV-7 contains the foams having the most promising properties. They indeed present a good compromise between all requested properties, i.e., a thermal conductivity lower than $0.040 \text{ W}\cdot\text{m}^{-1}\cdot\text{K}^{-1}$ and a compressive strength that can reach 0.08 MPa. Those properties are slightly better than those of other closely related materials having a similar thermal conductivity of $0.040 \text{ W}\cdot\text{m}^{-1}\cdot\text{K}^{-1}$ but presenting a compressive stress not higher than 0.06 MPa for tannin-furanic foams prepared with blowing agent (Basso et al., 2011), or of 0.03 MPa for meringue foams prepared with hexamine as crosslinker (Szcurek et al., 2014). Fig. IV-7 also has the advantage of showing that no thermal conductivity lower than the values represented by the dashed line can be expected with this kind of materials, such “diagonal” in the plot corresponding to the best insulators that might be prepared.

Representing those optimal foams in the tannin – furfuryl alcohol – catalyst ternary diagram, one can better see the kind of formulations leading to the best foams (see Fig. IV-8). These are formulations with a high amount of furfuryl alcohol, a low amount of catalyst to avoid a violent expansion due to such large amount of furfuryl alcohol, and a low amount of tannin too.

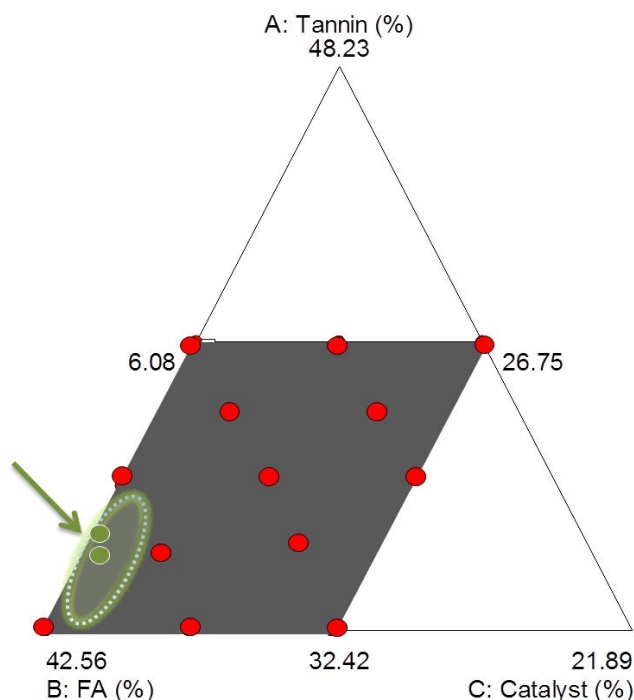


Fig. IV-8. Area (dotted contour) corresponding to the optimum formulations in the tannin – furfuryl alcohol – catalyst ternary diagram. The two green points inside the dotted contour are the formulations employed to prove the relevance of the model.

Two foams represented in Fig. IV-7 and Fig. IV-8 by two green points inside the optimal area were prepared, and their properties were measured in order to prove the efficiency of the model. Those two optimum formulations, OF1 (34.69 wt. % tannin, 39.97 wt. % furfuryl alcohol and 6.4 wt. % catalyst) and OF2 (34.83 wt. % tannin, 40.13 wt. % furfuryl alcohol and 6.1 wt. % catalyst), were thus expected to show a good compromise between thermal conductivity and mechanical properties. The corresponding experimental results are gathered in Table IV-5, together with the values predicted by the multiple-regression model. As can be seen, there is an excellent agreement between measured and predicted values, indicating the effectiveness of the model.

Table IV-5. Validation of the model: measured versus predicted values.

Sample	ρ_b (g·cm ⁻³)	Experimental			Predicted by the model		
		Compressive strength (MPa)	Elastic modulus (MPa)	Thermal Conductivity (W·m ⁻¹ ·K ⁻¹)	Compressive strength (MPa)	Elastic modulus (MPa)	Thermal Conductivity (W·m ⁻¹ ·K ⁻¹)
OF1	0.046	0.069	1.14	0.0381	0.066	1.18	0.0389
OF2	0.058	0.078	1.45	0.0394	0.076	1.39	0.0394

IV/4. Conclusion

Tannin-furanic foams prepared without formaldehyde, blowing agent and isocyanate are environment-friendly alternatives to the contemporary synthetic foams for thermal insulation. For that purpose, a low thermal conductivity is mandatory, but good mechanical properties are also important for practical use.

It is well known that improving the thermal insulation properties of foams having mainly open cells requires an as-high-as-possible porosity. This is indeed the only way of approaching the conductivity of air, 0.026 W·m⁻¹·K⁻¹ at room temperature and pressure, which behaves as a very good insulator. But increasing the porosity necessarily decreases the mechanical properties of the foams, since less solid is present. In this context, thermal insulation and mechanical resistance are antagonistic properties, justifying the search for a compromise. Such study was carried out here

through the use of an effective and efficient tool: experimental design and related statistical analysis of the results.

Doing so, the impact of the major ingredients of tannin-furanic foams could be explored, the results were modelled, and based on the model the properties of other formulations within the investigated range of formulations could be predicted. As a result, the most suitable combinations of the three main ingredients (tannin, furfuryl alcohol and catalyst) were selected for obtaining foams being both enough thermally insulating and mechanically strong. The corresponding formulations contained a high amount of furfuryl alcohol, a moderate amount of tannin and a low amount of catalyst.

The effectiveness of the experimental design and its model was tested through the preparation of foams having the expected optimal properties, and measuring their thermal conductivity, elastic modulus and compressive strength. The results showed that the corresponding properties were in excellent agreement with the values predicted by the model. As a consequence, the latter was shown to be a very useful tool for developing environment-friendly tannin-furanic foams with desired features and for the industrialisation of the technology.

IV/5. Bibliography

- Antony, J., Roy, R.K., 1998. Improving the process quality using statistical design of experiments: a case study. *Qual. Assur. San Diego Calif* 6, 87–95.
- Basso, M.C., Giovando, S., Pizzi, A., Celzard, A., Fierro, V., 2013a. Tannin/furanic foams without blowing agents and formaldehyde. *Ind. Crops Prod.* 49, 17–22. doi:10.1016/j.indcrop.2013.04.043
- Basso, M.C., Lagel, M.-C., Pizzi, A., Celzard, A., Abdalla, S., 2015. First Tools for Tannin-Furanic Foams Design. *Bioresources* 10, 5233–5241.
- Basso, M.C., Li, X., Fierro, V., Pizzi, A., Giovando, S., Celzard, A., 2011. Green, formaldehyde-free, foams for thermal insulation. *Adv. Mater. Lett.* 2, 378–382. doi:10.5185/amlett.2011.4254
- Basso, M.C., Pizzi, A., Celzard, A., 2013b. Influence of formulation on the dynamics of preparation of tannin-based foams. *Ind. Crops Prod.* 51, 396–400. doi:10.1016/j.indcrop.2013.09.013
- Basso, M.C., Pizzi, A., Celzard, A., 2013c. Dynamic Monitoring of Tannin-based Foam Preparation: Effects of Surfactant. *Bioresources* 8, 5807–5816.

- Fahimirad, B., Asghari, A., Rajabi, M., 2017. Photo-degradation of basic green 1 and basic red 46 dyes in their binary solution by La₂O₃-Al₂O₃nanocomposite using first-order derivative spectra and experimental design methodology. *Spectrochim. Acta. A. Mol. Biomol. Spectrosc.* 179, 58–65. doi:10.1016/j.saa.2017.02.022
- Fang, K.-T., Yang, Z.-H., 2000. On uniform design of experiments with restricted mixtures and generation of uniform distribution on some domains. *Stat. Probab. Lett.* 46, 113–120. doi:10.1016/S0167-7152(99)00095-4
- Gardziella, D.A., Pilato, D.L.A., Knop, D.A., 2000. Phenolic Resins: Chemistry, Reactions, Mechanism, in: *Phenolic Resins*. Springer Berlin Heidelberg, pp. 24–82.
- Gibson, L.J., Ashby, M.F., 2001. *Cellular solids: structure and properties*, 2. ed., 1. paperback ed. (with corr.), transferred to digital printing. ed, Cambridge solid state science series. Cambridge Univ. Press, Cambridge.
- Lacoste, C., Basso, M.C., Pizzi, A., Laborie, M.-P., Garcia, D., Celzard, A., 2013. Bioresourced pine tannin/furanic foams with glyoxal and glutaraldehyde. *Ind. Crops Prod.* 45, 401–405. doi:10.1016/j.indcrop.2012.12.032
- Lacoste, C., Pizzi, A., Laborie, M.-P., Celzard, A., 2014. Pinus pinaster tannin/furanic foams: Part II. Physical properties. *Ind. Crops Prod.* 61, 531–536. doi:10.1016/j.indcrop.2014.04.034
- Liang, Y., Fang, K., Xu, Q., 2001. Uniform design and its applications in chemistry and chemical engineering. *Chemom. Intell. Lab. Syst.* 58, 43–57. doi:10.1016/S0169-7439(01)00139-3
- Lundstedt, T., Seifert, E., Abramo, L., Thelin, B., Nystrom, A., Pettersen, J., Bergman, R., 1998. Experimental design and optimization. *Chemom. Intell. Lab. Syst.* 42, 3–40. doi:10.1016/S0169-7439(98)00065-3
- Montgomery, D.C., 2008. *Design and Analysis of Experiments*. John Wiley & Sons.
- Szczurek, A., Amaral-Labat, G., Fierro, V., Pizzi, A., Masson, E., Celzard, A., 2011. Porosity of resorcinol-formaldehyde organic and carbon aerogels exchanged and dried with supercritical organic solvents. *Mater. Chem. Phys.* 129, 1221–1232. doi:10.1016/j.matchemphys.2011.06.021
- Szczurek, A., Fierro, V., Pizzi, A., Stauber, M., Celzard, A., 2014. A new method for preparing tannin-based foams. *Ind. Crops Prod.* 54, 40–53. doi:10.1016/j.indcrop.2014.01.012
- Tondi, G., Pizzi, A., 2009. Tannin-based rigid foams: Characterization and modification. *Ind. Crops Prod.* 29, 356–363. doi:10.1016/j.indcrop.2008.07.003
- Tondi, G., Zhao, W., Pizzi, A., Du, G., Fierro, V., Celzard, A., 2009. Tannin-based rigid foams: A survey of chemical and physical properties. *Bioresour. Technol.* 100, 5162–5169. doi:10.1016/j.biortech.2009.05.055
- Zhang, X.D., Macosko, C.W., Davis, H.T., Nikolov, A.D., Wasan, D.T., 1999. Role of Silicone Surfactant in Flexible Polyurethane Foam. *J. Colloid Interface Sci.* 215, 270–279. doi:10.1006/jcis.1999.6233
- Zhao, W., Fierro, V., Pizzi, A., Du, G., Celzard, A., 2010. Effect of composition and processing parameters on the characteristics of tannin-based rigid foams. Part II: Physical properties. *Mater. Chem. Phys.* 123, 210–217. doi:10.1016/j.matchemphys.2010.03.084

Chapter V: Flammability of tannin-based foams

V/1. Introduction

The massive use of some polymers in our everyday life is driven by their remarkable combination of properties, especially low density, specific mechanical resistance, and ease of processing. It is, therefore, not surprising that fire retardance and related properties such as emission of smoke or dripping of inflamed particles became very critical parameters to be considered in applications such as transportation, packaging or thermal and acoustic insulation, amongst others. Consequently, improving the fire retardant behaviour of those materials is a major challenge for extending their use to others applications. Safety requirements are currently becoming more and more drastic in terms of polymers' reaction to fire. Chemical and/or physical modification of polymers to incorporate flame retardant additives is a usual procedure in the industry, but such additives might be toxic and have an impact on the environment and on human health (Laoutid et al., 2009).

Some of the most used commercial products for thermal and acoustic insulation are polyurethane or polystyrene foams which are well-known for their relatively high flammability, most often accompanied by the production of corrosive or highly toxic gases and smoke during combustion. Those problems call for the use of fire retardants, but the latter generally produce a loss of physical and mechanical properties on the material, despite the many efforts already carried out for minimising such effects (Singh and Jain, 2008). Poor fire resistances and high flammability are generally characteristic for the natural and biodegradable products too (Mngomezulu et al., 2014).

The fire properties of the first formulation of tannin-based foams, Standard Tannin Foams (presented in the subsection *I/3.4.5 Fire behaviour*), were studied some years ago (Celzard et al., 2011), and those foams presented excellent fire retardance. After this work was published, not much more research has been carried out about that topic on tannin-based foams. Only a few tests with similar results were carried out with formaldehyde-free tannin foams (Celzard et al., 2015). All those initial results turned those foams into a very interesting materials since, in addition to their renewable, cost-effective, and environment-friendly properties, they exhibit much better fire retardant properties than most commercial thermally insulating materials (polyurethane or polystyrene foams). However, despite tannin foams seem have very attractive properties, they

need to be investigated more in-depth since many other formulations with new ingredients and new foaming methods have been developed recently, and which might induce a change in their fire properties. Such work is presented in the present chapter.

The flammability of a material is not a straightforwardly determined property. Inflammation can be due to thermal energy from an external heat source (radiation, convection or conduction), by a chemical process occurring inside the material (fermentation, oxidation, etc.) or by the exothermicity of the initiation of a combustion reaction (Lyon et al., 2014). The amount of energy required to initiate combustion generally depends on the physical and chemical characteristics of the material. Thus, an exhaustive study of the most relevant parameters influencing the fire retardance behaviour of our foams is of paramount importance for being able to enhance and control those properties. The flammability can be tested through different fire testing techniques (Laoutid et al., 2009; Price et al., 2001; Wichman, 2003). These techniques involve the measurement of parameters such as ignitability (ignition temperature, delay time, critical heat flux), burning rates (heat release rate, solid degradation rate), spread rates (flame, pyrolysis, and smoulder), analysis of degradation products (emissions of toxic products, smoke), etc., by appropriate tests (Carvel et al., 2011; Laoutid et al., 2009; Price et al., 2001; Scharrel et al., 2007; Wilkie, 1999).

The research work about tannin foams' fire properties presented in this chapter has been developed from different perspectives detailed hereafter, combining various measurement techniques. Initially, the flammability of the main types of tannin foams has been studied and their European class has been estimated, in order to compare the corresponding values with those of other materials that are currently on the market. Afterwards, the influence of the formulation on the fire properties of the foams has been analysed. For that purpose, foams with some modifications in their composition and in the foaming procedure have been studied in order to observe the effect such preparation parameters on the flammability of the foams. Finally, for completing the study, the combustion products of the two main and most different tannin foams, standard and meringue, have been identified.

All the fire tests performed were carried out in the research group "Reaction and Resistance to Fire (R2Fire)" of the laboratory Unité Matériaux Et Transformations (UMET) - CNRS UMR 8207, hosted by the École Nationale Supérieure de Chimie de Lille (ENSCL) in Villeneuve

d'Ascq (University of Lille 1), during a one-week research training there in 2016. Special thanks go to Prof. Serge Bourbigot for giving me the access to their devices of fire testing and analysis of materials submitted to fire.

V/2. European fire testing of building products

In the past, all the materials related to building were traditionally tested and classified according to national building codes in most countries of the world. The different countries of the European Union used to have different fire tests supporting their own national regulations and, consequently, it was extremely difficult to compare with each other the data arising from different fire tests. Manufacturers thus have had to make tests in every country to sell their products. Therefore, in the last decade, a common European system for reaction to fire testing and classification, known as the Euroclass, was developed (Commission Decision 2000/147/EC, 2000). The Single Burning Item (SBI), used for testing, and the FIGRA (FIre Growth RAte) parameter, used for evaluating materials reaction to fire properties, were introduced (Sundström, 2007).

In the Euroclass system, building products are divided into seven classes based on their reaction-to-fire properties. This system affects mainly surface covering materials, insulation materials, floor coverings, pipe insulation materials and cables. Surface covering materials and products are classified by the FIGRA (FIre Growth Rate) index ($W \cdot s^{-1}$), which is defined as the maximum value of heat release rate divided by elapsed time, and it is a good estimation of the spread (rate) and the size of a fire.

The classification of the performance of construction products in terms of reaction to fire made in February 2000 by the European Commission (Commission Decision 2000/147/EC, 2000) is shown in Table V-1, together with the test methods and classification criteria.

Table V-1. Classes of reaction to fire performance for construction products excluding floorings - (EN 13501-1, 2007).

Class	Test method(s)	Classification criteria	Additional classification
A1	EN ISO 1182 ⁽¹⁾ ; <i>And</i>	$T \leq 30^{\circ}\text{C}$; <i>and</i> $m \leq 50\%$; <i>and</i> $t_f = 0$ (i.e. no sustained flaming)	-
	EN ISO 1716	$\text{PCS} \leq 2.0 \text{ MJ.kg}^{-1}$ ⁽¹⁾ ; <i>and</i> $\text{PCS} \leq 2.0 \text{ MJ.kg}^{-1}$ ⁽²⁾ ^(2a) ; <i>and</i> $\text{PCS} \leq 1.4 \text{ MJ.m}^{-2}$ ⁽³⁾ ; <i>and</i> $\text{PCS} \leq 2.0 \text{ MJ.kg}^{-1}$ ⁽⁴⁾	-
A2	EN ISO 1182 ⁽¹⁾ ; <i>Or</i>	$T \leq 50^{\circ}\text{C}$; <i>and</i> $m \leq 50\%$; <i>and</i> $t_f \leq 20\text{s}$	-
	EN ISO 1716; <i>And</i>	$\text{PCS} \leq 3.0 \text{ MJ.kg}^{-1}$ ⁽¹⁾ ; <i>and</i> $\text{PCS} \leq 4.0 \text{ MJ.m}^{-2}$ ⁽²⁾ ; <i>and</i> $\text{PCS} \leq 4.0 \text{ MJ.m}^{-2}$ ⁽³⁾ ; <i>and</i> $\text{PCS} \leq 3.0 \text{ MJ.kg}^{-1}$ ⁽⁴⁾	-
	EN 13823 (SBI)	$\text{FIGRA} \leq 120 \text{ W.s}^{-1}$; <i>and</i> $\text{LFS} < \text{edge of specimen}$; <i>and</i> $\text{THR}_{600\text{s}} \leq 7.5 \text{ MJ}$	Smoke production ⁽⁵⁾ ; <i>and</i> Flaming droplets/ particles ⁽⁶⁾
B	EN 13823 (SBI); <i>And</i>	$\text{FIGRA} \leq 120 \text{ W.s}^{-1}$; <i>and</i> $\text{LFS} < \text{edge of specimen}$; <i>and</i> $\text{THR}_{600\text{s}} \leq 7.5 \text{ MJ}$	Smoke production ⁽⁵⁾ ; <i>and</i> Flaming droplets/ particles ⁽⁶⁾
	EN ISO 11925-2 ⁽⁸⁾ ; <i>Exposure = 30s</i>	$\text{Fs} \leq 150\text{mm}$ within 60s	
C	EN 13823 (SBI); <i>And</i>	$\text{FIGRA} \leq 250 \text{ W.s}^{-1}$; <i>and</i> $\text{LFS} < \text{edge of specimen}$; <i>and</i> $\text{THR}_{600\text{s}} \leq 15 \text{ MJ}$	Smoke production ⁽⁵⁾ ; <i>and</i> Flaming droplets/ particles ⁽⁶⁾
	EN ISO 11925-2 ⁽⁸⁾ ; <i>Exposure = 30s</i>	$\text{Fs} \leq 150\text{mm}$ within 60s	
D	EN 13823 (SBI); <i>And</i>	$\text{FIGRA} \leq 750 \text{ W.s}^{-1}$	Smoke production ⁽⁵⁾ ; <i>and</i> Flaming droplets/ particles ⁽⁶⁾
	EN ISO 11925-2 ⁽⁸⁾ ; <i>Exposure = 30s</i>	$\text{Fs} \leq 150\text{mm}$ within 60s	
E	EN ISO 11925-2 ⁽⁸⁾ ; <i>Exposure = 15s</i>	$\text{Fs} \leq 150\text{mm}$ within 20s	Flaming droplets/ particles ⁽⁷⁾
F	No performance determined		

- (*) The treatment of some families of products, e.g. linear products (pipes, ducts, cables etc.), is still under review and may necessitate an amendment to this decision.
- (¹) For homogeneous products and substantial components of non-homogeneous products.
- (²) For any external non-substantial component of non-homogeneous products.
- (^{2a}) Alternatively, any external non-substantial component having a $PCS \leq 2.0 \text{ MJ.m}^{-2}$, provided that the product satisfies the following criteria of EN 13823(SBI) : $FIGRA \leq 20 \text{ W.s}^{-1}$; and $LFS < \text{edge of specimen}$; and $THR_{600s} \leq 4.0 \text{ MJ}$; and $s1$; and $d0$.
- (³) For any internal non-substantial component of non-homogeneous products.
- (⁴) For the product as a whole.
- (⁵) $s1 = SMOGRA \leq 30\text{m}^2.\text{s}^{-2}$ and $TSP_{600s} \leq 50\text{m}^2$; $s2 = SMOGRA \leq 180\text{m}^2.\text{s}^{-2}$ and $TSP_{600s} \leq 200\text{m}^2$; $s3 = \text{not } s1 \text{ or } s2$.
- (⁶) $d0 = \text{No flaming droplets/ particles in EN13823 (SBI) within 600s}$; $d1 = \text{No flaming droplets/ particles persisting longer than 10s in EN13823 (SBI) within 600s}$; $d2 = \text{not } d0 \text{ or } d1$; Ignition of the paper in EN ISO 11925-2 results in a $d2$ classification.
- (⁷) Pass = no ignition of the paper (no classification); Fail = ignition of the paper ($d2$ classification).
- (⁸) Under conditions of surface flame attack and, if appropriate to end-use application of product, edge flame attack.

FIGRA, the main parameter for classification of building products, is based on the SBI (Single Burning Item) (EN 13501-1, 2007) test in the so-called Euroclass-system which evaluates the potential contribution of a surface lining to the development of a fire. It simulates a single burning item in a corner of a room. Such test needs that each specimen has an area of 2.25 m^2 , and an infrastructure that we did not have access to. Therefore, we calculated a kind of FIGRA index for the tannin-based foams and other insulation materials using Cone Calorimeter technique in order to compare and have an idea of the fire class of the material. Thus, it has been assumed that the Heat Release Rate (HRR), rate at which heat is generated by the fire, per unit area measured in the Cone Calorimeter is the same as the one obtained from surface elements in the room submitted to fire. Such assumption is not necessarily true as the burning environment in the cone may differ from that of the room, for example in terms of air supply and sample orientation. However, a Cone Calorimeter is able to predict an approximate FIGRA index value that allows us to define the most likely fire class of the material (Bourbigot et al., 2001; Chen et al., 2012; Giraud et al., 2005). Moreover, Cone Calorimeter testing is easier as soon as several versions of one material have to be quickly tested, so that it allows finding which one performs best and hence investigating the impact of formulation and preparation protocol.

Some of the main types of insulation product associated to each Euroclass are gathered in Fig.V-1. As tannin is a polyphenolic molecule, tannin-based foams are expected to present fire properties somewhat similar to those of phenolic foams, and thus probably belong to the group B of the Euroclass.

Euroclass for some typical insulation products

Euroclass	Type of insulation product
A1	Glass wool, stone wool, foam glass
A2	High density foam stoned and glass wool
B	Some phenolic foams tannin-based foams??
C	Some polyisocyanurate foams
D	Most polyisocyanurate foams, wood
E	Flame-retarded expanded polystyrene, polyurethane foams
F	Non flame-retarded expanded polystyrene

Fig. V-1. Euroclass classification for the main insulation product on the market.

V/3. Experimental

V/3.1. Foam preparation

Twelve different tannin-based foams have been prepared and analysed in the present study. They are a representative selection of all the types of tannin foams that exist until this moment. The foam formulations were carefully selected in order to be able to analyse the effect of the content of surfactant, plasticiser, furfuryl alcohol and crosslinker, as well as of the way of foaming, temperature of curing and type of tannin (mimosa, quebracho FintanT and quebracho FintanQ). Therefore, foams with very different compositions and features were developed as shown in Fig. V-2.



Fig. V-2. All the tannin-based foams studied in this work.

Standard Tannin Foams were prepared using two different kinds of tannin, mimosa (STD-M) and quebracho FintanT (STD-Q), following the specific methodology described in *I/3.3. Formulations of tannin foams*. The standard formulation with mimosa was also slightly modified by adding a plasticiser (PEG-M), as well as with different kinds of surfactant (Pluro-M and Triton-M); they are derived from a recent work of our team reported elsewhere (Letellier et al., 2017). On the other hand, Standard Formaldehyde-free Tannin Foams were also prepared from two kinds of tannin, mimosa (SF-M) and quebracho FintanT (SF-Q). Some formaldehyde-free foams containing a little amount of surfactant, helping the stabilisation of the foaming, were also prepared (P21-Q), whereas other were modified by adding furfuryl alcohol (P24-Q). Finally, some foams were prepared following different methods of foaming and curing, such as meringue foam (Meringue-M) based in mechanical foaming with polymerisation at 85°C and a new confidential method based in the mechanical foaming with auto-polymerisation (C200-Q' and LNSA3-Q').

More information about the origin and the justification of the foam formulations used in this work can be found in Chapter I of the thesis. The detailed compositions of the foams prepared for carrying out this study are gathered in Table V-2. Only the formulations C200-Q' and LNSA3-Q' have not been detailed because they are part of the confidential work carried out together with a company during the thesis (Table V-2).

Table V-2. Formulation of the different types of foams.

	Chemical foaming + auto-polymerisation												Mechanical foaming + reaction at 85°C	Confidential foams: mechanical foaming + auto-polymerisation		
	Mimosa						Quebracho Fintan T								Mimosa	Quebracho Fintan Q
	STD-M	PEG-M	Triton-M	Pluro-M	SF-M		STD-Q	SF-Q	P21-Q	P24-Q					Meringue-M	C200-Q'
Tannin (g)	30	30	30	30	30		30	30	30	30			20			
Furfuryl alcohol (g)	10.5	10.5	10.5	10.5	21		10.5	21	21	24			-			
Water (g)	6	6	6	6	6		6	6	6	6			30			
Formaldehyde (37% in water) (g)	7.4	7.4	7.4	7.4	-		7.4	-	-	-			-			
Plasticiser (g)	-	8	8	8	-		-	-	-	-			-			
Diethyl ether (g)	6	6	6	5	3		3	3	3	3			-			
Surfactant (g)	-	-	0.6 ^A	0.6 ^B	-		-	-	3 ^C	3 ^C			3 ^D			
pTSA (65% in water) (g)	11	11	11	11	11		11	11	11	11			1.12*			
Hexamine (g)	-	-	-	-	-		-	-	-	-			1.45			
Density (g·cm ⁻³)	0.039	0.055	0.057	0.044	0.028		0.060	0.038	0.065	0.048			0.065	0.120	0.081	

Surfactant: ^A Triton X-100; ^B Pluronic PE 7400; ^C Cremophor ELP; ^D Tween80

Plasticiser: Polyethylene glycol with molecular weight 400, PEG

Catalyst: paratoluenesulphonic acid, pTSA. *pTSA solid, not in solution

V/3.2. Foam properties

Flammability is the ability of a substance to burn or ignite, causing fire or combustion. It is characterised by different parameters such as the ignitability, flame spread rate and heat release. A number of small, intermediate and/or full-scale flammability tests are used in industrial and/or academic laboratories to quantify it (Mngomezulu et al., 2014). The single most important variable in the definition of fire growth is the Heat Release Rate (HRR). The HRR can be viewed as the engine driving the fire. This tends to occur in a positive-feedback way: heat makes more heat (Babrauskas and Grayson, 2009). It controls the growth of a fire and, therefore, the production of undesirable effects of fire such as toxic gases, smoke and other types of fire hazards. Since the probability of such effects increases with the heat release rate, the latter represents the best variable to assess the hazard of a fire.

The ignition time is also one of the most important variables in the characterisation of the flammability of a material. It is defined as the time at which a continuous flame is supported on the material surface (Mouritz and Gibson, 2006). It is always recommended to control ignition sources and to use materials poorly prone to ignition, whenever possible. Indeed, neither HRR nor any other consequences of fire will come into play as long as there is no ignition. However, when an ignition does occur, limiting the HRR means that the fire has a chance to be controllable and not disastrous. High HRR fires, however, are intrinsically dangerous.

On the other hand, the peak HRR, the total amount of HR as well as the smoke generation and toxicity are interesting parameters that are worth highlighting too. The peak HRR occurs over a very short period of time and often shortly after ignition, and is usually a good indicator of the maximum flammability of a material. The average HR is the total heat released averaged over the combustion period, and is considered as the most reliable measure of the heat contribution to a sustained fire. Finally, as it was mentioned earlier, it is also very important to control the toxic gases released during combustion as they cause the greatest health hazard (Mouritz and Gibson, 2006).

The flammability testing techniques used in this work to obtain some of those fire parameters for tannin-based foams were: cone calorimetry, pyrolysis combustion flow calorimetry (PCFC),

and thermogravimetric analysis coupled with Fourier-transform infrared spectroscopy (TGA-FTIR).

V/3.2.1 Cone calorimetry studies

Cone calorimetry is one of the most effective medium-sized fire test devices used to study the rate of heat released by materials exposed to a radiant heat flux. It has been standardised in the United States (ASTM E-1354-90) and in an international standard (ISO 5660) which allow comparing the fire behaviour of materials with each other. In general, the principle of cone calorimeter experiment is based on the measurement of the decreasing oxygen concentration in the combustion gases of a sample subjected to a given heat flux. Typical levels of heat flux are 25, 35, 50 and 75 kW·m⁻² and they represent low thermal aggression situation, mild fire scenario, flashover situation and strong and sudden fire, respectively (Babrauskas, 1984). The surface of the test specimen is exposed to a constant level of heat irradiance from a conical heater. Volatile gases from the heated specimen are ignited by an electrical spark igniter. The gas analysis makes possible to calculate heat release rate. The specimen is mounted on a load cell which records the mass loss rate of the specimen during combustion.

Fig. V-3 illustrates the experimental set-up of a cone calorimeter in details. In the measurement carried out in this work, the used equipment followed the procedure defined in ASTM E-906. The equipment is identical to that used in oxygen consumption cone calorimetry (ASTM E-1354-90), except that a thermopile in the chimney was used to obtain heat release rate (HRR) rather than employing the oxygen consumption principle. The samples (100 × 100 × 20 mm) were horizontally placed in a sample holder on a load cell for evaluation of the mass loss during the experiment. The samples were wrapped in aluminium foil leaving the upper surface exposed to the heater and placed on a ceramic backing board at a distance of 25 mm from the cone base. A conical radiant electrical heater uniformly irradiated the sample from above with a heat flux of 50 kW·m⁻². The combustion was triggered by an electrical spark. The combustion gases that were produced passed through the heating cone and were captured by means of an exhaust duct system with a centrifugal fan and an extraction hood (Carvel et al., 2011; Guillaume et al., 2014; Laoutid et al., 2009).

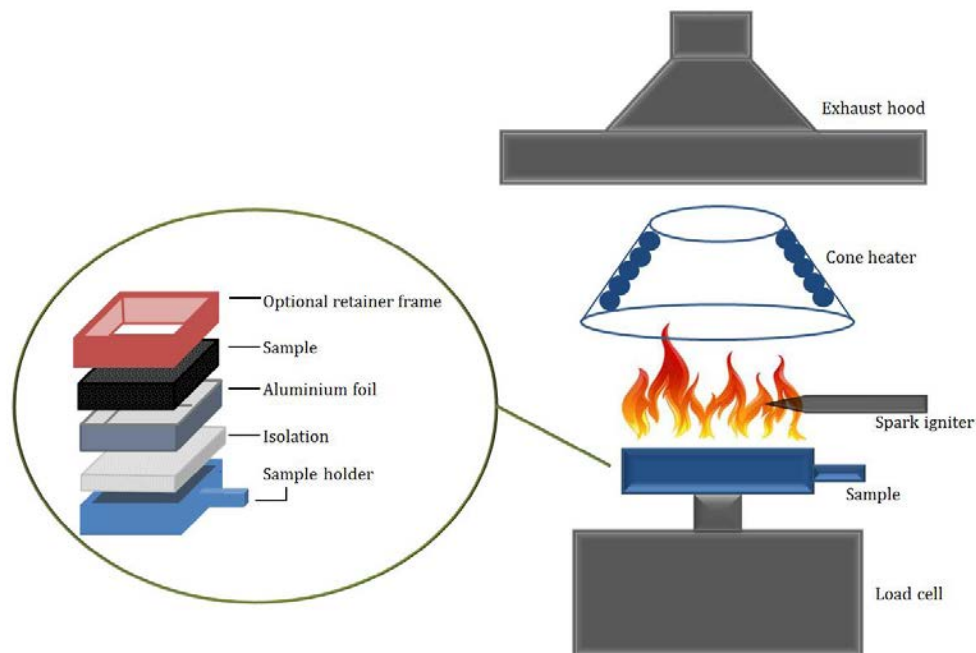


Fig. V-3. Schematic representation of a cone calorimeter.

The quantity of heat released per unit of time and surface area, the HRR (heat release rate), expressed in $\text{kW}\cdot\text{m}^{-2}$ was, therefore, measured. Moreover, the time to ignition (TTI) and the FIGRA (fire growth rate) index were calculated too.

Thus, in general, the cone calorimeter enables to obtain the ignition delay time and the critical heat flux for ignition, which are the two parameters that will qualitatively establish the capability of a fuel to spread a flame. The longer the ignition delay time, the greater the amount of energy required to spread the flame, the higher the critical heat flux for ignition, and the higher the threshold required to achieve sufficient production of pyrolysis gases to sustain ignition.

V/3.2.2 Pyrolysis combustion flow calorimetry (PCFC)

Pyrolysis-combustion flow calorimetry (PCFC) is a fire test method for evaluating the combustibility of milligram-sized samples by simulating the burning of a polymer as it would normally be the case in a fire situation. It is also known as microscale combustion calorimetry (MCC). The method consists in reproducing separately the solid-state and gas-phase processes of

flaming combustion in a non-flaming test by controlled pyrolysis of the sample in an inert gas stream, followed by high-temperature oxidation of the volatile pyrolysis products (Lyon and Walters, 2004; Morgan et al., 2009; Morgan and Galaska, 2008; Scharrel et al., 2007). It combines the constant heating rate and flow characteristics of thermal analysis with the ability to determine the heat of combustion that is typical of calorimetry. It is nowadays a standardised technique classified as ASTM D7309-07.

PCFC device used in this work was supplied by Fire Testing Technology Ltd. and is schematically represented in Fig. V-4. The samples, weighing 10-20 mg, were heated under nitrogen flow at a constant rate of $1^{\circ}\text{C}\cdot\text{s}^{-1}$ up to 750°C . The pyrolysis gases generated during the temperature rise are sent to a tube furnace by the nitrogen purge gas, where a total combustion of those gases takes place. The combustor temperature was fixed at 900°C , and the inlet of oxygen/nitrogen flow was $20/80\text{ cm}^3\cdot\text{min}^{-1}$. Combustion products that exit the combustor are removed by the scrubbers, and the nitrogen and the residual oxygen pass through the flow meter and oxygen analyser. Deconvolution of the oxygen consumption signal is performed numerically during the test and the different parameters are calculated and displayed.

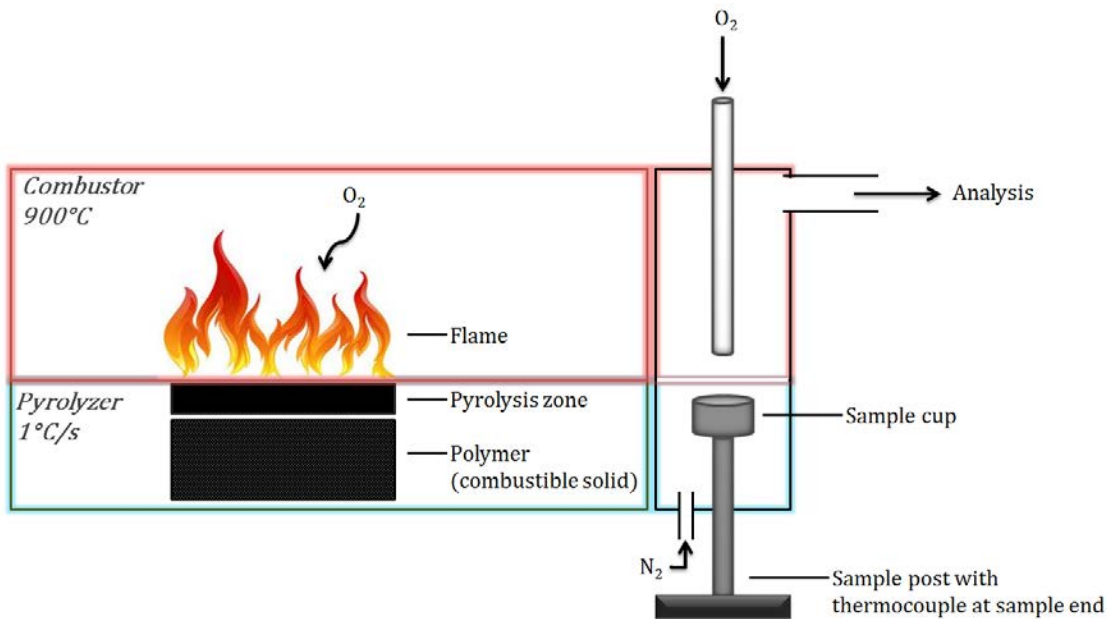


Fig. V-4. Schematic representation of a pyrolysis-combustion flow calorimeter.

Two repetitions were performed for each formulation and no significant differences were noticed between the repetitions. Interesting parameters were extracted from these measurements: maximum (peak) specific heat release rate (pHRR, $\text{W}\cdot\text{g}^{-1}$) at a given heating rate, heat release capacity (HRC, $\text{J}\cdot\text{g}^{-1}\cdot\text{K}^{-1}$), onset temperature of combustion (T_0 , °C), total amount of heat release (HR, $\text{kJ}\cdot\text{g}^{-1}$) and temperature at maximum pyrolysis rate (T_{max} , °C).

V/3.2.3 Thermogravimetric analysis coupled with Fourier transform infrared spectroscopy (TGA-FTIR)

Thermogravimetric Analysis (TGA) coupled to Fourier-Transform Infrared Spectrometry (FTIR) apparatus is a very useful technique to probe and understand thermal degradation processes (Wilkie, 1999). The sample gases originated from the TGA pass through the heated transfer line into the beam-conforming heated flow cell placed in the FTIR sample compartment, where FTIR spectra are collected and stored for further processing. Qualitative measurements are possible from sample masses typically in the milligram range.

The mass loss characteristics and composition of the gas emission products of two different formulations of tannin foams were investigated with this technique on a TA Instrument TGA Q5000IR coupled with a Thermo Scientific Nicolet iS10 spectrometer. The temperature was raised from room temperature, 30°C, to 800°C at a heating rate of $10^\circ\text{C}\cdot\text{min}^{-1}$ after preliminary stabilisation of 30 min at 30°C. The experiments were carried out under air or nitrogen flow. Gases evolved during the TGA experiment were detected continuously by the FTIR device. The spectra were recorded every 10 seconds with the OMNIC® software in a spectral range of 4000–650 cm^{-1} with a 4 cm^{-1} resolution. The temperature of the transfer line between the TGA and the FTIR instrument was set to 225°C to avoid condensation of the evolved gases.

V/4. Results and discussion

V/4.1. Cone calorimetry studies

Three different kinds of tannin foams have been analysed using cone calorimetry in order to have some insight about their flammability and, in particular, for comparing the former tannin formulations with the new generations of foams. The flammability of standard tannin foams (STD-M-type) and formaldehyde-free foams (SF-M-type) has already been investigated some years ago in (Celzard et al., 2011) and (Celzard et al., 2015), respectively. Those results, which were briefly presented in subsection *I/3.4.5 Fire behaviour* of the thesis, have been analysed in detail, completed and compared with the results from new tests carried out with Meringue tannin-based foams prepared by physical whipping and polymerisation at 80°C.

Standard foams with different densities and, for some of them, modified through the incorporation of typical fire retardant materials such as boric and/or phosphoric acids, were tested under different external heat fluxes (35, 50 and 60 kW·m⁻²) (Celzard et al., 2011). That study is very interesting and precious because, in addition of being the first one providing information about the fire properties of tannin foams according to strict and reliable protocols, it is very complete. The main findings are described hereunder.

The peak heat release rates (pHRR) of those foams under a heat flux of 50 kW·m⁻² were not greater than 12 kW·m⁻², on average, and the time to ignition was around 100 s which led to the conclusion that such foams present outstanding fire retardance (Fig. V-5). On the other hand, the tests under different external heat fluxes showed that the peak HRR always remained the same. The latter is very important because it reflects that the gases released and the contribution of the material to the fire is constant regardless to the external heat flux, i.e., to the different fire scenarios. This is a sign of robustness of the material's performance. Finally, it was also shown that the flammability of the material was not modified by the density of the foam, despite highly porous lightweight foams might have appeared to have a faster flame propagation rate and a high thermal emission as observed for PU foams (Weil et al., 1996).

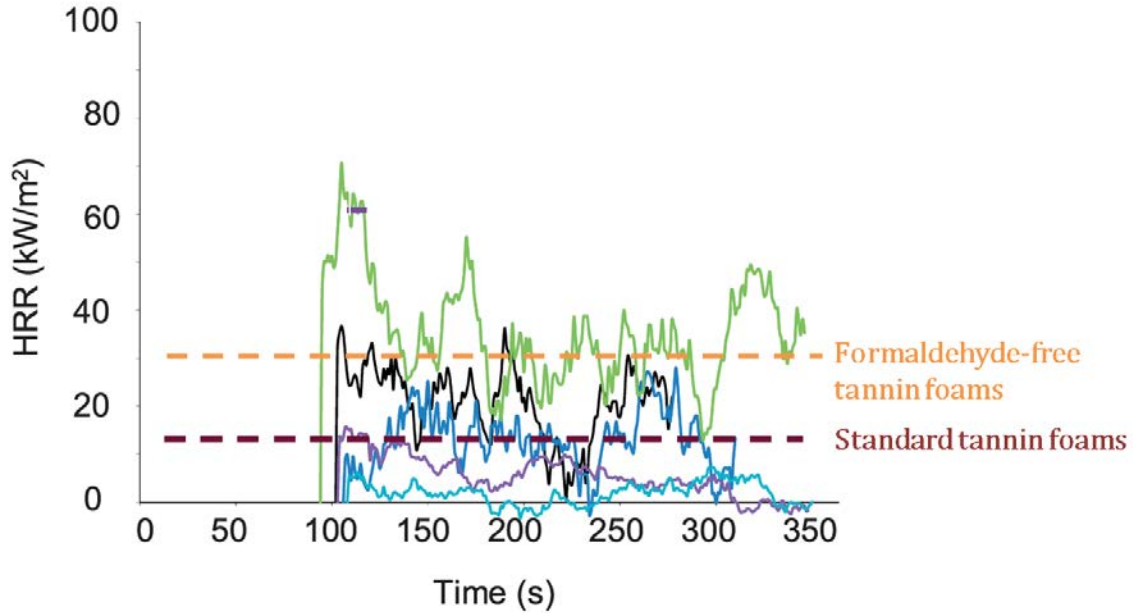


Fig. V-5. HRR of standard and formaldehyde-free tannin foams submitted to a radiant heat flux of $50 \text{ kW}\cdot\text{m}^{-2}$.

Fire properties of formaldehyde-free foams were also analysed (Celzard et al., 2015), but were not as detailed as for standard foams. pHRR of formaldehyde-free foams submitted to a radiant heat flux of $50 \text{ kW}\cdot\text{m}^{-2}$ was around $30 \text{ kW}\cdot\text{m}^{-2}$, and the average time to ignition was 90 s. Thus, the fire retardance was slightly lower than that of standard tannin foams, but remained excellent (see again Fig. V-5).

Meringue foams with two different surfactants were analysed by cone calorimetry in the same conditions as for the former tannin foams. The meringue formulations differ from the others two studied formulations in several points such as the absence of furfuryl alcohol, the presence of surfactant, the large amount of water, a different crosslinker and a different heat source for polymerization. These foams presented one order of magnitude higher pHRR, $120 \text{ kW}\cdot\text{m}^{-2}$, and their ignition time was ten times shorter, 9 s, than the previously analysed tannin foams (Fig. V-6). No significant difference was observed due to the kind of surfactant.

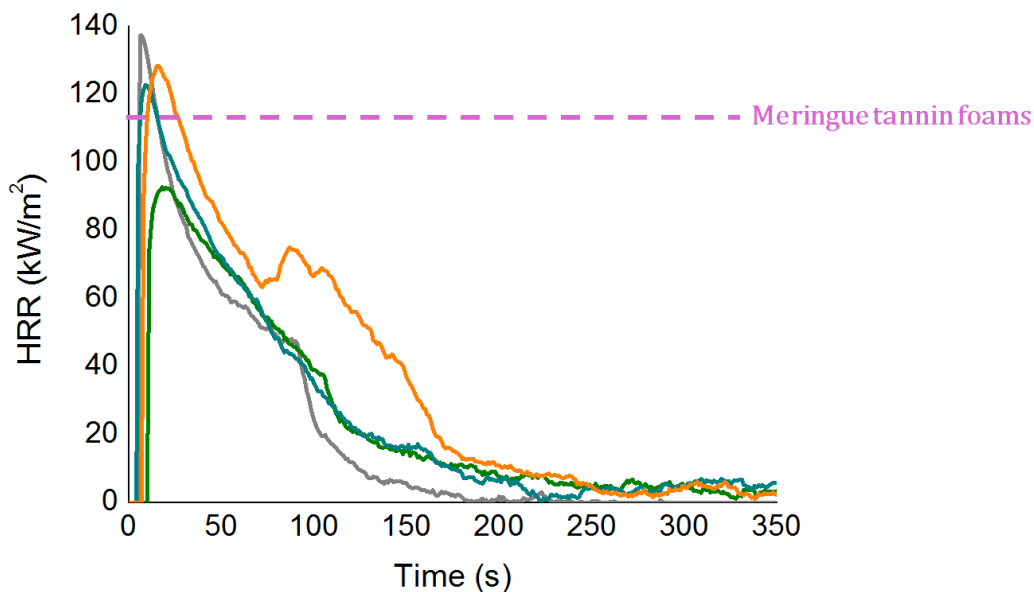


Fig. V-6. HRR of meringue tannin foams submitted to a radiant heat flux of $50 \text{ kW}\cdot\text{m}^{-2}$.

Very useful information has been obtained from a deeper analysis of these results. Meringue foams show a very high initial peak at around 20 s and then the HRR drops until a rather value similar to that found for other tannin foams studied (Fig. V-6). That initial peak corresponds to the flame that is observed in the photos taken along the cone calorimeter test (Fig. V-7 at 10 s). After 100 s of the assay, and without additional application of heat, the flame disappeared and the released heat decreased to a value as low as about $2 \text{ kW}\cdot\text{m}^{-2}$.

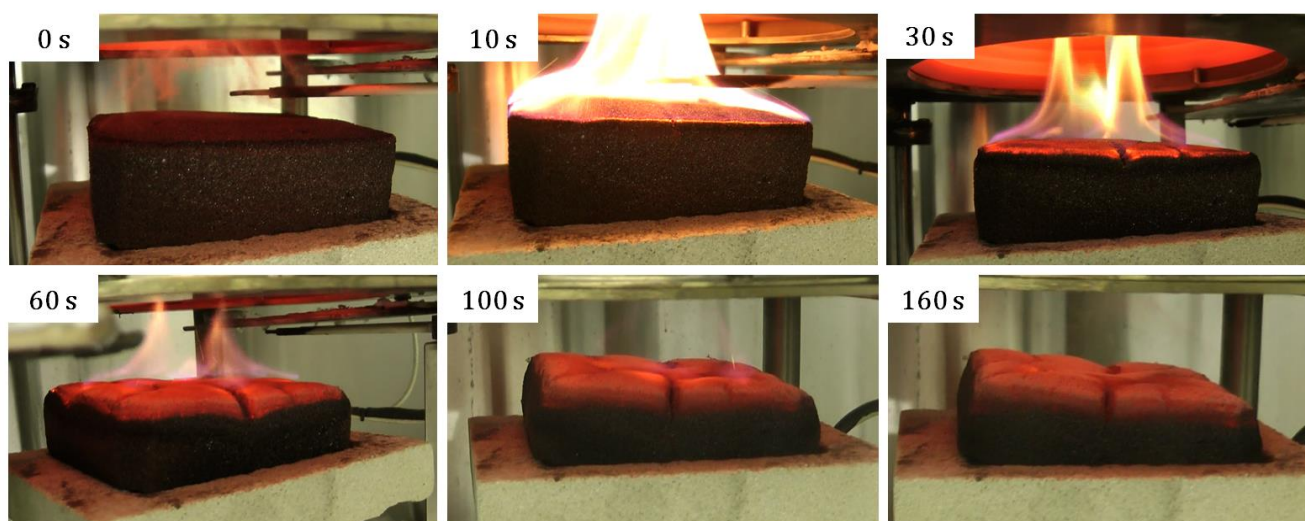


Fig. V-7. Meringue foam during cone calorimeter test as a function of time.

These large initial HRR values might be due to the presence of surfactant that might be initially released and cause flames, hardly seen with the standard and formaldehyde-free formulations. It may also be due to the large amount of water contained in the formulation. Similar effect with these two parameters, surfactant and water content, was also observed elsewhere for polyurethane foams (Lefebvre et al., 2005). The surfactant content had a negative impact, decreasing all fire properties of the polyurethane foams, and an increase of water index involved an increase in the intensity of the first peak of HRR and in the production of smoke. The latter effect was also observed at the beginning of the test with Meringue foams. Those points will be developed further in the next section, supported by the results from PCFC.

It may also be thought that the reason of the decrease of fire retardance of the meringue foam could be due to a weaker polymer network formed with hexamine as crosslinker than that formed by polymerization of furfuryl alcohol and tannin. However, such possibility is not that obvious. In fact, in the two previous examples, it was observed that eliminating the formaldehyde weakened the structure and produced slightly lower fire properties, but the induction time was not significantly changed. Thus, if only the polymer structure was involved, the decrease of fire retardance would be affected in different aspects, which was not the case here.

In general, the critical heat flux for ignition of all tannin foams, including meringue foams, is very high as no ignition was detected under a heat flux of $25 \text{ kW}\cdot\text{m}^{-2}$ in any of the foams tested. Materials with such ignition characteristics are generally expected to propagate a flame very slowly or to self-extinguish, unless a very strong external heat flux is applied (Chen et al., 2012). Most polymers and natural materials, with the exception of those being highly retardant, exhibit a critical heat flux which is much higher than that of tannin-based foams (Dasari et al., 2013; Freivalde et al., 2014; Lee et al., 2011). The huge amount of radiant heat that is required for maintaining the combustion which respect to the resultant HRR explains the high self-extinguishing capacity of tannin foams.

Maximum heat released rate (pHRR), ignition time and FIGRA index (calculated as explained above in the section “*European fire testing of building products*”) of tannin foams are gathered in Table V-3, together with those of other interesting materials having the same potential applications. The aim is to compare and to place tannin foams in the thermal insulation market as a function of their fire properties. The materials selected for the comparison are: phenolic foams,

which present a similar polymeric structure as that of tannin foams, epoxy foams, polyurethane and expanded polystyrene foams that are their main competitors on the market, and some natural and organic materials for thermal insulation.

Table V-3. Fire parameters of tannin foams and other thermal insulation materials obtained by cone calorimetry under heat flux of $50 \text{ kW}\cdot\text{m}^{-2}$.

	pHRR ($\text{kW}\cdot\text{m}^{-2}$)	Ignition time (s)	FIGRA ($\text{W}\cdot\text{s}^{-1}$)
Standard foam	12	100	1.2
Formaldehyde-free tannin foam	30	95	3.2
Meringue foam	117	9	130
Pure epoxy foam (Auad et al., 2007)	314	2	1570
Pure phenolic foam (Auad et al., 2007)	106	6	177
Polyurethane foam (Lorenzetti et al., 2012)	550	4	1375
Expanded polystyrene foam (Chen et al., 2012)	256	9	284
Insulating non-woven hemp fibres (Freivalde et al., 2014)	284	3	710
Insulating agro-materials from flax short fibres ($35 \text{ kW}\cdot\text{m}^{-2}$) (Lazko et al., 2013)	126	11	115

The results gathered in Table V-3 show that tannin foams are the materials unambiguously presenting the highest ignition times and the lowest heat release rates of this list of materials. As might be expected, phenolic foams have the most similar properties to tannin foams, and especially to meringue foams. The insulating agro-materials looks to have similar properties but the tests were performed at a lower heat flow. On the other hand, epoxy and polyurethane foams ignite instantly and also release a high amount of heat. Thus, tannin-based rigid foams have in general higher fire retardance properties than other cellular materials of similar density and applications. Very difficult ignition and very low heat release rate are the main features of these materials.

Finally, as it was explained in the previous point “*European fire testing of building products*”, the method described in the regulations is not what has been used in our experiences. However, a comparative FIGRA index has been calculated by cone calorimeter technique that allows us to

place those materials on the European classification. Tannin foams have a FIGRA index located basically on the B level of the classification (Table V-1) in the most unfavourable situation, i.e., when considering meringue foams that are very close to the limit of the group B. It can then be concluded that tannin foams belong to level B of the European classification, confirming the supposition done in Fig. V-1. In contrast, other materials such as epoxy or polyurethane foams belong the level E of the European Fire Classification (see again Table V-1).

V/4.2. Pyrolysis combustion flow calorimetry (PCFC)

A PCFC device has been used to determine the flammability characteristics of twelve tannin-based foams at the milligram scale, in order to further investigate the effects that some elements of the formulation may have on the fire performances of the foams. It is a useful instrument to determine the fuel content of the volatile thermal degradation products of a material, and it offers a valuable insight into the effect that some additives can have on the flammability of materials. Each sample was tested in duplicate, and the reproducibility of the data in PCFC was very high since less than 2% of deviation between two analyses (for both pHRR and HRC) was obtained.

The main parameters obtained from the PCFC that are associated with flammability and hazard in case of fire have been calculated for all the tannin foams. The specific heat release rate HRR ($\text{W}\cdot\text{g}^{-1}$) at a given sample heating rate ($\text{K}\cdot\text{s}^{-1}$) was calculated from oxygen consumption. Furthermore, the heat release capacity HRC ($\text{J}\cdot\text{g}^{-1}\cdot\text{K}^{-1}$) corresponds to the peak of heat release rate (pHRR) measured in PCFC divided by the heating rate (Lyon and Walters, 2004). This value is not dependent on the heating rate and is an intrinsic characteristic of a material. At $1\text{ K}\cdot\text{s}^{-1}$, the HRC is equal to the pHRR in the case of a single-step decomposition as for the Meringue foam (Fig. V-8(a) and Table V-4). In the case of a multistep decomposition, Lyon et al. (Lyon et al., 2009) proposed to use the sumHRC which is the sum of the HRC of each peak after deconvolution (Schartel et al., 2007; Shi et al., 2009). On the other hand, the total heat release (Total HR, $\text{kJ}\cdot\text{g}^{-1}$) is the specific heat release rate HRR integrated over the entire duration of the experiment. The heat release temperature T_{max} ($^{\circ}\text{C}$) is the sample temperature at pHRR. All those parameters obtained for the 12 tannin-based foams averaged over two samples of each type are summarised in Table V-4.

Table V-4. PCFC results for tannin-based foams.

	HRC ($\text{J}\cdot\text{g}^{-1}\cdot\text{K}^{-1}$)	Peak HRR ($\text{W}\cdot\text{g}^{-1}$)	Total HR ($\text{kJ}\cdot\text{g}^{-1}$)	T_{\max} ($^{\circ}\text{C}$)
STD-M	20.152	14.552	2.286	378.2
PEG-M	34.479	18.077	3.498	257.5
Triton-M	41.655	23.613	4.057	260.8
Pluro-M	40.272	22.138	4.148	255.9
SF-M	23.433	14.171	2.961	365.5
STD-Q	19.607	12.807	2.192	375.2
SF-Q	19.753	12.541	2.266	376.1
P21-Q	27.313	18.125	4.309	415.9
P24-Q	26.985	18.233	4.280	425.4
Meringue-M	51.178	49.578	6.001	376.4
C-200-Q'	35.729	24.029	4.476	406.8
L-NSA3-Q'	46.568	24.245	5.516	412.1

The dynamic flammability data derived from PCFC of all the foams are shown in Fig. V-8(a), where the heat release rate (HRR) is presented as a function of temperature. The different shapes of the curves of HRR allow roughly separating the foams into four main groups (Fig. V-8(b)) depending on their thermal degradation process, i.e., depending on the amount of heat released and the number of steps in their degradation. Three groups correspond, as it could be expected, to the three existing types of foaming (chemical foaming + auto-polymerization, mechanical foaming + polymerisation at 85°C and mechanical foaming + auto-polymerization). A last additional group could also be defined for a special situation where the foams contained additives and surfactant.

In general, the initial peak for those foams whose decomposition is divided in two steps is due to the presence of additives and surfactants in the formulation and the second peak, or the single one in the case of a single-step degradation, is due to the decomposition of the polymeric structure of the foam. Such assignment is consistent as most polymers and organic material such as lignin, cellulose, etc. degrade between 350-450°C (Dorez et al., 2014; Ferry et al., 2015; Prieur et al., 2017). Moreover, the plasticiser and the surfactants are thermally unstable and decompose,

usually above around $\sim 180^{\circ}\text{C}$, having an adverse effect on the fire retardance of the material (Dasari et al., 2013). Fig. V-8(c) shows the attribution of those peaks.

The peak around 400°C is indeed the main difference between foams obtained from different foaming methods. If we focus on that peak related to polymeric structure, it is observed that the peak is higher for the foams made by mechanical foaming + polymerisation at 85°C (Meringue-M), followed by foams made by mechanical foaming + auto-polymerisation (C200-Q' and LNSA3-Q') and, finally, the foams made by chemical foaming + auto-polymerisation (STD-type). This order is also observed in the heat release capacity of the foams (Table V-4). The amount of water present in the formulation follows exactly the same trend of the heat released, i.e., the higher the amount of water, the higher the heat release capacity. This finding leads to the conclusion that a higher percentage of water in the initial formulation of the foams might lead to a polymeric structure that is much easier to degrade. Some studies have already reported similar behaviour on the failure of their materials in fire (Feih et al., 2008; Lefebvre et al., 2005). Especially interesting is the work carried out by (Feih et al., 2008) in which phenolic composites under fire evidenced a high influence of the water content in the material. It was proved that the vaporisation of water within the phenolic matrix caused explosive delamination and cracking of the matrix, increasing the degradation of the material. This is probably what occurs in tannin foams during the fire test, where the high water content in the polyphenolic structure results in high internal pressures generated by vaporisation that favours the degradation of the foam. This effect is increased as the amount of water present in the foam increases, in agreement with the results of cone calorimetry where Meringue-M had lower fire retardance properties than STD-M.

Analysing Meringue-M more deeply, it can be observed that this foam does not have an initial peak around 180°C despite having a significant amount of surfactant in its formulation. This suggests that the curing of the foam at 85°C has already removed the surfactant or has integrated it into the polymer network, which makes its release more difficult unlike what happens when polymerization by self-generated heat takes place and when the surfactant is not part of the structure and degrades easily. This finding eliminates the surfactant as the cause of the worsening of fire properties of Meringue foams and corroborates the explanation of the amount of water as the main influential factor.

As for C200-Q' and LNSA3-Q', obtained by mechanical foaming + auto-polymerisation, these materials also showed a behaviour very consistent with what was described above. They indeed exhibit two peaks, an initial one due to the high amount of surfactant used in their preparation and a second one related to the degradation of the polymeric structure. The second HRR peak is in-between those of STD and Meringue foams as its initial amount of water is also in-between. It may be objected here that those foams were prepared with different tannin, which might influence in a way the HRR. However, it should not have any impact here, since it will be demonstrated below in the study that the effect of the kind of tannin on the fire properties is not very significant.

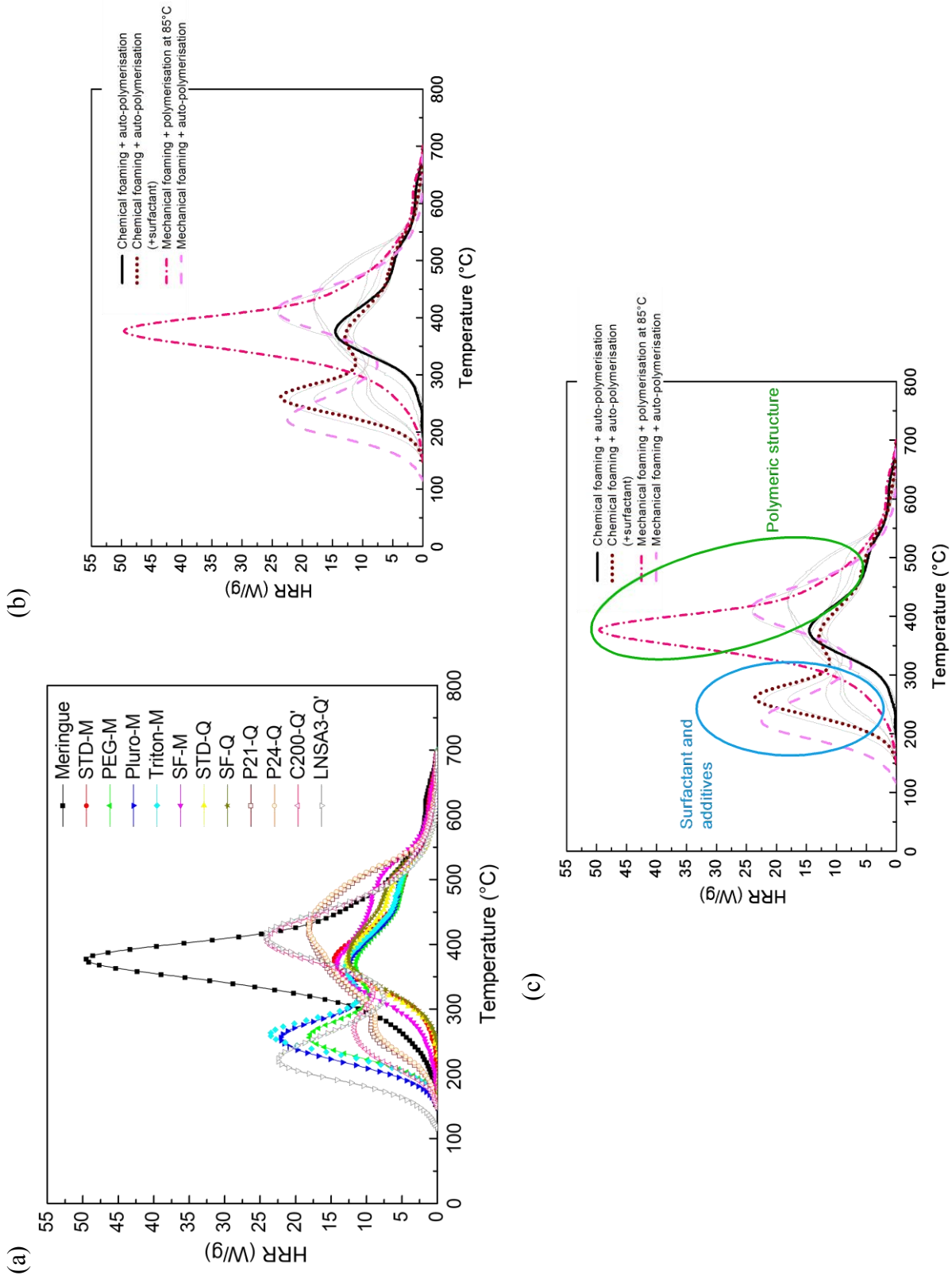


Fig. V-8. Heat release rate curves measured by PCFC at 1 K s^{-1} for several tannin-based foams: (a) investigated foams; (b) highline main, corresponding, kinds of thermal degradation process; (c) assignment of the degradation peaks.

The tannin-based foams analysed by PCFC were prepared conscientiously in order to be able to detect the effect of some parameters such as the presence of surfactant and plasticiser, the amount of furfuryl alcohol, the type of tannin, etc. on the fire properties of the foam. Thus, tannin foams with exactly the same formulation but differing by the type of tannin, mimosa or quebracho, were analysed (Fig. V-9). The results show that the foams with quebracho have a slightly lower heat release capacity (Table V-4) and, therefore, quebracho slightly improves the behaviour of the foams under fire. However, in general, the foams show very similar flammability which is really interesting from the manufacturing point of view as it means that the foams can be prepared from a considerably more available resource (the supply of Mimosa tannin being limited). Fig. V-9 also shows the effect of elimination of formaldehyde from the STD foams. Upon the elimination of formaldehyde (SF formulations), the total heat release and the heat release capacity of the foam slightly increased, more remarkably for foams with mimosa than for those with quebracho (Table V-4). That increase is consistent with the increase found from cone calorimetry results and, as it was pointed out at that moment, it is probably due to the weaker polymer network that formed in the absence of formaldehyde.

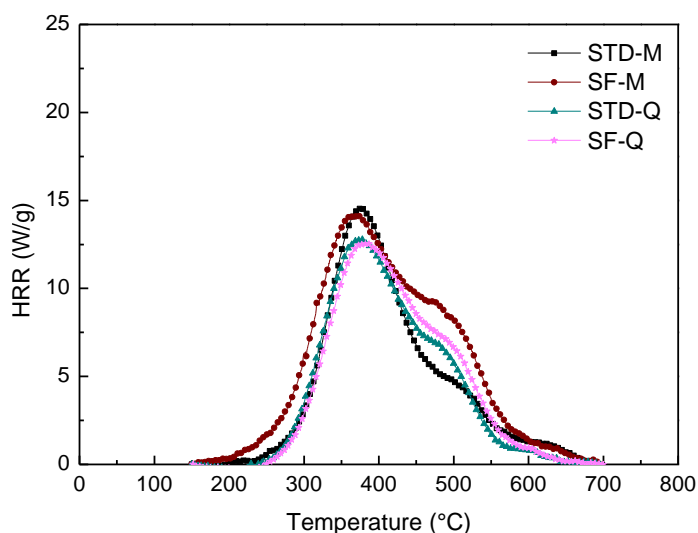


Fig. V-9. Effect of the type of tannin and of the elimination of formaldehyde on the flammability of tannin foams.

On the other hand, the effect of plasticiser on the flammability of the foams was studied by adding a little amount of plasticiser on the formulation of STD-M foam, maintaining everything else constant. After that, the same procedure as before for analysing the effect of the surfactant

was carried out. Thus, it was shown in Fig. V-10 that all the additives on the STD formulation alter significantly the thermal decomposition profile of the foam. Pure STD foam primarily decomposes in one single step, but PEG-M, Pluro-M and Triton-M have a multi-step decomposition process.

As seen in Fig. V-10, the incorporation of PEG to the foam led to an earlier decomposition of the foam. It indeed produced a high initial degradation peak at 250°C due to the degradation and volatilization of the plasticiser which was not present in STD-M. That effect considerably increased with the additional incorporation of surfactant. Those components increased the HRC of the Standard foam from $20 \text{ J}\cdot\text{g}^{-1}\cdot\text{K}^{-1}$ to $34 \text{ J}\cdot\text{g}^{-1}\cdot\text{K}^{-1}$ with the addition of PEG and up to $40 \text{ J}\cdot\text{g}^{-1}\cdot\text{K}^{-1}$ with the addition of PEG plus surfactant, the flammability of the foam with surfactant being two times higher than the original formulation. A similar effect was observed for polyurethane foams wherein the surfactant content decreased the fire properties (Lefebvre et al., 2005).

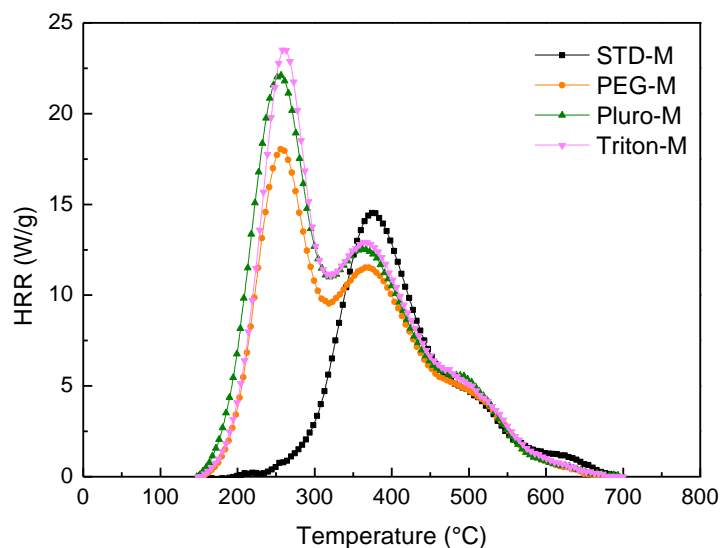


Fig. V-10. Effect of addition of plasticiser and surfactant on the flammability of tannin foams.

The effect of the amount of furfuryl alcohol on the flammability of tannin foams was also analysed by testing two foams with different amounts of furfuryl alcohol, P21-Q and P24-Q. The results obtained were very similar (see Table V-4), suggesting that this increase of furfuryl alcohol had no significant effect. Those foams were also prepared with a little amount of surfactant which is revealed by a shoulder around 250°C (Fig. V-8(a)).

In summary, the flammability of tannin-based foams strongly depends on the chemicals used in their formulation. All the components and additives for changing the features of the foams were found to have a non-negligible influence on the fire properties of the materials.

As a general remark, the PCFC results do not entirely agree with the cone calorimeter results due to different sample sizes and test conditions. Moreover, unlike in the cone calorimeter experiments, the solid phase reactions and the gas phase combustion reactions are separated in PCFC. However, the PCFC tests complement very well the cone calorimetry experiments, and the results are consistent and follow the same trends (Liu et al., 2017). Moreover, although it is a very recent technique, some studies have already been done by applying this technique to insulation materials. If the total HR of the latter is compared with the total HR of tannin foams (Table V-4), it is shown that tannin foams have superior fire properties. The same conclusion is obtained from cone calorimetry. Some of those insulation materials are of natural origin, such as rice husk + starch, barley straw + starch or barley straw + alginate with total HR of 6.5, 7.1 and 6.2 $\text{kJ}\cdot\text{g}^{-1}$, respectively, or are synthetic such as polystyrene and polyurethane foams with total HR of 38.7 and 13.5 $\text{kJ}\cdot\text{g}^{-1}$, respectively (Palumbo et al., 2015).

V/4.3. Thermogravimetric analyses coupled to Fourier Transform Infrared Spectroscopy (TGA-FTIR)

Thermo-oxidative and pyrolytic decomposition of two very different tannin-based foams, STD-M and Meringue-M were carried out, compared and represented in Fig. V-11. According to the TGA curves under the two atmospheres (flowing air or nitrogen), two main phases of thermal decomposition can be identified, a typical behaviour found for lignocellulosic materials, natural fibres, lignin, etc. (Lazko et al., 2013; Prieur et al., 2017). The first stage, until 350°C, is independent from the atmosphere as it is similar under air and nitrogen. On the other hand, the second stage of decomposition occurs in a temperature range of 350-550°C in air, which indicates the predominance of oxidative combustion phenomena. Thus, the point of fastest degradation is shifted to higher temperatures under oxidative conditions. The maxima of mass loss rate are reached for both samples at around 300°C under pyrolytic conditions and at around 450°C under oxidative conditions.

Fig. V-11 also shows several decomposition steps overlapping with each other in both tannin foams. However, they are more accentuated in STD-M, which is possibly due to the more complex structure of the polymer network since it was based on more components (tannin, furfuryl alcohol and formaldehyde) than in Meringue-M (tannin with hexamine as crosslinker).

It was also observed that under oxidative degradation, both tannin foams were completely degraded and no residue was left at 600°C, while under pyrolysis conditions, 45 wt. % of residue remained from STD-M and slightly less, 35 wt. %, from Meringue-M.

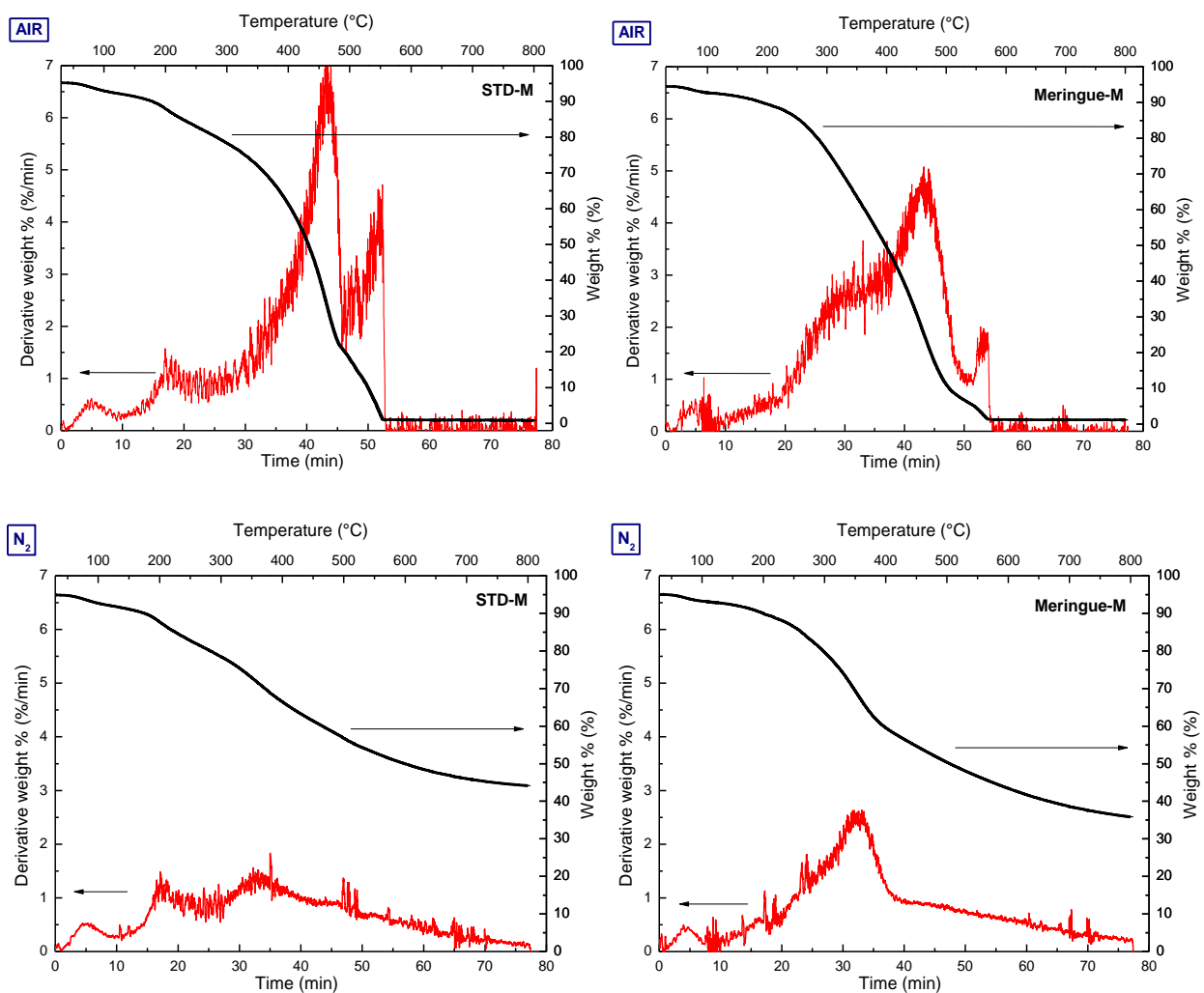


Fig. V-11. Thermal stability of tannin-based foams, STD-M (left) and Meringue-M (right), under air (top) and N₂ (bottom) atmospheres (heating rate: 10 °C·min⁻¹).

The major factor limiting the rate of heat release in the PCFC (in a fire) is normally the thermal decomposition of the polymer that releases volatile fuels and feeds the flame (Prieur et al., 2017; ScharTEL et al., 2007; Wilkie, 1999). A good way to verify such assumption is comparing PCFC and TGA (under N₂) methods, since both are used at a constant heating rate and under nitrogen atmosphere.

Fig. V-12 shows the comparison of STD-M and Meringue-M foams and, in general, the results of TGA correlate very well with the data of PCFC. The temperature at the maximum heat release rate was slightly shifted to higher temperatures because of the higher heating rate in PCFC ($1^{\circ}\text{C}\cdot\text{s}^{-1}$ for PCFC versus $10^{\circ}\text{C}\cdot\text{min}^{-1}$ for TGA) (ScharTEL et al., 2007). The shapes of the curves are quite similar, showing approximatively a single-step thermal decomposition with both methods. The correspondence of the curves is really good for the Meringue-M foam, however, STD-M has a secondary peak between 180°C and 250°C of mass loss but no combustion is noticed at that temperature although some products evolve. This means that the decomposition products between 180°C and 250°C are not combustible in those conditions. This observation suggests that dehydration and decarboxylation are the main reactions occurring at the beginning of the heating (release of water and carbon dioxide) which is in good agreement with what was observed in other phenolic materials such as lignin (Prieur et al., 2017).

The good correlation between TGA behaviour in an inert atmosphere and thermal stability in nitrogen proves that the main factor controlling the heat release rate of tannin-based foams is their thermal decomposition, as already anticipated above. The higher weight loss of Meringue-M indeed produces a higher heat release rate than for STD-M. Such a good qualitative correlation between the mass loss and the heat released by the material makes TGA a useful technique to understand thermal degradation pathways (Wilkie, 1999). Even though PCFC delivers more information about the heat release rate, which is the accepted characterization tool for fire risks, TGA also provides interesting data.

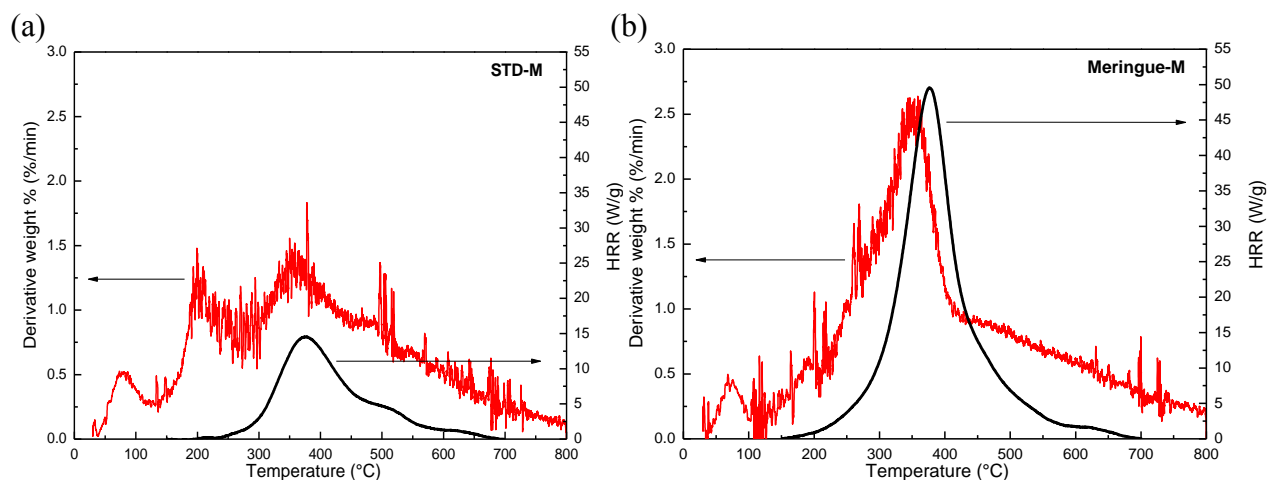


Fig. V-12. Comparison between heat release rate and mass loss rate monitored with PCFC (right axis) and TGA (left axis), respectively, for (a) STD-M and (b) Meringue-M.

The identification of the decomposition gases, released during combustion of tannin-based foams, was also done using TGA-FTIR device under air flow. With the FTIR device used in this study, quantification was not possible but the profiles were normalised by the Gram–Schmidt orthogonalisation method, making possible the comparison of the different peaks. That study gives us a valuable idea of the gases that might be released in a real fire, although we are aware that the gases released in a true fire test are not exactly the same as those obtained by simply heating at $10^{\circ}\text{C}\cdot\text{min}^{-1}$ in air flow. The conditions of a real combustion (uncontrolled temperature, self-generated heat, propagation of a flame, etc.) are indeed not the same as in this test and it is likely that the emitted gases don't present exactly the same compositions. However, such test can provide interesting information about the possible components to be found in the gases emitted by tannin foam combustion. STD-M and Meringue-M were studied by this method too.

Two figures represent the obtained results for each foam: Fig. V-13 for STD-M, and Fig.V-14 for Meringue-M. In both figures, the intensity of gas signal recorded by FTIR during all the experience time is presented as (a), showing lines that mark the temperatures at which the infrared signal will be studied more in-depth, as well as the FTIR spectra at the temperatures mentioned in the previous graph with the same scale but shifted for better observing the peaks, and identifying each peak (b).

Firstly, it can be observed that the intensity of the emitted gases collected by the infrared analyser in the Fig. V-13(a) and V-14(a) coincides consistently with the mass loss rate recorded on the TGA under air atmosphere (Fig. V-11).

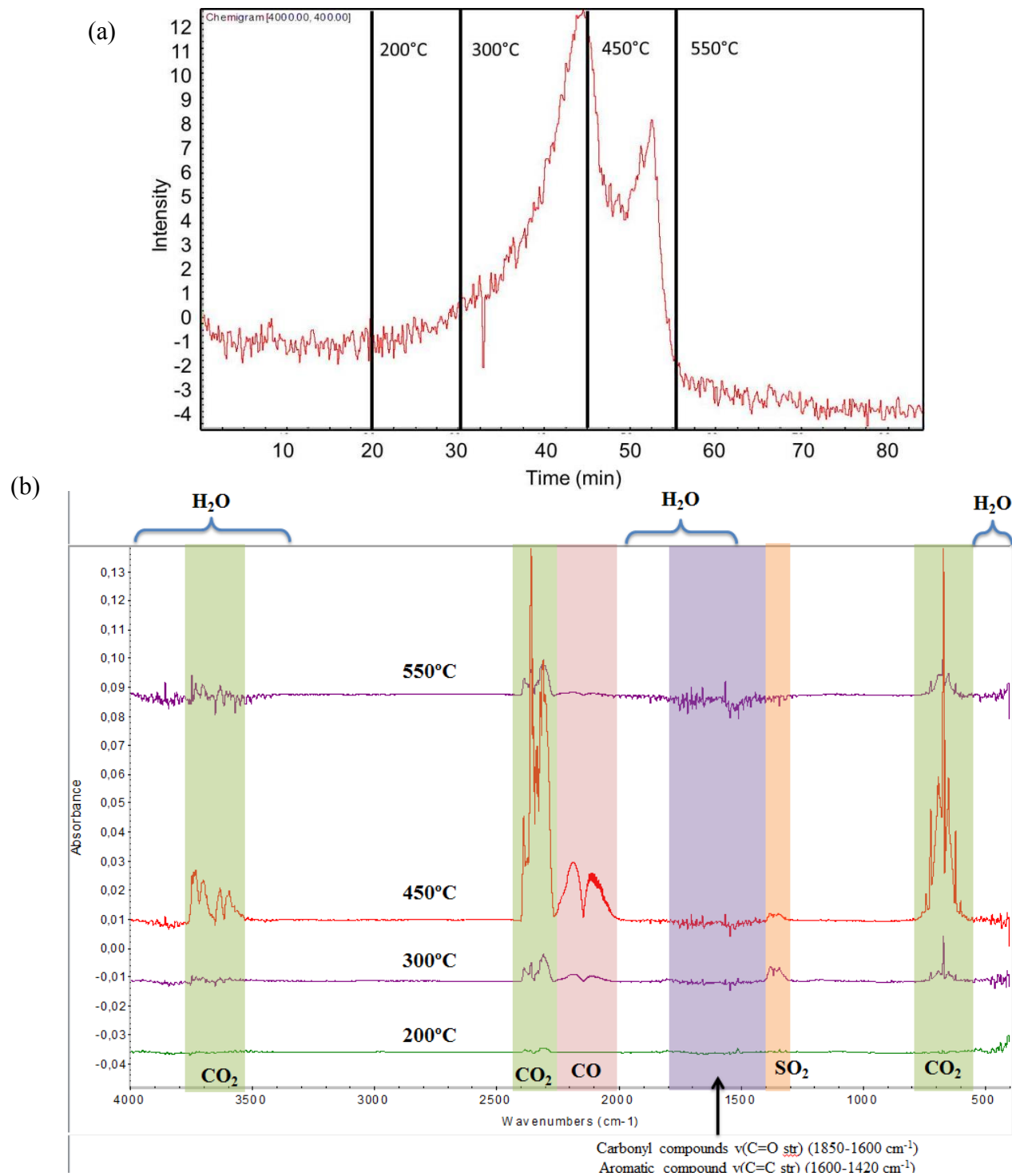


Fig. V-13. Results obtained from the TGA-FTIR analysis of STD-M foam.

Fig.V-13(b) show mainly CO₂ peaks due to the combustion of the organic foam. At the point where the combustion is the fastest, i.e., corresponding to the highest mass loss rate, the appearance of two CO peaks indicates that the combustion is slightly incomplete. It can also be observed a very small signal in the 1800-1400 cm⁻¹ area due to the release of some carbonyl and aromatic components, although this is not very significant as in that area the presence of water vapour is detected too. The emitted gases also contain SO₂, which is attributed to the high amount of para-toluene sulfonic acid used as catalyst in the STD formulation (Tondi et al., 2008).

As for the Meringue foam (Fig.V-14(b)), its FTIR spectra show a combustion more incomplete than for STD-M combustion. This is suggested by the presence of compounds such as methane and ethylene in the gases released, especially at low temperatures, and by the increase of the CO peak areas. CO, methane and acetylene peaks are not perfectly synchronised because CO still appears at high temperatures while the other two gases practically disappear at 450°C. Also worth noticing in the spectra of Meringue foam is the appearance of N₂O and NO_x compounds such as NO₂ and NO. All these nitrogen-based compounds are associated to the use of hexamine as crosslinker that increases the concentration of nitrogen in the foam. Finally, the peak of SO₂ that appeared in STD-M spectra does not appear here because the quantity of acid used in this case was very low.

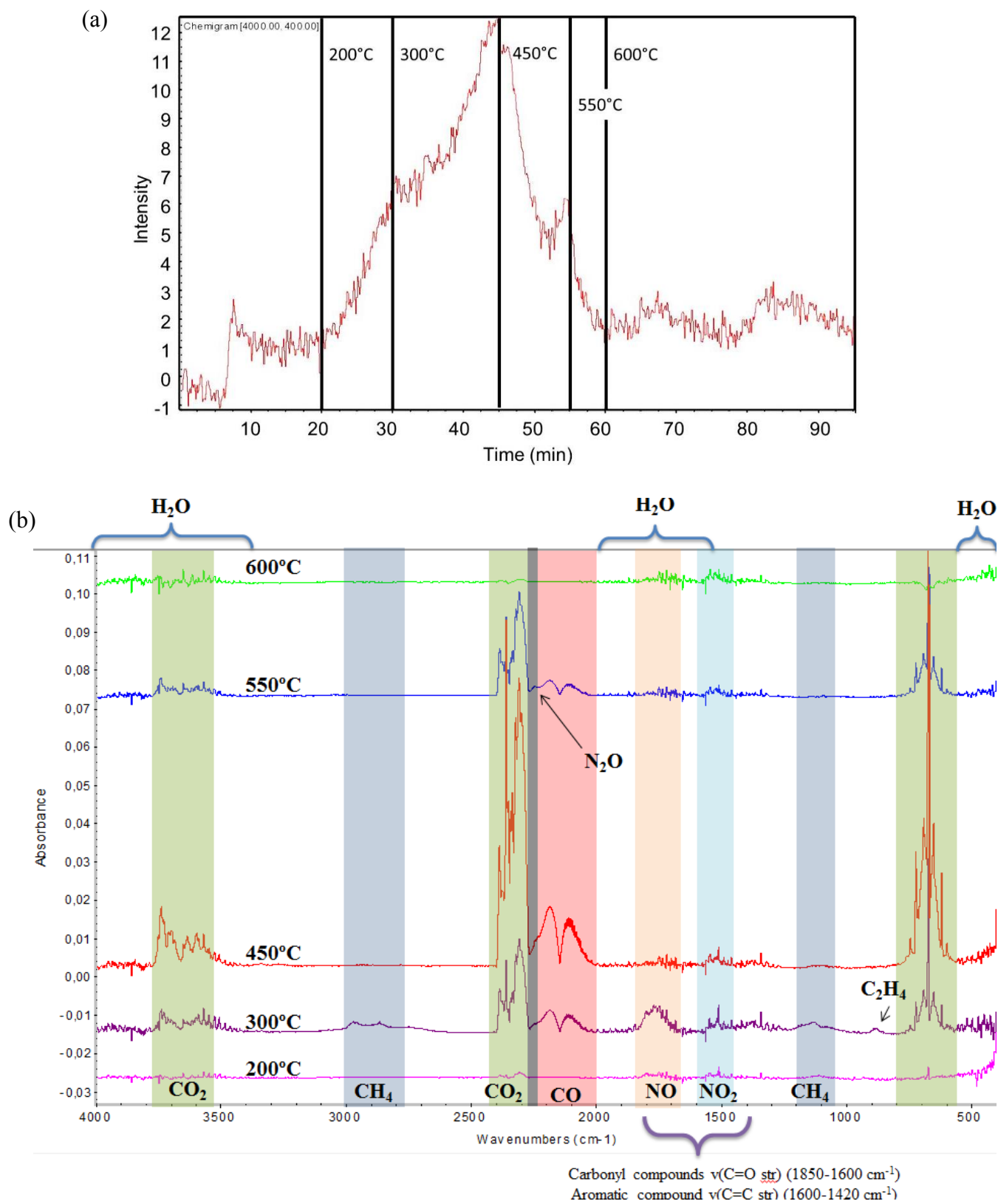


Fig. V-14. Results obtained from the TGA-FTIR analysis of Meringue-M foam.

V/5. Conclusion

The good fire retardance of tannin-based foams is mainly due to the aromatic composition of the matrix that forms a resistant polymer network with low weight loss during the decomposition process. As a result, little hydrocarbon fuel is provided by the foams to drive the combustion process, which increases the ignition delay time and reduces the heat release. This was evidenced by the good correlation between TGA behaviour in an inert atmosphere and the heat released rate from PCFC experiments.

On the other hand, it has been observed that the flammability of tannin-based foams strongly depends on the chemical and not that much on the structural properties of the foams. The density and the porosity are indeed quantities that have to be controlled during foam processing but that are not really essential for the flammability of the tannin foam (Celzard et al., 2011). However, all the components and additives for changing the features of the foams have a big influence on the fire properties of the material. Actually, it was revealed that different tannin foams could perform very differently in fire scenarios, depending on the presence of surfactant and additives and, more importantly, on their initial water content in their formulation. The latter is really important as the vaporisation of the water weakens the structure, facilitating the thermal degradation of the foam. Thus, reducing the water content in the formulation of the foam may improve the performances of tannin foams submitted to fire.

In general, tannin-based organic rigid foams were found to exhibit excellent fire retardance in all their variations. The corresponding results were compared with those of the main insulating materials presently commercialised such as polystyrene, polyurethane and phenolic foams, confirming that insulation based on tannin foams presents a better behaviour in case of fire. Their low flammability together with other remarkable properties such as low weight, low thermal conductivity, biosourced, etc. definitely makes tannin-based foams very interesting polymer materials.

V/6. Bibliography

- Auad, M.L., Zhao, L., Shen, H., Nutt, S.R., Sorathia, U., 2007. Flammability properties and mechanical performance of epoxy modified phenolic foams. *J. Appl. Polym. Sci.* 104, 1399–1407. doi:10.1002/app.24405
- Babrauskas, V., 1984. Development of the cone calorimeter. A bench-scale heat release rate apparatus based on oxygen consumption. *Fire Mater.* 8, 81–95. doi:10.1002/fam.810080206
- Babrauskas, V., Grayson, S.J., 2009. Heat release in fires. Interscience communications, Place of publication not identified.
- Bourbigot, S., Flambard, X., Poutch, F., Duquesne, S., 2001. Cone calorimeter study of high performance fibres—application to polybenzazole and p-aramid fibres. *Polym. Degrad. Stab.* 74, 481–486. doi:10.1016/S0141-3910(01)00175-6
- Carvel, R., Steinhaus, T., Rein, G., Torero, J.L., 2011. Determination of the flammability properties of polymeric materials: A novel method. *Polym. Degrad. Stab., Fire Retardant Polymers Meeting Poznan 2009* 96, 314–319. doi:10.1016/j.polymdegradstab.2010.08.010
- Celzard, A., Fierro, V., Amaral-Labat, G., Pizzi, A., Torero, J., 2011. Flammability assessment of tannin-based cellular materials. *Polym. Degrad. Stab.* 96, 477–482. doi:10.1016/j.polymdegradstab.2011.01.014
- Celzard, A., Szczurek, A., Jana, P., Fierro, V., Basso, M.-C., Bourbigot, S., Stauber, M., Pizzi, A., 2015. Latest progresses in the preparation of tannin-based cellular solids. *J. Cell. Plast.* 51, 89–102. doi:10.1177/0021955X14538273
- Chen, H.-B., Wang, Y.-Z., Sánchez-Soto, M., Schiraldi, D.A., 2012. Low flammability, foam-like materials based on ammonium alginate and sodium montmorillonite clay. *Polymer* 53, 5825–5831. doi:10.1016/j.polymer.2012.10.029
- Commission Decision 2000/147/EC, 2000. Commission Decision 2000/147/EC. *Off. J. Eur. Communities* 14–18.
- Dasari, A., Yu, Z.-Z., Cai, G.-P., Mai, Y.-W., 2013. Recent developments in the fire retardancy of polymeric materials. *Prog. Polym. Sci.* 38, 1357–1387. doi:10.1016/j.progpolymsci.2013.06.006
- Dorez, G., Ferry, L., Sonnier, R., Taguet, A., Lopez-Cuesta, J.-M., 2014. Effect of cellulose, hemicellulose and lignin contents on pyrolysis and combustion of natural fibers. *J. Anal. Appl. Pyrolysis* 107, 323–331. doi:10.1016/j.jaap.2014.03.017
- EN 13501-1, 2007. Fire Classification of Construction Products and Building elements.
- Feih, S., Mathys, Z., Mathys, G., Gibson, A.G., Robinson, M., Mouritz, A.P., 2008. Influence of water content on failure of phenolic composites in fire. *Polym. Degrad. Stab.* 93, 376–382. doi:10.1016/j.polymdegradstab.2007.11.027
- Ferry, L., Dorez, G., Taguet, A., Otazaghine, B., Lopez-Cuesta, J.M., 2015. Chemical modification of lignin by phosphorus molecules to improve the fire behavior of polybutylene succinate. *Polym. Degrad. Stab.* 113, 135–143. doi:10.1016/j.polymdegradstab.2014.12.015
- Freivalde, L., Kukle, S., Andžs, M., Bukšāns, E., Grāvītis, J., 2014. Flammability of raw insulation materials made of hemp. *Compos. Part B Eng.* 67, 510–514. doi:10.1016/j.compositesb.2014.08.007

- Giraud, S., Bourbigot, S., Rochery, M., Vroman, I., Tighzert, L., Delobel, R., Poutch, F., 2005. Flame retarded polyurea with microencapsulated ammonium phosphate for textile coating. *Polym. Degrad. Stab.*, 9th European Conference on Fire Retardant Polymers 88, 106–113. doi:10.1016/j.polymdegradstab.2004.01.028
- Guillaume, E., Marquis, D., Saragoza, L., 2014. Calibration of flow rate in cone calorimeter tests. *Fire Mater.* 38, 194–203. doi:10.1002/fam.2174
- Laoutid, F., Bonnaud, L., Alexandre, M., Lopez-Cuesta, J.-M., Dubois, P., 2009. New prospects in flame retardant polymer materials: From fundamentals to nanocomposites. *Mater. Sci. Eng. R Rep.* 63, 100–125. doi:10.1016/j.mser.2008.09.002
- Lazko, J., Landercy, N., Laoutid, F., Dangreau, L., Huguet, M.H., Talon, O., 2013. Flame retardant treatments of insulating agro-materials from flax short fibres. *Polym. Degrad. Stab.* 98, 1043–1051. doi:10.1016/j.polymdegradstab.2013.02.002
- Lee, B.-H., Kim, H.-S., Kim, S., Kim, H.-J., Lee, B., Deng, Y., Feng, Q., Luo, J., 2011. Evaluating the flammability of wood-based panels and gypsum particleboard using a cone calorimeter. *Constr. Build. Mater.* 25, 3044–3050. doi:10.1016/j.conbuildmat.2011.01.004
- Lefebvre, J., Bastin, B., Le Bras, M., Duquesne, S., Paleja, R., Delobel, R., 2005. Thermal stability and fire properties of conventional flexible polyurethane foam formulations. *Polym. Degrad. Stab.*, 9th European Conference on Fire Retardant Polymers 88, 28–34. doi:10.1016/j.polymdegradstab.2004.01.025
- Letellier, M., Szczurek, A., Basso, M.-C., Pizzi, A., Fierro, V., Ferry, O., Celzard, A., 2017. Preparation and structural characterisation of model cellular vitreous carbon foams. *Carbon* 112, 208–218. doi:10.1016/j.carbon.2016.11.017
- Liu, X., Salmeia, K.A., Rentsch, D., Hao, J., Gaan, S., 2017. Thermal decomposition and flammability of rigid PU foams containing some DOPO derivatives and other phosphorus compounds. *J. Anal. Appl. Pyrolysis* 124, 219–229. doi:10.1016/j.jaap.2017.02.003
- Lorenzetti, A., Modesti, M., Gallo, E., Schartel, B., Besco, S., Roso, M., 2012. Synthesis of phosphinated polyurethane foams with improved fire behaviour. *Polym. Degrad. Stab.* 97, 2364–2369. doi:10.1016/j.polymdegradstab.2012.07.026
- Lyon, R.E., Safronava, N., Quintiere, J.G., Stoliarov, S.I., Walters, R.N., Crowley, S., 2014. Material properties and fire test results. *Fire Mater.* 38, 264–278. doi:10.1002/fam.2179
- Lyon, R.E., Takemori, M.T., Safronava, N., Stoliarov, S.I., Walters, R.N., 2009. A molecular basis for polymer flammability. *Polymer* 50, 2608–2617. doi:10.1016/j.polymer.2009.03.047
- Lyon, R.E., Walters, R.N., 2004. Pyrolysis combustion flow calorimetry. *J. Anal. Appl. Pyrolysis, Practical Applications of Analytical Pyrolysis (special section)* 71, 27–46. doi:10.1016/S0165-2370(03)00096-2
- Mngomezulu, M.E., John, M.J., Jacobs, V., Luyt, A.S., 2014. Review on flammability of biofibres and biocomposites. *Carbohydr. Polym.* 111, 149–182. doi:10.1016/j.carbpol.2014.03.071
- Morgan, A.B., Galaska, M., 2008. Microcombustion calorimetry as a tool for screening flame retardancy in epoxy. *Polym. Adv. Technol.* 19, 530–546. doi:10.1002/pat.1100
- Morgan, A.B., Wolf, J.D., Gulians, E.A., Fernando, K.A.S., Lewis, W.K., 2009. Heat release measurements on micron and nano-scale aluminum powders. *Thermochim. Acta* 488, 1–9. doi:10.1016/j.tca.2009.01.016
- Mouritz, A.P., Gibson, A.G., 2006. *Fire properties of polymer composite materials, Solid mechanics and its applications.* Springer, Dordrecht.

- Palumbo, M., Formosa, J., Lacasta, A.M., 2015. Thermal degradation and fire behaviour of thermal insulation materials based on food crop by-products. *Constr. Build. Mater.* 79, 34–39. doi:10.1016/j.conbuildmat.2015.01.028
- Price, D., Anthony, G., Carty, P., 2001. 1 - Introduction: polymer combustion, condensed phase pyrolysis and smoke formation, in: *Fire Retardant Materials*. Woodhead Publishing, pp. 1–30.
- Prieur, B., Meub, M., Wittemann, M., Klein, R., Bellayer, S., Fontaine, G., Bourbigot, S., 2017. Phosphorylation of lignin: characterization and investigation of the thermal decomposition. *RSC Adv.* 7, 16866–16877. doi:10.1039/C7RA00295E
- Schartel, B., Pawlowski, K.H., Lyon, R.E., 2007. Pyrolysis combustion flow calorimeter: A tool to assess flame retarded PC/ABS materials? *Thermochim. Acta* 462, 1–14. doi:10.1016/j.tca.2007.05.021
- Shi, Y., Kashiwagi, T., Walters, R.N., Gilman, J.W., Lyon, R.E., Sogah, D.Y., 2009. Ethylene vinyl acetate/layered silicate nanocomposites prepared by a surfactant-free method: Enhanced flame retardant and mechanical properties. *Polymer* 50, 3478–3487. doi:10.1016/j.polymer.2009.06.013
- Singh, H., Jain, A.K., 2008. Ignition, combustion, toxicity, and fire retardancy of polyurethane foams: A comprehensive review. *J. Appl. Polym. Sci.* NA–NA. doi:10.1002/app.29131
- Sundström, B., 2007. The development of a european fire classification system for building products test methods and mathematical modelling. Department of Fire Safety Engineering. Lund University, Sweden.
- Tondi, G., Pizzi, A., Masson, E., Celzard, A., 2008. Analysis of gases emitted during carbonization degradation of polyflavonoid tannin/furanic rigid foams. *Polym. Degrad. Stab.* 93, 1539–1543. doi:10.1016/j.polymdegradstab.2008.05.016
- Weil, E.D., Ravey, M., Gertner, D., 1996. Recent progress in flame retardancy of polyurethane foams. Presented at the Recent advances in flame retardancy of polymeric materials, Stamford.
- Wichman, I.S., 2003. Material flammability, combustion, toxicity and fire hazard in transportation. *Prog. Energy Combust. Sci.* 29, 247–299. doi:10.1016/S0360-1285(03)00027-3
- Wilkie, C.A., 1999. TGA/FTIR: an extremely useful technique for studying polymer degradation. *Polym. Degrad. Stab.* 66, 301–306. doi:10.1016/S0141-3910(99)00054-3

Chapter VI: New methods for mechanical characterisation of tannin-based foams

VI/1. Introduction

This chapter is dedicated to the testing and characterisation of different tannin-based foams. More specifically, it deals with their mechanical properties, which are an important point to consider when carrying out a complete investigation of a new material. Elastic modulus, compressive strength, Poisson's ratio¹ and shear modulus are the main parameters to define the mechanical properties of a material.

Until now, and to the best of our knowledge, all the studies carried out about the mechanical characterisation of tannin-based foams focused on elastic modulus and compressive strength measurements, the latter indeed being quite useful quantities as far as applications in the building industry are concerned. However, there are other parameters such as Poisson's ratio, shear modulus or loss factor², which have never been measured so far on tannin-based foams, and which might be very important for studying them further and for exploring other possible applications. For example, materials with different Poisson's ratio (ν) behave very differently mechanically (Greaves et al., 2011): for instance, Poisson's ratio of rubbers, for which stress primarily results in shape change, is close to 0.5; in most well-known solids such as metals, polymers and ceramics, $0.25 < \nu < 0.35$, and in glasses and minerals, ν is close to 0.

Those intrinsic parameters such as Poisson's ratio or loss factor that define the elastic and damping properties of the foams are for instance fundamental for quality controls or accurate predictions of the foams' acoustic efficiency for sound absorption in buildings. The use of tannin

¹Poisson's ratio is the ratio of transverse contraction strain to longitudinal extension strain in the direction of stretching force. Tensile deformation is considered positive and compressive deformation is considered negative. The definition of Poisson's ratio contains a minus sign so that usual materials have a positive ratio. However, the theory of isotropic linear elasticity (Sokolnikoff, 1983) allows Poisson's ratios in the range from -1 to 1/2 for an object with free surfaces with no constraint. This range is derived from concepts of stability. For an object without constraint to be stable, the elastic parameters (measuring the material's stiffness) must be positive. Poisson's ratio is interrelated with these parameters; the usual relationships assume isotropy, linearity and elasticity.

² Loss factor is the ability of a material to convert part of the acoustic energy into heat instead of transferring or radiating it as airborne noise. This parameter is used as a measure of the capacity of a material to damp structure-borne sound. The theoretical maximum loss factor is 1. An undamped 1-mm thick steel panel can have a loss factor as low as roughly 0.001, whereas soft rubber with large loss factor may improve remarkably the sound absorption performance of a whole structure (Liu and Sheng, 2008).

foams as an acoustic insulation material is a very promising application but that still needs to be fully explored. Only one study about this has been carried out until now, which described tannin foams as potential biosourced sound absorbers with acoustic properties somewhat comparable to those of commercially available materials (Lacoste et al., 2015).

On the other hand, the knowledge of mechanical parameters is very interesting from the point of view of foams' modelling. In fact, in general, many efforts are and have been carried out to model the mechanical behaviour of cellular materials, but the prediction of parameters such as elastic modulus, Poisson's ratio and shear modulus is usually quite limited (Gong et al., 2005).

During the last years, new experimental methods have been proposed to characterise the elastic and damping parameters of porous materials (Jaouen et al., 2008). The interest for those methods is partly due to the efforts to find a unique technique of characterisation, or at least a limited set of methods suitable for most porous materials, which is not that straightforward. For instance, tannin foams present mechanical properties that may vary from hard and brittle to semi-rigid or even purely soft and elastic, depending on the composition, and therefore making a proper characterisation is difficult through the use of only one single technique. Moreover, as stated before, the search for new methods of characterisation is also motivated by the attempt to improve and to develop a material with multiple interesting applications.

Nowadays, there is no consensus about the most suitable technique that would be able to provide all the main parameters describing the elastic properties of materials. The most commonly used experimental methods for the determination of elastic parameters of porous materials are roughly divided in two kinds: destructive and non-destructive. Among the latter, quasi-static methods wherein inertia effects are neglected, and dynamic methods which are usually resonant, can be found.

The present chapter is, in large part, focused on the determination of the elasticity modulus of a broad selection of tannin foams with very different mechanical properties by using two different techniques: one dynamic and destructive, and the other one quasi-static and non-destructive. The conventional method is mechanical compression, by which the complete stress-strain compression characteristics of the material are determined by applying continuously increasing loads and measuring the resultant deformation. Despite it is destructive, it is still the

most commonly used method for the study of stress-strain relationships in porous materials (Celzard et al., 2010; Shen and Nutt, 2003). On the other hand, our foams were also tested by a new, non-destructive, technique based on quasi-static mechanical vibration that in addition allows the determination of additional parameters such as Poisson's ratio and loss factor (Etchessahar et al., 2005; Jaouen et al., 2008; Sahraoui et al., 2000).

Hereinafter, the mechanical behaviour of tannin foams analysed in previous studies is recalled, and a brief description of the studied tannin foams is presented in the first part of the chapter. Afterwards, the description of both methods is given, the parameters that can be obtained are presented, and the advantages and drawbacks of each are summarised. Finally, the results from the two methods used to characterise tannin-based foams are analysed, compared and discussed in order to suggest appropriate recommendations.

VI/2. Experimental

VI/2.1. Foams preparation

The tannin-based foams prepared and analysed in Chapter V of the thesis were used to carry out this work too. As explained in *V/3.1. Foam preparation*, they represent all the different types of tannin foams that exist until this moment. Indeed, for their preparation, several types of foaming methods, crosslinkers, curing temperatures and additives were employed in order to develop foams with very different features. The set of samples comprises 12 different foams with densities ranging from 0.039 to 0.120 g·cm⁻³, and having very different mechanical properties, i.e., being either qualitatively fragile or elastic, flexible, resistant, weak, etc. This allows testing and comparing the two aforementioned methods of characterisation, covering all the possible scenarios that can be found with tannin-based foams.

A general description of the foams, together with their detailed composition, can be found in *V/3.1. Foam preparation* and in *Table V-2*, respectively. Furthermore, additional information about the origin, justification and process of preparation of the foams has been given in *I/3.3. Formulations of tannin foams*.

VI/2.2. Mechanical properties characterisation

The mechanical properties of tannin-based foams have been described in several articles in the recent past, e.g. (Celzard et al., 2010). The nature and the amount of the components used in the preparation of the foams, as well as the method of foaming and polymerisation, are key parameters for obtaining materials with very different mechanical behaviours. The sections *I/3.3. Formulations of tannin foams* and *I/3.4.2 Mechanical properties* of Chapter I summarise the research carried out so far on this topic. Briefly, for making a short overview of the state-of-the-art, the original tannin-based foams, i.e., “standard” tannin foams (STD-M), present a brittle fracture (Zhao et al., 2010), but this characteristic could be changed through the development of new formulations. For example, the elimination of formaldehyde and the addition of surfactant increases the degree of elasticity of the foams (Basso et al., 2015, 2013) as it happens with the addition of plasticiser (Li et al., 2012).

However, the objective of this chapter was not to study the mechanical properties as a function of composition, but to analyse the mechanical properties by two different methods of characterisation and to compare their outcomes. The broad selection of tannin foams analysed below was expected to allow collecting representative results.

The two methodologies used in this work for testing tannin-based foams are explained carefully now. The setup apparatus, the experimental approach for doing the measurements, the parameters obtained in each technique, as well as some other information that can be interesting for understanding the results, are described below.

VI/2.2.1 Classical, destructive, method

The foams were investigated by compression using the same procedure and the same equipment as what was presented in section *IV/2.4.3 Mechanical properties* of the thesis, i.e., an Instron 5944 universal testing machine equipped with a 2 kN head, and using a load rate of 2.0 mm·min⁻¹. All the samples were cut in the form of parallelepipeds, all having the same dimensions of 30 × 30 × 15 mm to avoid any difference due to size effects, and tested along the growing (vertical) direction to minimise as much as possible effects of minor anisotropy. During the compression tests, stress and deformation were continuously recorded.

As the applied stress can be transmitted in different ways to the sample, the distribution of load, and hence the rupture mechanism inside the foam, may vary. Two load transfer methods were used here: without and with plates glued to the opposite sample surfaces in contact with the compression platens:

- (i) Without plates: the “classic”, conventional way, compression test, wherein the foam sample is placed directly between the compression platens of the testing machine;
- (ii) With plates: the method by which the opposite faces of the sample are glued to rigid plates (here polymethylmethacrylate (PMMA) plates) using a highly-resistant epoxy adhesive (Araldite®) before testing, see Fig. VI-1.



Fig. VI-1. Tannin-based foams glued to plastic plates, ready for compression test.

Compression with plates was carried out because the mechanical behaviour of brittle foams was indeed shown to be strongly affected by the bonding – or not – of the specimen ends to the loading platens. The bonding of the specimen ends to the stiff loading platens leads to a more homogeneous distribution of the load through the section and, consequently, to higher – more representative – values of elastic modulus and compressive strength (Brezny and Green, 1993; Letellier et al., 2017; Mora and Waas, 2002; Szczurek et al., 2015).

In general, three well-identified zones can be observed in the standard compression curve of a cellular material (Gibson and Ashby, 2001). In compression without plates, there is first a linear elastic region at low stresses, followed by a collapse plateau and finally a densification regime. All of them are explained in detail in the section *IV/2.4.3 Mechanical properties* of Chapter IV.

On the other hand, in compression with plates, there is also a linear elastic region but which a sometimes far higher slope than before, and which is followed by a collapse of the sample where the stress drops abruptly; at this point, almost all the energy is released. After that point, the test is stopped. In the present study, the post-linear elastic parts in both kinds of test, with and without plates, have not been considered and only the elastic modulus and the maximum compressive strength obtained at the end of the linear part were discussed, see below.

In another research to which I participated at the beginning of the thesis, and which directly inspired the present chapter, similar experiments were carried out about the mechanical properties of tannin-based vitreous carbon foams through a comparative analysis of samples either with or without rigid plates glued to their opposite faces and submitted to compression (Letellier et al., 2017). That study, whose results are not detailed here but are worth mentioning briefly here, is very interesting since it was carried out under the same conditions as for the organic tannin-based foams and, therefore, it can help to understand the present results. The main conclusions of that previous study are the following. The compressive strength of the foams had similar values in the case of the tests with and without plates, however, the compression modulus was very sensitive to the method, leading to different values whether measured with or without plates. The way the load transfer was made impacted dramatically the modulus only, leading for some foams to values more than one order of magnitude higher using glued plates than those obtained without plates. In plate-free tests, the stress was indeed localised on the struts in contact with the platens, which were progressively broken by bending. The only important parameters that affected the modulus were the apparent density, i.e., the overall porosity which is linked to the stiffness of the struts and hence their dimensions, and the cell size which is linked to the area of struts in contact with the load. Nevertheless, in the case of tests with plates, significantly different behaviours were observed, and the foams could thus be divided into three main types: open cell foams, closed cell foams, and “semi-open” foams that possess, despite their open cells, moduli similar to closed foams. Fig. VI-2 gathers some of the main results.

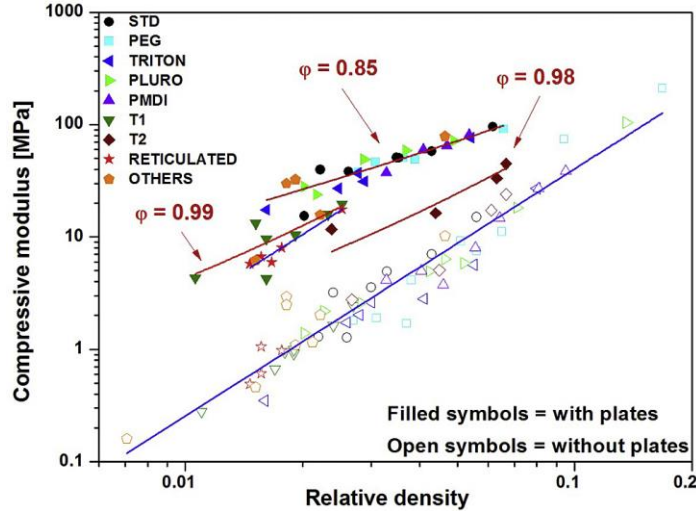


Fig. VI-2. Compressive modulus of tannin-based vitreous carbon foams tested with and without plates, as a function of their relative density (Letellier et al., 2017). Different relations coming from the Gibson and Ashby model (Gibson and Ashby, 2001) were fitted, and the fraction of solid only contained in the struts, ϕ , is shown. STD, PEG, TRITON, PLURO, etc. correspond to the different formulations of the former tannin-based foams, some of them being similar to those used in this work.

In the present study, three samples with bonded plates and three samples without plates were systematically tested for each of the 12 types of tannin foams considered herein.

VI/2.2.2 Non-destructive method

The quasi-static mechanical analysis (QMA) is a recent and not very well-known method used to identify simultaneously the values of elastic modulus, Poisson's ratio and loss factor of poroelastic materials (Langlois et al., 2001). It is based on polynomial relations between compression stiffness (rigidity K , i.e., a measure of the resistance offered by a material to deformation), elastic modulus (E), Poisson's ratio (ν) and shape factor (s , here defined as half the radius-to-length ratio, $s = R/2L$) from high-order axisymmetric finite-element simulations on a cylindrical foam sample under static compression. Those relations hold in the low-frequency range —below any resonance— and account for the fact that the cylindrical foam sample expands sideways when compressed between rigid plates.

All the quasi-static compression tests were performed by a Quasi-static Mechanical Analyzer (Mecanum, Canada) based on standard ISO 18437-5. Several samples of different shape factors were analysed, i.e., based on wider-than-tall cylindrical samples sandwiched between two rigid plates. The lower plate is axially excited by an electrodynamic shaker while the upper plane is fixed. The plates are covered with sandpaper to avoid sliding of the sample with respect to them; these boundary conditions allow being close to clamped conditions without explicitly gluing the sample to the plates. A schematic sketch with the parts that constitute the equipment and a photo of this one are shown in Fig. VI-3(a) and Fig. VI-3(b), respectively.

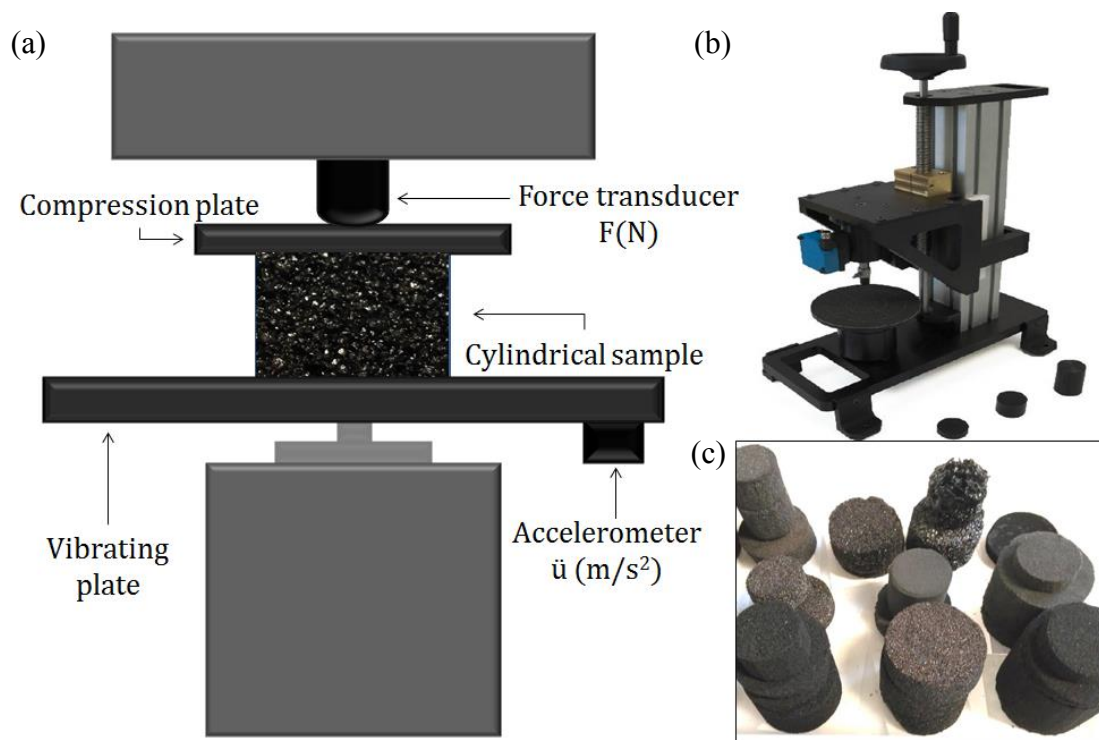


Fig. VI-3. Quasi-static mechanical analyser (QMA) details: (a) schematic representation of measurement setup, (b) real photo and (c) tannin cylindrical foam samples ready for testing.

Tannin-based foam specimens of different lengths from 10 to 40 mm and different diameters from 25 to 40 mm, whose combinations give rise to shape factors ranging from 0.3 to 0.8, were analysed (see some of the samples in Fig. VI-3(c)). A shaker using a pseudo-random noise in a frequency range of 0–50 Hz was used to excite the bottom plate, connected with an accelerometer. A force transducer was connected to the top plate. The accelerometer measured the acceleration of the bottom plate, while the force transducer measured the reaction force

applied on the top plate. To ensure linearity in the porous material's behaviour, the initial strains applied to the sample should not exceed 5%. In the present measurements, an initial strain of 1.3% was applied, guaranteeing that this value was within the linear part wherein the elastic properties do not vary with the initial strain (Pritz, 1994). The measured transfer function of the foam, together with polynomial relations, leads to the loss factor of the foam and to a system of two equations with two unknowns. The solution of the system yields the elastic modulus and Poisson's ratio of the foam. The measurement protocol and all the theory behind the development of the polynomial relations are explained in detail elsewhere (Langlois et al., 2001). A brief description of the protocol of calculation, together to the main equations on which the measure is based, will be introduced hereafter for helping understand the method.

The initial concept behind the development of the polynomial relations is based on Biot's theory (Biot and Tolstoy, 1992) in isotropic open-cell poroelastic materials. The isotropic condition might appear not totally true with our materials. However, despite some studies have shown that the foams can have a marked anisotropy in the direction of foaming, much attention has been paid in our work for limiting such effect as much as possible. Thus, some of the foams have been prepared following the instruction detailed elsewhere in the thesis of Letellier (Letellier, 2015). In the latter, the anisotropy of the foams was studied in detail, especially by micro-computed tomography, and a relatively high and constant sphericity was obtained, suggesting that the cells are only very slightly elongated, and above all that their shape is repeatable from one foam to another. It was therefore assumed that the anisotropy remains relatively low or at least similar for all the foams. Moreover, when the degree of anisotropy is low, it has been shown that an isotropic model for the elastic properties gives better results than an anisotropic model (Dauchez, 1999).

Coming back to the measurement device, the accelerometer in the bottom plate measures the acceleration $\ddot{u}(\omega)$ and the force transducer measures the reaction force $F(\omega)$, as it was stated before. A Fast Fourier Transformation analyser integrates twice the accelerometer signal, to obtain the displacement $u(\omega)$, and calculates the transfer function $Z(\omega)$ measuring how much a structure resist when subjected to a harmonic force. That (complex) transfer function, corrected from perturbations, can be written by separating its real and imaginary parts as follows:

$$Z(\omega) = \frac{F(\omega)}{u(\omega)} = K(\omega) + jX(\omega) \quad (\text{VI-1})$$

where the real part, $K(\omega)$, is the compression stiffness or mechanical resistance of the test sample at angular frequency ω , and the imaginary part, $X(\omega)$, its reactance.

The relationship between the compression stiffness and the elastic modulus is given by $K = E \cdot A/L$ where A is the cross-section area of the cylindrical sample, and L its length. The modulus is an intensive property of the material and the stiffness is an extensive property that depends on the material and its shape and boundary conditions. In the present case, the sample is affected substantially by the Poisson's effect and boundary conditions, leading to an apparent elastic modulus, E' :

$$K(\omega) = \text{Re}(Z(\omega)) = \text{Re}\left(\frac{F(\omega)}{u(\omega)}\right) = \frac{E'A}{L} \quad (\text{VI-2})$$

That situation creates a problem because the true elastic modulus cannot be directly calculated. The investigation with axisymmetric finite element simulations showed that the measured compression stiffness K can be correlated to the shape factor, s , of the test specimen for different Poisson's ratios, ν . This correlations takes the form of polynomial relations $P(s,\nu)$ that can be used to link the apparent elastic modulus to the true elastic modulus of the material:

$$E = \frac{E'}{P(s,\nu)} \quad (\text{VI-3})$$

These polynomial expressions can be used to determine both the elastic modulus and the Poisson's ratio of the material. Measuring the compression stiffness (real part of the transfer function) on two cylindrical specimens of different shape factors s_1 and s_2 yields:

$$E = \frac{E'_1}{P(s_1,\nu)} \quad \text{and} \quad E = \frac{E'_2}{P(s_2,\nu)} \quad (\text{VI-4})$$

Since the true elastic modulus is unique for the tested material, the equation can be drawn as follow and Poisson's ratio can be calculated:

$$\frac{E'_1}{P(s_1,\nu)} - \frac{E'_2}{P(s_2,\nu)} = 0 \quad \xrightarrow{\text{1 equation, 1 unknown } (\nu)} \nu \quad (\text{VI-5})$$

Once the Poisson's ratio of the material is found, one of the two equalities in Eq. (VI-4) can be used to retrieve the true elastic modulus of the material.

Finally, in these conditions of low frequencies, the reactance, $X(\omega)$, is approximated as the mechanical resistance multiplied by the loss factor of the material. If we replace the latter in Eq. (VI-1), one gets:

$$Z(\omega) \cong K(\omega) + jK(\omega)\eta(\omega) \quad (\text{VI-6})$$

Consequently, the loss factor is given directly by the imaginary part of the measured quasi-static transfer function:

$$\text{Im}(Z(\omega)) = K(\omega) \cdot \eta(\omega) \quad \xrightarrow{K(\omega)=\text{Re}(Z(\omega))} \quad \eta(\omega) = \frac{\text{Im}(Z(\omega))}{\text{Re}(Z(\omega))} \quad (\text{VI-7})$$

VI/3. Results and discussion

For comparing the results of various characterised foams with each other, the relative density has been used as it is one of the most representative parameters of such materials. Indeed, and unlike apparent density, it allows comparing foams with different chemical compositions leading to different polymer intrinsic densities, which corresponds to the present situation. Moreover, it is relatively easy to obtain, and it affects in a global manner all the properties of the foams, especially mechanical ones.

The relative density (dimensionless) is defined as $\rho_{relative} = \rho_{app} / \rho_s$, where ρ_{app} ($\text{g}\cdot\text{cm}^{-3}$) is the apparent density (mass / volume ratio of a representative sample) and ρ_s ($\text{g}\cdot\text{cm}^{-3}$) is the skeletal density (density of the solid constituting the structure). The apparent density was obtained by simple weighing samples of simple geometry and measuring their dimensions, whereas the skeletal density was measured by helium pycnometry, as explained in section *III/2.3.1 Morphological characterisation*.

VI/3.1. Destructive mechanical compression

The mechanical properties of tannin-based foams were first analysed by destructive mechanical compression. The foams were characterised by the two methods described in the above experimental part, i.e., with and without plates. Three samples of the same foam were tested for each method; the results were averaged and gathered in Table VI-1.

Table VI-1. Experimental results of mechanical compression for the 12 foams' formulations.*

	ρ_{app} (g·cm ⁻³)	$\rho_{relative}$	Compressive strength (MPa)	Elastic modulus (MPa) with plates	Elastic modulus (MPa) without plates
STD-M	0.039	0.027	0.099 ± 0.010	4.71 ± 0.20	1.94 ± 0.06
PEG-M	0.055	0.038	0.180 ± 0.002	11.06 ± 0.40	1.65 ± 0.10
Triton-M	0.057	0.040	0.159 ± 0.020	9.50 ± 0.60	1.65 ± 0.05
Pluro-M	0.044	0.031	0.115 ± 0.010	7.42 ± 1.10	1.53 ± 0.02
SF-M	0.028	0.019	0.029 ± 0.001	0.61 ± 0.15	0.61 ± 0.15
STD-Q	0.060	0.041	0.142 ± 0.008	7.96 ± 0.05	2.84 ± 0.01
SF-Q	0.038	0.027	0.038 ± 0.010	2.51 ± 1.00	0.55 ± 0.10
P21-Q	0.065	0.046	0.128 ± 0.003	2.10 ± 1.10	2.10 ± 1.10
P24-Q	0.048	0.034	0.089 ± 0.001	2.20 ± 0.50	2.70 ± 0.50
Meringue-M	0.056	0.040	0.189 ± 0.030	11.96 ± 1.30	3.33 ± 0.20
C-200-Q'	0.120	0.084	0.408 ± 0.020	18.50 ± 0.60	18.5 ± 0.60
L-NSA3-Q'	0.081	0.057	0.130 ± 0.002	3.75 ± 0.30	3.75 ± 0.30

*Data are presented as means ± standard deviation.

The values of compressive strength of all foams were similar whether the tests were carried out with or without plates. This is the reason why no distinction has been done between them in Table VI-1. All the formulations clearly led to one single linear (increasing) trend when plotted in a double-logarithmic scale (Fig. VI-4). This behaviour was evidenced by extensive analytical, numerical and experimental works (Gibson and Ashby, 2001) and is usually described by the following equation:

$$\text{Compression strength, } \sigma \propto \sigma_s \cdot \rho_{relative}^n \quad (\text{VI-8})$$

where σ_s is the yield strength of the (non-porous) solid, and the exponent n is associated to the structure and deformation mechanics of the cellular material. According to Sanders and Gibson (Sanders and Gibson, 2003), the theoretical values of n are 1.5 and 2 if the foams are based on open cells and closed cells, respectively.

Eq. (VI-8) was successfully fitted to the data of Fig. VI-4, giving the value of 1.51 for the exponent n . This exponent suggests that the porosity is practically open. This finding is in complete agreement with has been reported about organic tannin foams (Celzard et al., 2010).

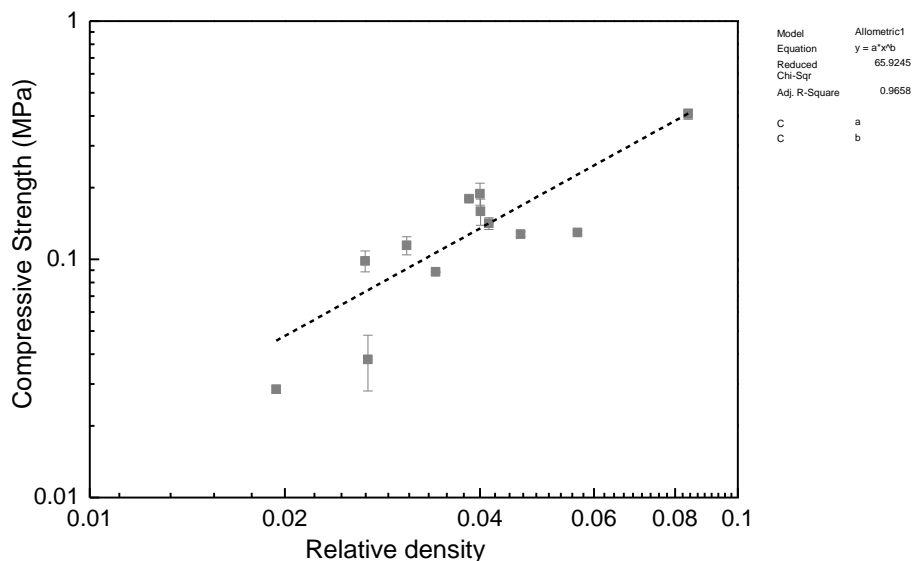


Fig. VI-4. Compressive strength obtained by destructive mechanical compression as a function of tannin foams' relative density. The same results were obtained with or without plates. The dashed line corresponds to the application of Eq. (VI-8).

With reference to the elastic modulus, which is the main parameter under study in this work, some foams presented significantly different results, whether the latter were obtained with or without plates. The elastic modulus of all samples tested without plates indeed followed the same trend as a function of the relative density of the foams (Fig. VI-5(a)). It can be assumed that, in the linear elastic part from which the modulus was determined, the struts progressively break by bending when in contact with the platens. In this case, the load transfer through the structure is quite poor and, whatever the nature of the latter, the only important parameter seems to be the stiffness of the struts and hence their dimensions, themselves function of relative density and cell size. Similar results were observed in vitreous tannin-based carbon foams tested without plates by (Letellier et al., 2017).

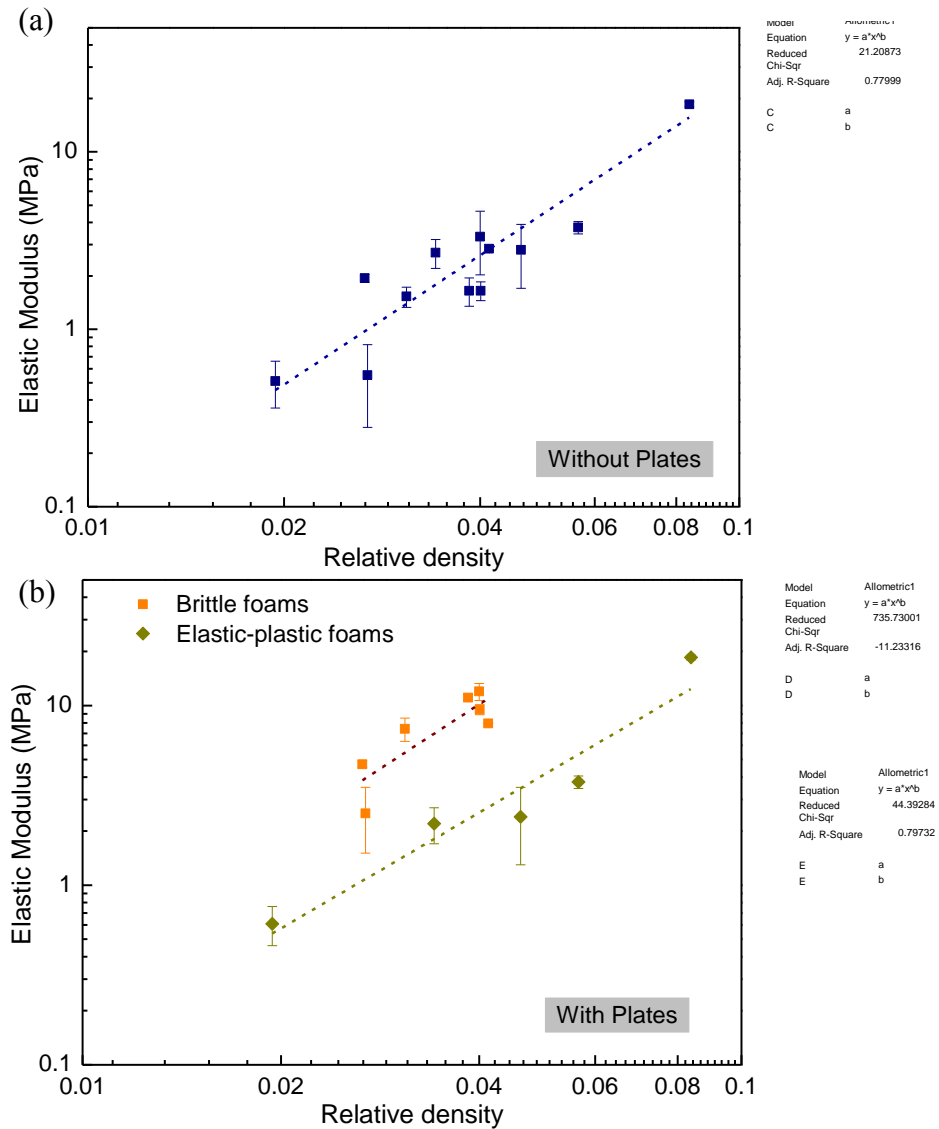


Fig. VI-5. Elastic modulus obtained by destructive mechanical compression as a function of relative density of tannin foams tested: (a) without plates; and (b) with plates. The dashed lines correspond to the application of Eq. (VI-9).

However, analysing the modulus obtained from the compression with plates, it can be clearly observed that there are two groups of foams, both with a modulus increasing with the relative density of the foam (Fig. VI-5(b)). These two groups can be identified by observing the way tannin foams collapsed when submitted to compression with plates in the stress-strain curves of Fig. VI-6. There are foams whose stress dropped suddenly to zero, i.e., brittle foams, and foams with a compressive behaviour similar to the one without plates, i.e., elastic-plastic foams. In

elastic-plastic foams, the linear elastic domain may extend to a strain almost as high as 10%, while it only goes up to 5% if the foams are fragile.

In the group formed by brittle foams, the stress drops suddenly to zero because the energy stored in the foam is released, and there is a momentary loss of contact due to the foam breaking. That behaviour is the one observed in all tannin-derived vitreous carbon foams analysed in a former work (Letellier et al., 2017). Their moduli are much higher than those of the elastic-plastic foams at similar relative density. On the other hand, the compression of elastomeric or elastic-plastic foams does not lead to any sudden rupture. Moreover, the elastic moduli of this second group of foams are similar to those obtained without plates, showing that load can sometimes be transmitted without plates almost as efficiently as it actually is with plates.

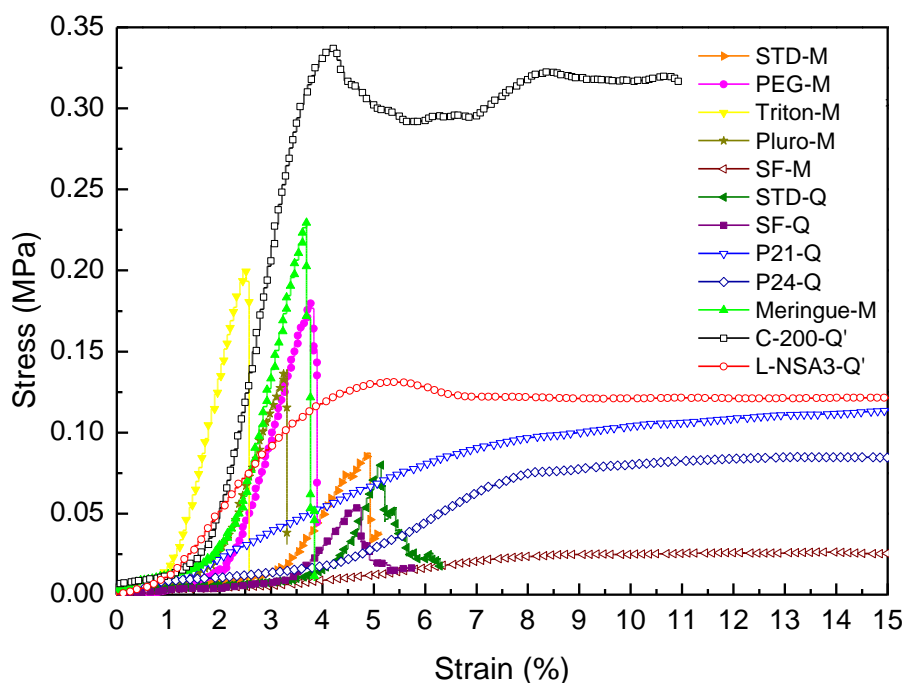


Fig. VI-6. Stress-strain curves of tannin-based foams by destructive mechanical compression with plates.

Going a little further, and similar to the analyses of compression strength, it can be observed in Fig. VI-5 that the values of elastic modulus both with and without plates obey a power law dependence of relative density (linear trend in double logarithmic plotting) such as:

$$\text{Elastic modulus, } E \propto E_s \cdot \rho_{\text{relative}}^m \quad (\text{VI-9})$$

where E_s is the elastic modulus of the solid from which the cellular material is made, and m is an exponent whose value depends on the failure mode. Eq. (VI-9) was indeed well fitted to the data of Fig. VI-5, giving the following values for the exponent m : 2.42 in tests without plates, and 2.38 and 2.14 in tests with plates for brittle and elastic-plastic foams, respectively. Those exponents indicate that the elastic forces acting in the organic foams are more or less similar in all the foams. According to percolation theory (see for example Sahimi, 1998, and refs therein.), the value of m depends on the intrinsic characteristic of the bonds. In three-dimensional systems as the actual foams are, two values are widely accepted: one close to 2 when the elastic forces are purely central, the other one being close to 4 for forces acting against changes of angle at the struts nodes. The analysed tannin foams, and especially the brittle ones, would thus be mainly dominated by central forces where each strut behaves as a spring and where no angle-changing forces are present. Similar results were already found for others physically blown tannin foams (Celzard et al., 2010; Li et al., 2012) and meringue foams (Szczyrek et al., 2014). Moreover, such values are also characteristic of highly regular open-celled foams, which is consistent with what was previously obtained.

VI/3.2. Quasistatic mechanical analysis

At least two cylindrical samples of different shape factors are necessary for the calculation of the mechanical parameters by quasi-static mechanical analysis (QMA), as it was explained in the experimental part. However, sometimes and as in the present study, the lack of convergence during the inversion process in the numerical computations with the polynomial relations $P(s,\nu)$ necessitates the measurement of more samples having other, different, shape factors. Five samples of each kind of foam were thus tested in this study.

Table VI-2 gathers all the measurements of elastic modulus, Poisson's ratio and loss factor of the foams obtained by QMA. In spite of the efforts made to obtain precise and representative results for all the foams measuring several samples of different shape factor, in some cases, it was impossible to obtain the Poisson's ratio of the foam and, consequently, neither the elastic modulus. For three of the samples listed in Table VI-2, it was impossible to find a value of Poisson's ratio and the elastic modulus was obtained after inputting different Poisson's ratios and observing that there were no variation in the elastic modulus. Concurrently, the loss factor was

directly calculated by the imaginary part of the measured transfer function, i.e., it is not affected by the Poisson's ratio (see again Eq. (VI-7)).

Table VI-2. QMA results for the 12 foams' formulations.*

	$\rho_{\text{app}} (\text{g}\cdot\text{cm}^{-3})$	ρ_{relative}	Elastic modulus (MPa)	Poisson's ratio	Loss factor
STD-M	0.039	0.027	1.69 ± 0.37	-	0.139 ± 0.010
PEG-M	0.055	0.038	1.71 ± 1.10	0.353 ± 0.01	0.151 ± 0.024
Triton-M	0.057	0.040	2.25 ± 0.83	0.270 ± 0.01	0.162 ± 0.017
Pluro-M	0.044	0.031	1.98 ± 0.73	0.429 ± 0.01	0.159 ± 0.009
SF-M	0.028	0.019	0.74 ± 0.31	0.392 ± 0.01	0.112 ± 0.015
STD-Q	0.060	0.041	4.09 ± 1.50	0.279 ± 0.01	0.151 ± 0.023
SF-Q	0.038	0.027	0.52 ± 0.24	0.403 ± 0.01	0.082 ± 0.010
P21-Q	0.065	0.046	1.53 ± 0.65	0.258 ± 0.01	0.082 ± 0.017
P24-Q	0.048	0.034	1.84 ± 0.74	-	0.094 ± 0.019
Meringue-M	0.056	0.040	4.60 ± 1.17	0.232 ± 0.01	0.224 ± 0.022
C-200-Q'	0.120	0.084	15.65 ± 3.38	-	0.172 ± 0.003
L-NSA3-Q'	0.081	0.057	3.83 ± 0.94	0.282 ± 0.01	0.179 ± 0.025

*Data are presented as means \pm standard deviation.

Regarding the elastic modulus results, represented in Fig. VI-7(a), all the foams follow the same trend and no distinction can be made between elastic-plastic and fragile foams. The modulus of the foams increases with relative density according to a power law. Eq. (VI-9) was indeed quite well applied to the QMA elastic modulus and the exponent was $m = 1.99$. An exponent so close to 2 again indicates that the elastic forces are purely central, in agreement with the results obtained by mechanical compression in the previous section and with tannin foams analysed in others works.

An interesting point that is worth noticing is the intrinsic limits of the equipment for elastic modulus measurements, which range approximately from 10^{-3} to 10 MPa. That means that the Foam C-200-Q' is above the limit and thus the obtained value is probably not very accurate. Such limits reduce the range of application of this technique, leaving outside high-density foams with high elastic modulus.

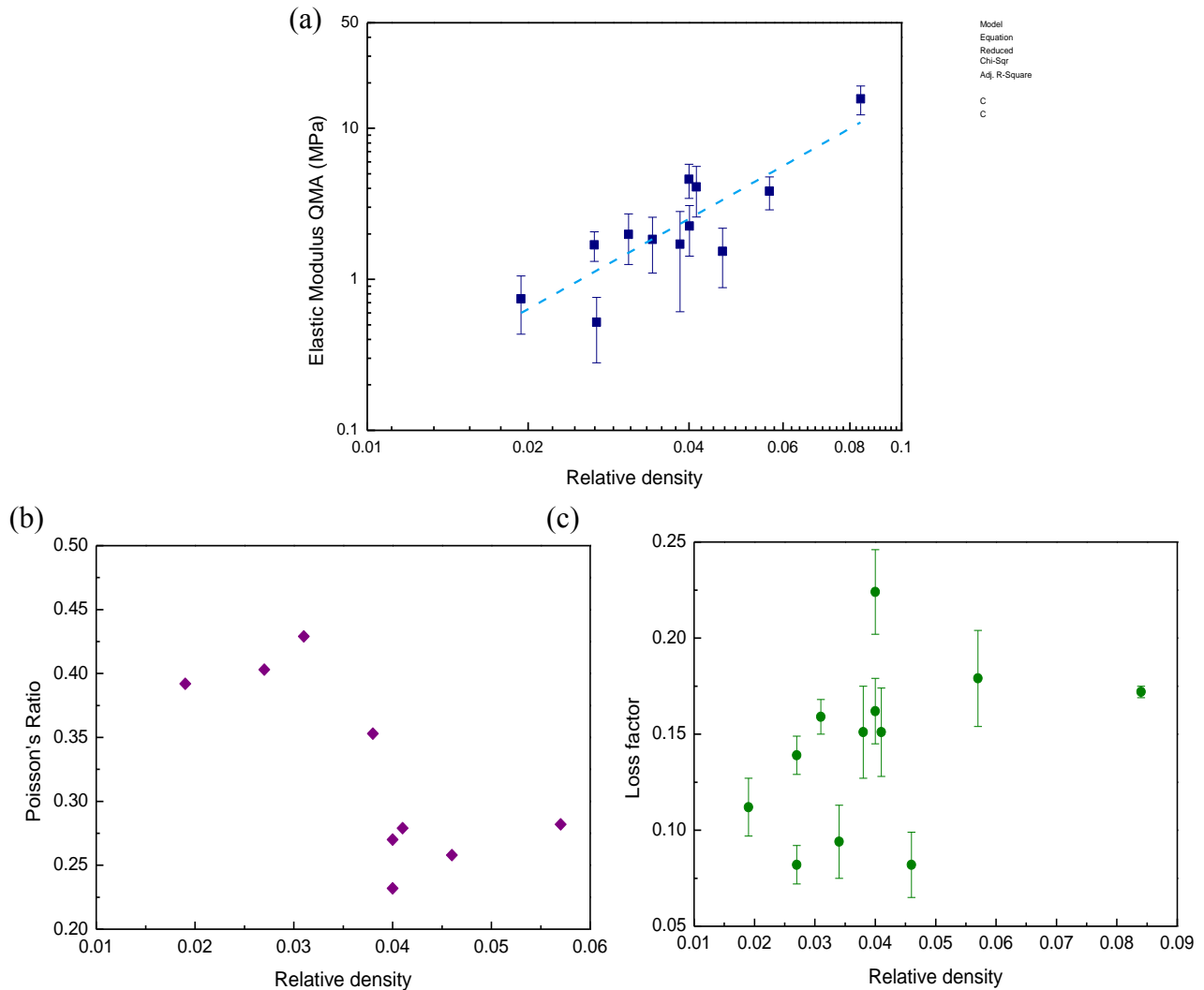


Fig. VI-7. Elastic parameters obtained by QMA as a function of relative density: (a) Elastic modulus; (b) Poisson's ratio and (c) loss factor.

The mean values of Poisson's ratio calculated for the tannin-based foams range from 0.2 to 0.4. They agree with typical values for other conventional foams (Gibson and Ashby, 2001; Langlois et al., 2001; Mott and Roland, 2009; Sahraoui et al., 2000), and do not seem to have any correlation with the composition of the foams. Fig. VI-7(b) only suggests a slight trend according to which Poisson's ratio of the foams roughly decreases, on average, when the relative density of the foams increases. The same was also observed in studies that investigated the Poisson's ratio of open-cell foams (Zhu et al., 2000).

On the other hand, the loss factor of tannin-based foams was found to range from 0.08 to 0.22 (see Table VI-2), and did not show any clear trend with the relative density of the foam in

Fig. VI-7(c). They are higher than the loss factor of 0.045 obtained for melamine foam – widely used for acoustic insulation applications– using the QMA in the same conditions (Langlois et al., 2001). This is an *a priori* good indication that those tannin foams may have good properties for acoustic insulation. There is not much data of other materials with which tannin foams can be compared. In fact, great care should be used when comparing damping values measured by different methods and in different environments, owing to their inevitably nonhomogeneous nature.

For analysing and comparing the acoustic insulation properties of different materials, sound absorption is the most important property. All the elastic and acoustic parameters obtained in the current characterisation (elastic modulus, Poisson's ratio and loss factor), together with other properties of the material such as tortuosity or airflow resistivity, can be used to feed the Biot-Allard poroelastic model (Allard and Atalla, 2009) for predicting the sound absorption of the foams. Indeed, the company Mecanum has developed a simulation software, MNS/Nova 2.0, based on the Biot-Allard model that is able to produce good numerical prediction of sound absorption and transmission loss of single or multilayer materials. Their results present a good correlation with the values obtained by standing wave tube measurements (Langlois et al., 2001). Thus, all the parameters obtained in this work are, therefore, truly interesting for future studies on acoustic properties of foams as well as for simulations.

VI/3.3. Comparison of destructive method (with and without plates) vs non-destructive one (QMA)

The results of QMA have been compared to the results of destructive mechanical compression with and without plates. For that purpose, the elastic modulus obtained by QMA has been plotted versus the one obtained by compression analyses, with and without plates, in Fig. VI-8(a) and Fig. VI-8(b), respectively. Obviously, similar values for both kinds of analysis lead to points aligned along the main diagonal of the graph.

The results verifying such alignment on the plot are those belonging to foams that are not fragile and brittle, regardless of their density. Foams being very dense but presenting elastic-plastic behaviour indeed lead to very similar results using both methods. However, the data of brittle foams analysed by QMA are much lower than those obtained by compression with plates.

On the other hand, a very good agreement is observed between QMA moduli and those derived from compression without plates, see Fig. VI-8(b).

These results suggest that QMA is not suitable for determining accurately the elastic modulus of fragile foam. This finding was somewhat surprising since the foam was fixed between two rough plates that "prevented" any lateral movement, thereby producing a system close to clamped conditions without explicitly bonding the sample to the platens, and therefore resembling the setup of compression with plates. Thus, as we deal with a quasi-static method in which the whole sample is submitted to low-vibration frequencies, one would have expected a global elastic modulus as a result.

However, this assumption was found to be wrong, since the QMA results were rather similar to those obtained by compression without plates, which is suitable for elastic-plastic foams but not for brittle foams. In fact, the elastic modulus of brittle foams is underestimated by QMA. The latter new method thus only determines the elastic modulus of the struts in contact with the platens and not the global elastic modulus of the foam.

On the other hand, the QMA device was mainly developed with the aim of characterising materials designed for acoustic isolation. Those materials with good acoustic insulation properties are, in general, soft, bendable, or elastic-plastic porous materials which would suggest that the equipment is not really adapted for brittle and fragile foams but instead for elastic-plastic foams. Elastic-plastic foams are indeed among the most used materials for acoustic insulation purposes (Jaouen et al., 2008; Tiuc et al., 2016; Wang et al., 2012).

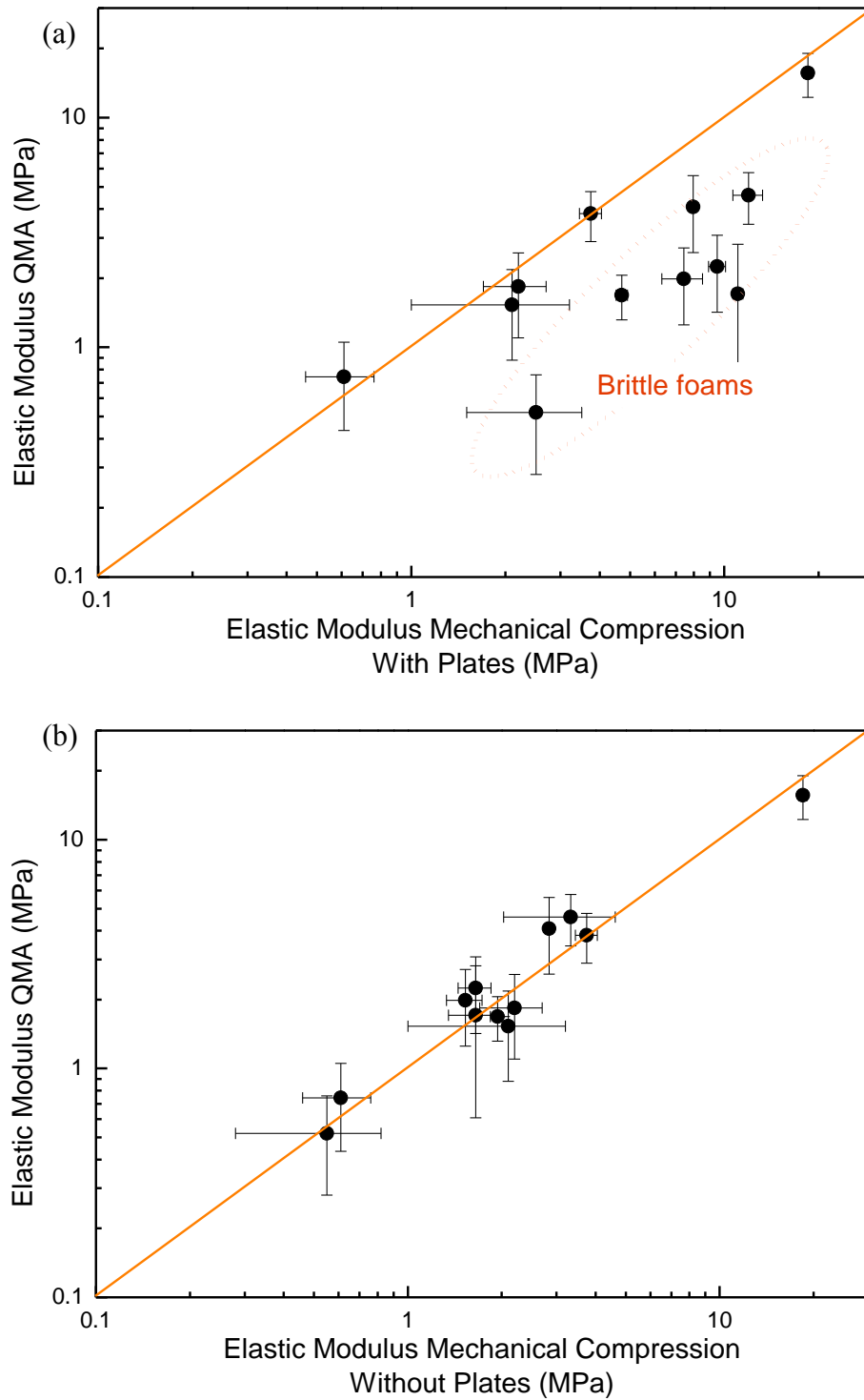


Fig. VI-8. QMA elastic modulus versus elastic modulus from destructive mechanical compression method: (a) with plates and (b) without plates.

In summary, classical mechanical compression with plates is the most suitable method to determine the elastic modulus and the compression strength of all kinds of tannin foams, despite it has the disadvantage of being destructive. In contrast, QMA is only suitable for determining the elastic modulus of elastic-plastic materials that do not present a fragile behaviour. It can also provide parameters such as Poisson's ratio and loss factor that are very interesting and important particularly from the point of view of acoustic applications.

VI/4. Conclusion

12 tannin-based foams, very different from each other, were analysed by the well-known mechanical – destructive – compression technique, with and without plates. It was found that bonding the specimen ends to the stiff loading platens is a key point for the appropriate characterisation of fragile foams. Gluing the brittle foams to rigid plates indeed induces a much better load distribution through the section of the foam, and leads to the sudden collapse of the whole material instead of a progressive break and, consequently, to much higher but far more representative elastic moduli. In contrast, the effect of the adhesion to rigid plates in the elastic-plastic foams is barely noticeable since, in this type of materials, the correct positioning of the load plate in the whole section of the foam is much simpler, so that similar results are obtained with or without glued plates. However, whatever the type of foam and whether the experiments were carried out with or without plates, the same value of compressive strength was always recovered. Modulus and strengths were both found to depend on density through power laws, whose exponents were found to correspond to open-cell foams and to central forces, respectively. Such results are fully consistent with what is known for this kind of cellular materials.

The present work has also presented and discussed a rather new technique for determining the elastic properties of tannin-based foams: quasi-static analysis (QMA). The method is based on the use of polynomial relationships linking compression stiffness, elastic modulus, Poisson's ratio, and shape factor derived from high-order axisymmetric finite-element simulations on a cylindrical sample under static compression. Some of the parameters calculated such as Poisson's ratio and loss factor had never been measured before for this kind of materials.

The results of elastic modulus obtained by the new methodology were compared to those from the destructive mechanical compression method. A very good correlation was found between the QMA elastic modulus and that obtained by compression without plates. However, QMA did not agree with compression with plates, more specifically as far as the elastic modulus of brittle foams was concerned. It was indeed observed that, although the foam was well fixed between two platens in the new method, the distribution of load was not enough homogeneous through the section of the fragile foams and, just like compression without glued plates, no elastic modulus representative of the whole material was obtained.

Thus, QMA and destructive compression testing without plates are both suitable for foams with elastic-plastic properties; however, they are not appropriate for fragile foams. Fragile and brittle foams need to have their opposite faces submitted to compression glued to rigid plates for providing a homogeneous distribution of the load throughout all the section. In conclusion, the safest way to characterise the mechanical properties of a porous material is to use a combination of methods, depending on the quantity under study.

Finally, all the measured elastic properties can also be used to predict the sound absorption coefficient of the foams through the Biot poroelasticity theory. Thus, this work can be the starting point of a new research about the acoustic insulation properties of tannin-based foams.

VI/5. Bibliography

- Allard, J.-F., Atalla, N., 2009. Propagation of sound in porous media: modelling sound absorbing materials, 2nd ed. ed. Wiley, Hoboken, N.J.
- Basso, M.C., Lagel, M.-C., Pizzi, A., Celzard, A., Abdalla, S., 2015. First Tools for Tannin-Furanic Foams Design. *Bioresources* 10, 5233–5241.
- Basso, M.C., Pizzi, A., Celzard, A., 2013. Dynamic Monitoring of Tannin-based Foam Preparation: Effects of Surfactant. *Bioresources* 8, 5807–5816.
- Biot, M.A., Tolstoy, I., 1992. Acoustics, elasticity, and thermodynamics of porous media: twenty-one papers. Published by the Acoustical Society of America through the American Institute of Physics.
- Brezny, R., Green, D.J., 1993. Uniaxial Strength Behavior of Brittle Cellular Materials. *J. Am. Ceram. Soc.* 76, 2185–2192. doi:10.1111/j.1151-2916.1993.tb07753.x
- Celzard, A., Zhao, W., Pizzi, A., Fierro, V., 2010. Mechanical properties of tannin-based rigid foams undergoing compression. *Mater. Sci. Eng. A* 527, 4438–4446. doi:10.1016/j.msea.2010.03.091

- Dauchez, N., 1999. Etude vibroacoustique des matériaux poroélastiques par éléments finis (phdthesis). Université du Maine ; Université de Sherbrooke.
- Etchessahar, M., Sahraoui, S., Benyahia, L., Tassin, J.F., 2005. Frequency dependence of elastic properties of acoustic foams. *J. Acoust. Soc. Am.* 117, 1114–1121. doi:10.1121/1.1857527
- Gibson, L.J., Ashby, M.F., 2001. Cellular solids: structure and properties, 2. ed., 1. paperback ed. (with corr.), transferred to digital printing. ed, Cambridge solid state science series. Cambridge Univ. Press, Cambridge.
- Greaves, G.N., Greer, A.L., Lakes, R.S., Rouxel, T., 2011. Poisson's ratio and modern materials. *Nat. Mater.* 10, 823–837. doi:10.1038/nmat3134
- Jaouen, L., Renault, A., Deverge, M., 2008. Elastic and damping characterizations of acoustical porous materials: Available experimental methods and applications to a melamine foam. *Appl. Acoust.* 69, 1129–1140. doi:10.1016/j.apacoust.2007.11.008
- Lacoste, C., Basso, M.-C., Pizzi, A., Celzard, A., Ella Ebang, E., Gallon, N., Charrier, B., 2015. Pine (*P. pinaster*) and quebracho (*S. lorentzii*) tannin-based foams as green acoustic absorbers. *Ind. Crops Prod.* 67, 70–73. doi:10.1016/j.indcrop.2014.12.018
- Langlois, C., Panneton, R., Atalla, N., 2001. Polynomial relations for quasi-static mechanical characterization of isotropic poroelastic materials. *J. Acoust. Soc. Am.* 110, 3032–3040. doi:10.1121/1.1419091
- Letellier, M., 2015. Optimisation de mousses de carbone dérivées de tannin par l'étude et la modélisation de leurs propriétés physiques (Thèse de doctorat). Université de Lorraine, France.
- Letellier, M., Delgado-Sanchez, C., Khelifa, M., Fierro, V., Celzard, A., 2017. Mechanical properties of model vitreous carbon foams. *Carbon* 116, 562–571. doi:10.1016/j.carbon.2017.02.020
- Liu, Z., Sheng, M., 2008. Study on Characteristics of Sound Absorption of Underwater Visco-elastic Coated Compound Structures. *Mod. Appl. Sci.* 3, 32. doi:10.5539/mas.v3n1p32
- Li, X., Pizzi, A., Cangemi, M., Fierro, V., Celzard, A., 2012. Flexible natural tannin-based and protein-based biosourced foams. *Ind. Crops Prod.* 37, 389–393. doi:10.1016/j.indcrop.2011.12.037
- Mora, R.J., Waas, A.M., 2002. Strength scaling of brittle graphitic foam. *Proc. R. Soc. -Math. Phys. Eng. Sci.* 458, 1695–1718. doi:10.1098/rspa.2001.0938
- Mott, P.H., Roland, C.M., 2009. Limits to Poisson's ratio in isotropic materials. *Phys. Rev. B* 80. doi:10.1103/PhysRevB.80.132104
- Pritz, T., 1994. Dynamic Young's modulus and loss factor of plastic foams for impact sound isolation. *J. Sound Vib.* 178, 315–322. doi:10.1006/jsvi.1994.1488
- Sahimi, M., 1998. Non-linear and non-local transport processes in heterogeneous media: from long-range correlated percolation to fracture and materials breakdown. *Phys. Rep.* 306, 213–395. doi:10.1016/S0370-1573(98)00024-6
- Sahraoui, S., Mariez, E., Etchessahar, M., 2000. Mechanical testing of polymeric foams at low frequency. *Polym. Test.* 20, 93–96. doi:10.1016/S0142-9418(00)00006-4
- Sanders, W.S., Gibson, L.J., 2003. Mechanics of hollow sphere foams. *Mater. Sci. Eng. A* 347, 70–85. doi:10.1016/S0921-5093(02)00583-X
- Shen, H., Nutt, S., 2003. Mechanical characterization of short fiber reinforced phenolic foam. *Compos. Part Appl. Sci. Manuf.* 34, 899–906. doi:10.1016/S1359-835X(03)00136-2
- Sokolnikoff, I.S., 1983. Mathematical theory of elasticity. R.E. Krieger Pub. Co, Malabar, Fla.

- Szczurek, A., Fierro, V., Pizzi, A., Stauber, M., Celzard, A., 2014. A new method for preparing tannin-based foams. *Ind. Crops Prod.* 54, 40–53. doi:10.1016/j.indcrop.2014.01.012
- Szczurek, A., Ortona, A., Ferrari, L., Rezaei, E., Medjahdi, G., Fierro, V., Bychanok, D., Kuzhir, P., Celzard, A., 2015. Carbon periodic cellular architectures. *Carbon* 88, 70–85. doi:10.1016/j.carbon.2015.02.069
- Tiuc, A.-E., Vermeşan, H., Gabor, T., Vasile, O., 2016. Improved Sound Absorption Properties of Polyurethane Foam Mixed with Textile Waste. *Energy Procedia, EENVIRO-YRC 2015 - Bucharest* 85, 559–565. doi:10.1016/j.egypro.2015.12.245
- Wang, D., Zhang, Luo, S., Li, S., 2012. Preparation and Property Analysis of Melamine Formaldehyde Foam. *Adv. Mater. Phys. Chem.* 02, 63–67. doi:10.4236/ampc.2012.24B018
- Zhao, W., Fierro, V., Pizzi, A., Du, G., Celzard, A., 2010. Effect of composition and processing parameters on the characteristics of tannin-based rigid foams. Part II: Physical properties. *Mater. Chem. Phys.* 123, 210–217. doi:10.1016/j.matchemphys.2010.03.084
- Zhu, H.X., Hobdell, J.R., Windle, A.H., 2000. Effects of cell irregularity on the elastic properties of open-cell foams. *Acta Mater.* 48, 4893–4900. doi:10.1016/S1359-6454(00)00282-2

Conclusions et perspectives

Les différents travaux réalisés dans cette thèse pour développer et améliorer les mousses à base de tanin ont donné lieu à un grand nombre d'expériences avec des résultats intéressants et originaux. Les principaux points à souligner sont énumérés ci-dessous:

→ Les formulations les plus récentes et les plus prometteuses de mousses de tanin, c'est-à-dire des mousses dites « meringues » et des mousses furaniques de tanin sans formaldéhyde, ni isocyanate, ni agent moussant, ont été étudiées et optimisées. Pour cela, des méthodes qui n'avaient jamais été utilisées avec ce type de matériaux ont été mises en œuvre et se sont révélées très utiles.

D'une part, tous les facteurs qui affectent les mousses de type « meringue » ont été optimisés et étudiés grâce à un appareil très peu répandu fonctionnant sur la base de l'analyse de la lumière rétrodiffusée. Cela a permis de connaître comment la température, la quantité de tensioactif ou le temps d'agitation affectent la stabilité de la mousse liquide et, par conséquent, les propriétés physiques et structurales de la mousse rigide finale. De cette manière, cette méthode d'étude a permis de développer une mousse liquide stable plus longtemps, ce qui donne plus de possibilités pour tester d'autres agents de réticulation par exemple, entre autres ingrédients.

D'autre part, dans l'optimisation des mousses furaniques de tannin, des plans d'expériences ont été utilisés. L'impact des principaux ingrédients de la mousse dans deux de ses caractéristiques finales les plus importantes, la conductivité thermique et la résistance mécanique, a été exploré et modélisé. Ainsi, les propriétés de toute autre formulation de mousse qui se situe dans les bornes de l'étude peuvent être prévues. En conséquence, les combinaisons les plus appropriées de leurs ingrédients ont permis d'obtenir le meilleur compromis conduisant à des mousses à la fois assez isolantes thermiquement et mécaniquement résistantes.

Ainsi, ces deux types d'études ont permis de mieux connaître le comportement des formulations. Les outils mis en œuvre ont permis de connaître certaines des caractéristiques des mousses sans avoir besoin de les préparer réellement, et ainsi de prévoir s'il était possible ou non d'atteindre des valeurs données de propriétés.

→ La détérioration des propriétés d'isolation thermique des mousses de tannin dans des conditions d'humidité élevée a été soigneusement analysée. Des informations précieuses sur le comportement des mousses soumises à différentes valeurs d'humidité relative ont été obtenues à partir de l'étude et de la comparaison de mousses hydrophobisées par rapport à des échantillons non traités. Une hydrophobisation totale de la mousse de tanin est impossible car la vapeur d'eau peut toujours pénétrer dans le réseau de polymère de la mousse. Néanmoins, le traitement a limité significativement l'augmentation de la conductivité thermique, ce qui permet à ces mousses de conserver leur potentiel d'isolation thermique.

Ainsi, au lieu d'essayer d'imiter complètement le comportement des mousses synthétiques déjà utilisées pour l'isolation thermique, les mousses à base de tanin devraient être considérées comme les matériaux dérivés de ressources naturelles qu'ils sont, avec des propriétés différentes mais néanmoins avantageuses. Essentiellement, les mousses à base de tanin hydrophobisées ont montré une augmentation limitée de la conductivité thermique avec l'humidité relative, mais ont toujours conservé suffisamment leur caractère hydrophile pour leur permettre de « respirer ». Ainsi, ces mousses pourraient offrir une bonne isolation thermique combinée à la possibilité d'améliorer la qualité de l'air intérieur, en régulant l'humidité source de nombreuses pathologies du bâtiment. De telles caractéristiques font de ce produit un candidat idéal pour le marché de l'isolation thermique biosourcée.

→ Une étude détaillée des propriétés de réaction au feu des mousses de tanin a aussi été réalisée dans cette thèse. Cela a permis de connaître, outre leur excellent comportement retardant, tous les paramètres des mousses qui influencent ces propriétés. Il a été observé que l'inflammabilité des mousses dépend fortement de leur formulation et pas tant de leurs propriétés structurales. En fait, il a été observé que le comportement des mousses pendant un incendie peut être très différent selon la présence ou non de certains ingrédients et additifs dans leur formulation. La présence de tensioactifs et d'additifs comme des plastifiants et, plus important encore, la teneur initiale en eau des formulations dégradent les propriétés au feu des mousses. La quantité d'eau initiale dans les mousses est particulièrement importante car la vaporisation de l'eau sous l'effet de la chaleur affaiblit la structure, ce qui facilite la dégradation thermique de la mousse. La réduction de la teneur en eau dans la formulation peut donc améliorer les performances des mousses de tanin soumises au feu.

Il a aussi été vérifié que la retardance au feu des mousses est principalement due à la composition aromatique de la matrice polymérique, qui forme un réseau macromoléculaire résistant à la chaleur, avec une faible perte de masse au cours de sa décomposition thermique. En conséquence, seule une très faible quantité de gaz inflammables est produite, augmentant de fait le temps d'ignition, réduisant le dégagement de chaleur, et interdisant tout caractère auto-entretenu de la combustion. Ces propriétés au feu des mousses de tanins ont été comparées à celles des principaux matériaux isolants actuellement commercialisés, tels que le polystyrène expansé, la mousse de polyuréthane et les mousses phénoliques, montrant que les mousses de tanin ont des propriétés très supérieures de ce point de vue.

→ La dernière partie de la thèse est centrée sur l'étude d'une nouvelle méthode de caractérisation des propriétés mécaniques des mousses. Cette nouvelle technique est non destructive et repose sur des relations polynomiales connectant plusieurs paramètres élastiques des mousses sous compression statique au travers de simulations axisymétriques à éléments finis. Cette nouvelle méthode s'est révélée appropriée pour caractériser les mousses élastiques-plastiques, mais ne convient pas aux mousses fragiles qui doivent avoir leurs faces opposées collées à des plaques rigides pour assurer une répartition homogène de la charge dans toute leur section droite. La nouvelle méthode a également permis de déterminer le coefficient de Poisson et le facteur de perte, qui n'avaient jamais été mesurés jusqu'à présent pour des mousses de tannin, et qui sont des paramètres très intéressants du point de vue de la modélisation des mousses ou pour explorer d'autres applications telles que l'isolation acoustique.

En conclusion, les études menées dans cette thèse ont apporté des progrès majeurs dans les recherches sur les mousses de tanin. Cette thèse a notamment permis d'évaluer les performances et de mieux comprendre les propriétés de ces matériaux prometteurs, respectueux de l'environnement, principalement à base de produits naturels et avec un procédé de production relativement écologique. Nous espérons ainsi favoriser une possible mise sur le marché. Même si beaucoup de travail a été réalisé au cours de cette thèse, le potentiel des mousses de tanin n'a pas été entièrement exploré pour autant. Il y a certains points ou pistes de développement qui n'ont pas encore pu être plus amplement abordés, et qui à notre avis restent d'un grand intérêt.

Un sujet qui serait particulièrement très intéressant à étudier et qu'on a déjà mentionné est l'application de ces mousses de tanin à l'isolation acoustique. Une seule étude à ce sujet a été effectuée jusqu'à présent, qui décrit ces mousses comme des absorbeurs de sons biosourcés potentiels, avec des propriétés acoustiques comparables à celles des matériaux disponibles sur le marché. Par conséquent, le développement de mousses de tanin avec de bonnes propriétés acoustiques, une faible conductivité thermique et une excellence retardance au feu, serait certainement très attrayant dans le contexte actuel où les matériaux multifonctionnels sont très recherchés.

La valorisation des déchets de mousse de tanin est aussi un point très important pour compléter l'étude de ces matériaux, et qui n'a été que très peu explorée. Un processus intéressant de récupération pourrait être leur application dans le traitement des eaux usées. En fait, de courtes études sur l'adsorption de quelques polluants dans l'eau tels que des colorants, tensioactifs et médicaments sur des mousses de tannin broyées ont déjà donné des résultats très encourageants. Ces études mériteraient d'être complétées et élargies à l'adsorption de métaux lourds, ou au traitement d'effluents industriels avec de multiples contaminants.

Il serait également très intéressant d'étudier la biodégradabilité des mousses de tanin. Une étude poussée sur les possibles attaques d'insectes et de champignons sur ces mousses n'a jamais été conduite. Les tanins jouent un rôle de défense pour les végétaux car ils sont difficilement assimilables par les insectes et les champignons, et ont un goût astringent pour les herbivores. Mais il serait donc intéressant de voir s'il en va de même dans le cas des mousses à base de tanins, dont la pureté n'est pas totale. En effet, la présence de polysaccharides dans le tanin industriel non raffiné devrait théoriquement les rendre vulnérables aux attaques fongiques à long terme. Il devrait alors être possible de moduler la biodégradabilité, selon le temps de décomposition souhaitée, en incorporant plus ou moins de polysaccharides aux formulations.

Pour finir, un dernier point et non des moindres concerne le passage de l'échelle du laboratoire à l'échelle (semi-) industrielle pour la préparation des mousses de tanin. Il est en effet connu que les effets de masse sont extrêmement importants dans la polycondensation de ces systèmes tanin-alcool furfurylique, et des mousses très différentes sont obtenues à formulation identique selon le volume de matière utilisé, la nature et la taille du moule, la température ambiante, etc. Ces problèmes ne pourront être réglés qu'au travers de la modélisation du procédé de moussage, par

l'incorporation des données de la formulation dans le modèle et avec comme variables de sortie la température au cœur de la mousse en formation, sa vitesse d'expansion, son volume final, sa variation de masse au cours du temps, etc. De telles études sont actuellement en cours dans une autre thèse réalisée dans notre équipe de recherche.

List of figures

Fig. I-1. Status of the European thermal insulation market in 2014.....	29
Fig. I-2. Some examples of tannin-rich plants and corresponding tannin extracts.	31
Fig. I-3. Tannin classification and examples of structures.	32
Fig. I-4 Structures of the two possibilities of each phenolic ring and the flavonoid units present in the condensed tannins (Arbenz and Avérous, 2015).....	33
Fig. I-5. Reaction between tannin and formaldehyde.....	35
Fig. I-6. Example of crosslinking of tannin through benzylamine bridges by reaction with an amino-imino methylene base obtained by decomposition of hexamine in the presence of tannins (Pichelin et al., 1999).	37
Fig. I-7. Production of furfuryl alcohol from pentoses.	38
Fig. I-8. Reactions proposed for the polycondensation and chain extension of furfuryl alcohol resins in the presence of acids and other electrophiles (Choura et al., 1996; Dunlop and Peters, 1953).....	39
Fig. I-9. Products of the reaction between tannin and furfuryl alcohol (Arbenz and Avérous, 2015).....	39
Fig. I-10. Reaction of furfuryl alcohol with formaldehyde.	40
Fig. I-11. Schematic arrangement of foams: a) ideal: made only of tetrakaidecahedra; b) real: 75% tetrakaidecahedra and 25% dodecahedra.	43
Fig. I-12. Standard tannin-based foams.....	45
Fig. I-13. Scheme explaining how different tannin-based foam families could be prepared so far.	47
Fig. I-14. Foaming process and composition of a standard tannin foam.....	48
Fig. I-15. Foaming process and composition of a tannin meringue foam.	51
Fig. I-16. Meringue tannin foam: a) a detail of its surface observed by scanning electron microscopy (SEM); b) its complementary image obtained by 3D X-ray micro-computed tomography (the colour coded the size distribution).....	54

Fig. I-17. Comparative mechanical resistance of a standard foam – STD (with formaldehyde and a blowing agent), a SF foam (without formaldehyde but with a blowing agent) and a foam M1 without formaldehyde and without a blowing agent (Basso et al., 2013a).....	55
Fig. II-1. Preparation of a liquid meringue tannin-based foam.	72
Fig. II-2. Views of the Turbiscan setup: (a) open, empty sample holder; (b) liquid tannin-based foam in the closed sample holder; (c) scheme of the sample environment in the Turbiscan device, showing light source and detectors; (d) Turbiscan Tower analyser, admitting up to 6 samples. ..	74
Fig. II-3. Typical Δ -backscattering profiles of tannin-based liquid foams recorded by the optical analyser: top = with crosslinker (hexamine); bottom = without crosslinker.	76
Fig. II-4. Foaming capacity at 25°C of liquid formulations (30 g of water, 20 g of tannin, 1.42 g of hemaxine and 1.12 g of pTSA) prepared with different amounts of surfactant as a function of stirring time. The dotted lines are just guides for the eye.	79
Fig. II-5. Effect of the presence of crosslinker (hexamine) on: (a) foaming capacity as a function of stirring time; (b) drainage and sedimentation at the sample’s bottom; (c) coalescence and coarsening in the middle of the foam; and (d) average bubble diameter. The typical uncertainties on these curves are $\leq 5\%$	82
Fig. II-6. Effect of whipping time on: (a) volume of drained liquid; (b) drainage and sedimentation at the sample’s bottom; (c) coalescence and coarsening in the middle of the foam; and (d) average bubble diameter.	85
Fig. II-7. Effect of surfactant amount on: (a) volume of drained liquid; (b) drainage and sedimentation at the sample’s bottom; (c) coalescence and coarsening in the middle of the foam; and (d) average bubble diameter.	88
Fig. II-8. Δ -backscattering profiles of foams evaluated by the analyser at 25, 40, 60 and 80°C	91
Fig. II-9. Effect of temperature on liquid foams as a function of time: (a) drainage and polymerisation at the sample’s bottom; (b) coalescence and coarsening in the middle of the foam; (c) variation of average bubble diameter; and (d) starting point of polymerisation.	93
Fig. II-10. Application of Eq. (II-4) to the data of Fig. II-9(d), accounting for the polymerisation of tannin in liquid foam formulations.	95
Fig. II-11. General scheme of the study using the Turbiscan analyser.	96

Fig. III-1. Schematic representation of the grafting process of organosilane compounds on a material surface bearing hydroxyl groups.	104
Fig. III-2. Tannin-based foams: (a) Meringue and (b) Standard.	106
Fig. III-3. Prorobinetinidin, the main compound of Mimosa tannin.	109
Fig. III-4. Water contact angle measured by Washburn method (see next section for details) at the surface of untreated foam samples formerly conditioned at various values of relative humidity.	110
Fig. III-5. Determination of the mean linear cell density by counting the numbers of cells along lines of known length by the use of the « cell counter » tool of ImageJ software. The markers here correspond to the counts of the cells along the 9 horizontal lines, and the same is repeated along the vertical lines.	112
Fig. III-6. Vario EL Cube elemental analyser and diagram of the measurement.	113
Fig. III-7. Details of contact angle measurements: (a) Sessile drop method and (b) Washburn method.	115
Fig. III-8. (a) 3Flex apparatus and (b) types of adsorption isotherms classified according to IUPAC (Ng and Mintova, 2008).	118
Fig. III-9. HotDisk TPS 2500 device and details of the probe.	120
Fig. III-10. FTIR spectra of untreated and treated tannin foams based on standard (top) and meringue (bottom) formulations.	123
Fig. III-11. Top view of a droplet of water deposited on C8Me-grafted foams: (a) Standard; (b) Meringue.	125
Fig. III-12. Surface energy and their dispersive and polar parts, determined using OWRK method with contact angle data from sessile drop and liquid penetration techniques, for raw and treated foams (top: standard, and bottom: meringue), and corresponding water contact angles.	127
Fig. III-13. Sorption - desorption isotherms of water on pristine tannin-based foams.	128
Fig. III-14. Sorption isotherms of water on pristine and treated foams on dry basis (d.b.) (top: standard foams; bottom: meringue foams). The inset shows the sorption behaviour of 3 structural PVC (Airex® C70) and polyurethane (Kapex® C51 and Saitec®) foam core materials for sandwich panels. The curves were calculated by Eq. (10).	130
Fig. III-15. Schematic picture of grafted tannin-based foam in a moist environment.	132

Fig. III-16. Thermal conductivity of pristine and treated tannin-based foams as a function of relative humidity (top: standard foams; bottom: meringue foams).....	136
Fig. III-17. Thermal conductivity of pristine and treated tannin-based foams, as a function of water uptake. The dotted lines are just guides for the eye, evidencing two groups of samples, Meringue and Standard, having different slopes.....	137
Fig. IV-1. Example of tannin-furanic foam samples prepared and tested in this work.....	149
Fig. IV-2. Distribution of experimental design points in the investigated range of parameters <i>A</i> (tannin), <i>B</i> (furfuryl alcohol), and <i>C</i> (catalyst: 65 wt. % aqueous solution of phenol-sulphonic acid).....	154
Fig. IV-3. Universal test machine INSTRON 5944 equipped with its compression plates. ...	156
Fig. IV-4. Stress-strain curves of some tannin-based foams studied in this work.	159
Fig. IV-5. Normal probability plot of residuals for: (a) thermal conductivity, (b) compression strength, and (c) elastic modulus. Numerical values of those properties increase from blue to red.	162
Fig. IV-6. Contour plots (first row, left) and surface plots (second row, right) of the effect of tannin, furfuryl alcohol and catalyst amounts on: (a) thermal conductivity; (b) compressive strength; (c) elastic modulus. Numerical values of the responses increase from blue to red.....	165
Fig. IV-7. Thermal conductivity versus compressive strength calculated by application of Eqs. (IV-3)-(IV-5), using compositions inside the ranges given in Eq. (IV-1). The best compromise between low thermal conductivity and high mechanical properties is highlighted by the dotted contour, and the two green points inside the dotted contour are the formulations employed to prove the relevance of the model. The dashed line is just a guide for the eye, indicating the lower boundary of thermal conductivity that can be expected with this kind of materials.....	165
Fig. IV-8. Area (dotted contour) corresponding to the optimum formulations in the tannin – furfuryl alcohol – catalyst ternary diagram. The two green points inside the dotted contour are the formulations employed to prove the relevance of the model.	166
Fig. V-1. Euroclass classification for the main insulation product on the market.	178
Fig. V-2. All the tannin-based foams studied in this work.....	179
Fig. V-3. Schematic representation of a cone calorimeter.	184
Fig. V-4. Schematic representation of a pyrolysis-combustion flow calorimeter.	185

Fig. V-5. HRR of standard and formaldehyde-free tannin foams submitted to a radiant heat flux of $50 \text{ kW} \cdot \text{m}^{-2}$	188
Fig. V-6. HRR of meringue tannin foams submitted to a radiant heat flux of $50 \text{ kW} \cdot \text{m}^{-2}$	189
Fig. V-7. Meringue foam during cone calorimeter test as a function of time.	189
Fig. V-8. Heat release rate curves measured by PCFC at 1 K s^{-1} for several tannin-based foams: (a) investigated foams; (b) highline main, corresponding, kinds of thermal degradation process; (c) assignment of the degradation peaks.	196
Fig. V-9. Effect of the type of tannin and of the elimination of formaldehyde on the flammability of tannin foams.	197
Fig. V-10. Effect of addition of plasticiser and surfactant on the flammability of tannin foams.	198
Fig. V-11. Thermal stability of tannin-based foams, STD-M (left) and Meringue-M (right), under air (top) and N_2 (bottom) atmospheres (heating rate: $10 \text{ }^\circ\text{C} \cdot \text{min}^{-1}$).	200
Fig. V-12. Comparison between heat release rate and mass loss rate monitored with PCFC (right axis) and TGA (left axis), respectively, for (a) STD-M and (b) Meringue-M.	202
Fig. V-13. Results obtained from the TGA-FTIR analysis of STD-M foam.	203
Fig. V-14. Results obtained from the TGA-FTIR analysis of Meringue-M foam.	205
Fig. VI-1. Tannin-based foams glued to plastic plates, ready for compression test.....	217
Fig. VI-2. Compressive modulus of tannin-based vitreous carbon foams tested with and without plates, as a function of their relative density (Letellier et al., 2017). Different relations coming from the Gibson and Ashby model (Gibson and Ashby, 2001) were fitted, and the fraction of solid only contained in the struts, ϕ , is shown. STD, PEG, TRITON, PLURO, etc. correspond to the different formulations of the former tannin-based foams, some of them being similar to those used in this work.	219
Fig. VI-3. Quasi-static mechanical analyser (QMA) details: (a) schematic representation of measurement setup, (b) real photo and (c) tannin cylindrical foam samples ready for testing.	220
Fig. VI-4. Compressive strength obtained by destructive mechanical compression as a function of tannin foams' relative density. The same results were obtained with or without plates. The dashed line corresponds to the application of Eq. (VI-8).	225

Fig. VI-5. Elastic modulus obtained by destructive mechanical compression as a function of relative density of tannin foams tested: (a) without plates; and (b) with plates. The dashed lines correspond to the application of Eq. (VI-9).226

Fig. VI-6. Stress-strain curves of tannin-based foams by destructive mechanical compression with plates.227

Fig. VI-7. Elastic parameters obtained by QMA as a function of relative density: (a) Elastic modulus; (b) Poisson's ratio and (c) loss factor.230

Fig. VI-8. QMA elastic modulus versus elastic modulus from destructive mechanical compression method: (a) with plates and (b) without plates.233

List of tables

Table II-1. Effect of stirring time on: onset of sedimentation, foaming capacity and sigmoidal model parameters for liquid drainage.....	83
Table II-2. Effect of surfactant amount on: onset of sedimentation, foaming capacity and sigmoidal model parameters for liquid drainage.....	87
Table II-3. Effect of temperature on: final fraction of air in the foam, onset of polymerisation, and time required to reach the set point.	90
Table III-1. Mimosa tannin-based foams formulations. All amounts are expressed in grams.	107
Table III-2. Description of hydrophobisation reagents.	108
Table III-3. Surface tension and corresponding polar and dispersive parts of liquids used for the determination of surface energy (Jańczuk and Białopiotrowicz, 1989).....	117
Table III-4. Main features of the two studied tannin-based foam samples.	121
Table III-5. Ultimate analysis of the two studied tannin-based foams.....	121
Table III-6. Measured contact angles of various liquids on tannin-based foams, and calculated values of their total surface energy γ_s , as well as their dispersive γ_s^d and polar γ_s^p parts. All measurements were made at 20°C and 40% RH. ^A	124
Table III-7. Sorption parameters derived from the application of the GAB equation (III-10) to the data of Fig. III-14. The correlation factor R^2 is also provided.	134
Table IV-1. Representative example of foam formulation.....	149
Table IV-2. Uniform experimental design scheme for the preparation of foams.....	154
Table IV-3. Experimental results for the 14 foams' formulations.	158
Table IV-4. ANOVA for Eqs. (IV-3)-(IV-5).....	161
Table IV-5. Validation of the model: measured versus predicted values.....	167
Table V-1. Classes of reaction to fire performance for construction products excluding floorings - (EN 13501-1, 2007).....	175
Table V-2. Formulation of the different types of foams.....	181
Table V-3. Fire parameters of tannin foams and other thermal insulation materials obtained by cone calorimetry under heat flux of 50 kW·m ⁻²	191

List of tables

Table V-4. PCFC results for tannin-based foams.....	193
Table VI-1. Experimental results of mechanical compression for the 12 foams' formulations.*	224
Table VI-2. QMA results for the 12 foams' formulations.*.....	229

List of works

Publications in scientific journals

Published

- ✦ G. Rangel, H. Chapuis, M.C. Basso, A. Pizzi, **C. Delgado-Sanchez**, V. Fierro, A. Celzard, C. Gerardin-Charbonnier, 2016. Improving Water Repellence and Friability of Tannin-Furanic Foams by Oil-Grafted Flavonoid Tannins. *Bioresources* 11, 7754–7768. doi:10.15376/biores.11.3.7754-7768

- ✦ **C. Delgado-Sánchez**, M. Letellier, V. Fierro, H. Chapuis, C. Gérardin, A. Pizzi, A. Celzard, 2016. Hydrophobisation of tannin-based foams by covalent grafting of silanes. *Ind. Crops Prod.* 92, 116–126. doi:10.1016/j.indcrop.2016.08.002

- ✦ **C. Delgado-Sánchez**, V. Fierro, S. Li, A. Pasc, A. Pizzi, A. Celzard, 2017. Stability analysis of tannin-based foams using multiple light-scattering measurements. *Eur. Polym. J.* 87, 318–330. doi:10.1016/j.eurpolymj.2016.12.036

- ✦ M. Letellier, **C. Delgado-Sánchez**, M. Khelifa, V. Fierro, A. Celzard, 2017. Mechanical properties of model vitreous carbon foams. *Carbon* 116, 562–571. doi:10.1016/j.carbon.2017.02.020

- ✦ **C. Delgado-Sánchez**, G. Amaral-Labat, L.I. Grischechko, A. Sánchez-Sánchez, V. Fierro, A. Pizzi, A. Celzard, 2017. Fire-resistant tannin–ethylene glycol gels working as rubber springs with tuneable elastic properties. *J. Mater. Chem. A* 5, 14720–14732. doi:10.1039/C7TA03768F

- ✦ M. Letellier, J. Macutkevic, D. Bychanok, P. Kuzhir, **C. Delgado-Sánchez**, H. Naguib, S.G. Mosanenzadeh, V. Fierro, A. Celzard, 2017. Modelling the physical properties of glasslike carbon foams. *J. Phys. Conf. Ser.* 879, 012014. doi:10.1088/1742-6596/879/1/012014

- ✦ J. Encalada, K. Savaram, N.A. Travlou, W. Li, Q. Li, **C. Delgado-Sánchez**, V. Fierro, A. Celzard, H. He, T.J. Badosz, 2017. Combined effect of porosity and surface chemistry on the

electrochemical reduction of oxygen on cellular vitreous carbon foam catalyst. *ACS Catal.*
doi:10.1021/acscatal.7b01977

Submitted

✦ F.J. Santiago-Medina, **C. Delgado-Sánchez**, A. Pizzi, A. Celzard, V. Fierro, L. Delmotte, C. Vaultot, 2017. Understanding and distinguishing condensed tannins with the same origin but influenced by sulfitation. *ProLigno*.

✦ **C. Delgado-Sánchez**, F.J. Santiago-Medina, V. Fierro, A. Pizzi, A. Celzard, 2017. Methodical optimisation of blowing agent-free and formaldehyde-free tannin-furanic foams for thermal insulation through experimental design. *Materials & Design*.

✦ F.J. Santiago-Medina, **C. Delgado-Sánchez**, M.C. Basso, A. Pizzi, V. Fierro, A. Celzard, 2017. Mechanically blown wall-projected tannin-based foams. *Industrial Crops and Products*.

Oral communications

✦ M. Khelifa, V. Fierro, A. Celzard, M. Letellier, **C. Delgado-Sánchez**. FE analysis of carbon foam under multiple compressive loading. *18th International Conference on Composite Structures (ICCS18)*, Lisbon (Portugal) 15 – 18 Juin 2015

✦ M. Letellier, J. Macutkevic, D. Bychanok, P. Kuzhir, **C. Delgado-Sánchez**, H. Naguib, S. Ghaffari Mosanenzadeh, V. Fierro, A. Celzard. Matériaux alvéolaires modèles en carbone vitreux pour la science des matériaux et les sciences de l'ingénieur. *Journées Scientifiques de la Société Francophone d'Etude des Carbons (SFEC 2016)*, Carqueirane (Var), 20 Mai 2016 : CONFERENCE INVITÉE

✦ M. Letellier, J. Macutkevic, D. Bychanok, P. Kuzhir, **C. Delgado-Sánchez**, H. Naguib, S. Ghaffari Mosanenzadeh, V. Fierro, A. Celzard. Modelling the physical properties of glasslike carbon foams. *International Conference Carbon 2016*, State College (PA, USA) 10 – 15 Juillet 2016

✦ M. Letellier, **C. Delgado-Sánchez**, J. Macutkevic, D. Bychanok, P. Kuzhir, H. Naguib, S. Ghaffari Mosanenzadeh, V. Fierro, A. Celzard. Etude des propriétés physiques de mousses

modèles en carbone vitreux. *Séminaire annuel du LCTS (Laboratoire des Composites Thermo-Structuraux)*, Bordeaux, 11 octobre 2016 : CONFERENCE INVITÉE

✦ **C. Delgado-Sánchez**, M. Letellier, V. Fierro, H. Chapuis, C. Gérardin, A. Pizzi, A. Celzard. Hydrophobisation of tannin-based foams by covalent grafting of silanes. *JEMP2016: 13^{èmes} Journées d'Etudes des Milieux Poreux*, Anglet (France) 12 – 14 Octobre 2016

✦ M. Letellier, J. Macutkevic, D. Bychanok, P. Kuzhir, **C. Delgado-Sanchez**, H. Naguib, S. Ghaffari Mosanenzadeh, V. Fierro, A. Celzard. Physical properties of model, reticulated and cellular vitreous carbon foams. *5th France - Russia Conference NAMES'16 (New Achievements in Materials and Environmental Science)*, Nancy 7-9 Novembre 2016

Poster communications

✦ **C. Delgado-Sánchez**, V. Fierro, A. Celzard. Study of tannin-based foam stability using new optical analyzer Turbiscan. *JEMP2016: 13^{èmes} Journées d'Etudes des Milieux Poreux*, Anglet (France) 12 – 14 Octobre 2016

Abstract

In this thesis, foams based on more than 90% of natural products and with an exceptionally low thermal conductivity have been studied in depth. The main objective of this work was to improve some of the weaknesses of those materials and to solve problems that might be encountered during use, for allowing them to compete with other synthetic foams that are currently on the thermal insulation market. New methodologies have been proposed to optimise tannin-based foams from different points of view. First, liquid foams were analysed in terms of stability and polymerisation process using a backscattered light analyser, in order to convert them into improved rigid tannin-based foams. Experimental design was also used to improve the mechanical properties of physically blown rigid foams without prejudicing their thermal conductivity. On the other hand, hydrophobisation treatments were suggested for reducing the sensitivity of those foams to water in liquid or vapour form, and the effect of formulations' ingredients on their fire properties were elucidated. Finally, two techniques of mechanical characterisation were investigated and compared, leading to Poisson's coefficient and loss factor, and evidencing the precautions to be taken for characterising brittle foams.

Résumé

Dans cette thèse, des mousses produites à plus de 90% à partir de produits naturels et à très faible conductivité thermique ont été étudiées en détail. L'objectif principal de ce travail était d'améliorer certaines faiblesses de ces matériaux et de résoudre les problèmes qui pourraient être rencontrés lors de leur utilisation, pour leur permettre de concurrencer d'autres mousses synthétiques actuellement sur le marché de l'isolation thermique. De nouvelles méthodologies ont été proposées pour optimiser les mousses à base de tanin de différents points de vue. Tout d'abord, des mousses liquides ont été analysées en termes de stabilité et de processus de polymérisation à l'aide d'un analyseur de lumière rétrodiffusée, afin de les transformer en mousses rigides de tanin plus performantes. Des plans d'expériences ont également été utilisés pour améliorer les propriétés mécaniques de mousses rigides, produites par moussage physique, sans porter préjudice à leur conductivité thermique. D'autre part, des traitements d'hydrophobisation ont été réalisés pour réduire la sensibilité de ces mousses à l'eau, qu'elle soit sous forme liquide ou vapeur, et l'effet des ingrédients des formulations sur leurs propriétés au feu a été élucidé. Enfin, deux techniques de caractérisation mécanique ont été étudiées et comparées, ce qui a permis de déterminer le coefficient de Poisson et le facteur de perte, et de mettre en évidence les précautions à prendre pour caractériser les mousses fragiles.